TRANSMISSION DYNAMICS OF COVID-19: MATHEMATICAL MODELS FOR EFFECTIVE CONTROLS

A THESIS SUBMITTED TO THE

CENTRAL DEPARTMENT OF MATHEMATICS
INSTITUTE OF SCIENCE AND TECHNOLOGY
TRIBHUVAN UNIVERSITY
NEPAL

FOR THE AWARD OF
DOCTOR OF PHILOSOPHY
IN MATHEMATICS

BY
KHAGENDRA ADHIKARI

December 2023

TRANSMISSION DYNAMICS OF COVID-19: MATHEMATICAL MODELS FOR EFFECTIVE CONTROLS

A THESIS SUBMITTED TO THE

CENTRAL DEPARTMENT OF MATHEMATICS
INSTITUTE OF SCIENCE AND TECHNOLOGY
TRIBHUVAN UNIVERSITY
NEPAL

FOR THE AWARD OF
DOCTOR OF PHILOSOPHY
IN MATHEMATICS

BY
KHAGENDRA ADHIKARI

December 2023

TRIBHUVAN UNIVERSITY

Institute of Science and Technology

DEAN'S OFFICE

Kirtipur, Kathmandu, Nepal

Reference No.:

Institute of Science & Technology
Dean's Office
Kirtipur, 2025

EXTERNAL EXAMINERS

The Title of Ph.D. Thesis: " Transmission Dynamics of COVID-19: Mathematical Models for Effective Controls "

Name of Candidate: Khagendra Adhikari

External Examiners:

(1) Prof. Dr. Dil Bahadur Gurung
Kathmandu University
Dhulikhel, NEPAL

(2) Prof. Dr. Kapil Kumar Sharma
South Asian University
Delhi, INDIA

(3) Prof. Dr. Libin Rong
University of Florida
Gainesville, USA

April 04, 2024

(Dr. Surendra Kumar Gautam)
Asst. Dean

DECLARATION

Thesis entitled **"Transmission Dynamics of COVID-19: Mathematical Models for Effective Controls "** which is being submitted to the Central Department of Mathematics, Institute of Science and Technology(IOST), Tribhuvan University, Nepal for the award of the degree of Doctor of Philosophy (Ph.D.), is a research work carried out by me under the supervision of Prof. Dr. Kedar Nath Uprety of Central Department of Mathematics, Tribhuvan University, Nepal and co-supervised by Prof. Dr. Naveen K. Vaidya, Department of Mathematics, San-Diego State University, San Diego, CA USA.

This research is original and has not been submitted earlier in part or full in this or any other form to any university or institute, here or elsewhere, for the award of any degree.

.....

Khagendra Adhikari

RECOMMENDATION

This is to recommend that **Khagendra Adhikari** has carried out research entitled **"Transmission Dynamics of COVID-19: Mathematical Models for Effective Controls"** for the award of Doctor of Philosophy (Ph.D.) in **Mathematics** under our supervision. To our knowledge, this work has not been submitted for any other degree.

He has fulfilled all the requirements laid down by the Institute of Science and Technology (IOST), Tribhuvan University, Kirtipur for the submission of the thesis for the award of Ph.D. degree.

.....
Kedar Nath Uprety, Ph.D.
Supervisor
(Professor)
Central Department of Mathematics
Tribhuvan University
Kirtipur, Kathmandu, Nepal

.....
Naveen K Vaidya, Ph.D.
Co-Supervisor
(Professor)
Department of Mathematics
San Diego State University
CA, USA

December 2023

Phone No. :00977- 14331977

TRIBHUVAN UNIVERSITY

CENTRAL DEPARTMENT OF MATHEMATICS

Institute of Science and Technology

KIRTIPUR, KATHMANDU
NEPAL

Ref No.

CENTRAL DEPARTMENT OF MATHEMATICS
TRIBHUVAN UNIVERSITY
KIRTIPUR

Date: April 09, 2024

Letter of Approval

On the recommendation of Prof. **Dr. Kedar Nath Uprety** and **Prof. Dr. Naveen Vaidya**, this Ph.D. thesis submitted by **Mr. Khagendra Adhikari**, entitled **"Transmission Dynamics of COVID-19: Mathematical Models for Effective Controls"** is forwarded by Central Department Research Committee (CDRC) to the Dean, IOST, T.U..

Chet Raj Bhatta, PhD
Professor and Head

ACKNOWLEDGEMENTS

Foremost, I would like to express my deep and sincere gratitude to my supervisor Prof. Dr. Kedar Nath Uprety and co-supervisor Prof. Dr. Naveen K. Vaidya. Their continuous guidance, encouragement with insightful comments and immense knowledge were instrumental in shaping the direction of my research and refining my analytical skills. Their unwavering belief in my abilities motivated me to push the boundaries of knowledge and strive for excellence. This dissertation would hardly exist without their contribution.

I extend my heartfelt thanks to Prof. Dr. Tanka Nath Dhamala, head of the Central Department of Mathematics, for his invaluable scientific support during my research period. My gratitude also goes to my colleagues, Mr. Ramesh Gautam and Anjana Pokharel, whose collaborative spirit and idea-sharing created a supportive community throughout this journey. I am greatly appreciative of the professors, faculties, and colleagues within the department for their constructive input, and the efficient administrative services provided by the department's staff and the Dean's office were instrumental in ensuring a smooth and productive research experience.

I express my sincere gratitude to the Nepal Academy of Science and Technology (NAST) for the PhD fellowship, the International Mathematical Union (IMU) for the Graduate Research Assistantships in Developing Countries (GRAID) Program, and the Nepal Mathematical Society for providing the NMS-Fellowship award. I would also like to express my sincere thanks to CIMPA and IIT Indore for the opportunity of my research visit during this journey. I owe my warm gratitude to Amrit Campus, Kathmandu, Nepal, for the support in various forms.

Finally, I want to express my deep gratitude and love to my wife, Shobha Khatiwada, my mother, Januka Devi Adhikari, my father, Raghu Nath Adhikari, my brother, Umanath Adhikari, my sister-in-law, Sunita Pokharel, my sisters, Bhagawati and Sita, and my brothers-in-law, Lambodher Poudel and Ramesh Timsina, who encouraged me to take this step and took all hardships of our family life. I extend my endless love to my son, Sukhad Adhikari, as well as our cousins, Unnati, Pragati, Eliza, Alina, Anup, and Asmita, who have been a constant source of strength and fulfillment beyond my wildest dreams.

Khagendra Adhikari

शोध सार

महामारी रोगको प्रार्दुभावले प्रायः विश्वव्यापी स्वास्थ्य सेवा प्रणालीमा अनपेक्षित चुनौतीहरू प्रस्तुत गरेको छ । विशेष गरी नेपाल जस्ता निम्न र मध्यम आय भएका राष्ट्रहरूलाई यसले असर गरेको छ । संक्रामक रोगहरूको गणितीय मोडेलिङले प्रभावकारी जनस्वास्थ्य हस्तक्षेप र स्रोत विनियोजनको कार्यान्वयनलाई सक्षम पार्दै रोगहरूको गतिशीलता भविष्यवाणी गर्न र बुझ्न मद्दत गर्दछ । यसले महामारीलाई कम गर्न प्रमाणमा आधारित नीतिगत निर्णयहरूमा योगदान पुऱ्याउदछ । विश्वव्यापी प्रयास र खोप विकासको बावजुद, कोभिड-१९ महामारीले एक देशबाट अर्को देशमा उल्लेखनीय रूपमा भिन्न हुने विनाशकारी विश्वव्यापी प्रभावहरू पारेको छ जसले रोग र यसको नियन्त्रण रणनीतिहरूको गहिरो बुझाइको लागि देश-विशिष्ट अध्ययनहरू आवश्यक बनाएको छ । यस शोध प्रबंधले कोभिड-१९ प्रसारण गतिशीलताको व्यापक विश्लेषण गर्न निर्माण गरिएका नवीनतम गणितीय मोडेलहरू प्रस्तुत गर्दछ । हाम्रा मोडेलहरूको विश्वसनीयता र वैधता बढाउन बहुआयामिक तथ्याङ्कहरु संग कडाइका साथ प्रमाणीकरण गरिएको छ ।

कोभिड-१९ को पहिलो लहरको अध्ययनका लागि हाम्रो गणितीय मोडेलले जसमा उच्च आयामी प्रणालीमा गैर-रैखिक साधारण अवकल समीकरणहरू छन्; विशेष गरी नेपाल र भारत बीचको खुला सीमाना पार गर्नेहरूको संख्याको आकलन गर्ने महत्वपूर्ण क्षमता राख्दछ । विदेशबाट फर्किनेहरूको अस्थायी ढाँचा अनुमान गर्न हामीले गैर-स्वायत्त सुविधाहरू प्रस्तुत गरेर गणितीय मोडेललाई थप परिष्कृत गरेका छौं । Next Generation Matrix विधि प्रयोग गरेर हामी आधारभूत प्रजनन संख्या (R_0) र प्रभावकारी प्रजनन संख्या (R_t) गणना गर्छौं जसले सफलतापूर्वक रोगहरूको प्रक्षेपणको र Bifurcating प्रकृतिको भविष्यवाणी गर्छ । यस मोडेलद्वारा हामीले नेपालमा महामारीको पहिलो लहरमा लागू गरिएका विभिन्न नियन्त्रण उपायहरूको प्रभावकारिता मूल्याङ्कन गरेका छौं । हामीले नेपालमा कोभिड-१९ को पहिलो लहरको समयमा लागू गरिएका तीनवटा प्रमुख हस्तक्षेप नीतिहरूको प्रभावबारे विशेष रूपमा अनुसन्धान गरेका छौ,: पहिलो लकडाउन, दोस्रो सीमा जाँच एवम् क्वारेन्टाइन र तेस्रो रोगीहरुको पहिचान एवम् अलग । हाम्रा खोजहरूले कोभिड-१९ प्रसारणको न्यूनीकरणमा तिनीहरूको प्रभावकारिता उजागर गर्दछन् ।

यसका साथै हामी नेपालमा कोभिड-१९ को दोस्रो लहरको डेल्टा भेरियन्टमा केन्द्रित छौं । हामीले यो अत्यधिक सर्न सक्ने भेरिएन्टसँग सम्बन्धित प्रसारण गतिशीलता र सेरोप्रिभलेन्समा प्रकाश पार्छौं । यसबाहेक, हामी नेपालमा आइसियू शैया र भेन्टिलेटरहरू सहित चिकित्सा स्रोतहरूमा अपेक्षित बोझको अनुमान गर्छौं जसले स्वास्थ्य सेवा तयारीको लागि महत्वपूर्ण अन्तरदृष्टि प्रदान गर्दछ । हामी सम्भावित महामारी नियन्त्रण विधिहरूका रूपमा खोप कार्यक्रमहरू र लकडाउन उपायहरूलाई क्रमशः खुकुलो बनाउने बारे अनुसन्धान गर्छौं जुन नेपाल जस्तो स्रोत-सीमित देशमा महत्वपूर्ण छ जहाँ राम्रो स्वास्थ्य सेवा व्यवस्थापन महत्त्वपूर्ण छ । हाम्रो कामले देखाउछ कि हाम्रो गणितीय मोडेलले डेल्टा भेरिएन्टको वृद्धिको समयमा सेरोप्रिभलेन्सको सफलतापूर्वक भविष्यवाणी गरेको थियो जुन अनुमानहरू राष्ट्रव्यापी सेरोप्रिभलेन्स सर्वेक्षण मार्फत सरकारद्वारा प्राप्त परिणामहरूसाग मिल्दोजुल्दो छ । यस खोजले रोग गतिशीलता पहिल्याउन र बुझ्नमा मोडेलको क्षमता, विश्वसनीयता र प्रभावकारिता देखाउदछ जुन संक्रामक रोग प्रकोपको समयमा सार्वजनिक स्वास्थ्य योजना र कार्यान्वयनको लागि महत्वपूर्ण छ । यसले जनस्वास्थ्य संकटहरूको मूल्याङ्कन र व्यवस्थापन गर्ने हाम्रो क्षमतामा सुधार गर्दै वास्तविक तथ्याङ्कहरु सङ्कलन प्रयासहरूलाई पूरक र प्रमाणीकरण गर्न गणितीय मोडलिङको सम्भावनालाई पनि उजागर गर्दछ ।

हामी महामारीको समयमा संक्रमण र अस्पताल भर्नाको वास्तविक-समय जोखिमको अनुमानको लागि तथ्याङ्क-संचालित मोडेलहरू पनि विकास गर्छौं । संक्रमणको जोखिमको अनुमानको लागि हाम्रो सम्भावित मोडेलले संवेदनशील जनसंख्या, सक्रिय संक्रमित, व्यक्तिहरूको सम्पर्क ढाँचा, र प्रभावकारी प्रजनन संख्या समावेश गर्दछ । यसले प्रजनन संख्या मार्फत मात्र प्राप्त गर्न सकिने भन्दा महामारीको प्रसारण ढाँचाको थप सटीक विवरण प्रदान गर्दछ । हामी महामारीको समयमा अस्पताल भर्नाको अस्थायी ढाँचाको दर अनुमान गर्नको लागि गणितीय मोडेल निर्माण गर्न अधिकतम सम्भावना प्रकार्य पनि प्रयोग गर्छौं । यी मोडेलहरू नेपाल र यसका सात प्रान्तका नयाँ कोभिड-१९ केसहरू

र अस्पतालमा भर्ना भएकाहरूको अद्वितीय तथ्याङ्कहरुमा लागू गरिएको छ, जसले हामीलाई रोगको सर्ने मूल्याङ्कन गर्न र महामारीको बोझ कम गर्न स्वास्थ्य सेवा स्रोतहरूलाई प्रभावकारी रूपमा व्यवस्थापन गर्न सक्षम बनाउँछ । यी तथ्याङ्कहरु -संचालित मोडेलहरूले नवीन प्रविधिहरू प्रस्तुत गर्छन् र रोमाञ्चक परिणामहरू प्राप्त गरेका छन् जसले महामारीको समयमा संक्रमण र अस्पतालमा भर्ना हुने जोखिमबारे हाम्रो बुझाइलाई अगाडि बढाउँछ । यी खोजहरूले महामारी नियन्त्रणका लागि दिशानिर्देशहरू र रणनीतिहरू सूचित गर्ने सम्भाव्यता राख्छन्, विशेष गरी विनाशकारी प्रकोपहरूको सामनामा । हाम्रा जैविक रूपमा यथार्थपरक मोडेलहरू, तथ्याङ्कहरु एकीकरण विधिहरू, र सम्भाव्य दृष्टिकोणहरूले जीवन विज्ञान, गणित, र कम्प्युटेसनल विज्ञानलाई समेट्ने फराकिलो वैज्ञानिक क्षेत्रहरूमा योगदान पुऱ्याउँछन् ।

ABSTRACT

The emergence of a pandemic disease often presents unforeseen challenges to the global healthcare system, particularly affecting low and middle-income nations like Nepal. Mathematical modeling of infectious diseases helps to predict and understand the dynamics of the diseases enabling the implementation of efficient public health interventions and resources allocation. This contributes to evidence-based policy decisions to mitigate a pandemic. Despite worldwide efforts and vaccine development, the COVID-19 pandemic has had devastating global impacts varying significantly from one country to another, making country-specific studies essential for a deeper understanding of the disease and its control strategies. This dissertation presents novel mathematical models designed to comprehensively analyze COVID-19 transmission dynamics. Our models have been rigorously validated with multiple datasets, enhancing their reliability and validity.

Our mathematical model for the first wave of COVID-19 in higher dimensional systems, characterized by non-linear ordinary differential equations, possesses a significant capability to assess the count of returnees, particularly those crossing the open border between Nepal and India. To estimate the temporal pattern of the returnees, we enhance the system by introducing non-autonomous features. By using the Next Generation Matrix Method, we calculate the Basic Reproduction Number (R_0) and Effective Reproduction number which successfully predict the bifurcating nature of diseases trajectories. By taking advantage of this model, we evaluate the effectiveness of various control measures implemented during the first wave of the pandemic in Nepal. We specifically investigate the impact of three key intervention policies enacted during the first wave of COVID-19 in Nepal: the 1st Lockdown, the 2nd Border Screening and Quarantine, and the 3rd Detection and Isolation. Our findings uncover their effectiveness in the mitigation of COVID-19 transmission in Nepal.

In addition, we focus on the Delta variant dominated second wave of COVID-19 in Nepal. We shed light on the transmission dynamics and seroprevalence associated with this highly transmissible variant. Furthermore, we estimate the expected burden on medical resources, including ICU beds and ventilators, in Nepal, providing crucial insights for healthcare preparedness. Additionally, we investigate vaccination programs and the gradual relaxation of lockdown measures as prospective pandemic control methods, which are especially important in resource-limited country like Nepal, where good healthcare management is critical. Our work demonstrates that our mathematical model successfully predicted the seroprevalence during the Delta surge with

estimates closely matching the results obtained by the government through a nationwide seroprevalence survey. This finding demonstrates the model's ability, reliability and effectiveness in tracking and understanding disease dynamics, which is crucial for public health planning and response during infectious disease outbreaks. It also highlights the potential for mathematical modeling to complement and authenticate real-world data collection efforts, improving our ability to assess and manage public health crises.

We also develop the data-driven models for the estimation of real-time risk of infection and hospitalization during a pandemic. Our probabilistic model for estimation of the risk of infection incorporates susceptible populations, active infectious cases, contact patterns of people, and the effective reproduction number. It offers a more precise description of pandemic's transmission patterns that can be achieved solely through the reproduction number. We also use Maximum Likelihood Function to construct the mathematical model for estimating the rate of the temporal pattern of hospitalization during a pandemic. These models are applied to unique datasets of new COVID-19 cases and hospitalization cases in Nepal including its seven provinces, enabling us to assess disease transmission and efficiently manage healthcare resources to minimize the pandemic's burden. These data-driven models introduce innovative techniques and yield exciting results that advance our understanding of the risk of infection and hospitalization during a pandemic. These findings hold the potential to inform guidelines and strategies for pandemic control, particularly in the face of catastrophic outbreaks. Our biologically realistic models, data integration methods, and probabilistic approaches contribute to the broader scientific fields encompassing life sciences, mathematics, and computational science.

Keywords: COVID-19, Nepal, Risk of Infection, Hospitalization, Vaccination, Data Driven Mathematical Models.

LIST OF ABBREVIATIONS

COVID-19	:Coronavirus Disease of 2019
SARS-CoV-2	:Severe Acute Respiratory Syndrome Coronavirus-2
DFE	:Disease Free Equilibrium
EE	:Endemic Equilibrium
RNA	:Ribonucleic Acid
DNA	:Deoxyribonucleic Acid
ODE	:Ordinary Differential Equation
WHO	:World Health Organization
CDC	:Centers of Disease Control and Prevention
ICU	:Intensive Cure Unit
MoHP	:Ministry of Health and Population
GoN	:Government of Nepal
MERS	:Middle East Respiratory Syndrome
HEOC	:Health Emergency Operation Center
GISAID	:Global Initiative on Sharing All Influenza Data
CBS	:Central Bureau of Statistics
CrI	:Credible Interval
IHME	:Institute for Health Metrics and Evaluation
MLM	:Maximum Likelihood Method
SPI-M	:Scientific Pandemic Influenza group on Modeling
NPIs	:Non-Pharmaceutical Interventions (NPIs)

LIST OF SYMBOLS

S	:Susceptible Population
E	:Exposed Population
I	:Infected Population
I_R	:Recorded Infected Population
I_N	:Non Recorded Infected Population
R	:Recovered Population
Q	:Quarantined Population
R_0	:Basic Reproduction Number
R_t	:Effective Reproduction Number

LIST OF FIGURES

LIST OF TABLES

TABLE OF CONTENTS

CHAPTER 1

INTRODUCTION

1.1 Context and Motivation

Since the first reported case in China in December 2019 as a case of pneumonia of unknown cause, the novel coronavirus disease (COVID-19) has spread rapidly all over the world, and on March 11, 2020, the World Health Organization (WHO) declared COVID-19 a pandemic [175]. As of September 15, 2023, more than 695 million cases of COVID-19 and more than 6 million deaths due to the disease have been reported worldwide [202]. Despite its global devastating effects on all aspects of human lives, the impact of the epidemic varies from country to country [96].

In Nepal, the first case of COVID-19 was confirmed on January 23, 2020, which was also the first COVID-19 case in South Asia [120]. Specifically, the second and third waves with the circulating Delta and Omicron variants, respectively, swept across the country from the beginning of April 2021, resulting in one million cases and 12,019 deaths [122] until December 1, 2022. During the peak of the second wave of COVID-19 (end of May, 2021), Nepal experienced a terrifying shortage of hospital beds, ICU beds, ventilators, and oxygen cylinders, which resulted in a loss of potentially preventable lives [23, 28].

Mathematical modeling of infectious diseases plays a pivotal role in public health and epidemiology [4, 44, 133, 136]. It provides invaluable insights into the dynamics of disease transmission, aiding in prediction, resource allocation, and decision-making [158, 159]. By utilizing data, mathematical models enable policymakers to anticipate the course of an outbreak, allocate healthcare resources efficiently, and assess the effectiveness of various interventions such as social distancing and vaccination campaigns [144, 164, 177]. Models also enhance our understanding of how diseases spread

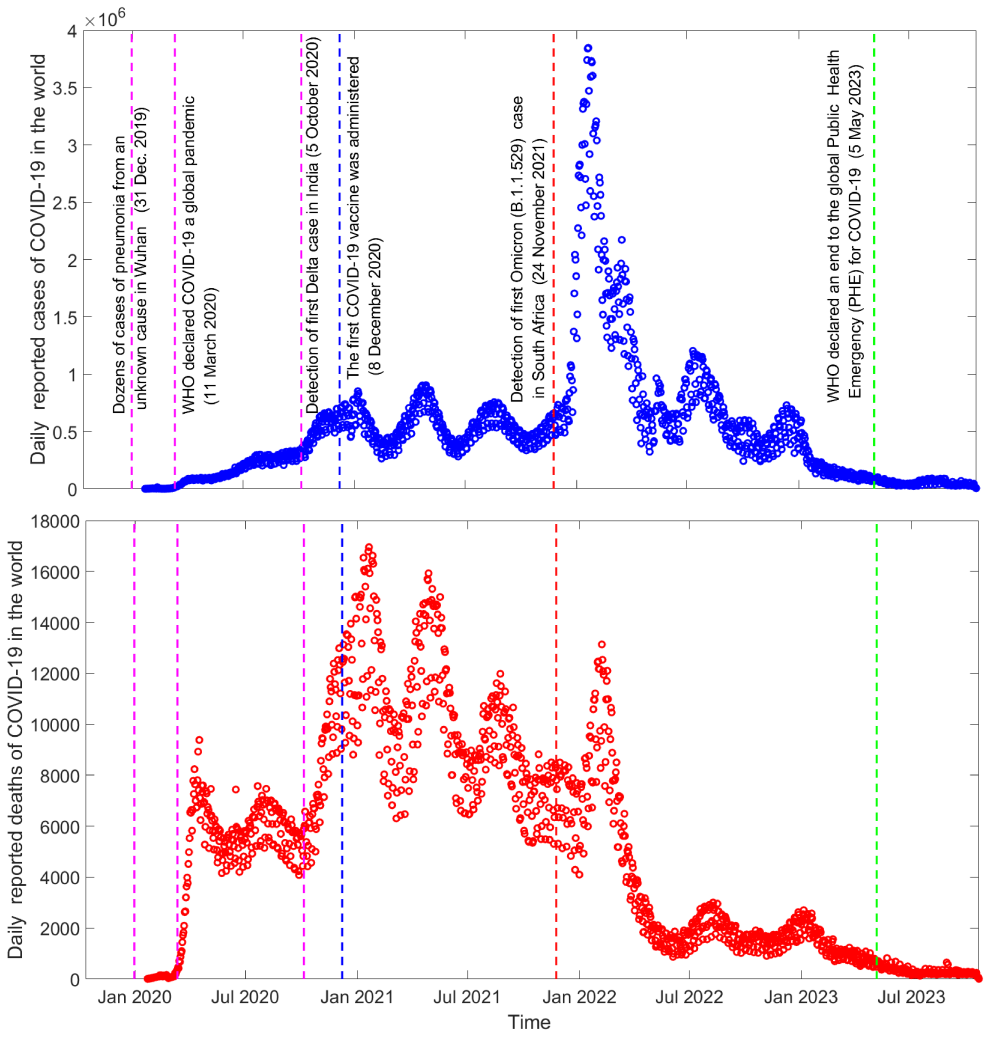

Figure 1: Daily reported COVID-19 new cases & deaths in the world from 22 January, 2020 to 21 October, 2023.
Data source `https://www.worldometers.info/coronavirus/`

within populations, helping us identify critical factors like reproduction number, the role of asymptomatic carriers and effectiveness of control measures [3, 173]. Moreover, mathematical modeling guides the vaccine development and distribution strategies, facilitates data interpretation, and supports scenario planning [35]. Through continuous refinement and adaptation, these models contribute significantly to our ability to manage and mitigate the impact of infectious diseases, ultimately saving lives and reducing the societal and economic burden of outbreaks.

Mathematical modeling has become an integral component of the strategic planning process employed by governments worldwide in response to recent outbreaks. A notable example is the UK Department of Health's well-established committee, the

Scientific Pandemic Influenza Group on Modeling (SPI-M), which offers guidance on novel respiratory infections [36, 52, 53]. A significant historical instance of such application occurred during the 2009 H1N1 pandemic, where the World Health Organization established a network comprising modeling groups and public health experts to delve into various facets of the outbreak [33, 129, 182]. These endeavors encompassed activities ranging from characterizing outbreak dynamics to assessing the efficacy of diverse intervention strategies. The incorporation of mathematical approaches into policy formulation underscores the invaluable insights that modeling and statistical analyses can contribute to understanding and effectively addressing public health crises.

Mathematical modeling of COVID-19 serves as a powerful tool to understand and combat the virus's impact on developing countries like Nepal. Nepal's unique challenges require tailored strategies, and mathematical models provide a scientific foundation for decision-making. These models can provide insight to researchers and policymakers to explore various scenarios, helping to optimize the distribution of healthcare resources and vaccines. Modeling can help optimize resource allocation, identify vulnerable populations, and inform evidence-based policy decisions. Moreover, in situations where data collection and reporting may be challenging, mathematical models can fill data gaps and provide valuable estimates of disease transmission. By contributing to a more nuanced understanding of COVID-19's dynamics in Nepal, mathematical modeling empowers the country to devise targeted interventions and policies that address its specific needs, ultimately aiding in the control and management of the pandemic.

1.2 Mathematical Modeling of the Biological System

It is important to understand that mathematical representations of systems are similar to snapshots. No single image can capture the entire scenario [75, 162]. Mathematical models serve as simplified, idealized, and approximate representations of the structure, mechanisms, and behavior of real-world systems [82, 112]. Scientific representations involve abstractions or idealizations, expressing only partial elements of humans or systems [115]. We should be aware that when we model something mathematically, we are simplifying a complicated biological reality. This acknowledgment emphasizes that there is no single mathematical model to accurately represent the variety of a

biological system [56, 82].

1.2.1 Philosophy of Mathematical Modeling

Universalism and pluralism are two contrasting philosophies of mathematical modeling that shape how mathematicians and scientists approach the development and use of mathematical models in various fields [198, 199].

1.2.1.1 Universalism

Universalism is a philosophy of mathematical modeling that emphasizes the idea that there exists a single, universal mathematical framework or language that can describe and explain all natural phenomena [165]. Proponents of universalism argue that mathematics is a unified and coherent system that provides a consistent and objective representation of reality [75]. They believe that there is a "best" or "optimal" mathematical model for any given problem or phenomenon, and the goal is to discover and use this model.

Key Features of Universalism
Unity of Mathematics: Universalists believe in the unity of mathematics, suggesting that the same mathematical principles and structures apply across different domains of science and engineering [75].

Search for Fundamental Laws: They seek fundamental mathematical laws and equations that govern the behavior of complex systems and phenomena [148].

Reductionism: Universalists often adopt a reductionist approach, breaking down complex problems into simpler mathematical components to understand them comprehensively [181].

1.2.1.2 Pluralism

Pluralism, on the other hand, is a philosophy of mathematical modeling that accepts and even embraces the existence of multiple mathematical frameworks, languages, or models to describe and explain different aspects of reality [8, 75, 115]. Proponents of pluralism argue that no single mathematical model can capture the full complexity of the natural world, and different models may be suitable for different purposes and contexts. They emphasize the importance of diversity in mathematical approaches

and tools [50].

Key Features of Pluralism

Diversity of Models: Pluralists advocate for the development and use of diverse mathematical models that may vary in their assumptions, simplifications, and methodologies [115].

Context-Dependent: They believe that the choice of mathematical model should be context-dependent, based on the specific goals, data availability, and practical constraints of a problem.

Interdisciplinary Approach: Pluralism often encourages collaboration between experts from various disciplines who bring different mathematical perspectives to solve complex problems.

1.2.2 Key Features of Mathematical Modeling

There are three fundamental aspects of mathematical modeling: **(i) the formulation of models, (ii) the analysis of models, and (iii) the fitting or comparison of models to data** [75].

The first aspect of mathematical modeling, formulation, involves constructing equations or algorithms that represent the behavior of biological systems. Secondly, the analysis of models involves examining their mathematical properties and behaviors using techniques from various mathematical fields. However, recent research has disproportionately focused on model analysis at the expense of creating new models, potentially limiting our ability to fully understand the complexities of biological systems. A balanced approach is crucial for the advancement of mathematical biology [35].

The third crucial aspect of mathematical modeling in biological systems is fitting or comparing mathematical models to data. This process involves several phases [12, 47, 70, 112].

Data Collection: Relevant data representing the biological system's behavior is collected through experiments or observations.

Estimation of Parameters: Parameters within mathematical models, which govern the system's behavior, are determined to best match observed data.

Model Validation: After achieving a satisfactory fit, the model's predictive ability is validated on new data to build confidence in its validity.

Model Selection: In cases with multiple competing models, researchers compare them using criteria like AIC or Bayesian model comparison to determine the best fit and complexity.

Uncertainty and Sensitivity Analysis: The uncertainties in both data and model parameters are considered, and sensitivity analysis helps identify which parameters have the most significant impact on model behavior and predictions.

1.3 Coronavirus

Coronaviruses, distinguished by their distinctive crown-like spikes visible under an electron microscope, belong to a family of large, enveloped, single-stranded RNA viruses. They are found in various mammalian species, including humans, dogs, cats, chickens, cattle, pigs, and birds. Coronaviruses are responsible for a range of diseases affecting the respiratory, gastrointestinal, and neurological systems. In clinical practice, the most frequently encountered Coronaviruses are 229E, OC43, NL63, and HKU1, typically cause mild cold symptoms in individuals with a competent immune system [208].

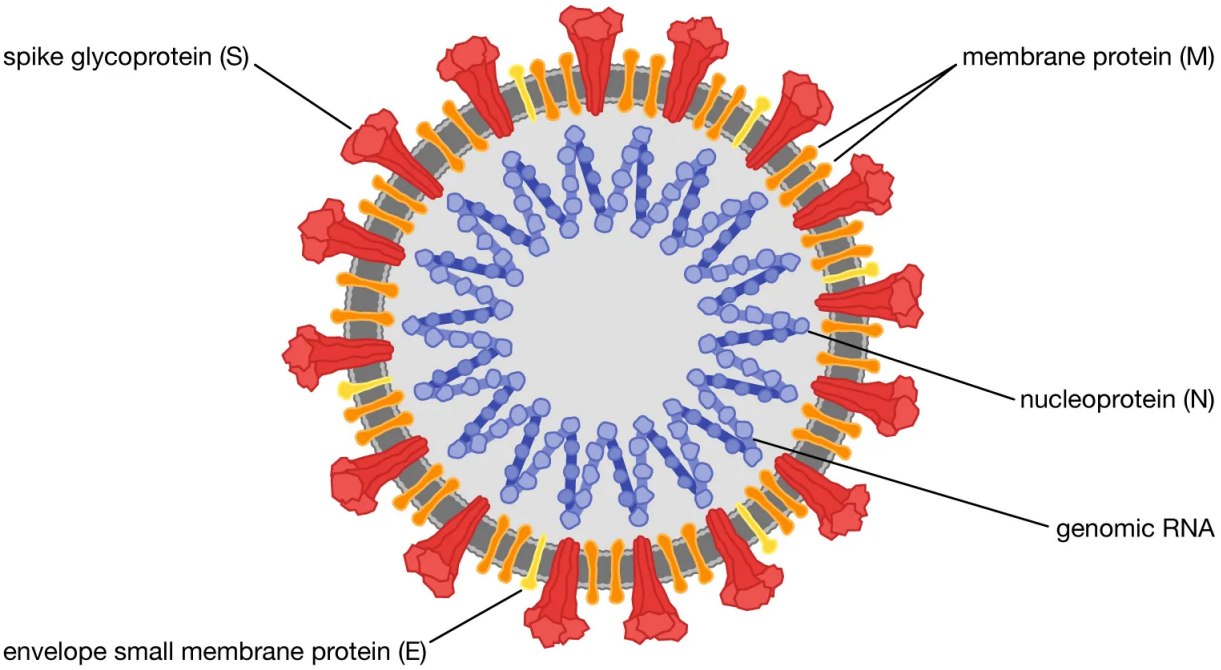

Figure 2: Schematic diagram of Coronavirus. Source: `https://www.britannica.com/science/coronavirus-virus-group`

Notably, SARS-CoV-2 marks the third instance in the past two decades where a coronavirus has caused severe disease on a global scale. The first such occurrence was the emergence of Severe Acute Respiratory Syndrome (SARS) in 2002-2003, believed to have originated in Foshan, China, and resulted in the SARS-CoV pandemic of that period [207]. Subsequently, the second severe coronavirus-induced disease emerged as the Middle East Respiratory Syndrome (MERS) in 2012, originating in the Arabian Peninsula [208].

1.4 COVID-19 in Nepal

1.4.1 Early Detection of COVID-19 Cases in Nepal

The first case of SARS-CoV-2 infection in Nepal was documented on January 23, 2020, involving a Nepalese individual who had recently arrived in Kathmandu from Wuhan, China [96].

1.4.2 The Initial Response of the Government of Nepal to COVID-19

The Ministry of Health and Population (MoHP) promptly initiated decisive actions to enhance the country's response in preventing the transmission of the virus [96]. These actions primarily involved strengthening health desks at Tribhuvan International Airport and subsequently at other domestic airports. Furthermore, additional health desks were established at the key entry points along the Nepal-China and Nepal-India borders. Travel restrictions were implemented on both sides of these border areas [118].

In addition to these initial measures, the Government of Nepal (GoN) undertook efforts to repatriate Nepalese nationals from Wuhan, China, resulting in the safe return of 175 Nepalese citizens. These individuals were subjected to a 14-day quarantine period and were allowed to return to their homes only after testing negative for the virus. To enhance the response, the MoHP activated the Incident Command System (ICS) and established the Health Emergency Operation Center (HEOC), coordinating comprehensive efforts to combat the virus [21].

On 2nd March 2020, the High-Level Coordination Committee (HLCC), under the leadership of the Deputy Prime Minister, was established. The HLCC subsequently made a series of pivotal decisions aimed at curtailing the spread of COVID-19 [118].

1.4.3 Detection of a Second Case and Announcement of Lockdown

Until March 17, 2020, there were no reported cases. However, on that date, a Nepalese individual returning from France was identified as carrying the virus [118]. The absence of detected cases between January 23, 2020, and March 17, 2020, raised concerns about the country's diagnostic capabilities. In response, on March 18, 2020, schools were shut down, and gatherings exceeding 25 people were discouraged [118].

Further measures were implemented by the Government of Nepal in subsequent days. On March 22, 2020, all international flights were prohibited, and the operations of nonessential businesses and domestic long-distance transportation were suspended. By March 23, 2020, international borders were completely closed. A nationwide lockdown was declared from March 24, 2020, to July 21, 2020. This lockdown included a ban on both domestic and international travel, closure of borders, and the shutdown

of nonessential services. During the initial phase of the nationwide lockdown, which began on March 24, 2020, there were only two recorded COVID-19 cases with no reported fatalities [118].

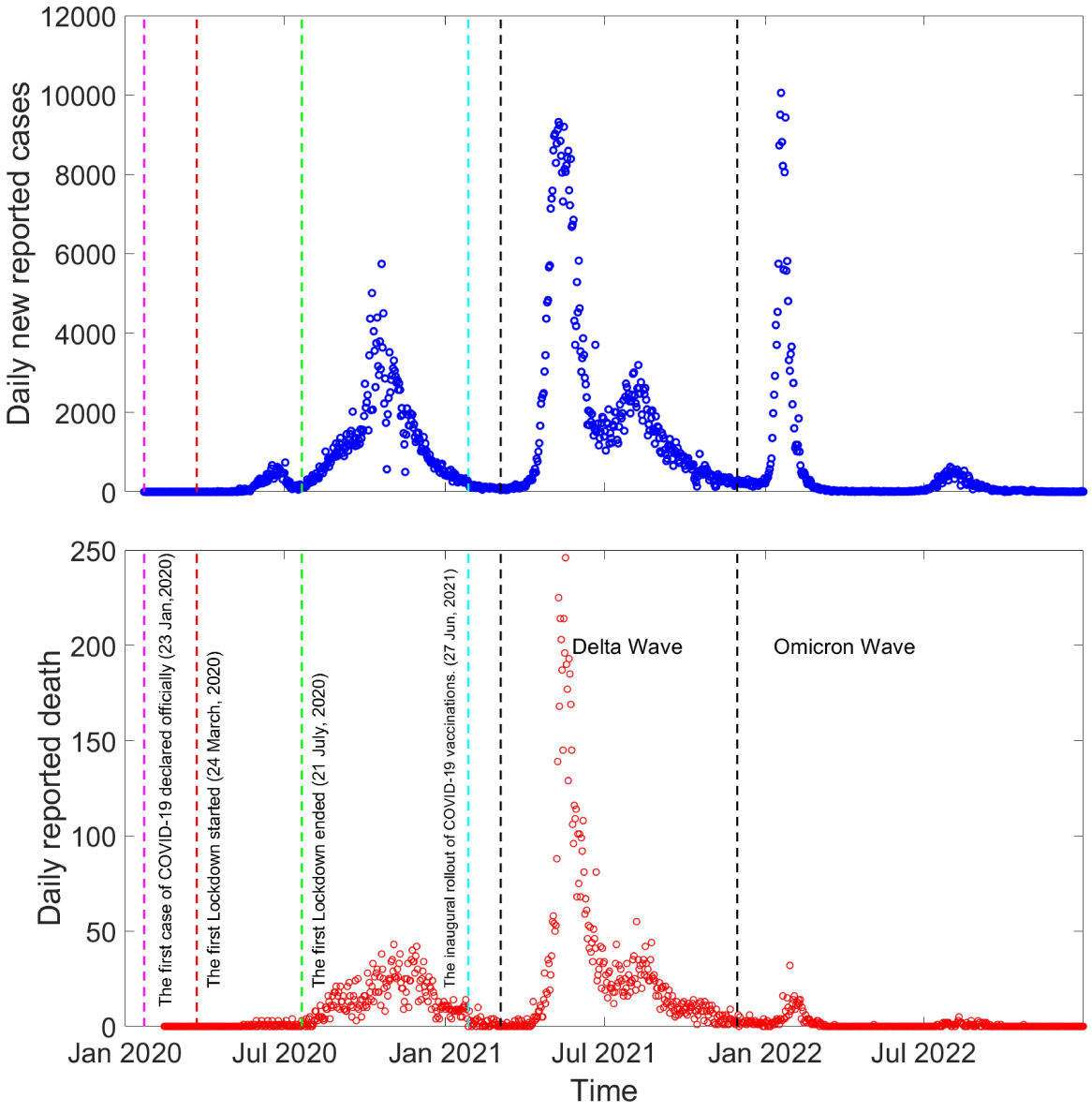

Figure 3: Daily reported COVID-19 new cases & deaths in Nepal from 23 January, 2020 to 30 December, 2022.
Data source `https://www.worldometers.info/coronavirus/`

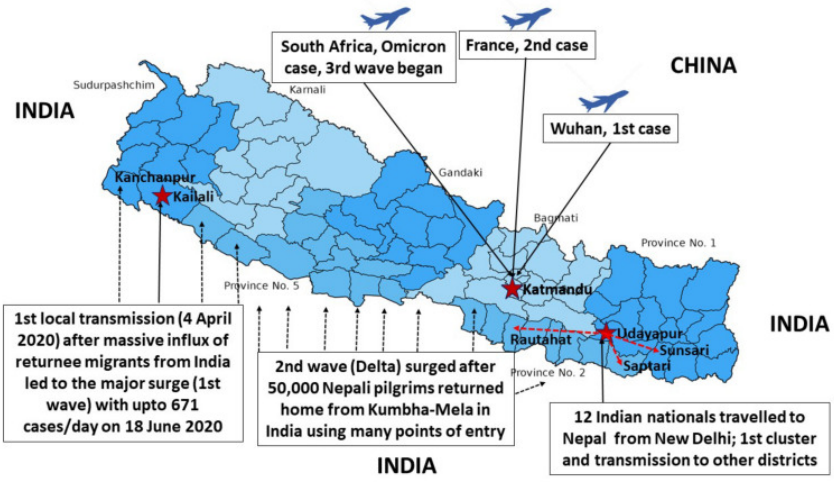

Figure 4: Map illustrating different surges of the Coronavirus entering Nepal [131].

1.4.4 The Second Wave (Delta) of COVID-19 in Nepal

In March 2021, the World Health Organization identified the new Delta variant, characterized as more virulent and infectious, first emerging in India [91]. During the spring, a substantial number of people gathered in the streets for political campaigns leading up to the May 2021 election. Additionally, the congregation for seasonal weddings and festivals added to the already large gatherings. In mid-April, amid a rising number of COVID-19 cases in India, an estimated 50,000 Nepali pilgrims traveled to northern India for Kumbha Mela, a Hindu festive gathering that typically attracts millions [44, 91]. Unfortunately, many of the pilgrims contracted COVID-19, potentially sparking the onset of the second wave in Nepal.

The second wave commenced in April 2021, with cases peaking in May. On May 11, 2021, the average daily case count reached 9,317, and daily deaths peaked at approximately 246. These figures closely aligned with the situation in India, where the Delta variant contributed to a surge, setting a global record with 414,188 cases recorded on May 6, 2021.

1.4.5 The Third Wave (Omicron) of COVID-19 in Nepal

From the peak of the second wave on May 11, 2021, the daily number of new cases began to decrease, marking a decline that extended into December 2021. On December 6, 2021, Nepal reported the presence of the Omicron (B.1.1.529) variant, just

two weeks after its initial identification in South Africa on November 24, 2021. The emergence of the Omicron variant triggered a notable increase in daily new cases, reaching a peak on January 20, 2022, with a record of over 10,000 cases MOHP2021.

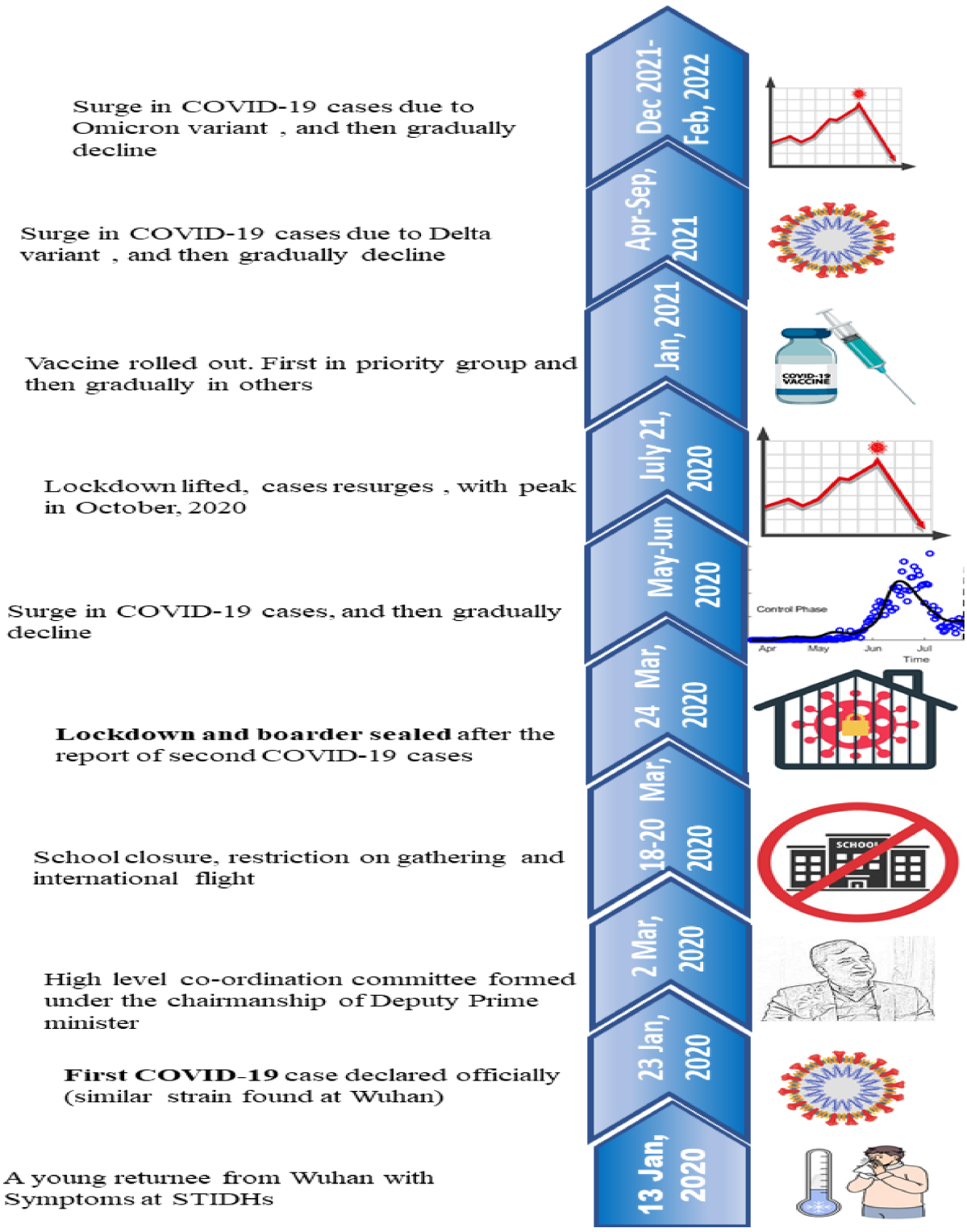

Figure 5: Chronology of key events of COVID-19 in Nepal.

1.5 Objectives of the Study

Mathematical modeling using epidemiological data can help policymakers to understand the impact of the various control strategies on transmission of the diseases and determine the effective control strategies. Despite the global devastating effects of COVID-19 on all aspects of human lives, the impact of the epidemic varies in different countries. Also, the study focused on a specific country can provide a better understanding of the disease and its control strategies. In this context, the main objectives of this study are:

- To develop a mathematical model and analyze transmission dynamics of COVID-19.
- To study the spatial heterogeneity of the transmission dynamics of COVID-19.
- To study the transmission dynamics of COVID-19 in Nepal and assess the possible control measures of COVID-19.
- To fit the mathematical model of COVID-19 with available data for the estimation of key parameters including basic reproduction number R_0 and the effective reproduction number R_t.

1.6 Literature Review

The use of mathematical modeling in the transmission dynamics of complex diseases has a rich and evolving history. Complex diseases are those that involve intricate interactions among various factors, including pathogens, hosts, and environmental conditions. Modeling these dynamics is crucial for understanding disease spread, designing effective control strategies, and predicting future outbreaks. The historical development of mathematical modeling in this field can be outlined as follows:

1.6.1 Early Epidemic Modeling (18th and 19th centuries)

The earliest attempts at modeling disease transmission can be traced back to the 18th century. Daniel Bernoulli's work on smallpox vaccination in the 1760s [25, 35, 67] followed in 1766 by a more complete exposition [24, 35] and Benjamin Gompertz's logistic growth model in the early 19th century were among the pioneering efforts. These early

models laid the groundwork for understanding the basic principles of epidemic spread [**?**]. En'ko creates a transmission model essentially from "first principles," i.e., based on some presumptions but without using previously published theory. He described the epidemics of measles and scarlet fever outbreaks occurred in two St. Petersburg boarding schools in 1875 and 1888 [63, 67]. In the 19th century, John Snow's investigation of the 1855 cholera epidemic in London pinpointed the Broad Street water pump as the infection source. Similarly, William Budd's work in 1873 revealed insights into typhoid transmission. Meanwhile, William Farr's 1840 study aimed to uncover the underlying laws governing epidemic rise and fall through statistical analysis [35].

W.H. Hamer offered a crucial hypothesis in 1906, asserting that the number of susceptible and infectious individuals influences how quickly an illness spreads [77]. In order to represent the frequency of new infections, he developed the idea of a mass action law, which has since grown to be an essential component of compartmental models. It is interesting that, between 1900 and 1935, prominent public health physicians such as Sir R.A. Ross, W.H. Hamer, A.G. McKendrick, and W.O. Kermack formulated the fundamental concepts of compartmental epidemiology rather than mathematicians [35, 67].

1.6.2 Compartmental Models (20th century)

The 20th century witnessed significant advancements in mathematical epidemiology. Major contributors to this field include Sir Ronald Ross [151, 152], who developed models for malaria transmission and awarded the second Nobel Prize in Medicine in 1902 for his demonstration of the dynamics of the transmission of malaria between mosquitoes and humans [35]. In 1911, Sir Ronald Ross developed a fundamental compartmental model that included both people and mosquitoes. The model illustrated the control of transmission by reducing mosquito populations below a critical threshold. It also introduced the concept of the fundamental reproduction number, which has remained a cornerstone in mathematical epidemiology ever since.

The first complete mathematical model for the infectious diseases which received the attention in the literature deterministic compartmental epidemic model in 1927 by Kermack-McKendrick [89, 95, 94, 93, 117] and Soper [163]. These models divided the population into compartments (e.g., susceptible, infected, and recovered) and used differential equations to describe how individuals moved between these states. The SIR (Susceptible-Infectious-Recovered) model became a fundamental tool for

modeling infectious disease dynamics. The basic reproduction number, now almost commonly indicated by R_0, is a threshold quantity in the work of Ross, Kermack, and McKendrick. This threshold quantity was not named or specified by Ross, Kermack, or McKendrick. It appears that MacDonald [110], in his study on malaria, was the first to specifically designate the threshold quantity.

The Kermack-McKendrick model has limitations in describing disease outbreaks because it assumes homogeneous mixing within compartments, which doesn't hold at the outbreak's start. Instead, a different model is needed to consider the stochastic nature of infection transmission, influenced by the initial small number of infective individuals and contact patterns within the population.

1.6.3 Stochastic Models (Middle of 20th Century)

Small populations pose challenges for deterministic models since infection spread is inherently random. Consequently, stochastic models play a crucial role in disease transmission modeling. The historical roots of stochastic epidemic modeling can be traced back to the late 19th century when P.D. En'ko's work in 1889 anticipated the stochastic nature of disease transmission [67]. In 1928, W.H. Frost introduced the chain binomial model, a seminal stochastic epidemic model [80]. Although the model was described in lectures at that time, it wasn't published until later [67]. This model laid the foundation for understanding stochastic elements in disease spread. Karl Dietz played a pivotal role in acknowledging the historical significance of P.D. En'ko's ideas, highlighting the early recognition of stochastic concepts in epidemiology [67]. M. Greenwood proposed an alternative version of the chain binomial model in 1931, offering a different perspective within the stochastic epidemic modeling framework . Stochastic epidemic modeling has continued to evolve, witnessing numerous extensions and modernization. D.J. Daley and J. Gani's book in 1999 provides a comprehensive account of some of the more recent developments in the field [70]. To further refine the understanding of stochastic disease transmission, Bartlett described a stochastic analog of the classic Kermack-McKendrick epidemic model in 1949 [35].

1.6.4 Computational Methods and Data-Driven Models (Use of Machine Learning and Artificial Intelligence)

With the advent of powerful computers and the availability of extensive data, mathematical epidemiology shifted towards more data-driven and computationally intensive approaches [72, 157]. Machine learning algorithms play a crucial role in enhancing infectious disease control by enabling precise spatial and temporal predictions of disease dynamics [200]. These algorithms are extremely important for processing extensive and complex datasets, uncovering intricate patterns, and identifying trends that might be escaped from human observations. Because of this, they are very suitable for forecasting infectious diseases, considering the complex interactions between variables such as human behaviors, environmental conditions, and population demographics. Many research that have used machine learning approaches to predict infectious diseases have shown promising results in recent years. [1, 5, 9, 11]. However, a primary challenge in utilizing machine learning for disease prediction pertains to the availability of high-quality, comprehensive data. Infectious disease surveillance systems collect data encompassing various factors, including reported case counts, outbreak locations, and infected individuals' demographics. Nonetheless, these datasets frequently suffer from incompleteness, bias, and noise, impacting machine learning model performance. To surmount these challenges, researchers have deployed a spectrum of machine learning algorithms, including decision trees, random forests, support vector machines, and deep-learning networks, applied across diverse data sources such as electronic health records, genomics, and social media posts [6, 104]. Overall, the study findings demonstrate that machine learning algorithms excel in accurately predicting infectious disease spread and onset, rivaling or surpassing traditional statistical methods. Examples of successful machine learning applications include forecasting disease case numbers based on historical and current data, identifying outbreak sources using pathogen genetics and infection patterns, and assessing an individual's risk of contracting an infectious disease based on personal attributes and behaviors [14, 69, 130, 153]. Although machine learning shows great potential in predicting infectious diseases, there are still challenges and limitations. These include the need for good data, the complexity of how diseases spread, and the risk of making predictions that are too specific [15].

1.7 Rational and Outline of the Thesis

This research work proposes mathematical modeling validated with the real time data of the transmission dynamics of COVID-19 to bring out some important insights. This works reveals some uncovered phenomenon of transmission dynamics of COVID-19 especially focusing on the developing country Nepal. We also proposed some novel ideas which describe the disease dynamics more precisely and accurately.

The research work is organized as follows:

In Chapter 2, we provide the relevant background of epidemiology and mathematical modeling. We also present various techniques for theoretical analysis used in this dissertation.

In Chapter 3, we develop a deterministic mathematical model, which incorporates the imported as well as locally generated cases along with various policies implemented for the control of COVID-19 in Nepal. Using case data from both the controlled and outgrown phases of epidemics in Nepal, we estimated key parameters as well as the basic and effective reproductive numbers. Using our model, we evaluated the control strategies implemented in Nepal. Furthermore, we applied our model to predict the long-term dynamics of COVID-19 in Nepal, and provided the simulations to demonstrate how these control strategies can curb the epidemics in Nepal.

In Chapter 4, we employed a data-driven modeling technique to investigate the COVID-19 transmission patterns in two distinct locations (high-risk and low-risk) during the Delta surge. Because of the Nepal-India open border and densely populated cities in some places, considering two distinct regions is critical in the context of Nepal. All Terai districts connected to India, as well as inhabited cities such Nepal Kathmandu, Surkhet, Pokhara, Lalitpur, Bhaktapur, and Chitwan, are considered high-risk areas. We verified our model by fitting it to various real-time data sets encompassing newly recorded cases from high- and low-risk regions, as well as hospitalized, ICU, and Ventilator patients, and estimated important model parameters in a simulation.

In Chapter 5, we developed data-driven models to predict the risk of infection and hospitalization in real time. Then we applied our models to COVID-19 data in Nepal to estimate province-specific time-dependent reproduction numbers, disease risk, and hospitalization risk. We compared the Delta and Omicron waves and their effects on provincial communities and healthcare systems using our models. Furthermore, we

used our model to assess the effects of intervention strategies on infection risk.

The sixth chapter is about the summary and conclusion in which the main result of the research findings, discussions, conclusions and recommendations are presented.

CHAPTER 2

BACKGROUND INFORMATION

In this chapter, we introduce some basic definitions of epidemiology, development of the epidemic model, some classical models with reproduction rate, and stability of disease-free equilibrium.

2.1 Basic Terminology in the Disease Modeling

2.1.1 Basic Terminology in Epidemiology

Susceptible Individual

Individuals who may be infected in the future with the disease that persists in some other individuals, are called susceptible.

Exposed Individuals

An exposed individual is someone who has encountered a pathogen but has not yet exhibited symptoms of the disease.

Infected and Infectious Individuals

When pathogens enter into the body it takes time for development in that exposed host. So host population who have immature disease is called infected individuals. Individuals who are capable of transmitting the disease are termed infectious. However, it's important to note that individuals who are infected may not be infectious for the entire duration of their infection.

Latent Period

The latent period is the time interval between when an individual is exposed to a disease causing agent (such as a virus or bacterium) and when they become infectious.

Incubation Period

The incubation period is the time interval between initial contact with an infectious agent and onset of the first sign or symptom of disease.

Incidence

Incidence is defined as the number of individuals who become ill during the specified interval of time (e.g. one day).

Recovered Individual

Individuals who are free from disease after infection are called recovered individuals. They may or may not reinfect depending on immunity gained against the disease. That is, if lifelong immunity is gained against the disease then reinfection by the disease does not happen.

Endemic

An infection is said to be endemic in a population when that infection is constantly maintained at a baseline level in a geographic area without external input (e.g., COVID-19, flu, Common-Cold, Malaria)

Epidemic

The extended but finite occurrence of an infectious disease at a low level within a community or region is referred to as an epidemic.

Outbreak

An outbreak usually refers to a sudden increase in the number of new cases of a disease in a limited geographic area. COVID-19 started as an outbreak in Wuhan,

the capital city of the Hubei province in China at the end of December 2019, when the Chinese government confirmed that it was treating dozens of cases of pneumonia of unknown cause.

Pandemic

A pandemic is defined as an epidemic that has spread across multiple countries or continents, affecting a large number of people within a short period, and where the infection is no longer under control. Pandemics usually occur when a new virus easily spreads among individuals who have little or no pre-existing immunity to it. COVID-19, declared a pandemic by the WHO on March 11, 2020, is the first known pandemic resulting from the emergence of a new coronavirus.

2.1.2 Mathematical Terminology

2.1.2.1 Basic Reproduction Number

The basic reproduction number R_0 is used to measure the transmission potential of a disease [55]. The basic reproduction number, symbolized as R_0, quantifies the number of new infections arising from a single infected individual within a population when all individuals are susceptible throughout the entire infectious period. In simplified models, R_0 can be expressed as follows:

$R_0 =$ (number of contacts at a time) $\times$ (probability of infection in a contact) $\times$ (duration of infectiousness during epidemics). For complicated models the next generation matrix (NGM) method is used in computing the R_0.

In the field of epidemiology, R_0 serves as a critical threshold. When R_0 is greater than one, it indicates the potential for epidemics, while an R_0 less than one suggests the absence of epidemics. The basic reproduction number (R_0) plays a pivotal role in guiding public health interventions and control strategies to prevent and manage disease outbreaks.

2.1.2.2 Effective Reproduction Number

In various real-world scenarios, it is rare for an entire population to be entirely susceptible to an infection. Some individuals may possess immunity, either due to prior

infection, which grants lifelong protection, or through previous immunization. Consequently, not all individuals who come into contact with the infectious agent will become infected, leading to a reduction in the average number of secondary cases arising from each infectious case, as compared to the basic reproduction number.

The concept of the effective reproductive number R_t, quantifies the average number of secondary cases per infectious case in a population composed of both susceptible and non-susceptible hosts [173]. When $R_t > 1$, the number of cases will increase, typically seen at the onset of an epidemic. When $R_t = 1$, the disease remains endemic within the population, and when $R_t < 1$, there is a decline in the number of cases.

The effective reproductive number, R_t, can be estimated by multiplying the basic reproductive number, R_0 by the fraction of the host population that is susceptible x, such that $R_t = R_0 x$.

For instance, if the basic reproductive number (R_0) for influenza is 12 in a population where half of the individuals are immune, the effective reproductive number for influenza is $12 \times 0.5 = 6$. In this scenario, a single case of influenza is expected to generate an average of 6 new secondary cases. To successfully eliminate a disease from a population, R_t needs to be maintained at a level less than 1.

2.1.3 Jacobian Matrix

The matrix of each of a vector-valued function's first-order partial derivatives is the function's Jacobian matrix [112]. The Jacobian matrix of a system of ODEs

$$\frac{dx}{dt} = f(x), \tag{2.1}$$

where $x = (x_1, x_2, x_3, ..., x_n)$ and $f = (f_1, f_2, f_3, ..., f_n)$ is the matrix of all partial derivatives of right side of system of equation 2.1 with respect to variable x given as

$$J = \begin{bmatrix} \frac{\partial f_1}{\partial x_1} & \frac{\partial f_1}{\partial x_2} & \cdots & \frac{\partial f_1}{\partial x_n} \\ \frac{\partial f_2}{\partial x_1} & \frac{\partial f_2}{\partial x_2} & \cdots & \frac{\partial f_2}{\partial x_n} \\ \frac{\partial f_3}{\partial x_1} & \frac{\partial f_3}{\partial x_2} & \cdots & \frac{\partial f_3}{\partial x_n} \\ \cdots & \cdots & \cdots & \cdots \\ \frac{\partial f_n}{\partial x_1} & \frac{\partial f_n}{\partial x_2} & \cdots & \frac{\partial f_n}{\partial x_n} \end{bmatrix}.$$

2.1.3.1 Eigenvalues and Spectral Radius

For a given square matrix A, an eigenvalue λ and its corresponding eigenvector v satisfy the equation $Av = \lambda v$. The spectral radius of A considers the absolute values of these eigenvalues and selects the largest one. The spectral radius of a square matrix A is denoted by $\rho(A)$ and is defined as $\rho(A)=max|\lambda i|; \quad i = 1, 2, 3, \cdots, n$, where λi are the eigenvalues of A [70, 112].

2.1.3.2 Next Generation Matrix

In the case of multiple infectious agents, an innovative next generation approach introduced in 1990 by Diekmann et al. [55] and subsequently standardized by Van den Driessche and Watmough [180] offers a valuable method. This method transforms a system of ordinary differential equations (ODEs) or partial differential equations (PDEs) within an infectious disease model into an operator. In this method, the basic reproduction ratio is precisely defined as the dominant eigenvalue (spectral radius) of this operator.

Now, let's analyze the following deterministic model:

$$\frac{dx_i(t)}{dt} = f_i(x), \quad x(0) \in \overline{\mathbb{R}}^n_+. \tag{2.2}$$

Here, $x_i(t)$ represents the population count in compartment i at time t. Initially, the population is in the non-negative orthant of $\mathbb{R}^n_+$, denoted as $x(0) \in \overline{\mathbb{R}}^n_+$. Let's define a set X as follows:

$$X = \{x \in \overline{\mathbb{R}}^n_+ : x_i = 0, 1 \leq i \leq m\}, \text{ where } m \leq n.$$

In this context, X represents a collection of disease-free states.

Now, considering the population dynamics, we have:

$$\frac{dx_i(t)}{dt} = F_i(x) - V_i(x), \tag{2.3}$$

where $F_i(x)$ represents the introduction of infection into compartment i. Here,

$$V(x) = V_i^-(x) - V_i^+(x),$$

where $V_i^-(x)$ denotes the transfer out of compartment i by other means and $V_i^+(x)$ denotes the transfer into compartment i by other means. $F(x)$ and $V(x)$ satisfy the following assumptions:

I. The rates of movement are non-negative, meaning that for $x \in \overline{\mathbb{R}}_+^n$, it follows that $F_i(x) \geq 0$ and $V_i^-(x) > 0$ for $1 \leq i \leq n$.

II. If a compartment is empty, movement out of that compartment is not possible, i.e., if $x_i = 0$, then $V_i^-(x) = 0$.

III. Movement of infection into non-infective classes is not possible, implying that $F_i(x) = 0$ for $i > m$.

IV. The disease-free subspace is invariant. When $x \in X$, both $F_i(x) = 0$ and $V_i^-(x) = 0$ for $1 \leq i \leq m$.

V. In the absence of new infections, the disease-free equilibrium is locally asymptotically stable. Specifically, when $F(x) = 0$, all eigenvalues of the matrix at the disease-free equilibrium must be negative or with negative real part.

For the disease-free equilibrium of 2.2, we define square matrices F and V as follows:

$$F_{ij} = \frac{\partial F_i}{\partial x_j} \text{ when } 1 \leq i, j \leq m$$
$$V_{ij} = \frac{\partial V_i}{\partial x_j} \text{ when } 1 \leq i, j \leq m.$$

Then, FV^{-1} is referred to as the Next Generation Matrix (NGM), and $R_0 = \rho(FV^{-1})$ represents the dominant eigenvalue (spectral radius) of the NGM.

2.1.4 Well-posedeness

A mathematical model is said to be well-posed if it satisfies three fundamental properties [70, 112]:

Existence: There exists at least one solution to the model within the specified domain. In other words, there is a solution that makes sense within the context of the problem being modeled.

Uniqueness: The solution is unique, meaning there is only one possible solution for a given set of initial or boundary conditions. This ensures that the model does not produce multiple conflicting solutions.

Stability: The solution is stable regarding small changes in the initial or boundary conditions. This means that small perturbations in the input do not make significantly

different in the solutions. Stability is particularly important in dynamical systems described by differential equations.

A well-posed mathematical model provides a solid foundation for understanding and solving real-world problems. Models that lack one or more of these properties can lead to ambiguous or unreliable results and may not accurately represent the physical or biological phenomena.

2.1.4.1 Stability of Solutions

Stability analysis is a fundamental aspect of dynamical system theory. Consider a continuous-time autonomous system represented by a set of ordinary differential equations (ODEs) of the form:

$$\frac{dx}{dt} = f(x), \tag{2.4}$$

where x is a vector representing the state of the system, and $f(x)$ is a vector field that describes how the state evolves over time.

Definition of Stability: [112] A steady-state solution $\bar{x}$ is said to be stable if, for any small perturbation $\epsilon > 0$, there exists a $\delta > 0$ such that if the initial condition $x(0)$ satisfies $\|x(0) - \bar{x}\| < \delta$, then the solution $x(t)$ will satisfy $\|x(t) - \bar{x}\| < \epsilon$ for all $t \geq 0$.

2.1.4.2 Asymptotic Stability Condition with Relation to Spectral Radius

Let $\bar{x}$ be a steady-state solution (i.e., $\frac{d\bar{x}}{dt} = 0$) of the system 2.4. The steady state $\bar{x}$ is asymptotically stable if and only if the following conditions hold:

1. The Jacobian matrix A of the system evaluated at the steady state $\bar{x}$ is negative definite, i.e., for all eigenvalues λ_i of A, we have $\mathrm{Re}(\lambda_i) < 0$, where $\mathrm{Re}(\lambda_i)$ denotes the real part of λ_i.

2. Alternatively, the spectral radius $\rho(A)$ of the Jacobian matrix A is less than one, i.e., $\rho(A) < 1$.

These conditions ensure that small perturbations from the steady state $\bar{x}$ will decay over time, and trajectories starting near $\bar{x}$ will converge to $\bar{x}$ as $t \to \infty$ [112].

2.1.5 Maximum Likelihood Method for the Estimation of the Effective Reproduction Number (R_t)

The effective reproduction number, R_t, is the real-time estimation of the reproduction number that represents the average number of secondary infections from an infected individual in his/her infectious period at time t [172]. Here, we used the Maximum Likelihood Method (MLM) described in the previous studies [49, 172] to estimate the effective reproduction number. Two data sets are required to estimate R_t using MLM: the number of new cases (incidence of cases) over time and the generation time (time duration between the primary and secondary infection). The generation time is usually not observable but can be approximated with the serial interval [98], which is defined as the time between the onset of symptoms of primary cases and that of secondary cases [184]. Many studies [42, 146, 166, 206] have reported that the serial interval follows a Gamma distribution with certain means and standard deviations.

Assuming that the secondary cases at time t generated by the infected cases at time s ($s = 1, 2, \ldots, t$) follow the Poisson distribution with mean $R_t\psi_t = R_t \sum_{s=1}^{t} I_{t-s} w_s$, where $\psi_t = \sum_{s=1}^{t} I_{t-s} w_s$ and w_s is a Gamma distribution of serial interval describing the infectiousness at time s after infection, the likelihood function of secondary cases is

$$L(R_t) = \frac{(R_t\psi_t)^{I_t}\ e^{-R_t\psi_t}}{I_t!}.$$

We assumed that the reproduction rate R_t remains constant over the small time period $[t-\tau,\ \ t]$ and is denoted as $R_{t,\tau}$. The likelihood of the secondary cases over the time period $[t-\tau,\ \ t]$ with given previous incidences $I_0, I_1, ..., I_{t-\tau-1}$ is

$$L(R_{t,\tau}) = \prod_{s=t-\tau}^{t} \frac{(R_{s,\tau}\psi_{s,\tau})^{I_s}\ e^{-R_{s,\tau}\psi_{s,\tau}}}{I_s!}. \tag{2.5}$$

Using a Bayesian framework with a Gamma distributed prior with parameters (a, b), the posterior joint distribution of $R_{t,\tau}$ is given by a Gamma distribution with the parameters

$$\left(a + \sum_{s=t-\tau}^{t} I_s,\quad \frac{1}{\frac{1}{b} + \sum_{s=t-\tau}^{t} \psi_s} \right).$$

2.2 Data Fitting

It is possible to approximation some unknown parameters of a model defined by a set of ordinary differential equations (ODEs) when fitting data to the model. These ODEs can be solved numerically by using MATLAB solvers like "ode15s" or "ode45." Together with these MATLAB solvers, the optimization functions "fminsearch" and "fmincon" are used. The least squares method is frequently used for data fitting. The goal of this fitting approach is to reduce the sum of squared residuals, which is a measure of the difference between the model's predictions and the equivalent values found in experimental data,

$$J(\Phi^*) = \sum_{i=1}^{n} \left[L(t_i) - \bar{L}(t_i) \right]^2,$$

where $\Phi^* = (\Phi_1, \Phi_2, ..., \Phi_m)$ is the set of m parameters to be estimated, and $L(t_k)$ and $\bar{L}(t_k)$ population obtained from the model and real time data of the respective population. Here, n represents the total number of data points used for the model fitting.

2.3 Computation of Confidence Intervals

In order to derive confidence intervals for the estimated parameters, we compute standard errors for Φ^* using a method outlined in Banks [20]. For this, we first compute the sensitivity matrix Υ of the parameters,

$$\Upsilon = \begin{bmatrix} \frac{\partial L_{t_1}}{\partial \Phi_1} & \frac{\partial L_{t_1}}{\partial \Phi_2} & \cdots & \frac{\partial L_{t_1}}{\partial \Phi_m} \\ \frac{\partial L_{t_2}}{\partial \Phi_1} & \frac{\partial L_{t_2}}{\partial \Phi_2} & \cdots & \frac{\partial L_{t_2}}{\partial \Phi_m} \\ \vdots & \vdots & \cdots & \vdots \\ \frac{\partial L_{t_n}}{\partial \Phi_1} & \frac{\partial L_{t_n}}{\partial \Phi_2} & \cdots & \frac{\partial L_{t_n}}{\partial \Phi_m} \end{bmatrix}.$$

Since we are unable to formulate the closed form of $\frac{\partial L_{t_k}}{\partial \Phi_j}$, $j = 1, 2, \ldots, m$, and $k = 1, 2, \ldots, n$ from the model, we use the following complex-step approximation to compute the partial derivatives.

We consider the Taylor expansion of L_{t_n} using a complex step ih, where h is taken to be a small positive constant ($h = 10^{-40}$) in our computations) and i is the unit imaginary number.

$L_{t_k}(\Phi_j + ih) \approx L_{t_k}(\Phi_j) + ihL_{t_k}^{'}(\Phi_j) - \frac{h^2}{2!}L_{t_k}^{''}(\Phi_j) + \ldots$

Taking the imaginary part of both sides of the above equation and dividing by h gives

$$L_{t_k}^{'}(\Phi_j) = \frac{\partial L_{t_k-}}{\partial \Phi_j} \approx \frac{Im[L_{t_k}(\Phi_j + ih)]}{h} + O(h^2),$$

where $O(h^2)$ represents terms of order 2 and higher. Therefore, the derivatives are given by

$$\frac{\partial L_{t_k}}{\partial \Phi_j} \approx D_h^j(L_{t_k}) = \frac{Im\left[L_{t_k}(\Phi_j + ih)\right]}{h},\ j = 1,\ 2,\ \ldots m, \text{ and } k = 1,\ 2,\ \ldots n.$$

With these, we compute an approximation to the sensitivity matrix Υ denoted by $\hat{\Upsilon}$. Then we take $\sqrt{(\sigma^2\{\hat{\Upsilon}^T\hat{\Upsilon}\}^{-1})_{ii}}$ where $\sigma^2 \approx \hat{\sigma}^2 = J(\Phi^*)/(n-m)$ and Φ^* are the basic estimated parameter values, to be the standard deviation for the parameter Φ_j, $j = 1,\ 2\ \ldots . m$.

2.4 Identifiability of the Parameters

A main difficulty is parameter estimation for dynamic biological models using non-linear ordinary differential equations (ODEs). A unique characteristic of biological models is that they frequently include a high number of factors that are correlated with one another [12, 47]. Identifiability is a critical concept in the field of parameter estimation and statistical modeling, particularly in contexts like system identification, machine learning, and data analysis. Identifiability refers to the ability to uniquely determine the values of model parameters from observed data. When a model is identifiable, it means that each parameter can be estimated without ambiguity, and the model is capable of accurately capturing the underlying relationships in the data.

One method to assess identifiability is based on the sensitivity matrix, which quantifies how changes in the model parameters affect the model's output [114].

Let $\Phi^* = (\Phi_1, \Phi_2, ..., \Phi_m)$ be the parameter vector of interest, which contains all the model parameters that we want to estimate. We calculate the sensitivity matrix as described in the section 2.3. A model is considered identifiable if the sensitivity matrix is of full rank. In other words, the number of linearly independent rows or columns in the matrix should be equal to the number of parameters to be estimated. If the sensitivity matrix is full rank, the model is identifiable, and we can estimate all the

parameters uniquely [90]. If the sensitivity matrix is not full rank, it indicates that some parameters are not identifiable using the available data and model structure. This could be due to redundancy in the model or insufficient information in the data to separate certain parameters.

CHAPTER 3

MATHEMATICAL MODEL FOR UNCOVERING THE EFFECTIVE CONTROLS OF FIRST WAVE OF COVID-19 IN NEPAL

In this chapter, we present a novel deterministic mathematical model based on the SEIR model to uncover the effective control strategies implemented by the government of Nepal during the first wave of COVID-19. This model accounts for both imported and locally generated COVID-19 cases, as well as the various policies implemented during the first wave of the pandemic in Nepal. By analyzing recorded data from both the controlled and uncontrolled phases of the epidemic in Nepal, we estimate crucial parameters, including the basic and effective reproductive numbers. Using our model, we assess the effectiveness of the COVID-19 control strategies employed in Nepal. Additionally, we use our model to examine the dynamics of COVID-19 in Nepal during the first wave (21 April, 2020 to 20 April, 2021) and provide simulations that illustrate the potential impact of these control strategies implemented on curbing the spread of the virus.

3.1 Introduction

In Nepal, the first confirmed case of COVID-19 was reported on January 23, 2020 [120]. Subsequently, until March 23, 2020, no new cases were reported. On March 24, 2020, the Nepalese government swiftly implemented a nationwide lockdown, business closures, travel restrictions, and stringent border screening, which effectively maintained a low number of COVID-19 cases (only 4% from local transmission) until mid-July 2020 [61]. However, the relaxation of these measures led to a significant surge in cases, resulting in a total of 58,327 cases by September 16, 2020, mostly originating from local transmission [59]. This bi-phasic epidemic trend in Nepal, transitioning

from a controlled phase to an outbreak phase, offers valuable insights into the impact of control strategies, notably given Nepal's open border with India, a country significantly affected by COVID-19.

Deterministic mathematical models, including the SEIR (Susceptible-Exposed-Infected-Recovered) model, have been widely used in quantitative studies of COVID-19 pandemics. While some models were used to estimate the parameters such as incubation period, and infectious period [17, 105, 107, 185], others examined the effectiveness of control strategies such as lockdown, detection and isolation, border screening, and medical resources [43, 45, 66, 78, 127, 159, 164, 204, 186]. The quarantine for the traveler and suspected cases were also studied as the effective control measures for mitigating COVID-19 [10, 79, 107, 205]. Regarding COVID-19 in Nepal, previous studies [29, 32, 143, 106] have provided some insights into doubling time of new infections, early transmission trend, and the timing of the daily incidence burden in Nepal. However, none of the previous models have considered the entry of cases through Nepal-India open border and border-related control strategies, which can be important factors because the travel history of recorded infectious people shows that more than 80% infectious cases came from abroad, especially from India, during the early period of epidemics [60, 126]. Also, despite Nepal government's effort of applying strategies such as border screening, quarantine and isolation, poor handling policy at the border does exist, allowing to enter many infected individuals into the community without quarantine [161].

Despite the COVID-19's global devastating effects on all aspects of human lives, the impact of the epidemic quite varies from country to country, in different waves, thus the study focused on a specific country can provide better understanding of the disease and its control strategies and mathematical modeling may able to uncover new insights of the effectiveness of control measures which may useful for the mitigation plan for future pandemic.

3.2 Method

3.2.1 Data Source

The data used in this study is obtained from the Ministry of Health and Population, Government of Nepal [59]. We use the data of COVID-19 from March 22 until September 16, 2020. The data including quarantine, new cases, cumulative cases,

and RT-PCR tests, were used in our model fitting and simulation. During the initial phase of epidemic, most of the PCR tests performed were for the quarantined people and a few for the community and front line workers (armed forces, hospital workers, civil workers, etc.). Therefore, we considered the 80% of PCR-tests performed were for the people who were quarantined.

3.2.2 Modeling of Basic Transmission Dynamics

The entire population is categorized into five distinct groups: S (those susceptible to the virus), E (individuals exposed to the virus), I_R (infectious individuals who are recorded), I_N (infectious individuals who are not recorded), and R (recovered individuals). In our model, susceptible people become exposed to the virus when they come into contact with non-recorded infectious individuals at a rate denoted as β. These exposed individuals then transition to being infectious at per capita rate δ, with a certain fraction, represented as θ, being recorded, and the remaining portion, represented as $1-\theta$, remaining unrecorded. Individuals in both the I_R and I_N groups either recover at a rate of η. k be the diseases induced death rate. The variables μ and Λ stand for the per capita rates of natural mortality and the natural recruitment of individuals into the susceptible group. The arrival of individuals from other regions, particularly across the Nepal-India border, is depicted using a time-dependent rate denoted as $\lambda(t)$, of which a proportion ρ are infected, while the remaining $(1-\rho)$ are still susceptible.

3.2.2.1 Modeling Control Strategies Implemented in Nepal

The main control strategies implemented by the government of Nepal during the first wave of COVID-19 were: (i) Border screen and quarantine, (ii) Lockdown, and (ii) Detection and isolation.

Border screen and quarantine. To model the border screen and quarantine strategy, we introduce a quarantined class, Q, to which $\phi\lambda(t)$ of individuals from abroad enters, where ϕ represents the rate of border screen. For these quarantined individuals PCR test is performed with rate τ and the tested individuals with positive result enter into the I_R class and are isolated. As the expected rate of positive test in people entering into the country is ρ, we assume that ρ represents the portion of the tested population getting positive result, while the remaining $(1-\rho)$ portion of the tested population show negative result and enter the susceptible class, S. Due to the limi-

tation of PCR test, there were cases of individuals, including some without onset of the symptoms, being released from the quarantine center without performing PCR test. We assume that individuals leave the quarantined class without PCR test at the rate of γ. Among them, the portion ρ enters non-recorded infectious class and the remaining $(1-\rho)$ enters the susceptible class.

Lockdown. Lockdown strategy reduces the contact among individuals, and we assume the reduction of contact by ξ resulting in the transmission rate $\beta \to (1-\xi)\beta$. Since the strategy was altered in two different phases, the controlled and the outgrown, we consider two different reduction rates of contact as follows:

$$\xi(t) = \begin{cases} \xi_c, & t \leq t_c, \\ \xi_o, & t > t_c, \end{cases}$$

where t_c represents the time when the epidemic phase changes corresponding to alteration of policies (July 21, 2020). As a result, the net infection rate becomes $\beta_c = (1-\xi_c)\beta$ and $\beta_o = (1-\xi_o)\beta$ before and after $t = t_c$, respectively.

Detection and isolation. As mentioned above, recorded infected individuals, I_R, in our model are isolated. Therefore, the detection and isolation strategy can be incorporated into our model by altering the rate θ. We introduce a parameter ψ to represent the effect of detection so that the rate of individuals in exposed class, who are detected and recorded, changes as $\theta \to \psi\theta$. Since the strategy of testing for individuals in general community are altered after the lockdown was lifted, we take two different detection rates for the controlled and outgrown phases as follows.

$$\psi(t) = \begin{cases} \psi_c, & t \leq t_c, \\ \psi_o, & t > t_c. \end{cases}$$

As a result, the net detection and isolation rate becomes $\theta_c = \psi_c\theta$ and $\theta_o = \psi_o\theta$ before and after $t = t_c$, respectively.

Combining all the control strategies implemented in Nepal into the basic transmission dynamics model, we obtain the model as shown in Figure 6.

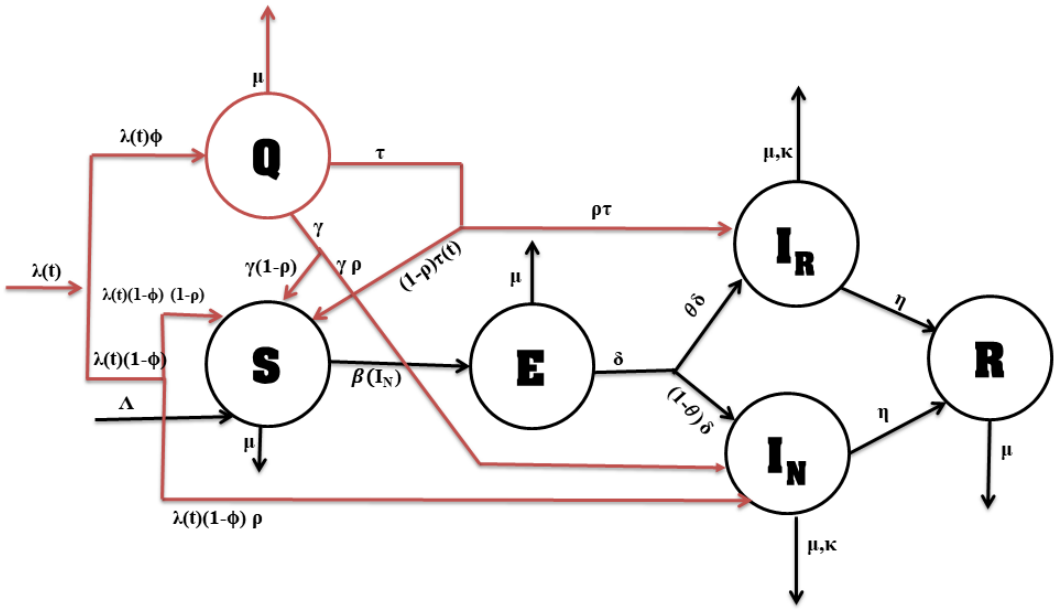

Figure 6: Compartmental diagram of the Model. The arrow along with parameters shows the rate of flow from one compartment to another. The part of figure with black color associates with basic $SEIR$ model and red part associates with control policies.

The model is described by the system of the following ordinary differential equations.

$$\frac{dQ}{dt} = \lambda(t)\phi - \tau Q - \mu Q - \gamma Q \tag{3.1}$$

$$\frac{dS}{dt} = \Lambda + \lambda(t)(1-\phi)(1-\rho) + \tau(1-\rho)Q + \gamma(1-\rho)Q - \frac{\beta(t)SI_N}{N} - \mu S \tag{3.2}$$

$$\frac{dE}{dt} = \frac{\beta(t)SI_N}{N} - (\delta + \mu)E \tag{3.3}$$

$$\frac{dI_R}{dt} = \delta\theta(t)E + \rho\tau Q - (\eta + \mu + k)I_R \tag{3.4}$$

$$\frac{dI_N}{dt} = \lambda(t)\rho(1-\phi) + \gamma\rho Q + \delta(1-\theta(t))E - (\eta + \mu + k)I_N \tag{3.5}$$

$$\frac{dR}{dt} = \eta I_N + \eta I_R - \mu R \tag{3.6}$$

Here, the total population is given by $N = Q + S + E + R + I_N + I_R$.

3.2.3 Basic Reproduction Number (R_0)

We first obtain the disease free equilibrium, $\mathcal{E}^*$, of the model system. Using the pre-pandemic condition $\lambda = \lambda(0)$ and the disease-free conditions $E = 0$, $I_R = 0$, $I_N = 0$, we obtain $\rho = 0$. Then the model system provides the following disease free

equilibrium:

$$\mathcal{E}^* = (S^*, Q^*, 0, 0, 0, 0),$$

where

$$S^* = \frac{\Lambda}{\mu} + \frac{\lambda(0)\{\tau + \gamma + \mu(1-\phi)\}}{\mu(\tau+\gamma+\mu)} \quad \text{and} \quad Q^* = \frac{\lambda(0)\phi}{\tau+\gamma+\mu}.$$

According to the next generation matrix method, we divide the compartments used in the model into two groups: infected $\vec{x} = (x_i, i = 1, 2, 3) = (E, I_R, I_N)$ and non-infected group $\vec{y} = (y_j, j = 1, 2, 3) = (S, Q, R)$. Then the model system can be written as:

$$x_i' = f_i(\vec{x}, \vec{y}) \text{ and } y_j' = g_j(\vec{x}, \vec{y}) \text{ for } i, j = 1, 2, 3.$$

We now write the right hand side of the system of infected compartments as $f_i(\vec{x}, \vec{y}) = F_i(\vec{x}, \vec{y}) - V_i(\vec{x}, \vec{y})$, where $F_i(\vec{x}, \vec{y})$ contains the terms representing the new infections in compartment i and $V_i(\vec{x}, \vec{y})$ contains the terms containing the difference between the transfer of individuals out of and into the compartment i:

$$\begin{pmatrix} F_1 \\ F_2 \\ F_3 \end{pmatrix} = \begin{pmatrix} \frac{\beta(t)SI_N}{S+Q+E+R+I_N+I_R} \\ 0 \\ 0 \end{pmatrix},$$

$$\begin{pmatrix} V_1 \\ V_2 \\ V_3 \end{pmatrix} = \begin{pmatrix} (\delta+\mu)E \\ (\eta+k+\mu)\, I_R - \delta\theta(t)E \\ (\eta+k+\mu)I_N - \delta(1-\theta(t))E \end{pmatrix}.$$

We now take the values $\beta(t) = \beta_c$ and $\theta(t) = \theta_c$ corresponding to the beginning of the epidemic, and construct the following two matrices using $F = \left(\frac{\partial F_i}{\partial x_j}\right)\Big|_{\mathcal{E}^*}$ and $V = \left(\frac{\partial V_i}{\partial x_j}\right)\Big|_{\mathcal{E}^*}$.

$$F = \begin{pmatrix} 0 & 0 & \frac{\beta_c S^*}{Q^*+S^*} \\ 0 & 0 & 0 \\ 0 & 0 & 0 \end{pmatrix}, \quad V = \begin{pmatrix} \delta+\mu & 0 & 0 \\ -\delta\theta_c & \eta+k+\mu & 0 \\ -\delta(1-\theta_c) & 0 & \eta+k+\mu \end{pmatrix}.$$

These matrices allow use to compute the second generation matrix as follows:

$$FV^{-1} = \begin{pmatrix} \frac{\beta_c\delta(1-\theta_c)S^*}{(\delta+k+\mu)(\eta+k+\mu)(Q^*+S^*)} & 0 & \frac{\beta_c S^*}{(\eta+k+\mu)(Q^*+S^*)} \\ 0 & 0 & 0 \\ 0 & 0 & 0 \end{pmatrix},$$

whose eigenvalues are 0, 0, and $\frac{\beta_c\delta(1-\theta_c)S^*}{(\delta+\mu)(\eta+k+\mu)(Q^*+S^*)}$. Then the basic reproduction number is given by the dominated eigenvalue. Therefore,

$$R_0 = \frac{\beta_c\delta(1-\theta_c)S^*}{(\delta+\mu)(\eta+k+\mu)(Q^*+S^*)}.$$

We used the Next Generation Matrix method [55, 180] to derive the expression of R_0 for our model (see Appendix) and obtained

$$R_0 = \frac{\beta_c \delta (1-\theta_c) S^*}{(\delta+\mu)(\eta+k+\mu)(Q^*+S^*)},$$

where

$$S^* = \frac{\Lambda}{\mu} + \frac{\lambda(0)\{\tau+\gamma+\mu(1-\phi)\}}{\mu(\tau+\gamma+\mu)} \quad \text{and} \quad Q^* = \frac{\lambda(0)\phi}{\tau+\gamma+\mu}.$$

As expected, we are able to theoretically establish R_0 as the outbreak threshold for our model, as stated in the following theorem:

Theorem 3.2.1 *Disease free equilibrium point of the system of equations (1-6) is asymptotically stable if $R_0 < 1$ and unstable if $R_0 > 1$.*

Proof: Jacobian of the system of equations (3.2-3.6) evaluated at the disease free equilibrium, $\mathcal{E}^*$, is

$$\begin{pmatrix} -\mu & \gamma(1-\rho_1)+(1-\rho)\tau & 0 & 0 & -\frac{\beta_c S^*}{Q^*+S^*} & 0 \\ 0 & -(\tau+\gamma+\mu) & 0 & 0 & 0 & 0 \\ 0 & 0 & -(\delta+\mu) & 0 & \frac{\beta_c S^*}{Q^*+S^*} & 0 \\ 0 & \rho\tau & \delta\theta_c & -(\eta+k+\mu) & 0 & 0 \\ 0 & \gamma\rho_1 & \delta(1-\theta_c) & 0 & -(\eta+k+\mu) & 0 \\ 0 & 0 & 0 & \eta & \eta & -\mu \end{pmatrix}.$$

The eigenvalues of this Jacobian are given by

$$\lambda_1 = -\mu, \lambda_2 = -\mu, \lambda_3 = -(\eta+k+\mu), \lambda_4 = -(\gamma+\tau+\mu),$$

$$\lambda_5 = \frac{-(\delta+\eta+2\mu+k) - \sqrt{(\delta+\eta+2\mu+k)^2 - 4(\delta+\mu)(\eta+\mu+k)\,(1-R_0)}}{2},$$

and

$$\lambda_6 = \frac{-(\delta+\eta+2\mu+k) + \sqrt{(\delta+\eta+2\mu+k)^2 - 4(\delta+\mu)(\eta+\mu+k)\,(1-R_0)}}{2}.$$

We can clearly observe that all the eigenvalues are negative if $R_0 < 1$. Therefore, the disease free equilibrium, $\mathcal{E}^*$, is asymptotically stable if $R_0 < 1$ and unstable if $R_0 > 1$. □

3.2.4 Estimation of Parameters and Population Size

Even though first case of COVID-19 in Nepal was confirmed on January 23, 2020, no additional cases were reported until March 23, 2020. Therefore, we consider March 22, 2020 as the initial time $t = 0$ for our dynamical system model. The total population of Nepal in the census year 2011 was 26,494,504, which was projected to reach 29,704,501 by the end of 2019 [40]. There are about 3 to 4 million Nepalese working in India [99, 170] and about 1.5 million Nepalese working in the Gulf countries and Malaysia [83, 73], making approximately the total of 5 million Nepalese as seasonal migrants. Therefore, deducting 5 million people as migrants from the total population of 29,704,501, we get $N(0)$=2,5000,000. 63 people came from aboard were sent to Kharipati quarantine (a quarantine center) on March 21 [171]. Therefore, we take $Q(0) = 63$. The first case identified on January 23, 2020 had been recovered [120] by the beginning of our dynamics, and hence we take $R(0) = 1$. Since the initial time of our dynamic model is the beginning of the epidemic, we assume $E(0) = 1,\ I_R(0) = 0$, and $I_N(0) = 1$.

Since the infected individuals remain in the exposed class for about 5.2 days until they become infectious [17, 100, 189], we take $\delta = 1/5.2 = 0.1923$ per day. Also, the infectious individuals get recovered in about 17 days [175], implying the average recovery rate $\eta = 1/17 = 0.0588$ per day. We estimate the rate of death due to COVID-19 using the data taken from the official website of Nepal government [120]. Specifically, we take the average death rate from March 22 to September 16, 2020, and obtain the per capita death rate $k = 0.000281$ per day. We take μ and Λ in such a way that the natural birth rate and death rate remain equal for the period of this pandemic. In addition, we use quarantine and PCR data along with the model to estimate parameters τ and γ, which are related to people leaving quarantine center. We estimate the remaining parameters $\phi, \beta_c, \beta_o, \theta_c, \theta_o$ and ρ by using the least square fitting of the model to the daily recorded new cases data.

3.2.5 Data Fitting

We implement the previous method [145] described in section 2.2 to perform the data fitting and to identify a reasonable confidence interval of the estimated parameters. In brief, the method involves thorough process of consecutive reduction of number of parameters until the reasonable confidence intervals are identified. The process allowed us to identify the parameters $\phi, \beta_c, \beta_o, \theta_c, \theta_o$ and ρ that can be reasonably

estimated from the available data. Further reduction of the number of parameters from the current six parameters provided a poor fit (F-test, p-value < 0.05).

For the model fitting the data available is the daily new cases of recorded infectious people. Using our model, the recorded new infections generated at time t, $L(t)$, can be computed using the following equation:

$$L(t) = \tau\rho Q(t) + \delta\theta E(t) \tag{3.7}$$

We obtain the best-fit set of parameters $\Phi^* = (\phi, \beta_c, \beta_o, \theta_c, \theta_o, \rho)$ via a nonlinear least squares regression method that minimizes the following sum of the squared residuals as described in the section 2.2. To obtain the confidence limits for the estimated parameters, we compute standard errors from the sensitivity matrix Υ by using the techniques described in the section 2.3. We find the matrix $\Upsilon^T\Upsilon$ to be of the full rank (rank = 6), which confirms the identifiability of the estimated parameters [114].

3.3 Results

3.3.1 Estimation of Border Screen

Given the open border of Nepal with India, one of the most COVID-19 infected countries, and related border screen and quarantine policies implemented by the Nepal government, the rate of border screen and quarantine is important for accurate evaluation of the policy. However, the official data of this information is not available. In this section, we use our model to estimate the rate of border screen and quarantine, $\phi\lambda(t)$, from the data of the active quarantine population, $\bar{Q}(t_i)$, and the number of PCR-tests performed, $PCR(t_i)$.

Since the natural death is negligible during the short period of the epidemic (i.e., $\mu \approx 0$), applying the model equation (3.1) at the data collected time t_i, we obtain the following approximation:

$$\phi\lambda(t_i) \approx \left.\frac{dQ}{dt}\right|_{t=t_i} + \tau Q(t_i) + \gamma Q(t_i) \approx \bar{Q}(t_i) - \bar{Q}(t_{i-1}) + \tau\bar{Q}(t_i) + \gamma\bar{Q}(t_i),$$

where $t_i - t_{i-1} = 1$ day, as the data was recorded every day. In this expression, $\tau\bar{Q}(t_i)$ is given by $PCR(t_i)$, and $\gamma\bar{Q}(t_i)$ represents those leaving quarantine center without PCR test ($no\text{-}PCR(t_i)$), implying

$$\phi\lambda(t_i) \approx \bar{Q}(t_i) - \bar{Q}(t_{i-1}) + PCR(t_i) + no\text{-}PCR(t_i).$$

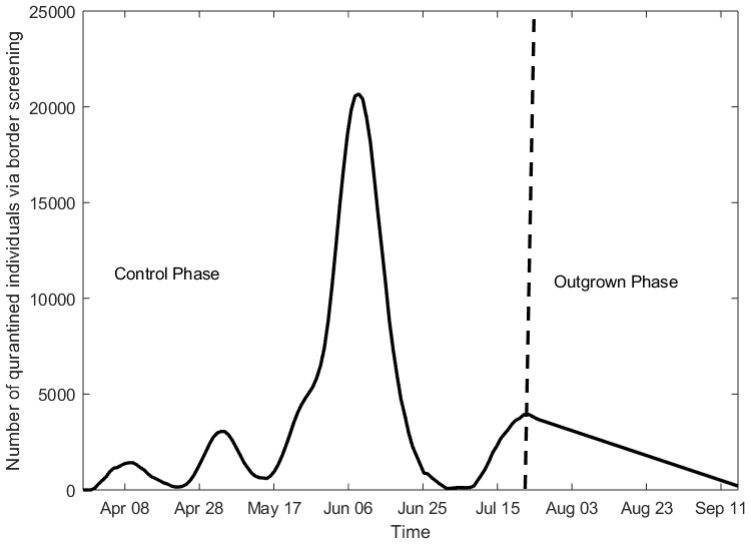

Figure 7: Number of daily quarantined individuals via border screening.

Since $\phi\lambda(t_i) \geq 0$, we obtain the minimum estimate of $no\text{-}PCR(t_i)$ as

$$no\text{-}PCR(t_i) \approx \begin{cases} \bar{Q}(t_i) - \bar{Q}(t_{i-1}) + PCR(t_i), & \text{if} \quad PCR(t_i) > \bar{Q}(t_{i-1}) - \bar{Q}(t_i), \\ 0, & \text{otherwise.} \end{cases}$$

Using data of active quarantine, $\bar{Q}(t_i)$, PCR tests, $PCR(t_i)$ and estimated population leaving quarantine center without PCR, $no\text{-}PCR(t_i)$, we then estimate the daily number of people border screened and entered into the quarantine, $\phi\lambda(t_i)$, until July 21, 2020 (the controlled phase). Our estimates show that the rate of border screen and quarantine was relatively low (less than 2 thousand per day) until the mid of May, 2020, and then the rate increased rapidly reaching a peak of about 16 thousand per day around mid June. After the peak, the rate began to fall and reached a low level by the end of the first phase of epidemic (Fig. 7). Data shows that, after July 21 (the outgrown phase), the active quarantined population continues to decrease indicating less impact of these individuals on the epidemic during the outgrown phase. Therefore, for simplicity, we assume that $\phi\lambda(t_i)$ decreases linearly after July 21 (Fig. 7).

Furthermore, we estimate the per capita rate of individuals leaving quarantine center with (τ) and without (γ) PCR test. We can approximate these rates as follows:

$$\tau \approx \frac{1}{n}\sum_{i=1}^{n} PCR(t_i) \quad \text{and} \quad \gamma \approx \frac{1}{n}\sum_{i=1}^{n} no\text{-}PCR(t_i).$$

Our calculation shows that the individuals leave the quarantine center at the rate $\tau = 0.06$ with PCR test and at the rate $\gamma = 0.00975$ without PCR test.

3.3.2 Epidemic Pattern and Model Validation

We fit our model to daily recorded new cases data of Nepal from both the controlled (March 22 to July 21) and the outgrown phases (July 21 to Sept 16), and estimated six parameters $\phi, \beta_c, \beta_o, \theta_c, \theta_o$, and ρ. The values of the best estimates along with their 95% confidence intervals are provided in Table 2. As shown in Fig. 11a the model has an excellent agreement with the data of recorded new cases from both phases of the epidemic. In addition, we estimated the cumulative cases of COVID-19 during the entire period of study and compared our estimates with the data (Fig. 11b). Our model is capable of accurately predicting the cumulative cases of COVID-19 in Nepal for both epidemic phases, thereby validating our modeling approach.

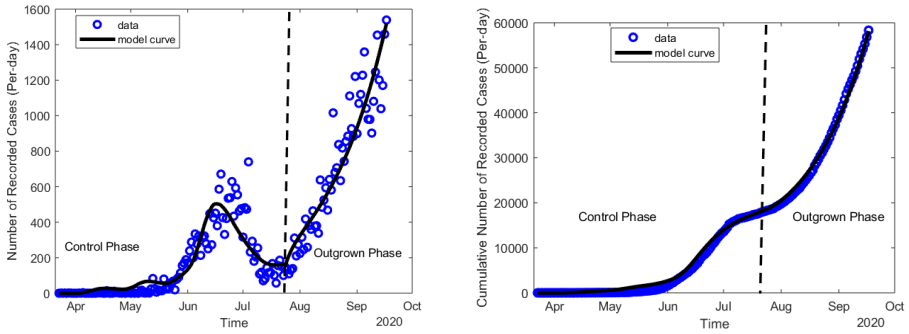

(a) **(b)**

Figure 8: (a) Model fitting with recorded new cases of COVID-19 and (b) the consistency of cumulative data of recorded new cases with the model.

Consistent with the data, the epidemic trend of the COVID-19 in Nepal predicted by our model shows that the recorded COVID-19 cases increased slowly until the mid of May, attained the peak of the controlled phase in the mid June, and then decreased until the end of the first phase (the controlled phase), when the policies were altered. After the controlled phase, the cases again started to rise with a higher rate until the end of the study, giving the outgrown phase following the controlled phase. It's worth noting that the first peak observed during the controlled phase is around the same time when the maximum number of returned migrants were border-screened and quarantined (Fig. 7).

Table 1: Values of estimated and fixed parameters.

Parameters	value	95% CI	Reference
β_c	0.052	[0.0085 0.0955]	Estimated
β_o	0.248	[0.20 0.29]	Estimated
θ_c	0.75	[0.64 0.85]	Estimated
θ_o	0.57	[0.49 0.65]	Estimated
ϕ	0.75	[0.64 0.85]	Estimated
ρ	0.052	[0.04 0.063]	Estimated
k	0.000281	Fixed	Calculated
γ	0.00975	Fixed	Calculated
τ	0.06	Fixed	Calculated
η	0.0588	Fixed	[103]
δ	0.1923	Fixed	[17, 100, 189]

3.3.3 Importation vs Local Transmission in COVID-19 Cases in Nepal

For countries like Nepal that shares open-border with another country (India) having one of the highest levels of COVID-19 cases, it is critical to identify the impact of importation through the border and the local transmission on the disease spread. We used our model to predict imported cases and the cases from local transmission, both recorded and non-recorded (Fig. 9). Our prediction shows that during the controlled phase of the epidemic, most of the COVID-19 cases in Nepal were Imported, indicating the local transmission was well controlled. During this phase, the imported cases gradually increased while the local transmission remained significantly lower than imported cases. The imported cases reached the maximum number (about 460) around July 01, consistent with the highest border screen (Fig. 7), and then gradually decreased for the entire period of our study.

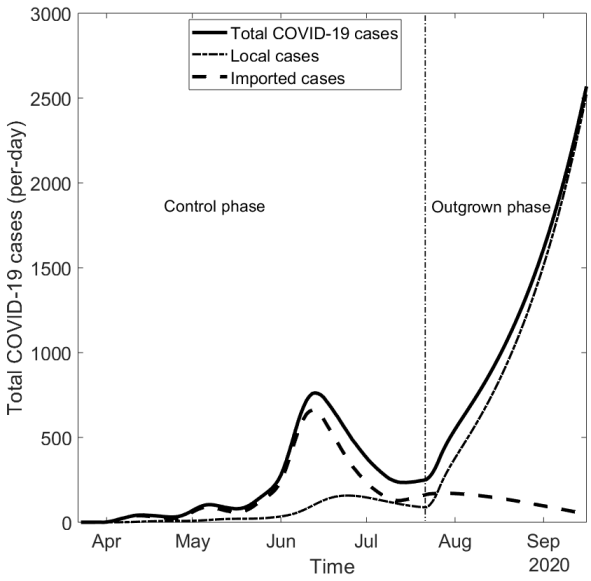

Figure 9: Local and imported cases.

While the local transmission was quite controlled during the controlled phase (only 6,577 $\approx$ 24% of the total cases), during the outgrown phase the local cases dramatically increased outcompeting the imported cases at the end of July. The outgrown phase (July 22-September 16, 2020) resulted in 67073 total cases (recorded and non-recorded), out of which 60123 ($\approx$ 90%) are from local transmission by September 16, 2020 the end date of our study. Note that the timing of the dominance of the local transmission over importation is consistent with the alteration of policies by the government of Nepal, especially the lifting of the lockdown.

3.3.4 Effectiveness of Control Strategies

From the epidemic trend it can be clearly seen that the major policies implemented by the government of Nepal, namely border screen and quarantine, lockdown, and detection and isolation, were significantly effective because the disease spread was well-controlled while the policies were in place and became out of controls once the policies were lifted. We can use our model parameters ϕ, ξ, and ψ to quantify the effectiveness of these policies, border screen and quarantine, lockdown, and detection and isolation, respectively, on controlling COVID-19 epidemic in Nepal during the controlled phase. Our model shows that the epidemic dynamics would have been quite worse (19090 new cases per day during the peak) if these policies were not implemented (Fig. 11a). Through these policies, 442,640 cases were prevented and

1,216 lives were saved during the period of controlled phase (real scenario: 17,994 cumulative cases and 40 deaths (official data); 27460 cumulative cases and 104 deaths (model values)).

We also estimate the effectiveness of each of the policies individually (Fig. 11b). Removing each policy at a time, our model predicts the peak infectious cases of 1339, 4199, 884 for the absence of border screen and quarantine, lockdown, and detection and isolation, respectively. In the absence of border screen and quarantine, lockdown, and detection and isolation, one at a time, the total cumulative cases would have reached 42050, 162400, 38920, respectively, taking the Nepalese lives of 162, 497, 138 respectively. Among these three policies lockdown was found to be the most significant, followed by the border screen and quarantine, and then by the detection and isolation. These results show that the detection and isolation does not seem to have significant impact on the reduction of infections and deaths on the early phase, compared to other two strategies, presumably because of the less local transmission due to the strict lockdown. However, the detection and isolation may have important role and significant impact during outgrown phase when the local transmission becomes the leading cause of infection.

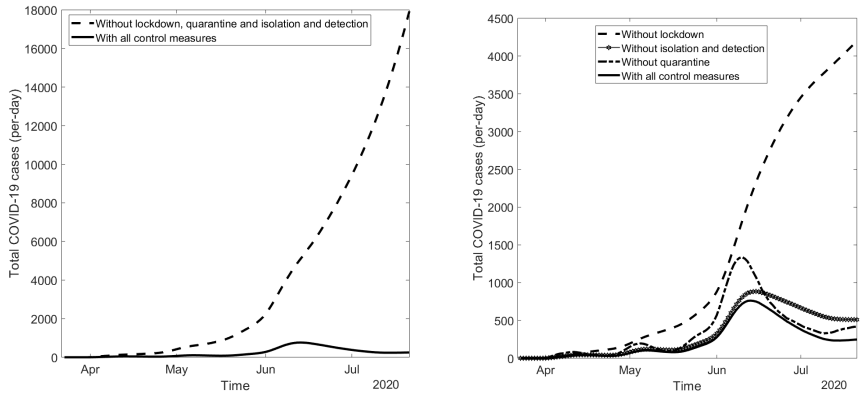

Figure 10: (a) Effect of Overall control strategies. (b) Effect of Lockdown and Quarantine (Border screening, quarantine, detection and isolation and lockdown.

3.3.5 Potential Control of First Wave of COVID-19 in Nepal

In this section, we use our model to predict epidemic outcome, especially the new cases, cumulative cases, and the total deaths, by the end of the year 2021. If the existing trend would be continued, our model predicted that the peak value of daily

new cases will reach 144,600 (82,420 recorded and 62,180 non-recorded) on March 4, 2021 (Fig. 11a). With this epidemic trend, Nepal would be suffer from the cumulative cases of 18.76 million (10.70 million recorded and 8.06 million non-recorded) and the total COVID-19-related deaths of 87 thousand by the end of 2021 (Fig. 11b) if no any Non-pharmaceutical interventions were implemented. But the number of cases would be subsequently decreased if transmission rate would be decreased by any NPIs or the non homogeneous mixing of susceptible.

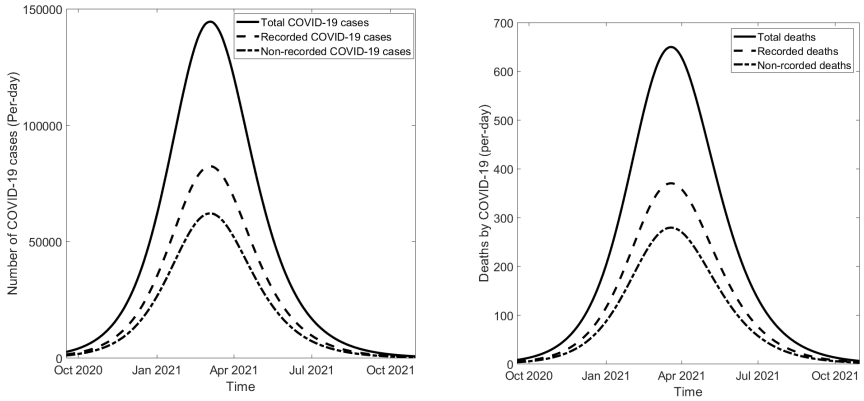

(a) **(b)**

Figure 11: Peak of new cases and number of deaths by COVID-19.

At the existing situation of the absence of pharmaceutical prevention, applying public health measures, including the ones the government of Nepal implemented during the controlled phase, are the most promising control measures [196, 190]. We now assess the impact of these control measures on curbing COVID-19 epidemics from September 2020 to December 2021. Since the existing trend (the outgrown phase) shows that the imported COVID-19 cases were not important compared to the local transmission, we particularly focus on two control strategies, the lockdown and the detection and isolation. Note that the existing value of infection rates is $\beta = \beta_o$ and the detection rate is $\theta = \theta_c$ (Table 2). In our model, the level of lockdown and detection and isolation can be incorporated using the parameters ξ and ψ, respectively.

Our model predicts that both the lockdown (reduction on β) and the detection and isolation (increment in θ) are significantly impact on curbing COVID-19 epidemic burden in Nepal (Fig. 12). For example, 50% reduction of contact through lockdown (i.e., $\xi = 0.5$) can reduce the cumulative number from the base-case of 18.7 million to 426 thousand and the total deaths from 87 thousand to 20 thousand. Similarly, 1.4 times increment in the detection and isolation rate (i.e., $\psi = 1.4$) can bring the

cumulative cases down to 494 thousand and the total death down to 13 thousand.

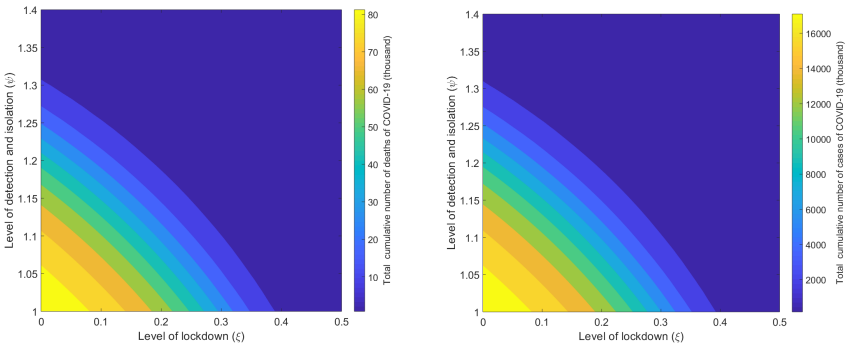

(a) **(b)**

Figure 12: Effect of control policy (ξ and ψ) to reduce the (a) total number of infectious and (b) deaths by COVID-19.

3.3.6 Reproduction Number

Using the estimated parameters, we find the value of $R_0 = 0.21$ for Nepal during the control phase (21 March, 2020 to 21 July 2020). $R_0 < 1$ implies that the outbreak was avoided at that time while the locally infected case was introduced in March 2020. The successful control was consistent with the fact that the local transmission during early epidemic period was negligible with the majority of infections coming from abroad. Furthermore, we find that if the government of Nepal had not timely implemented policies, the basic reproduction number would have been $R_0 = 1.8$ (i.e., replacing β_c by β_o and θ_c by θ_o). Using our model, we also perform analysis to identify the level of lockdown (ξ) and the detection and isolation (ψ) required to assure the value of R_0 less than unity so that the epidemic was avoided. The resulting combinations of these two policies, which can avoid the epidemic, are given in Fig. 9a. For example, a policy with combination of 22% reduction in contact due to lockdown ($\xi = 0.22$) and 20% increase in detection and isolation ($\psi = 1.2$) can avoid epidemic to occur.

The average number of the secondary infections varies over time, mainly due to alteration of implementation policies over the epidemic period. To describe the time varying average number of secondary cases more accurately, we consider the effective reproduction number, R_t. The value of R_t allows us to track whether the epidemic at time t is in increasing ($R_t > 1$) or decreasing ($R_t < 1$) trend. For our model, the effective reproduction number is given by

$$R_t = \frac{\beta(t)\delta(1-\theta(t))S(t)}{(\delta+\mu)(\eta+k+\mu)N(t)}.$$

Using the estimated parameters, we observed that the value of effective reproduction number $R(t)$ remains about 0.21 until July 21 (Fig. 13b), indicating that the local transmission is under control during the the controlled phase. However, around the July-21 (the date of end of policies), the effective reproduction number rapidly increased and reached 1.80 indicating the rapid local transmission during the outgrown phase. The long prediction of our model shows that the value of R_t remained greater than unity until March 2021 (increasing trend). After March 2021, the epidemic would be observed the decreasing trend (i.e, $R_t < 1$).

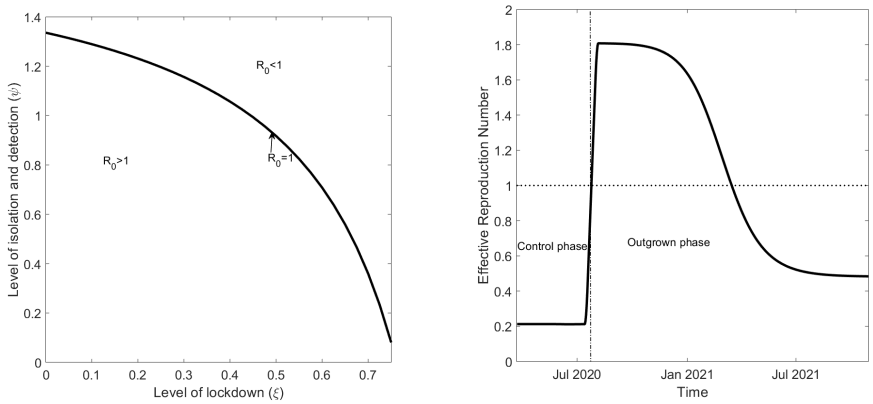

Figure 13: (a) Effect of control policy to prevent the raising of diseases by maintaining $R_t = 1$ and (b) change of reproduction number with time.

3.4 Discussion

In this study, we focused on modeling COVID-19 epidemic in Nepal, which shares open border with India, one of the most affected countries in the world. Since a large number of Nepalese, especially male labor migrants, work in India, the mobility across Nepal-India open border has directly affected COVID-19 cases in Nepal causing considerable number of imported cases through the migrant workers coming from India [61]. Despite a large number of inflow of COVID-19 cases from India, the timely implementation of Nepal Government's policies, namely (i) border screen and quarantine, (ii) lockdown, and (iii) detection and isolation, was successful in controlling the epidemic for about four months until these policies were lifted on July 21, 2020. After the policies were lifted, the cases surged uncontrollably, resulting in biphasic trend of COVID-19 in Nepal, the controlled phase (until July 21, 2020) and

the outgrown phase (after July 21, 2020). In order to evaluate these successful control policies, here we took advantage of modeling and data of unique epidemic in Nepal with biphasic trend resulting from the combination of inflow of cases through border and implementation of control policies. Our novel model, which is capable of excellently describing the COVID-19 data from Nepal, has provided number of important insights into transmission dynamics and related effective control policies.

Using our model and the available data from the ministry of health and population, we estimated the key parameters related to COVID-19 transmission and control in Nepal. Based on our model, we identified quite distinct transmission rate (β) and distinct rate of detection and isolation (θ) between two phases of epidemics, showing that the policies implemented were indeed significantly effective. The timely implementation of policies was able to maintain the low level of effective reproduction number (≈ 0.21) while the polices were in place, and upon lifting the policies the effective reproduction number rapidly rose to 1.80. As per our model evaluation, with these policies the government of Nepal was able to prevent more than 444 thousand cases and save more than 1200 lives. Among these three policies, "lockdown" was found to be the most effective, followed by "border screen and quarantine" and then by "detection and isolation".

Consistent with the data based on the travel history of recorded infectious people (more than 80% came from aboard, especially from India) [60, 126], our result also shows that about 70% of COVID-19 cases in Nepal were imported during the controlled phase. Despite inflow of significant number of COVID-19 cases from India, the local transmission remains well controlled during the controlled phase of epidemic, implying that the "border screen and quarantine" policy in combination with other policies implemented by the government of Nepal was key to avoid a potential early surge of cases from local transmission. Our model predicts high rate of local transmission, consistent with the data, during the outgrown phase (i.e., after the policies were lifted on July 21, 2020). As a result, the contribution of the local transmission to epidemics became significantly high out competing the imported cases after July 21, 2020. We note that along the line of our results, various reports and updates on the situation of Nepal [60, 64, 143, 169, 191, 192, 194] also claim that there were small number of local transmissions before July 21, 2020 and the mass community transmission had become noticeable only after lifting the policies on July 21, 2020.

Based on the existing epidemic trend identified by our model, we predicted that without any policy about 18 million Nepalese ($\sim$ 70% of the total population) will

be infected with COVID-19 by the end of 2021 in the absence of NPIs. The model predicts that the current increasing trend of daily new cases would be continued to increase reaching the peak level of about 144 thousand new cases per day on March 04, 2021. However, we also acknowledge that there was a possibility for the peak time to occur earlier, as projected by some studies [106], if the government reduces the testing of asymptomatic cases (i.e., reduces the detection and isolation in our model) as mentioned in [128]. Because Nepal is in the high risk zone of COVID-19 due to its poor health system and porous borders with India, potential epidemic outcomes predicted by our model strongly recommend the urgent implementation of control strategies.

Since the pharmaceutical controls of COVID-19 was unavailable during its first wave, most of the countries had been implementing the non-pharmaceutical approaches, including the ones implemented by the government of Nepal, for mitigating COVID-19 transmissions. As identified by our model in the context of Nepal, many countries, such as China, Taiwan, and South Korea, which had been successful to control the epidemics, also applied the strict lockdown, meticulous testing and tracking, and massive isolation of people, precise and widespread contact tracing and testing [16, 45, 46, 176] as effective means of epidemic control. Therefore, we also evaluated the local transmission related control strategies "Lockdown" and "Detection and isolation" in the context of Nepal, and identify the level of these policies required for successful mitigation of potential COVID-19 surge in Nepal. For example, our result shows that the lockdown level that can reduce the contact rate by 50% will decrease the peak of new cases of COVID-19 below the 2600, significantly less than the predicted base-case of 144 thousand. In this level of lockdown, the cumulative cases could also be reduced from 18 million to less than 200 thousand. Similarly, the total COVID-19 cases could be reduced to 494 thousand if the detection and isolation policy was increased by 1.4 times the base case. Importantly, our model has identified that for a significantly large level of the detection and isolation (for example, greater than 1.6 time the base case), the disease spread can be avoided without needing lockdown.

We acknowledge some limitations of this study. We used the limited data sets available publicly from the ministry of health and population of Nepal. Because of poor policy at the border, the data related to border screen need to be carefully considered. The detailed data with accurate border screen and quarantine will improve the predictions of our model. While the testing program for border screened population was better documented, the testing for local community is less understood,

which may have slightly impacted on our estimates of detection and isolation rate. However, we conducted sensitivity of this parameter over the wider range. We have ignored the spatial heterogeneity on the dynamics and policy implementation, especially among seven provinces of Nepal. Not all provinces equally share border with India and also cases distribution is not uniform. For example, Gandaki province has sporadic transmission [193] while other six provinces (Province 1, Province 2, Bagmati, Lumbini, Karnali and Sudurpaschim) show clusters of cases. Therefore, future studies on province-wise analysis of COVID-19 transmission along with inter-province mobility will help for better implementation of effective control strategies.

In summary, in this study, we develop a novel mathematical model to uncover effective control strategies that were implemented in unique biphasic epidemic trend in Nepal, under the influence of human mobility across open-border with India, one of the most COVID-19 affected countries in the world. Quantification of these successful control strategies through distinct two phases of epidemic in Nepal (the controlled phase and the outgrown phase) has provided us with opportunity to evaluate the impact of these strategies to curb potential surge in Nepal. Our results may provide important policy guidance for devising the appropriate control strategies for bringing Nepal out from the devastating pandemic.

CHAPTER 4

TRANSMISSION DYNAMICS OF DELTA VARIANT DOMINATED SECOND WAVE OF COVID-19 IN NEPAL

In this chapter, we present a data-driven modeling approach to study the delta variant dominated COVID-19 transmission dynamics focused on two separate regions (high-risk and low-risk). Considering two different regions is essential in the context of Nepal because of the Nepal-India open border and largely populated cities in some regions, making them higher than others. Especially all the districts of the Terai region connected to India and populated cities such as Kathmandu, Surkhet, Pokhara, Lalitpur, Bhaktapur, and Chitwan are taken as a high-risk region. We validated our model by fitting it to the multiple real-time data sets containing new recorded cases from the high- and low-risk regions as well as the hospitalized, Intensive Care Unit (ICU), and Ventilator cases, and estimating key parameters of the model in a realistic range. We estimated the effective reproduction number and predicted the hospital beds, ICU, and Ventilators that would be needed in Nepal until April 2022. Moreover, we extended our model to explore how various vaccination programs would reduce the epidemic burden in Nepal.

4.1 Introduction

The COVID-19 pandemic caused by the novel coronavirus (SARS-CoV-2) continues with multiple waves worldwide. The pandemic has already generated more than 587 million cases and 6.43 million deaths worldwide as of August 6, 2022 [201]. Among the several waves of COVID-19 caused by the different variants of the virus, the Delta variant (B.1.617.2) was the dominating strain during the second wave (June 2021 to December 2021 [71], until it was suppressed by new Omicron variant. The World Health Organization (WHO) classified the Delta variant as a global concern on May

10, 2021, when it had already spread to more than 30 countries [125]. Notably, the Delta variant circulating during the second wave was more infectious [34, 37, 38, 88, 197] than the wild type, and caused the highest number of cases and deaths compared to other waves in Nepal [118].

The crisis of Delta variant COVID-19 surge was catastrophic in Nepal, significantly ruining the fragile health care system after the second week of March 2021 [187] . With the country's population of only 30 million, infections during the second wave soared to over 9000 new cases per day recorded in the first week of May 2020 [118, 137]. As of September 1, 2021, the total COVID-19 related death in Nepal is 10,770, among which more than 7770 were during the second wave [118]. In May 2021, the whole-genome sequencing tests of 35 swab samples confirmed 34 of them as Delta variants (97%) [137]. Note that Alpha variant (B1.1.7) and K417N (AY.1.), a sub-lineage of B.1.617.2, have also been identified in Nepal [119].

In response to the second wave of COVID-19, the Government of Nepal implemented the lockdown on April 29, 2021, beginning from Kathmandu, the capital city, and later extending to all parts of the country [7]. Despite the lockdown for about four months and implemented vaccination, the transmission of the disease was still significantly high (2052 new cases and 20 deaths on September 1, 2021 ([118]). The potential devastation of this pandemic is highly unpredictable, primarily due to significant asymptomatic and undiagnosed cases [19, 103, 121, 149]. Moreover, the transmission dynamics of the second wave of COVID-19 was quite different from the first wave because of the availability of COVID-19 vaccination, improved treatment strategies, and a higher infectivity of the Delta variant [76, 85]. During the second wave, a higher reproduction number has been reported [62, 197], and also infected individuals experienced more severe infection resulting in a higher rate of hospitalization [18, 68, 74, 160]. Different vaccines are found to have varying effects in the community across different regions of the world depending on the variants [2, 109]. Therefore, it is critical to gain insight into the unique transmission pattern and potential burden of COVID-19 in Nepal to design policies for the proper management of health care facilities and vaccination.

4.2 Methods

4.2.1 Data

The data used in this study is obtained from the Ministry of Health and Population, Government of Nepal [118]. We used the data from 14 March to 15 September 2021 to fit the model. The six different data sets, the daily new cases of the whole country, the high-risk and low-risk regions, and number of patients in medical care, ICU, and ventilators were used in our model fitting and simulation.

4.2.2 Transmission Dynamics Model

To develop a transmission dynamics model based on the $SEIR$ framework, the total population is divided into high- and low-risk regions. The high-risk region consists of 22 districts, which have an open border with India and/or have highly populous cities, such as Kathmandu, Kaski, Chitawan, and Surkhet. The remaining districts belong to the low-risk region. The map of Nepal showing the high and low risk region is shown in the figure 14.

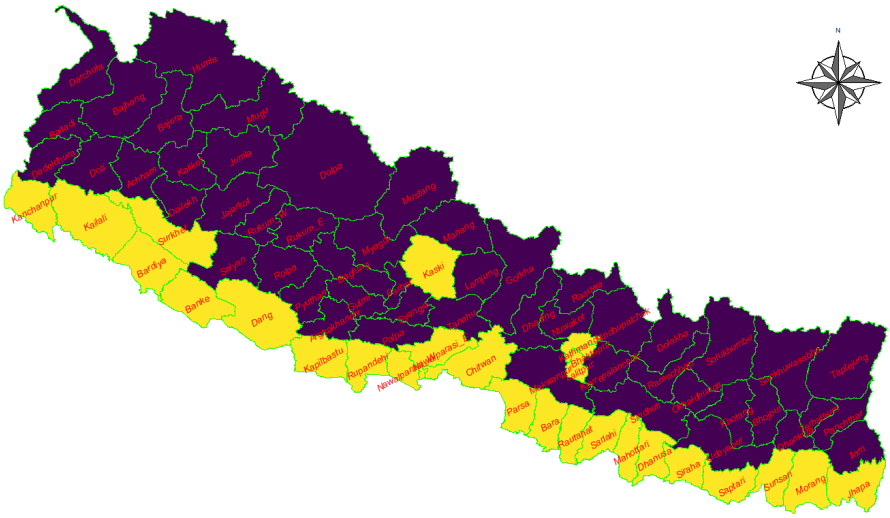

Figure 14: To create the map, the data (shapefile format) was obtained from the official web page (`http://dos.gov.np`) of the government of Nepal (Accessed on April 23, 2021). The map was then created using cartography package in R 4.3.1. The yellow region constitute the districts of high risk region and that of deep blue is low risk region.

The population of each region is divided into sixteen distinct compartments: S_H, S_L

(susceptible), E_H, E_L (exposed), I_{RH}, I_{RL} (recorded infectious), I_{RH}, I_{NL} (non-recorded infectious), M_H, M_L (Medical care), I_{cH}, I_{cL} (ICU), V_H, V_L (Ventilator) and R_H, R_L (recovered), where the suffixes H and L are used to indicate the high- and low-risk regions, respectively. Λ_H and Λ_L represent the birth rate in the high and the low-risk regions, respectively.

The immigrants from abroad enter only the high-risk region at the rate of $\lambda(t)$. Among the immigrants $\lambda(t)$, a portion ϕ is tested by the antigen, and the rest $(1-\phi)$ entered to the community without the antigen test. The portion ρ of the immigrants with a positive test result entered the recorded infected class (I_{RH}) of the high-risk region and the remaining immigrants (negative test result) entered the susceptible class. The immigrants without antigen test entered to the susceptible and non-recorded infectious (I_{NH}) with the same portion as that of tested immigrants. Since the low-risk region does not have a border with India, there is no recruitment from immigration in low-risk regions.

$\gamma(t)$ represents the mobility rate between two regions with corresponding classes (susceptible, exposed, non-recorded infectious, and recovered). The transmission rate from recorded infected individuals of both regions, non-recorded infectious individuals in the high-risk region, and non-recorded infectious individuals in low-risk region are denoted by β_1, $\beta_2(t)$, and $\beta_3(t)$, respectively. The exposed individuals become infectious at the rate of δ, among which a portion θ are recorded and the remaining $(1-\theta)$ remain non-recorded in both regions.

Among the recorded infectious, a portion ω of infected entered the medical care class, and the remaining $(1-\omega)$ enter the class without medical care in both regions. From the medical care class, the severe patients enter an extreme medical care class at the rate ν, among whom a portion ψ require the ventilators and the remaining $(1-\psi)$ portion are admitted to ICU. The rate of recovery from the recorded class without medical care and non-recorded infectious class is denoted by η and those from medical care, ICU, and ventilator are denoted by α_m, α_c, and α_v, respectively. The natural death rate is denoted by μ and the disease-induced death rate for recorded and non-recorded infectious are k and k', respectively. The disease-induced death rate for medical, ICU, and ventilator are k_1, k_2, and k_3, respectively. The schematic diagram of the model is shown in Fig. 15.

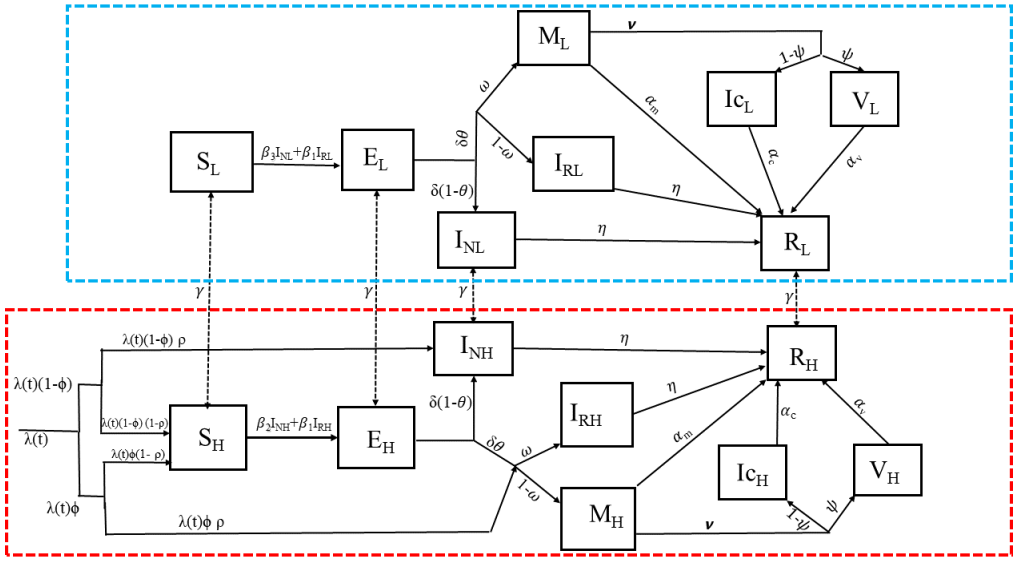

Figure 15: The compartmental diagram of the model. The compartments within the red box and the blue box belong to the high- and the low-risk regions, respectively. The arrow represents the transfer from one compartment to another. For clarity, the natural and disease-induced death rates are not shown in the diagram.

The dynamical system consisting of ODEs of the model is as follows:

$$\frac{dS_H}{dt} = \Lambda_H + \gamma S_L - \frac{(\beta_2 I_{\mathrm{NH}} + \beta_1 I_{\mathrm{RH}})\, S_H}{N_H} - (\gamma + \mu) S_H + \lambda(t)(1-\rho)(1-\phi) + \lambda(t)(1-\rho)\phi \tag{4.1}$$

$$\frac{dS_L}{dt} = \Lambda_L + \gamma S_H - \frac{(\beta_3 I_{NL} + \beta_1 I_{\mathrm{RL}})\, S_L}{N_L} - (\gamma + \mu) S_L \tag{4.2}$$

$$\frac{dE_H}{dt} = \frac{(\beta_2 I_{\mathrm{NH}} + \beta_1 I_{\mathrm{RH}})\, S_H}{N_H} + \gamma E_L - (\gamma + \delta + \mu) E_H \tag{4.3}$$

$$\frac{dE_L}{dt} = \frac{(\beta_3 I_{NL} + \beta_1 I_{RL})\, S_L}{N_L} + \gamma E_H - (\gamma + \delta + \mu) E_L \tag{4.4}$$

$$\frac{dI_{NH}}{dt} = \delta(1-\theta) E_H + \gamma I_{NL} - (\eta + k' + \mu) I_{NH} + \lambda(t)\rho(1-\phi) - \gamma I_{NH} \tag{4.5}$$

$$\frac{dI_{NL}}{dt} = \delta(1-\theta) E_L + \gamma I_{NH} - (\eta + k' + \mu) I_{NL} - \gamma I_{NL} \tag{4.6}$$

$$\frac{dI_{RH}}{dt} = \delta\theta(1-\omega) E_H + \lambda(t)\rho\phi(1-\omega) - (\eta + k + \mu) I_{\mathrm{RH}} \tag{4.7}$$

$$\frac{dI_{RL}}{dt} = \delta\theta(1-\omega)E_L - (\eta + k + \mu)I_{RL} \tag{4.8}$$

$$\frac{dM_H}{dt} = \delta\theta E_H\omega + \lambda(t)\rho\omega\phi - (k_1 + \mu + \alpha_m + \nu)\, M_H \tag{4.9}$$

$$\frac{dM_L}{dt} = \delta\theta\omega E_L - (\alpha_m + k_1 + \mu + \nu)\, M_L \tag{4.10}$$

$$\frac{dI_{cH}}{dt} = \nu(1-\psi)M_H - (\alpha_c + k_2 + \mu)\, I_{cH} \tag{4.11}$$

$$\frac{dI_{cL}}{dt} = \nu(1-\psi)M_L - (\alpha_c + k_2 + \mu)\, I_{cL} \tag{4.12}$$

$$\frac{dV_H}{dt} = \nu\psi M_H - (\alpha_c + k_2 + \mu)\, V_H \tag{4.13}$$

$$\frac{dV_L}{dt} = \nu\psi M_L - (\alpha_c + k_2 + \mu)\, V_L \tag{4.14}$$

$$\frac{dR_H}{dt} = \alpha_c I_{cH} + \alpha_m M_H + \eta(I_{RH} + I_{NH}) + \alpha_v V_H + \gamma R_L - (\mu + \gamma)R_H \tag{4.15}$$

$$\frac{dR_L}{dt} = \alpha_c I_{cL} + \gamma R_H + \alpha_m M_L + \eta(I_{NL} + I_{RL}) + \alpha_v V_L - (\gamma + \mu)R_L. \tag{4.16}$$

Here, $N_H = S_H + E_H + I_{RH} + I_{NH} + M_H + I_{cH} + V_H + R_H$ and $N_L = S_L + E_L + I_{RL} + I_{NL} + M_L + I_{cL} + V_L + R_L$.

4.2.3 Extension of Model to Integrate the Vaccination Program

We extended our model to incorporate the vaccination program by further dividing each compartment into vaccinated and non-vaccinated compartments except the recorded infectious compartments and medical compartments. For our study period, we assumed that there is no loss of immunity of vaccinated and recovered people. In the vaccinated compartments, there is a reduced infection rates and a reduced rates of hospitalization and medical care. The schematic compartmental diagram of the model with vaccination program is shown in Fig. 16.

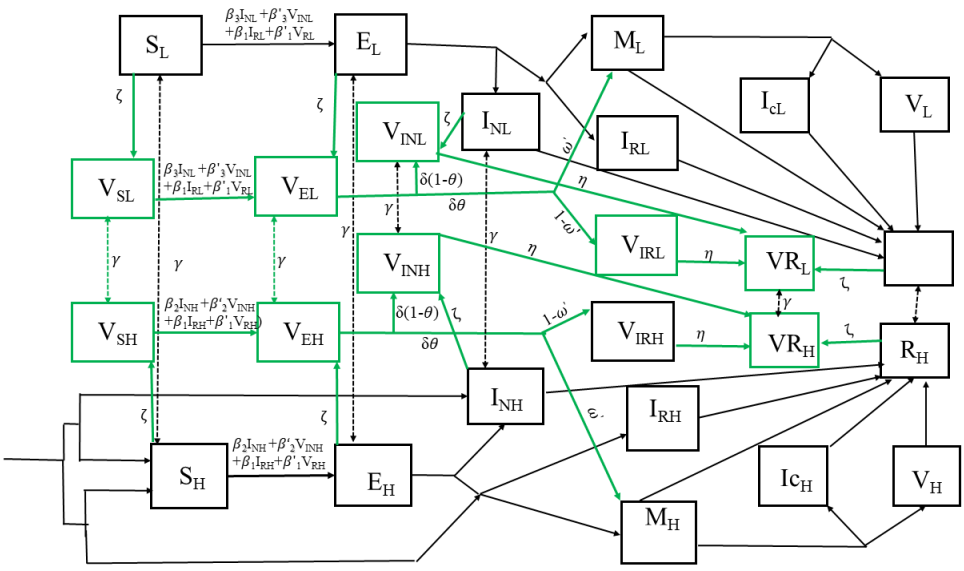

Figure 16: The compartmental diagram of the model with vaccination. The green boxes represent the vaccinated compartments. All other rates of transfer between compartments are the same as in Fig. 15 except transmission rates and hospitalization rates (β_i', $i = 1, 2, 3$, and ω').

4.2.4 Integration of Lockdown Policy in the Model

The lockdown in Kathmandu valley was started on March 29, 2021 and gradually extended to almost all parts of the country. To model this scenario, we define the transmission rate $\beta_2(t)$ and $\beta_3(t)$ as follows:

$$\beta_2(t) = \begin{cases} \beta_H, & \text{for } t \leq 47 \\ \beta_H((1-c_b)e^{(-r_H t)} + c_b), & \text{for } t \geq 47 \end{cases}$$

$$\beta_3(t) = \begin{cases} \beta_L, & \text{for } t \leq 47 \\ \beta_L((1-c_b)e^{(-r_L t)} + c_b), & \text{for } t \geq 47 \end{cases}$$

where β_H and β_L represent the transmission rates before lockdown on the high-risk region and the low-risk region, respectively. Following the lockdown, the transmission rates of high-risk and low-risk regions decay at the rates r_H and r_L, respectively. We further estimate the different values of r_H and r_L for different time periods according to the different levels of lockdown. We took $c_b = 0.3$ assuming up to 70% reduction on contacts during the prolonged lockdown period [132]. Note that the transmission of diseases by the recorded infectious remains the same regardless of the lockdown situation. Since the inter region mobility is quite different during the lockdown period from the per-lockdown period, we consider two different mobility rates $\gamma(t) = \gamma_1$,

and γ_2 for the period of pre-lockdown and lockdown, respectively. The remaining parameters were estimated from data fitting by using the least square method.

4.2.5 Initial Values of the State Variables

The new cases have been raised since March 14, 2021, so we take March 14, 2021, as initial time ($t = 0$). The total population of Nepal in the census year 2011 was 26,494,504 and it is projected to be 29,996,478 at the end of 2020 [40]. There are about 3 to 4 million Nepalese workings in India [99, 140] as a seasonal migrant workers, so we deduct 3.5 million people from the total population. The seroprevalence survey in Nepal [121] during the first wave also shows the 14.4% (95%CI 11.8-17.0) which was conducted in the first week of October 2020 when the first wave was in peak. By using our model [4] with fitting the remaining data (from 17 September 2020 to 13 March 2021), we approximately estimate the 24% seroprevalence up to 14 March 2021. We also deduct this population and finally take the initial susceptible $20,000,000$ for this study. Out of these susceptible, our high and low-risk regions constitutes about 65% and 35% population respectively[40] so, we take $S_H(0) = 13,000,000$ and $S_L(0) = 7,000,000$. Similarly, we have 24% seroprevalence in to two regions which gives us $R_H(0) = 4,700,000$ and $R_L(0) = 2,500,000$. We approximately assumed the values of other other remaining state variables as for the best fit of the model.

Table 2: Values of estimated and fixed parameters.

Description	State variables	Base Value	Reference
Susceptible population in high risk region	$S_H(0)$	12,818,000	Calculated
Susceptible population in low risk region	$S_L(0)$	6,479,000	Calculated
Exposed population in high risk region	$E_H(0)$	100	Assumed
Exposed population in low risk region	$E_L(0)$	80	Assumed
Recorded infectious population in high risk region	$I_{RH}(0)$	200	Assumed
Recorded infectious population in low risk region	$I_{RL}(0)$	100	Assumed
Non-Recorded infectious population in high risk region	$I_{NH}(0)$	1000	Assumed
Non-Recorded infectious population in low risk region	$I_{NL}(0)$	800	Assumed
Patients in medical care in high risk region	$M_H(0)$	0	Assumed
Patients in medical care in low risk region	$M_L(0)$	0	Assumed
Patients in medical care in high risk region	$I_{cH}(0)$	0	Assumed
Patients in medical care in low risk region	$M_{cL}(0)$	0	Assumed
Patients in medical care in high risk region	$V_H(0)$	0	Assumed
Patients in medical care in low risk region	$V_L(0)$	0	Assumed
Recovered population in high risk region	$R_H(0)$	4,608,000	Calculated
Recovered population in low risk region	$R_L(0)$	2,568,000	Calculated

4.2.6 Calculation of the Effective Reproduction Number

We use the approach developed by Thompson et. al [173] (describe in the section 2.1.5) for the estimation of effective reproduction numbers using the EpiEstem package of the R program. We take the mean serial interval as 4.7 days (95% CrI: 3.7, 6.0) days, with an SD of 2.9 days (95% CrI: 1.9, 4.9) days based on the study [127].

4.2.7 Parameter Estimation and Model Fitting to Data

The model is fitted to the multiple data sets, containing the daily new cases of the whole country, the high-risk and low-risk regions, and patients in medical care, ICU, and ventilators. From our model, the recorded new infections in Nepal, the high-risk region, and the low-risk region, the number of patients in medical care, ICU and

ventilator at time t can be computed using the following respective equations:

$$L_r(t) = \delta\theta E_H + \lambda(t)\phi\rho + \delta\theta E_L, \tag{4.17}$$

$$L_{rh}(t) = \delta\theta E_H + \lambda(t)\phi\rho, \tag{4.18}$$

$$L_{rl}(t) = \delta\theta E_L, \tag{4.19}$$

$$L_m(t) = \int_0^t (\delta\omega\theta(E_H+E_L)+\lambda(t)\phi\rho\omega-\alpha_m(M_H+M_L)-k_1(M_H+M_L)-\nu(M_H+M_L))dt, \tag{4.20}$$

$$L_c(t) = \int_0^t (\nu(1-\psi)(M_H+M_L) - (k_2+\alpha_c)(M_H+M_L))dt, \tag{4.21}$$

$$L_v(t) = \int_0^t (\nu\psi(M_H+M_L) - (k_3+\alpha_v)(V_H+V_L))dt. \tag{4.22}$$

We use the solutions to obtain the best-fit parameters via a nonlinear least-squares regression method (describe in the section 2.2). that minimizes the following sum of the squared residuals:

$$J(\Phi^*) = \sum_{i=1}^{n} \big[\big(L_r(t_i) - \bar{L_r}(t_i)\big)^2 + \big(L_{rh}(t_i) - \bar{L_{rh}}(t_i)\big)^2 + \big(L_{rl}(t_i) - \bar{L_{rl}}(t_i)\big)^2 + \big(L_m(t_i) - \bar{L_m}(t_i)\big)^2 + \big(L_c(t_i) - \bar{L_c}(t_i)\big)^2 + \big(L_v(t_i) - \bar{L_v}(t_i)\big)^2\big].$$

Here, $\Phi^* = (\beta_1, \beta_H, \beta_L, \theta, r_H, r_L, \gamma_1, \gamma_2, \omega, \nu, \psi, \alpha_m, \alpha_c, \alpha_v, \nu, k, k', k_1, k_2, k_3)$ is a vector of parameters to be estimated.

4.2.8 Computation of Basic Reproduction Number

4.2.8.1 Reproduction Number of the Whole Country

First we calculate the diseases free equilibrium point. At the disease free equilibrium point the portion of positive antigen test is zero, i.e $\rho = 0$, and we use the pre-pandemic condition $\lambda = \lambda(0)$ and $E_H = E_L = I_{RH} = I_{RL} = I_{NH} = I_{NL} = M_H = M_L = I_{cH} = I_{cL} = V_H = V_L = 0$. We get the following disease free equilibrium point: $E^* = (S_H^*, S_L^*, 0, 0, 0, 0, 0, 0, 0, 0, 0, 0, 0, 0, 0, 0, 0)$, where

$$S_H^* = \frac{\lambda(0)(\gamma+\mu) + (\gamma+\mu)\Lambda_H + \gamma\Lambda_L}{\mu(2\gamma+\mu)},\ S_L^* = \frac{\gamma\lambda(0) + \gamma\Lambda_H + (\gamma+\mu)\Lambda_L}{\mu(2\gamma+\mu)}.$$

We now divide the compartments into two groups: infected $\vec{x} = (x_i, i = 1, 2, ..., 12) = (E_H, E_L, I_{RH}, I_{RL}, I_{NH}, I_{NL}, M_H, M_L, I_{cH}, I_{cL}, V_H, V_L)$ and non-infected $\vec{y} = (y_j, j = 1, 2, 3, 4) = (S_H, S_L, R_H, R_L)$. Then the system (4.1-4.16) can be written as:

$$x_i' = f_i(\vec{x}, \vec{y}) \text{ and } y_j' = g_j(\vec{x}, \vec{y}) \text{ for } i = 1, 2, ..., 12, j = 1, 2, 3, 4.$$

The right hand side of the system of infected compartments can be written as: $f_i(\vec{x}, \vec{y}) = F_i(\vec{x}, \vec{y}) - V_i(\vec{x}, \vec{y})$, where $F_i(\vec{x}, \vec{y})$ contains the terms representing the new infections in compartment i and $V_i(\vec{x}, \vec{y})$ contains the terms containing the difference between the transfer of individuals out of and into the compartment i. Then we construct the following two matrices using $F = \left(\frac{\partial F_i}{\partial x_i}\right)$ and $V = \left(\frac{\partial V_i}{\partial x_i}\right)$ at the diseases free equilibrium (DFE) point as follows:

$$F = \begin{pmatrix} A_{6\times6} & 0_{6\times6} \\ 0_{6\times6} & 0_{6\times6} \end{pmatrix}, \quad V = \begin{pmatrix} B_{8\times6} & 0_{6\times6} \\ 0_{4\times6} & C_{6\times6} \end{pmatrix},$$

where

$$A = \begin{pmatrix} 0 & 0 & \frac{\beta_1 S_H^*}{N_L^*} & 0 & \frac{\beta_H S_H^*}{N_H^*} & 0 \\ 0 & 0 & 0 & \frac{\beta_1 S_L^*}{N_L} & 0 & \frac{\beta_L S_L^*}{N_L^*} \\ 0 & 0 & 0 & 0 & 0 & 0 \\ 0 & 0 & 0 & 0 & 0 & 0 \\ 0 & 0 & 0 & 0 & 0 & 0 \\ 0 & 0 & 0 & 0 & 0 & 0 \end{pmatrix},$$

$$B = \begin{pmatrix} \gamma+\delta+\mu & -\gamma & 0 & 0 & 0 & 0 \\ -\gamma & \gamma+\delta+\mu & 0 & 0 & 0 & 0 \\ -\delta\theta(1-\omega) & 0 & k+\eta+\mu & 0 & 0 & 0 \\ 0 & -\delta\theta(1-\omega) & 0 & k+\eta+\mu & 0 & 0 \\ -\delta(1-\theta) & 0 & 0 & 0 & \gamma+\eta+\mu+k' & -\gamma \\ 0 & -\delta(1-\theta) & 0 & 0 & -\gamma & \gamma+\eta+\mu+k' \\ -\delta\theta\omega & 0 & 0 & 0 & 0 & 0 \\ 0 & -\delta\theta\omega & 0 & 0 & 0 & 0 \end{pmatrix},$$

and

$$C = \begin{pmatrix} p & 0 & 0 & 0 & 0 & 0 \\ 0 & p & 0 & 0 & 0 & 0 \\ -\nu(1-\psi) & 0 & q & 0 & 0 & 0 \\ 0 & -\nu(1-\psi) & 0 & q & 0 & 0 \\ -\nu\psi & 0 & 0 & 0 & r & 0 \\ 0 & -\nu\psi & 0 & 0 & 0 & r \end{pmatrix}.$$

Here $p = k_1 + \mu + \alpha_m$, $\quad q = \alpha_c + k_2 + \mu$, and $r = k_3 + \mu + \alpha_v$.

The largest eigenvalue of the matrix FV^{-1} gives the basic reproduction number as follows:

$$R_0 = \frac{1}{2}\left(D + \sqrt{D^2 - 4E}\right), \tag{4.23}$$

where

$$D = \frac{\beta_1 T_1 S_H^* N_L^* + \beta_1 T_1 S_L^* N_H^* + \beta_2 T_3 S_H^* N_L^* + \beta_3 T_3 S_L^* N_H^*}{N_H^* N_L^*},$$

$$E = \frac{S_H^* S_L^* \left(\beta_1^2 T_1^2 - \beta_1^2 T_2^2 + (\beta_2 + \beta_3)\,\beta_1 T_1 T_3 - (\beta_2 + \beta_3)\,\beta_1 T_2 T_4 + \beta_2 \beta_3 \left(T_3^2 - T_4^2\right)\right)}{N_H^* N_L^*},$$

$$T_1 = \frac{\delta\theta(1-\omega)(\gamma+\delta+\mu)}{(\delta+\mu)(2\gamma+\delta+\mu)(\eta+k+\mu)}, \qquad T_2 = \frac{\gamma\delta\theta(1-\omega)}{(\delta+\mu)(2\gamma+\delta+\mu)(\eta+k+\mu)},$$

$$T_3 = \frac{\gamma\delta(1-\theta)\,(2\gamma+\delta+\eta+k'+2\mu)}{(\delta+\mu)N_L(2\gamma+\delta+\mu)\,(\eta+k'+\mu)\,(2\gamma+\eta+k'+\mu)},$$

$$\text{and} \quad T_4 = \frac{\delta(1-\theta)\,(\delta\eta+\delta\mu+\eta\mu+\gamma\,(2\gamma+\delta+\eta+k'+2\mu)+\delta k'+\mu k'+\mu^2)}{(\delta+\mu)(2\gamma+\delta+\mu)\,(\eta+k'+\mu)\,(2\gamma+\eta+k'+\mu)}.$$

At the Diseases Free Equilibrium (DFE) point, $S_H^* = N_H^*$, and $S_L^* = N_L^*$, then the basic reproduction number is obtained as:

$$R_0 = \frac{1}{2}\left(2\beta_1 T_1 + \beta_2 T_3 + \beta_3 T_3 + \sqrt{4\beta_2\beta_3 T_4^2 + 4\beta_1\beta_3 T_2 T_4 + 4\beta_1^2 T_2^2 + (\beta_2 - \beta_3)^{\,2} T_3^2 + 4\beta_1\beta_2 T_2 T_3}\right). \tag{4.24}$$

The corresponding effective reproduction number is obtained by making the respective state variables of Eqn. 4.23 as function of t.

4.2.8.2 Reproduction Number of the High Risk Region

Similar to the section 4.2.8.1, we construct the following two matrices for high risk region at DFE point as follows:

$$F_H = \begin{pmatrix} 0 & \frac{\beta_1 S_H^*}{N_H^*} & \frac{\beta_2 S_H^*}{N_H^*} & 0 & 0 & 0 \\ 0 & 0 & 0 & 0 & 0 & 0 \\ 0 & 0 & 0 & 0 & 0 & 0 \\ 0 & 0 & 0 & 0 & 0 & 0 \\ 0 & 0 & 0 & 0 & 0 & 0 \\ 0 & 0 & 0 & 0 & 0 & 0 \end{pmatrix}$$

$$V_H = \begin{pmatrix} \gamma+\delta+\mu & 0 & 0 & 0 & 0 & 0 \\ -\delta\theta(1-\omega) & k+\eta+\mu & 0 & 0 & 0 & 0 \\ -\delta(1-\theta) & 0 & k'+\gamma+\eta+\mu & 0 & 0 & 0 \\ -\delta\theta\omega & 0 & 0 & \mu+\nu+k_1+\alpha_m & 0 & 0 \\ 0 & 0 & 0 & -\nu(1-\psi) & \mu+k_2+\alpha_c & 0 \\ 0 & 0 & 0 & -\nu\psi & 0 & \mu+k_3+\alpha_v \end{pmatrix}.$$

and, furthermore,

$$F_H V_H^{-1} = \begin{pmatrix} \frac{\delta\theta(1-\omega)S_H^*\beta_1}{(\gamma+\delta+\mu)(k+\eta+\mu)N_H^*} + \frac{\delta(1-\theta)S_H^*\beta_2}{(\gamma+\delta+\mu)(k'+\gamma+\eta+\mu)N_H^*} & \frac{S_H^*\beta_1}{(k+\eta+\mu)N_H^*} & \frac{S_H^*\beta_2}{(k'+\gamma+\eta+\mu)N_H^*} & 0 & 0 & 0 \\ 0 & 0 & 0 & 0 & 0 & 0 \\ 0 & 0 & 0 & 0 & 0 & 0 \\ 0 & 0 & 0 & 0 & 0 & 0 \\ 0 & 0 & 0 & 0 & 0 & 0 \\ 0 & 0 & 0 & 0 & 0 & 0 \end{pmatrix}.$$

The dominated Eigenvalue of $F_H V_H^{-1}$ gives the basic reproduction number of the high-risk region as follows.

$$R_{H0} = \frac{S_H^*\delta\left(\beta_2(1-\theta)(\eta+k+\mu)+\theta\beta_1(1-\omega)(\gamma+\eta+k'+\mu)\right)}{N_H^*(\gamma+\delta+\mu)(\eta+k+\mu)(\gamma+\eta+k'+\mu)}. \tag{4.25}$$

. Using $N_H^* = S_H^*$ for DFE point, we obtain

$$R_{H0} = \frac{\delta\left(\beta_2(1-\theta)(\eta+k+\mu)+\theta\beta_1(1-\omega)(\gamma+\eta+k'+\mu)\right)}{(\gamma+\delta+\mu)(\eta+k+\mu)(\gamma+\eta+k'+\mu)}. \tag{4.26}$$

The corresponding effective reproduction number is obtained by making the respective state variables of Eqn. 4.25 as function of t.

4.2.8.3 Reproduction Number of the Low Risk Region

Similar to the high risk region, we construct the following two matrices for low risk region at DFE point as follows:

$$F_L = \begin{pmatrix} 0 & \frac{\beta_1 S_L^*}{N_L^*} & \frac{\beta_3 S_L^*}{N_L^*} & 0 & 0 & 0 \\ 0 & 0 & 0 & 0 & 0 & 0 \\ 0 & 0 & 0 & 0 & 0 & 0 \\ 0 & 0 & 0 & 0 & 0 & 0 \\ 0 & 0 & 0 & 0 & 0 & 0 \\ 0 & 0 & 0 & 0 & 0 & 0 \end{pmatrix}$$

and

$$V_L = \begin{pmatrix} \gamma+\delta+\mu & 0 & 0 & 0 & 0 & 0 \\ -\delta\theta(1-\omega) & k+\eta+\mu & 0 & 0 & 0 & 0 \\ -\delta(1-\theta) & 0 & k'+\gamma+\eta+\mu & 0 & 0 & 0 \\ -\delta\theta\omega & 0 & 0 & \mu+\nu+k_1+\alpha_m & 0 & 0 \\ 0 & 0 & 0 & -\nu(1-\psi) & \mu+k_2+\alpha_c & 0 \\ 0 & 0 & 0 & -\nu\psi & 0 & \mu+k_3+\alpha_v \end{pmatrix}.$$

Now, we have

$$F_L V_L^{-1} = \begin{pmatrix} \frac{\delta\theta(1-\omega)S_L^*\beta_1}{(\gamma+\delta+\mu)(k+\eta+\mu)N_L^*} + \frac{\delta(1-\theta)S_L^*\beta_3}{(\gamma+\delta+\mu)(k'+\gamma+\eta+\mu)N_L^*} & \frac{S_L^*\beta_1}{(k+\eta+\mu)N_L^*} & \frac{S_L^*\beta_3}{(k'+\gamma+\eta+\mu)N_L^*} & 0 & 0 & 0 \\ 0 & 0 & 0 & 0 & 0 & 0 \\ 0 & 0 & 0 & 0 & 0 & 0 \\ 0 & 0 & 0 & 0 & 0 & 0 \\ 0 & 0 & 0 & 0 & 0 & 0 \\ 0 & 0 & 0 & 0 & 0 & 0 \end{pmatrix}.$$

The dominated eigenvalue of $F_H V_H^{-1}$ gives the basic reproduction number as follows.

$$R_{L0} = \frac{S_L^*\delta\left(\beta_1\theta(1-\omega)(\gamma+\eta+k'+\mu)+\beta_3(1-\theta)(\eta+k+\mu)\right)}{N_L^*(\gamma+\delta+\mu)(\eta+k+\mu)(\gamma+\eta+k'+\mu)}. \tag{4.27}$$

Using $N_L^* = S_L^*$ for DFE point, we obtain

$$R_{L0} = \frac{\delta\left(\beta_1\theta(1-\omega)(\gamma+\eta+k'+\mu)+\beta_3(1-\theta)(\eta+k+\mu)\right)}{(\gamma+\delta+\mu)(\eta+k+\mu)(\gamma+\eta+k'+\mu)}. \tag{4.28}$$

The corresponding effective reproduction number is obtained by making the respective state variables of Eqn. 4.28 as function of t.

4.3 Results:

4.3.1 Pattern of the Second Wave of COVID-19 in Nepal and Model Validation

We used the extended model to fit the data and future predictions. The model was fitted to the multiple data sets consisting altogether 1116 data points simultaneously (186 data points of each of the daily recorded new cases in the whole country, the high-risk region, and the low-risk region, and cases in medical care, ICU, and ventilator Fig. 17). The large number of 6 different kinds of data points allowed us to estimate the unique parameters. In the beginning, the vaccination level in Nepal was negligible,

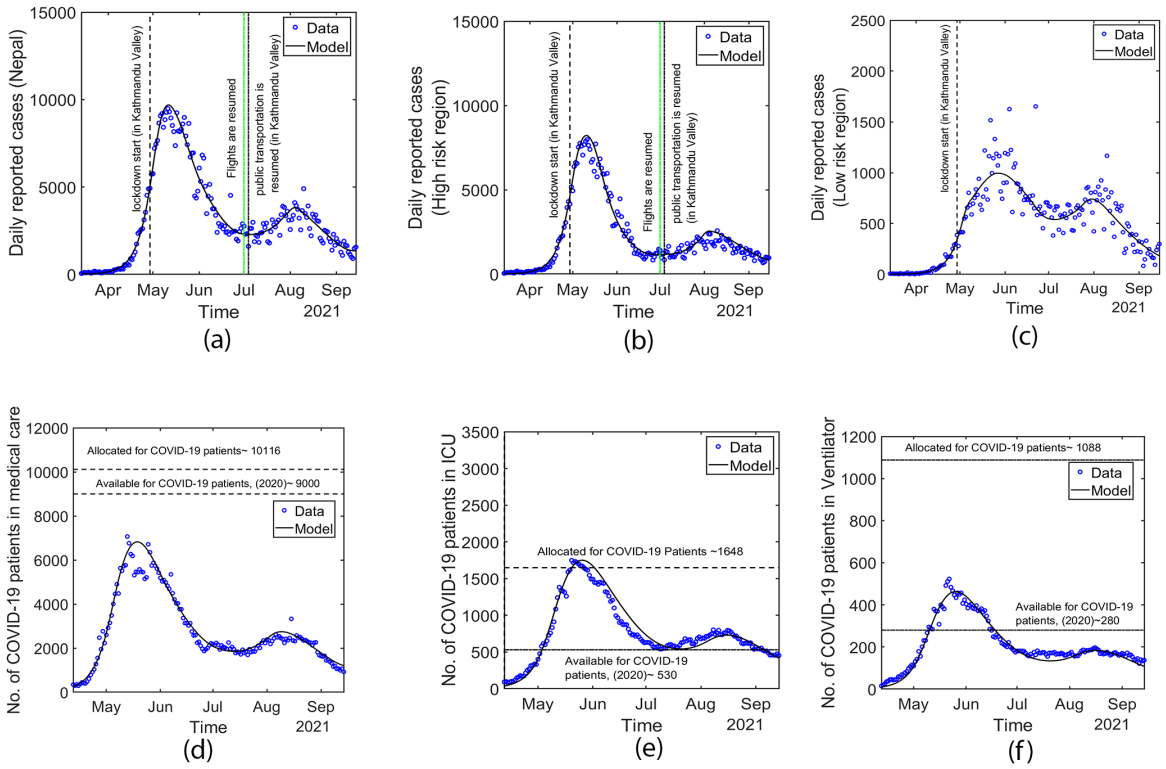

Figure 17: Model Fitting to Multiple Data Sets. Daily reported cases of the whole country Nepal (a), the high-risk region (b), and the low-risk region (b), and cases in medical care (d), ICU (e), and ventilator (f). Solid lines represent the model prediction, and the circles represent the data.

but from middle of July 2021, the vaccination rate was significantly increased. So, we also incorporated the realistic vaccination program in our basic model fitting. The model is in excellent agreement with each data set, asserting the validation of our model.

We take different decay rates r_H and r_L of transmission to address the different level of lockdown in different parts as follows:

$$r_H = \left\{ \begin{array}{l} 0, \ \text{ for } 0 \leq t \leq 47 \ \text{ Pre-lockdown period)} \\ 0.082, \ \text{ for } 47 \leq t < 52 \ \text{ Lockdown start at Kathmandu Valley)} \\ 0.13, \ \text{ for } 52 \leq t < 95 \ \text{ Lockdown to all regions)} \\ -0.05, \ \text{ for } 95 \leq t < 135 \ \text{ (Relaxation of lockdown)} \\ 0.035, \ \text{ for } 135 \leq t < 186 \ \text{ (Partial re-lockdown in some parts)} \end{array} \right\},$$

Table 3: Values of estimated and fixed parameters

Symbol	Value	References
β_1	0.005	Data fitting
β_H	0.525	Data fitting
β_L	0.235	Data fitting
θ	0.05	Data fitting
ϕ	0.1	Data fitting
ρ	0.1	[118]
k	0.0002	Data fitting
k'	0.00002	Data fitting
k_1, k_2, k_3	0.001,0.041,0.071	Data fitting
γ_1, γ_2	0.015, 0.0001	Data fitting
ω	0.1125	Data fitting
τ	0.1	Data fitting
ν	0.05	Data fitting
ψ	0.21	Data fitting
$\alpha_m, \alpha_c, \alpha_v$	0.092,0.1,0.0625	Data fitting
η	0.0588	[195]
δ	0.1923	[105]

$$r_H = \left\{ \begin{array}{l} 0, \text{ for } 0 \leq t \leq 47 \text{ Pre-lockdown period)} \\ 0.033, \text{ for } 47 \leq t < 105 \text{ Lockdown start and extend to other parts)} \\ -0.038, \text{ for } 105 \leq t < 135 \text{ (Relaxation of lockdown)} \\ 0.038, \text{ for } 135 \leq t < 186 \text{ (Partial re-lockdown in some parts)} \end{array} \right\},$$

The second wave increased rapidly until the 1st week of May 2021, hitting the highest new cases of 9,070 on May 6, 2021. The implementation of lockdown reduces the new cases in both the high- and low-risk regions, but the effect observed in the low-risk region was one month delayed compared to the high-risk region. Such spatial disparity under the same national-level program was also noted in the previous study (46), which performed the province-wise analysis of the first wave of COVID-19 in Nepal. After the relaxation in lockdown in some places of the high- and low-risk regions, the COVID-19 cases re-surged from mid-July of 2021, forcing these places to impose the second lockdown (For example, Jhapa district imposed the second lockdown from the last week of July 2021 and then relaxed from the second week of August 2021 [168]). The estimated parameters are given in Table 2.

4.3.2 Long-term Prediction of the Second Wave of COVID-19 in Nepal

Here, we used our extended model to predict the long-term trend of the epidemic from 16 September 2021 to the end of April 2022 with the scenario of gradual relaxation of lockdown to reach the pre-lockdown phase. We also used our model to evaluate the various vaccination programs that the Nepal Government could implement. The trend of the epidemic with the level of vaccination implemented by the government (Fig. 18) shows a steady decrease to an almost extinct level with no cases of hospitalization at the end of April 2022. However, we note that our prediction was for the scenario in which no novel strain of SARS-CoV-2 would dominate the transmission. As per model estimations, 111,300 new cases would be reported, with 11,890 people needing medical care, 3590 needing ICU, and 950 needing ventilators, from September 16, 2021, to April 30, 2022.

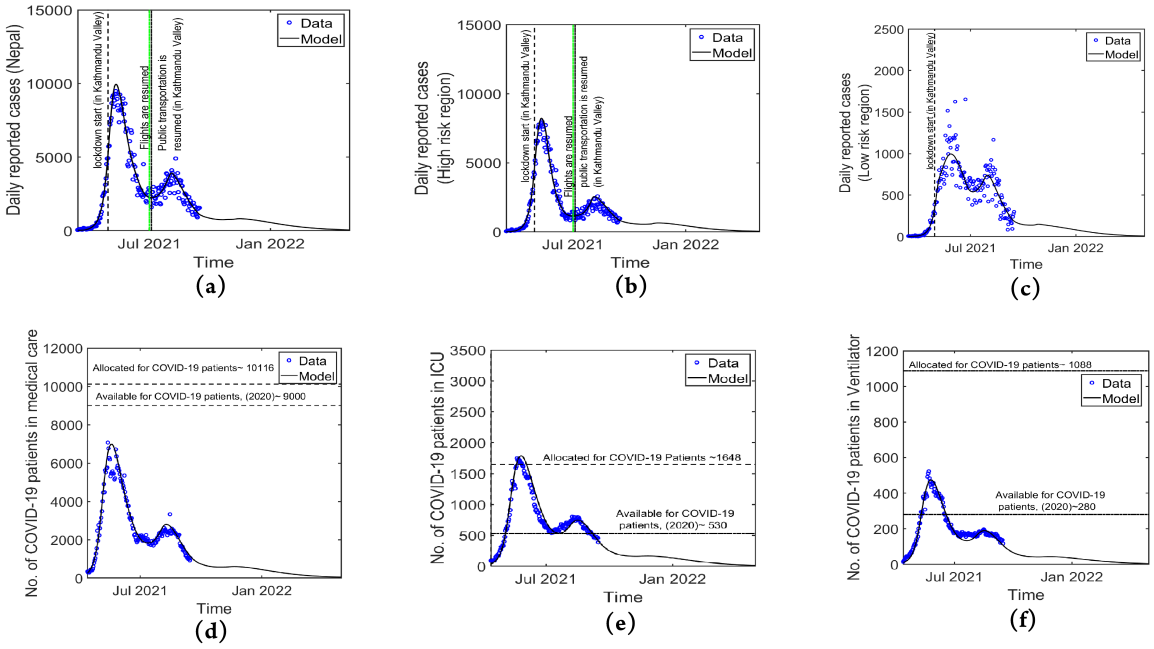

Figure 18: Long term Prediction of the Model. Prediction of daily reported cases of the whole country Nepal (a), the high-risk region (b), and the low-risk region (b), and cases in medical care (d), ICU (e), and ventilator (f), predicted by the model until April 30, 2022.

4.3.3 Estimation of Reproduction Number in Nepal

We first estimated the reproduction number (R_t) from the data using the Maximum Likelihood Method (MLM) described in the section (2.1.5). As mentioned earlier, the

April 14 was the starting date of the second wave of COVID-19 in Nepal.Taking the 7 day window for the calculation of R_t (see method section), we estimated the reproduction number from 21 April 2021-15 September 2021 (the last data considered). We observed that before the lockdown, R_t reached up to 2 in both the high- and low-risk regions as well as in the whole country (around the 3rd week of April), indicating that the significant community transmission of the disease had already occurred before the lockdown.

While (R_t) estimated from the data provides valuable information regarding the disease trend, it lacks the asymptomatic cases, which may be the dominating spreader of the disease. To overcome this limitation, we also estimated the time-dependent reproduction number (R_t) by using our model. As expected, the model predicted a higher value of the reproduction number of 4.2 due to the asymptomatic cases. (R_t) decreases rapidly after the implementation of the lockdown (Fig. 19). Around the 1st week of June, it fell below 1 and again raised following the partial relaxation of lockdown. This trend of (R_t) well-describes the trends of new cases in both high- and low-risk regions.

Under the complete national-level lockdown, it took one month longer in the low-risk region to bring (R_t) below 1 compared to the high-risk region. Our model also allowed us to predict a long-term (R_t) up until 30 April 2022. According to our model prediction, (R_t) remained less than the threshold value 1, indicating the decreasing trends of new cases in both regions (Fig. 19) throughout the pandemic until April 2022.

4.3.4 Estimates of Seroprevalence

The antibody of COVID-19 forms in the body due to the viral infection and/or vaccination. Estimating the seroprevalence is practically essential for COVID-19, mainly because of a large portion of unreported infected individuals. We assume that recovered and/or vaccinated people remain immune during the simulation period. We estimated 63.9% seroprevalence (Fig. 20) as of the end of July. We also used our model to predict the expected seroprevalence during the pandemic until April 2022 (Fig. 20). As predicted by our model, the seroprevalence will reach $\sim$ 90% in December 2021 and $\sim$ 95% in April 2022. Moreover, our model allows us to identify whether the seroprevalence achieved is due to vaccination, actual infection, or both. Among the 89% seroprevalence achieved by December 31, 2021, $\sim$ 7% are from vacci-

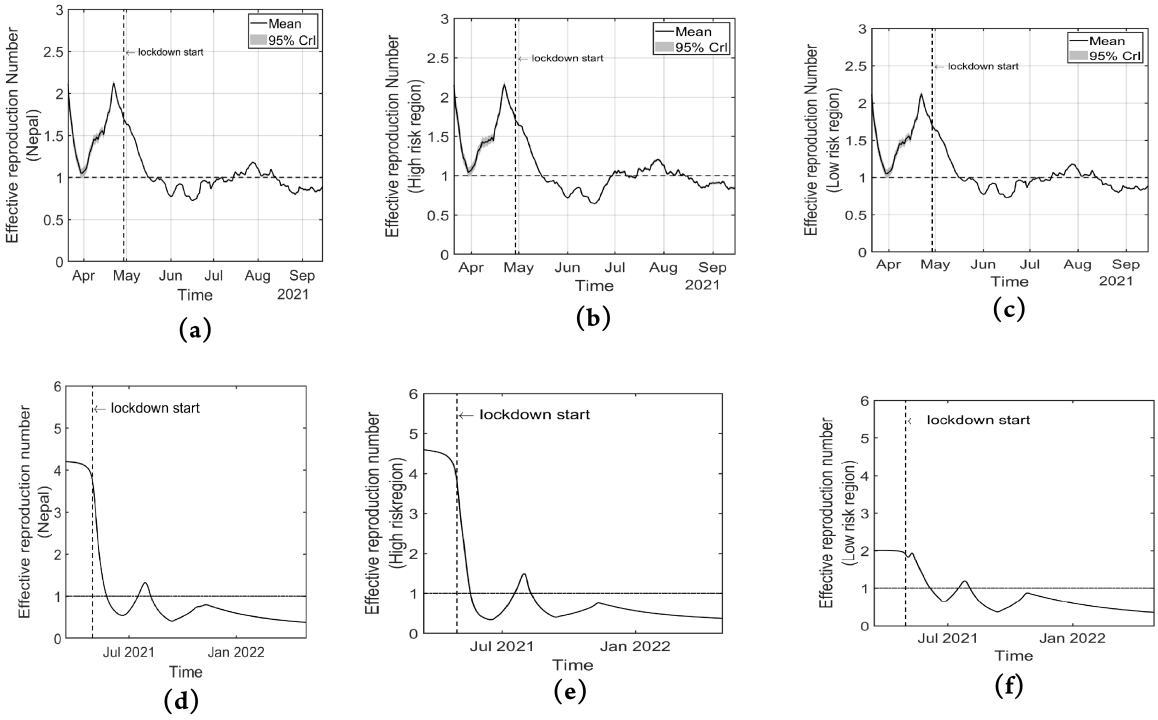

Figure 19: Reproduction number. Time-dependent reproduction number of COVID-19 estimated from the recorded data for the whole country Nepal (a), the high-risk region (b), and the low-risk region (c). Time-dependent reproduction number of COVID-19 estimated from the model for the whole country Nepal (d), the high-risk region (e), and the low-risk region (f). Note that the higher reproduction number estimated from the model is due to the infection from the unreported cases. The horizontal lines indicate the threshold value, $R_t = 1$, above (below) which shows an increasing (decreasing) trend of the disease spread.

nation, $\sim 52\%$ are from infection, and $\sim 30\%$ are from both vaccination and infection. Similarly, $\sim 7\%$, $\sim 42\%$, and $\sim 46\%$ are expected contributions from vaccination, infection, and both, respectively, towards the total seroprevalence of $\sim 95\%$ by April 30, 2022.

4.3.5 Role of Vaccination in the Mitigation of Second Wave of COVID-19 in Nepal

Here, we consider different vaccination scenarios under the complete relaxation of non-pharmaceutical interventions and used the model to predict the outcome of the pandemic under these vaccination programs. Based on the literature, we modeled the effectiveness of vaccination using a 50% reduction in infection and a 90% reduction in hospitalization for vaccinated people. While we used this level of effectiveness for demonstration purposes, the simulations with other values produce a similar qualita-

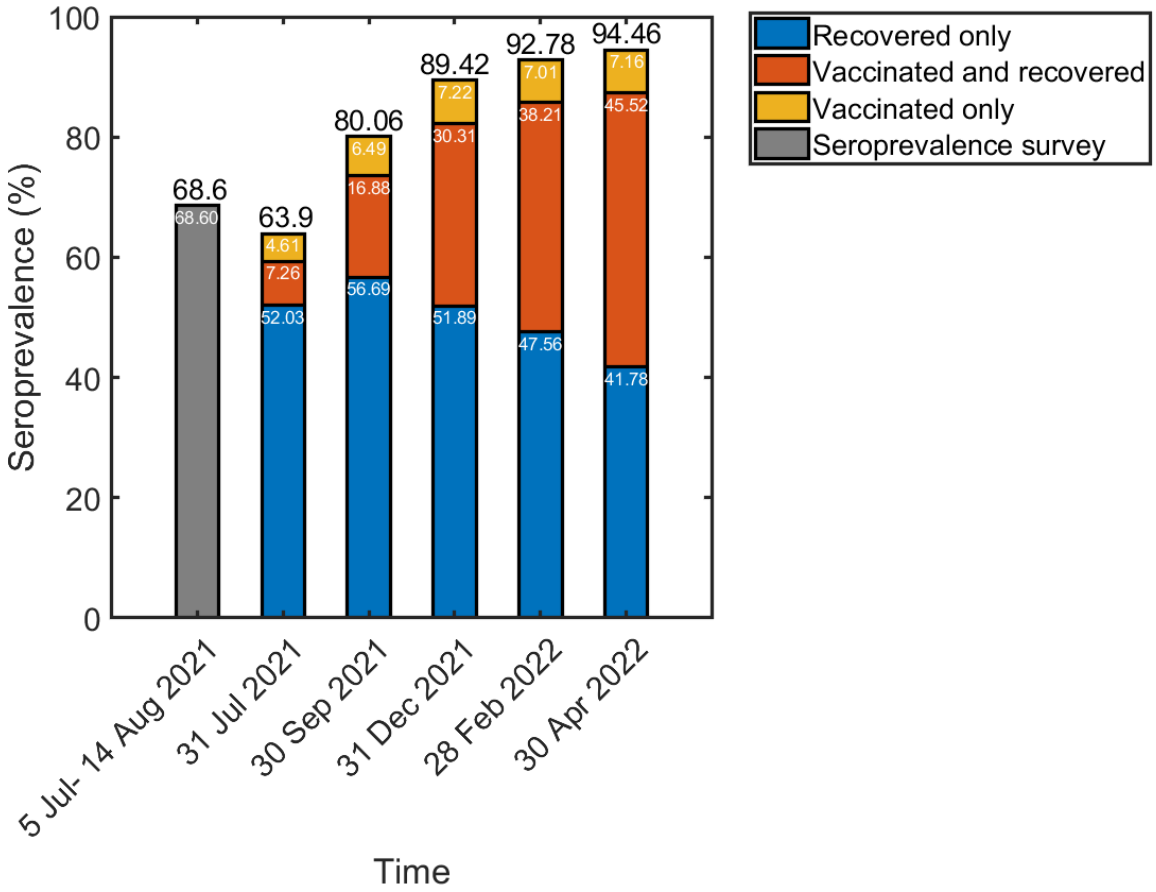

Figure 20: Estimation of seroprevalence: The predicted seroprevalence achieved due to actual infection only, vaccination only, and both. The first bar represents the survey data by the government of Nepal.

tive behavior with a slight quantitative difference.

The government of Nepal has set the target to vaccinate 71.6% of the people from the eligible age groups [118]. Therefore, we focus on vaccination programs targeting 71.6% of the eligible population by a specific time frame. The vaccination rate, ξ, in our model with the target to cover 71.6% eligible population by vaccination time frame, T , can be calculated using $\xi = (-\ln(1 - 71.6/100))/T$ [135]. For varying vaccination time frames from October 31, 2021, to April 30, 2022, and the varying level of lockdown from 0% to 9%, we simulated our model to predict maximum daily cases, the total cases, the total deaths, the total medical cares, the total ICUs, and the total ventilators, during the pandemic until April 2022 (Fig. 21).

With the existing level of vaccination and complete relaxation of the lockdown, the peak value of new cases would be 2232 per day. However, the peak can be reduced

to 1726, 1966, 2070, and 2134 per day, respectively, when the vaccination time frame was set to the end of October 2021, December 2021, February 2022, and April 2022. Our model simulations show that the total number of cases by the end of April 2022 could be reduced from 154000 to 62000, 94000, 119000, and 132000 by setting the vaccination time frame at the end of October 2021, December 2021, February 2022, and April 2022, respectively. With these vaccination programs, i.e., the time frame of the end of October 2021, December 2021, February 2022, and April 2022, the number of recorded deaths can be reduced from 1509 to 686, 1017, 1196, and 1316, respectively. Similarly, these vaccination time frames would reduce the total medical patients from 16610 to 5885, 9965, 12150 and 14080, respectively. In this case, the total ICU patients would be reduced from 4941 to 1964, 3147, 3790, 4220, respectively, and ventilator patients will be reduced from 1305 to 522, 836, 1007, 1122, respectively (Fig. 21).

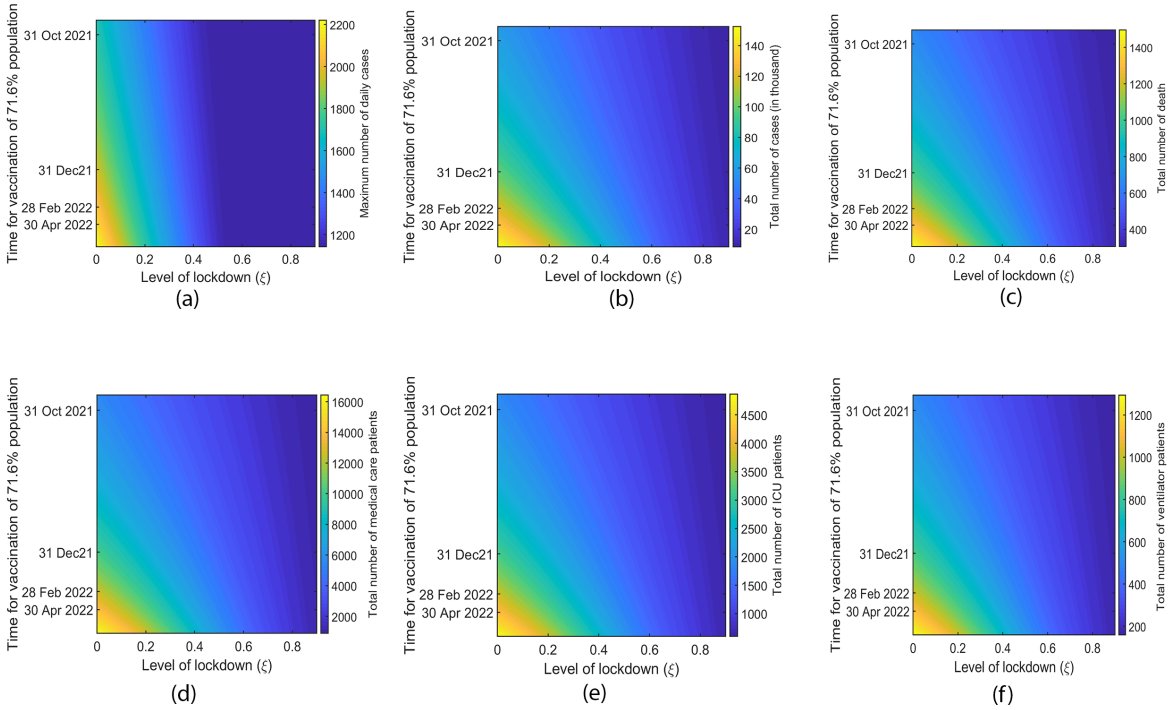

Figure 21: Assessment of vaccination and lockdown program combined. The predicted peak value of the daily cases (a), total cases (b), total death (c), medical care cases (d), ICU cases (e), and ventilator cases (f) during the period from September 01, 2021, and April 30, 2022, for varying vaccination target time frame and lockdown level.

4.4 Discussion

The timely characterization of the COVID-19 wave is essential for policy intervention to overcome the devastating impacts of the pandemic. In this chapter, we developed a data-driven mathematical model to describe Nepal's unique delta variant-dominated second wave of COVID-19. Using multiple data sets simultaneously and considering two distinct high- and low-risk regions are unique features with more practical applications in our model. Our results provide a great insight into some relevant scenarios of COVID-19 in Nepal and predict the impact of potential vaccination programs on mitigating the burden of the pandemic, helping policymakers design proper health care facilities and vaccination strategies.

We identified the distinct pattern of the Delta wave in high- and low-risk regions regarding its magnitude and time period. As expected, most of the cases ($> 80\%$) were recorded in high-risk region and it peaked about one month earlier than low-risk region. Such spatial disparity on the pandemic trend was also found in the previous study [133], which performed the province-wise analysis of the first wave of COVID-19 in Nepal. The increasing trend of the epidemics remained for the period of April-May 2021 in high-risk region and for the period of May-June 2021 in low-risk region.

The delta variant was the dominant variant during the second wave of COVID-19 in Nepal. As per our model estimates, the reproduction number of $R_t = 4.2$ at the beginning of the Delta variant dominated second wave was higher than the first wave (~ 1.8) [4], indicating a significantly higher virus transmission during the second wave than the first wave. The maximum likelihood method gives a relatively low effective reproduction number (~ 2) at the peak time of epidemic that is similar to the other study [51]. The higher transmissibility of the Delta variant observed in our study is supported by the previous studies in different parts of the world [34, 38, 68, 102, 155] and higher reproduction numbers in many other reports and studies (Campbell and Archer, 2021, Ito et al., 2021, WHO, 2021b). While the national implementation of lockdown caused the reproduction number to decrease to below the threshold value 1, the effect seen in the low-risk region was about a month delayed compared to the high-risk region. Such inter-regional disparity highlights that regional level policy, and thus regional level modeling, is needed for more effective control of the local-level outbreak. The inter-region discrepancy observed in our estimated R_t is consistent with the inter-provincial disparity identified in Pantha et al. [133] during the first wave of COVID-19 in Nepal.

The potential transmission from the undiagnosed cases is one of the most contributing factors to the uncertainty of the COVID-19 pandemic, causing extreme difficulty for its control. Estimating this critical transmission rate from undiagnosed cases requires a large-scale seroprevalence survey, which is often limited by resources in developing countries like Nepal. We implemented our data-driven dynamical system-based model to estimate this transmission rate. We found a significantly high transmission rate from undiagnosed cases ($\sim 95\%$), consistent with the seroprevalence survey of the Government of Nepal (MoHP). Our model predicts $\sim 63\%$ seroprevalence in Nepal at the end of July 2021, consistent with the result ($\sim 68.6\%$) from the Nepal Government's survey (MoHP). With the level of vaccination implemented, the model predicts that $\sim 95\%$) of people were immune to the circulating strains of COVID-19 by the end of April 2022. Among these immune people, about 46% had experienced both vaccination and actual infection.

For developing countries like Nepal, timely assessment of expected burden is critical to avoid an overwhelming situation in hospitals and medical facilities. Our simulation results identified the duration of hospitalization of the COVID-19 patients in Nepal (7 days in normal medical care, 7.2 days in ICU, and 7.5 days in ventilators) shorter than that noted in other studies [74, 103, 178, 183, 188]. As in many other studies [88, 155, 178, 183] , Nepal faced a significant increase in the hospitalization burden due to the delta-variant compared to the wild-type. Based on our model analysis, we found the hospitalization of $\sim 11.25\%$ of recorded cases in Nepal, similar to the rates identified in other countries ($\sim 9.2\% - 25\%$) [18, 74]. Among the hospitalized patients, $\sim 35\%$ of them needed extensive medical care, such as ICU and ventilator. According to the report on May 2020 [119], Nepal had 26,930 hospital beds, 1595 ICU beds, and 840 ventilators, including the government and private sectors. The Government of Nepal planned to allocate one-third of these facilities for COVID-19 patients. Later, the Government of Nepal extended its capacity to 10,116 hospital beds, 1648 ICUs, and 1088 ventilators for COVID-19 patients [118]. Interestingly, these data show that the predicted total hospitalization burden remains below the total capacity of Nepal even though the country is expected to have limited medical resources and prevention programs. However, we note that during the peak time (last of May 2021), many national and international media [27, 140, 188] covered the news about a shortage of hospital beds, ICU, ventilators, and oxygen cylinders. This discrepancy may be attributed to mismanagement of the hospital infrastructure and/or under-reporting of patients. We also note that the low hospital rate may partially be attributable to the hospitalization of only complicated cases or scarcity of the hospital beds at the

time of peak [27, 188, 140].

The significant impact of the vaccination, including against the new variants, has been reported [2, 109]. Both vaccination programs and the relaxation of lockdown were ongoing in Nepal after the September 2021. We implemented our model to predict the potential epidemic trends and medical care needed (hospital bed, ICU, ventilator) for various coverage rates of vaccination programs and levels of lockdown during the pandemic until April 2022 (Fig. 21). Our model predictions of 111,300 cases, 11,890 hospitalizations, 3590 ICUs, and 950 ventilators by the end of April 2022 is also compatible with the prediction of IHME model [81]. The results on vaccination and lockdown provide information on suitable strategies for Nepal to manage medical care and the pandemic burden.

We acknowledge some limitations of this study. Daily new cases may be affected by the number of tests and the positivity rate, which were not considered into our model. The inherent complexities of an unfolding epidemic, human behavior, implementation timing, and governmental policy change may have some impact on our predictions. We ignored the spatial heterogeneity in the dynamics within each region, the high- and low-risk regions. Furthermore, the in-homogeneity of the age structures of the study population was ignored. These questions can be addressed by heterogeneous and/or age-structured models, but more granular data is required. We considered high- and low-risk districts based on interconnections with India, a highly affected country by Delta variant, population density, and mobility pattern. The lack of data and information might have caused some uncertainty in categorizing districts into high- or low-risk regions. For example, our model classified the Makawanpur district, which is connected to high-risk districts (Chitwan, Lalitpur, and three Tarai districts), as low-risk due to its low density, low mobility pattern (a hilly district), and low infected cases. Moreover, because of the lockdown implemented during the second wave, there was less mobility across the districts, making Makawanpur a low-risk district despite its high-risk neighboring districts. Our long-term predictions were under the assumption that a novel strain would not appear for the study period. Therefore, the results need to be interpreted when the viral evolution and emergence of more severe strains are absent.

In summary, our data-driven model reveals some essential and insightful facts regarding the Delta-dominated second wave of COVID-19 in Nepal. In-depth exploration of the potential discrepancy between the actual epidemic burden and the recorded data suggests the policymakers revisit the gaps between the plan and practice of man-

agement of the pandemic. Estimated seroprevalence, new COVID-19 cases, and the hospitalization burdens under vaccination can provide helpful information for designing plans to control the pandemic in Nepal.

CHAPTER 5

DATA-DRIVEN MODELS FOR THE RISK OF INFECTION AND HOSPITALIZATION DURING A PANDEMIC: CASE STUDY ON COVID-19 IN NEPAL

In this chapter, we developed data-driven models to estimate the real-time risk of infection and hospitalization. Then we implemented our models on the data of COVID-19 in Nepal to estimate the province wise time dependent reproduction numbers, the risk of disease, and the risk of hospitalization. Using our models, we compared the Delta and Omicron waves and their impacts on the province-level community and healthcare systems. Furthermore, we used our model to evaluate the effects of intervention policies on the risk of infections.

5.1 Introduction

During the pandemic, a lack of knowledge about the risk of circulating new strains, which may be more contagious and capable of evading the immune response of previously infected individuals or vaccinated, may lead to unusually high cases [84]. Due to the uncertainty and variability in disease severity across different strains, there are often insufficient resources and preparedness, resulting in overwhelmed hospitalizations and shortages of medical staff, equipment, and beds. Consequently, individuals may postpone seeking medical attention and neglect preventive measures, which can ultimately increase the risk of death, as witnessed in Nepal and India during the Delta variant outbreak [3, 111]. The uncertainty on the risk of infection and hospitalization may have a greater impact, especially on developing countries like Nepal, because of the resource limitations. Thus, estimating the real-time risk of infection and hospitalization is crucial for assessing disease transmission and managing medical resources to minimize the burden of pandemics.

The effective reproduction number is widely used to assess the speed of an epidemic; if it is greater than one, the disease is rising [179]. However, due to the differences in the size of the susceptible population, the number of infected individuals, and the population's contact pattern, two localities with the same effective reproduction number may be vulnerable in different magnitudes (different magnitudes of incidence) during the pandemic. In such situations, estimating the risk of infection and hospitalization is essential, which can better describe epidemic status and healthcare capabilities. Limited clinical case studies [26, 57, 101, 147, 167, 203] and a handful of mathematical models [30, 113, 116, 185] estimate the risk of infection and hospitalization. However, none of these studies have combined mathematical models with real-time incidence data, active hospitalization, and population contact patterns, constituting the essential factors associated with disease transmission and controls. Such data-driven mathematical models can accurately estimate and quantify the real-time risk of infection and hospitalization during the pandemic [3, 124, 134].

5.2 Methods

5.2.1 Data

The countrywide and province-wise data were obtained from various available sources, including the official websites of the Ministry of Health and Population Nepal [122] and the Central Bureau of Statistics [40]. We considered the data containing the daily new COVID-19 cases and the active hospitalization cases in seven provinces of Nepal from 1 April 2021 to 31 March 2022, covering both Delta and Omicron waves. Based on the information about the circulating viral strains, we assumed that the Delta surge occurred between 1 April and 30 December 2021 and that the Omicron surge occurred from 1 January to 31 March 2022.

The contact rate, which depends upon the mobility of the population, plays a vital role in disease transmission. Since the population is a heterogeneous mixture of different age groups with different mobility and contact patterns, we utilized a previous study's age-specific contact rates for Nepal [123]. Here, a contact is defined as either skin-to-skin contact, such as a kiss or handshake (a physical contact), or a two-way conversation with three or more words in the physical presence of another person but no skin-to-skin contact (a nonphysical contact) [141]. Based on the previous studies [123, 141], we estimated an average of 19.31 contacts per person daily. The

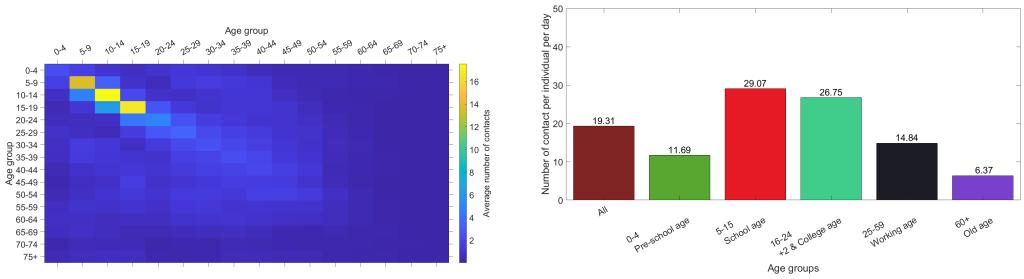

(a) **(b)**

Figure 22: (a) Age-specific contact matrix for Nepal. The two axes that start at the top left of the matrix represent the age groups that make up the population. (b) The average number of contacts per individual per day of different age groups in Nepal. The age groups are split into the following categories: preschool, school, $10 + 2$ and college, working, and old age.

contact matrix, including population mixing patterns and distribution of contacts by age groups, is presented in Fig. 22. We calculated the group-wise contact rate using the weighted arithmetic mean of contact rates of different age groups. Details of the study design and data collection procedure of contact rate are provided in the previous study [141].

The overall impacts of NPIs reflects in the reduction of contact rate. To estimate the impact of different level of control interventions (0%,40%, 70%) we reduced the contact rates by 0%,40%, 70% respectively. For impact of NPIs in age groups (schools, colleges, and working), we reduced the contact rate of respective age group by 70% keeping the unchanged contact rates of other groups and calculated the new average contact rates. With these assumptions and based on the previous study [123], we took the contact rates of 13.79 for closure of schools and colleges, 14.65 for closure of working places and 5.79 for lockdown.

The total population of Nepal and its seven provinces was taken from the recently published results of the population census of Nepal, 2021 [40]. Since about 7.45% of Nepalese are in foreign countries [40], we only took 92.55% of the total population for our study. The total population and population used in our study is given in Table 4.

Table 4: Total population of Nepal and its provinces. The third column contains the populations used in our study.

Regions	Total population	Population for the study (0.9255 × Total population)
Nepal	29,136,808	26,966,116
Province 1	4,972,021	4,601,605
Madhesh Province	6,126,288	5,669,880
Bagmati Province	6,084,082	5,630,818
Gandaki Province	2,479,745	2,295,004
Lumbini Province	5,124,225	4,742,470
Karnali Province	1,694,889	1,568,620
Sudur Paschim Province	2,711,270	2,509,280

5.2.2 Estimation of the Effective Reproduction Number (R_t)

We require two data sets to estimate R_t using MLM: the number of new cases (incidence of cases) over time and the generation time (time duration between the primary and secondary infection). The generation time is usually not observable but can be approximated with the serial interval [98], which is defined as the time between the onset of symptoms of primary cases and that of secondary cases [184]. Many studies [42, 146, 166, 206] have reported that the serial interval follows a Gamma distribution with certain means and standard deviations. We described the detail method in section 2.1.5.

5.2.3 Estimation of Risk of Infection

We assume that C_t represents the instantaneous contacts of an individual at time t and C is the average (expected) number of daily contacts. We assumed the contact (C_t) follows a Poisson distribution with mean C, i.e., $C_t \sim \text{Pois}(C)$. We further assumed that N is the total population, which we assumed to be constant during the short period of a single surge, and I_t and I_t^A are the number of new infections and active infections at time t, respectively. Taking ζ as the average infectious period (in days), $I_t^A = \sum_{s=t-\zeta}^{t} I_s$. Thus, the average contacts of an individual with the infectious people at time t is $C_t I_t^A / N$.

We now assume P_t to be the probability that a single contact with infectious people

leads to successful infection and S_t to be the number of susceptible individuals at time t. Then the number of new infections at time t is $C_t \frac{I_t^A}{N} P_t S_t$. Also, since the effective reproduction number is R_t, the number of new infections generated by a single infectious individual at time t is R_t/ζ. On average, the total new cases generated by all infectious people I_t^A at time t is $R_t I_t^A/\zeta$. Thus we have

$$\begin{aligned} C_t \frac{I_t^A}{N} P_t S_t &= R_t I_t^A/\zeta \\ \implies P_t &= R_t N/(\zeta C_t S_t), \end{aligned}$$

which gives the probability of infection at a single contact with an infectious person. Then, $(1 - P_t)$ represents the probability that a single contact with infectious people does not result in a successful infection. There are $C_t I_t^A/N$ contacts of an individual with infectious people at time t. Then, the probability that non of these contacts with infectious people results in a successful infection is $(1 - P_t)^{C_t I_t^A/N}$. Thus, the probability of infections (i.e., the risk of infection at time t) is

$$1 - (1 - P_t)^{C_t I_t^A/N}.$$

5.2.4 Estimation of Risk of Hospitalization

We consider time-to-hospitalization a random variable because it is randomly influenced by various factors, such as the severity of illness, access to healthcare, demographic factors, the geographic variation that are subject to variation and uncertainty. These factors can differ both across individuals and geographic regions, resulting in heterogeneity in the distribution of time-to-hospitalization. We assume g_h to be the probability distribution of the time-to-hospitalization after becoming infected at time h and $\mathcal{H}_t$ to be the risk of hospitalization at time t of an infection. Therefore, the number of new hospitalized cases at time t is $\mathcal{H}_t \sum_{h=1}^{t} I_{t-h} g_h = \mathcal{H}_t \lambda_t$, where $\lambda_t = \sum_{h=1}^{t} I_{t-h} g_h$. Denoting ν as the average duration of the stay at the hospital, the number of active hospitalized cases at time t is

$$\sum_{j=t-\nu+1}^{t} \mathcal{H}_j \lambda_j.$$

We assumed that the active hospitalization cases follow the Poisson process. Then the likelihood of active hospitalized cases H_t with given hospitalization rate $\mathcal{H}_t$, incidences

$I_0, I_1, I_2, ..., I_t$, and distribution g_h is:

$$P(H_t|I_0, I_1, I_2, ..., I_t, g_h, \mathcal{H}_t) = \frac{\left(\sum_{j=t-\nu+1}^{t} \mathcal{H}_j \lambda_j\right)^{H_t} \quad e^{-\sum_{j=t-\nu+1}^{t} \mathcal{H}_j \lambda_j}}{H_t!}.$$

Using a Bayesian framework with a Gamma distributed prior with parameters (θ, ϕ) for $\mathcal{H}_t$, i.e., $\mathcal{H}_t \sim \text{Gama}(\theta, \phi)$, the posterior joint distribution of $\mathcal{H}_t$ is

$$\begin{aligned} & P(\mathcal{H}_t|I_0, I_1, I_2, ..., I_t, H_t, g_h) \\ \propto \;& P(H_t|I_0, I_1, I_2, ..., I_t, g_h, \mathcal{H}_t)\; P(\mathcal{H}_t) \\ = \;& \frac{\left(\sum_{j=t-\nu+1}^{t} \mathcal{H}_j \lambda_j\right)^{H_t} \quad e^{-\sum_{j=t-\nu+1}^{t} \mathcal{H}_j \lambda_j}}{H_t!} . \frac{\mathcal{H}^{\theta-1} e^{-\frac{\mathcal{H}}{\phi}}}{\Gamma(\theta)\phi^{\theta}}. \end{aligned}$$

Since the stay in hospital is shorter than the surge period, we assumed that $\mathcal{H}_t$ is constant for the time period $t - \nu$ to t. Then we obtained

$$\begin{aligned} & P(\mathcal{H}_t|I_0, I_1, I_2, ..., I_{t-\nu}, H_t, g_h) \\ \propto \;& \frac{\mathcal{H}_t^{H_t} \left(\sum_{j=t-\nu+1}^{t} \lambda_j\right)^{H_t} \quad e^{-\mathcal{H}_t \sum_{j=t-\nu+1}^{t} \lambda_j}}{H_t!} \frac{\mathcal{H}_t^{\theta-1} e^{-\frac{\mathcal{H}_t}{\phi}}}{\Gamma(\theta)\phi^{\theta}} \\ \propto \;& \left(\mathcal{H}_t^{H_t+\theta-1} \; e^{-\mathcal{H}_t \left(\sum_{j=t-\nu+1}^{t} \lambda_j + 1/\phi\right)}\right) \frac{\left(\sum_{j=t-\nu+1}^{t} \lambda_j\right)^{H_t}}{H_t!}. \end{aligned}$$

Note that we used the Gamma distributed prior conjugate to the Poisson likelihood. From the expression above, the posterior distribution of $\mathcal{H}_t$, given the new cases and active hospitalized cases, conditional on the post-infection hospitalization timing distribution g_h, is a Gamma distribution with parameters

$$\left(\theta + H_t, \quad \frac{1}{\frac{1}{\phi} + \sum_{j=t-\nu+1}^{t} \lambda_j}\right).$$

We obtained a sample of a certain size (m) drawn from this posterior distribution of $\mathcal{H}_t$ given new cases and active hospitalized data from which the posterior mean and 95% Credible Interval (CrI) of $\mathcal{H}_t$ were computed. Since the exact time of infection is not observable and people only admit to the hospital if they feel some complications, the time between the infection and hospitalization can not be precisely measured. For our simulation, we considered a gamma-distributed duration between infection and hospital admission, with a mean of 3 days and a standard deviation of 2 days.

5.2.5 Impact of Non-Pharmaceutical Interventions (NPIs)

To model different levels of control interventions, we applied corresponding percentage reductions in average contact rates, e.g., a 70% control intervention would result in a 70% reduction in contact rates. As the Nepal Government implemented a significant level of lockdown during the Delta wave, we considered the 70% control intervention as the base case. During the Omicron wave, only primary and secondary schools were closed for a short period (from 11 January to 29 January 2022) [92], which we did not expect to have a significant impact, so we assumed a 0% control intervention for the Omicron wave.

In our modeling, the overall impact of NPIs was represented by the reduction of contact rate, which we considered to be 0%, 40%, and 70% for simulations with different levels of control interventions. For the impact of NPIs in age groups (schools, colleges, and working), we reduced the contact rate of the respective age group by 70% while keeping the contact rates of other groups unchanged and calculated the corresponding average contact rates. With these assumptions and based on the previous study [123], we estimated the contact rates of 13.79 for the closure of schools and colleges, 14.65 for the closure of working places, and 5.79 for the lockdown.

5.3 Results

5.3.1 Reproduction Number

The reproduction number indicates the trend of disease spread throughout the population [54]. Specifically, if it is more than 1, the disease spread has an increasing trend, and if it is less than 1, the spread has a decreasing trend [179].

In Fig. 23 (left column), we present our estimates of the effective reproduction number

in Nepal and its provinces from 21 April to 31 December 2021 (the Delta wave). The reproduction number was higher than the threshold value one at the beginning of April 2021. Except for Gandaki province, the reproduction number in Nepal and all of its provinces exceeded two and peaked in the middle of April 2021 (Nepal: 2.20, 95% CrI [2.166, 2.23], Province 1: 2.18, 95% CrI [2.04, 2.32], Madhesh: 2.61, 95% CrI [2.12, 3.14], Bagmati: 2.28, 95% CrI [2.23, 2.33], Gandaki: 1.84, 95% CrI [1.79, 1.89], Lumbini: 2.29, 95% CrI [2.28, 2.30], Karnali: 2.44, 95% CrI [1.68, 3.32], and Sudur Paschim: 2.63, 95% CrI [2.38, 2.89]). These early R_t values indicate that at the beginning of the Delta wave, the infections were rapidly spreading across the country in a short period of time. The reproduction rate in Nepal and its provinces began to fall below the threshold value one after the middle of May 2021 (Nepal: May 17; Province 1, Bagmati, and Gandaki: May 16; Madhesh: May 25; Lumbini: May 14; Karnali: May 24; Sudur Paschim: May 14 2021). Madhesh, Karnali, and Sudur Paschim provinces, where fewer cases were reported, showed greater fluctuations in the temporal pattern of the effective reproduction number.

The first incidence of Omicron in Nepal was detected on 6 December 2021 [138]. After the first week of January 2022, cases surged and spread rapidly. On January 23 2022, 80% of new cases were Omicron [139]. So, we estimate the effective reproduction number from 1 January to 31 April 2022 to characterize the period of the Omicron surge (Fig. 23, right column). The reproduction number in Nepal and all provinces were at the threshold level ($R_t = 1$) in December 2021 during the Delta wave (Fig. 23, left column). After that, it rose quickly, peaking around the middle of January (Nepal: 2.17, 95% CrI [2.14, 2.21]; Province 1: 2.26, 95% CrI [2.15, 2.38]; Madhesh: 2.38, 95% CrI [2.21, 2.56]; Bagmati: 2.16, 95% CrI [2.13, 2.19]; Gandaki: 2.24, 95% CrI [2.130, 2.34]; Lumbini: 2.43, 95% CrI [2.27, 2.60]; Karnali: 2.52, 95% CrI [2.12, 2.96]; and Sudur Paschim: 2.85, 95% CrI [2.47, 3.25]), before rapidly dropping below the threshold value of one from the last week of January 2022 for the rest of the year.

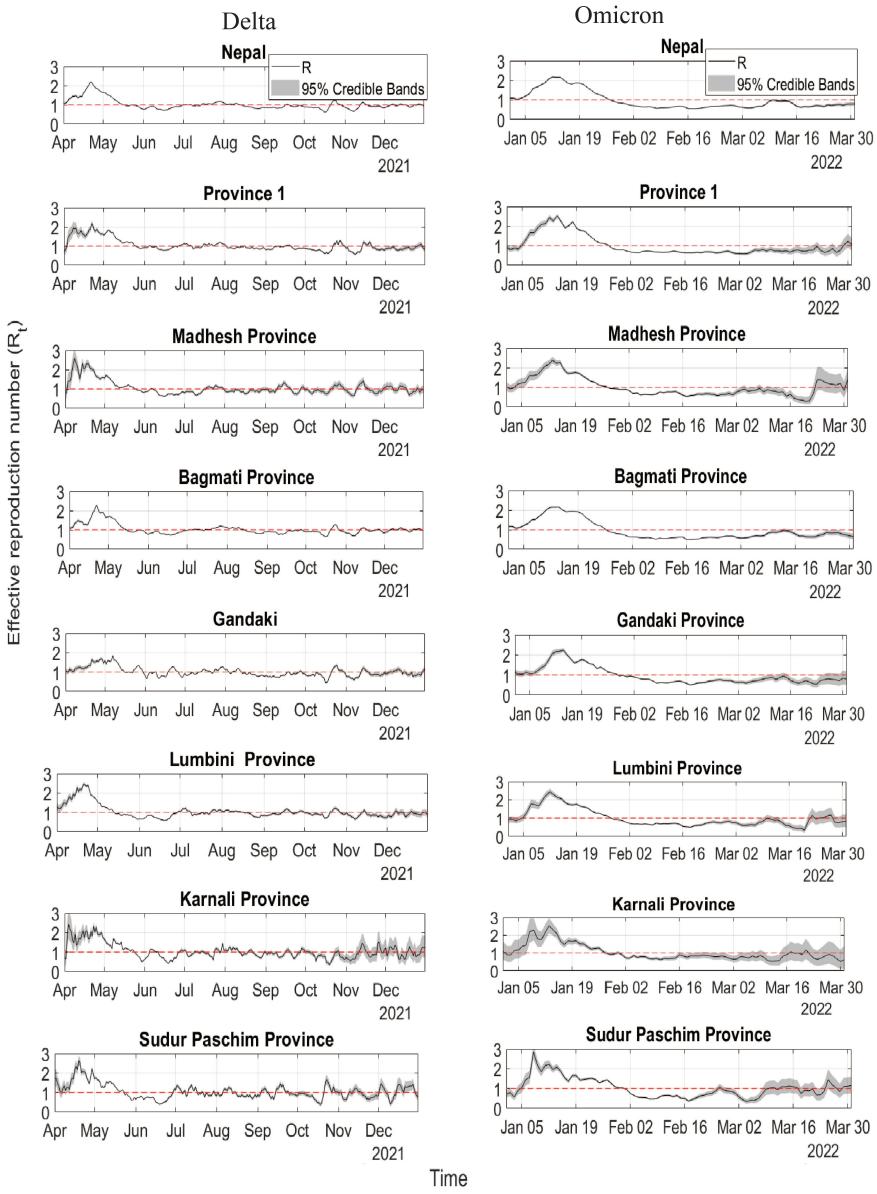

Figure 23: The time-dependent effective reproduction number of COVID-19 in Nepal and its seven provinces during the Delta (Left column) and Omicron (Right column) waves. The gray-shaded region is the 95% credible interval for R_t. The horizontal red dashed line indicates the threshold value $R_t = 1$. The left column is the effective reproduction number during the Delta wave, and the right column is for the Omicron wave.

We observed that the reproduction number remained greater than one for about a month (1st to last week of January 2022) during the Omicron surge. In certain provinces (Madhesh, Lumbini, Karnali, and Sudur Paschim), we noticed a wider range of credible intervals for the estimated R_t at the end of April 2022. This increased variability may be due to the fact that there were fewer reported new cases, with

more fluctuations. The results shown in Fig. 23 reveal that the reproduction numbers related to the Omicron and Delta variants are not considerably different even though quite different COVID-19 cases were reported in Nepal and all its provinces.

5.3.2 Risk of Infection

The timely estimation of the risk of infection is essential to track the dynamics of the diseases and valuable to determine the need for amplification or the relaxation of public health control measures. We used our model to compare the risk of infection of COVID-19 during Delta and Omicron surges in Nepal and its provinces. The estimated maximum risk of infection of Delta surge in Nepal and its provinces is shown in Table 5. The temporal pattern of the risk of infection during the Delta and Omicron surges is shown in Fig. 24.

The risk of infection during the Delta wave increased sharply from mid-April 2021 and peaked in the second week of May 2021 in Nepal (Fig. 24, left column). The Bagmati province, which contains Nepal's most densely populated capital city, had the peak risk for infection two weeks sooner than the other provinces (first week of May 2021). Our estimates showed that Bagmati province was the highest risk zone (98.94, 95% CrI [32.99, 181.31] per hundred thousand), while Madhesh province remained the lowest risk zone (12.16, 95% CrI [4.05, 22.29] per hundred thousand) (Table 5). Interestingly, despite being the most densely populated province (600 people/km^2) [40] and having a larger R_t value, the Madhesh province had a lower risk of infection compared to other regions.

Table 5: The maximum risk of infection and time of highest risk of COVID-19 during Delta and Omicron variant of Nepal and its seven provinces.

Risk of infection of Delta variant			
Regions	Risk of infection (per 100000)	95% CrI	Time of highest risk
Nepal	42.19	[14.06, 77.33]	11 May, 2021
Province 1	27.49	[9.16, 50.40]	23 May, 2021
Madhesh	12.16	[4.05, 22.29]	19 May, 2021
Bagmati	98.94	[32.99, 181.31]	7 May, 2021
Gandaki	44.53	[14.84, 81.62]	26 May, 2021
Lumbini	42.89	[14.30, 78.63]	8 May, 2021
Karnali	31.16	[10.39, 57.13]	14 May, 2021
Sudur Paschim	33.26	[11.08, 60.97]	17 May, 2021
Risk of infection of Omicron variant			
Nepal	30.42	[17.61 46.43]	30 Jan, 2022
Province 1	16.30	[9.87, 24.03]	31 Jan, 2022
Madhesh	5.01	[2.63, 7.65]	1 Feb, 2022
Bagmati	89.62	[56.61, 132.05]	30 Jan, 2022
Gandaki	21.35	[13.48, 31.47]	1 Feb, 2022
Lumbini	8.46	[4.90, 12.47]	31 Jan, 2022
Karnali	3.00	[1.74, 4.43]	31 Jan, 2022
Sudur Paschim	8.03	[4.64, 11.83]	27 Jan, 2022

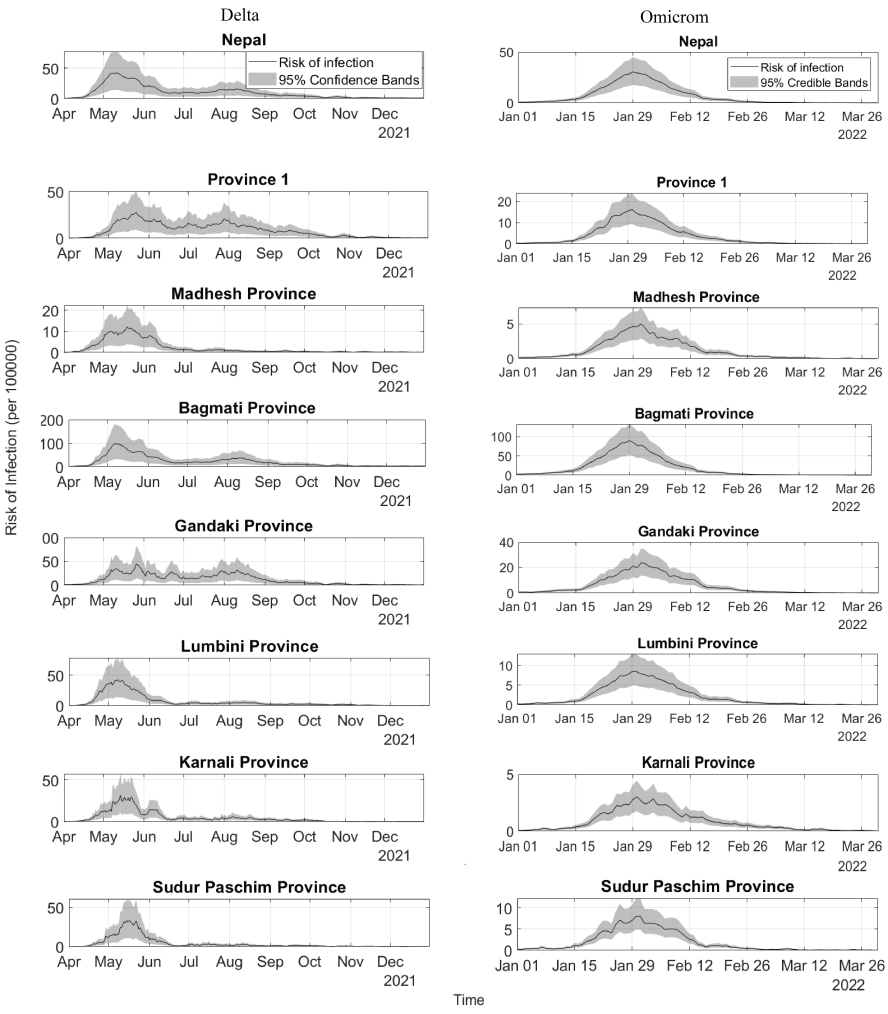

Figure 24: Risk of infection (per thousand hundred) due to Delta and Omicron variants of Nepal and its seven provinces. The first column is the risk of infection during the Delta wave, and the second column is the risk of infection during the Omicron wave. The scaling on the y-axis differs depending on the province and wave.

We also estimated the risk of COVID-19 during the Omicron wave (1 January to 31 March 2022). The temporal pattern of the risk of infection during the Omicron surge is shown in Fig. 24 (right column), and the estimated risk is shown in Table 5. Starting from a minimal risk at the beginning of January 2022, the risk of infection reached the highest level among provinces in a short period of time (3 weeks) around the fourth week of January 2022. During this time, we observed a considerable disparity in maximum risk of infection across Nepal and its provinces, ranging from 3.00, 95% CrI [1.74, 4.43] per hundred thousand in Karnali to 89.62, 95% CrI [56.61, 132.05] per hundred thousand in Bagmati. Furthermore, during the Delta surge, Madhesh

province had a low (5.01, 95% CrI[2.63, 7.65] per hundred thousand) risk of infection at the peak time of the Omicron surge. The higher uncertainty, i.e., a larger width of credible intervals, for estimates may attribute to the fluctuation of the data set of new cases. The fluctuation of daily new cases may be due to the poor recording of daily testing and detected positive cases.

We found a considerable difference in the patterns of risk of infection between the two waves of COVID-19 in Nepal. The risk of infection during the Delta wave was abruptly increased, and with a complete lockdown, it took about one month to decline, but in the Omicron wave, it climbed and fell quickly without lockdown. Furthermore, during the Delta surge, the maximum risk of infection was slightly higher than the Omicron surge in Nepal (38.69%) and Bagmati province (10%) but significantly higher in Gandaki (96.44%), Lumbini (407%), Karnali (942%), and Sudur Paschim (314%) than that of the Omicron surge. The Bagmati province was the most vulnerable to both Delta and Omicron surges, while the rest of the provinces were more vulnerable to the Delta surge than the Omicron surge.

5.3.3 Risk of Hospitalization

We calculated the risk of hospitalization using our model to the available data on active hospitalizations with COVID-19 in Nepal and its provinces. The results shown in Fig. 25 (left column) illustrate the risk that COVID-19 patients are admitted to hospitals in Nepal and its provinces during the Delta surge (1 May to 31 December 2021).

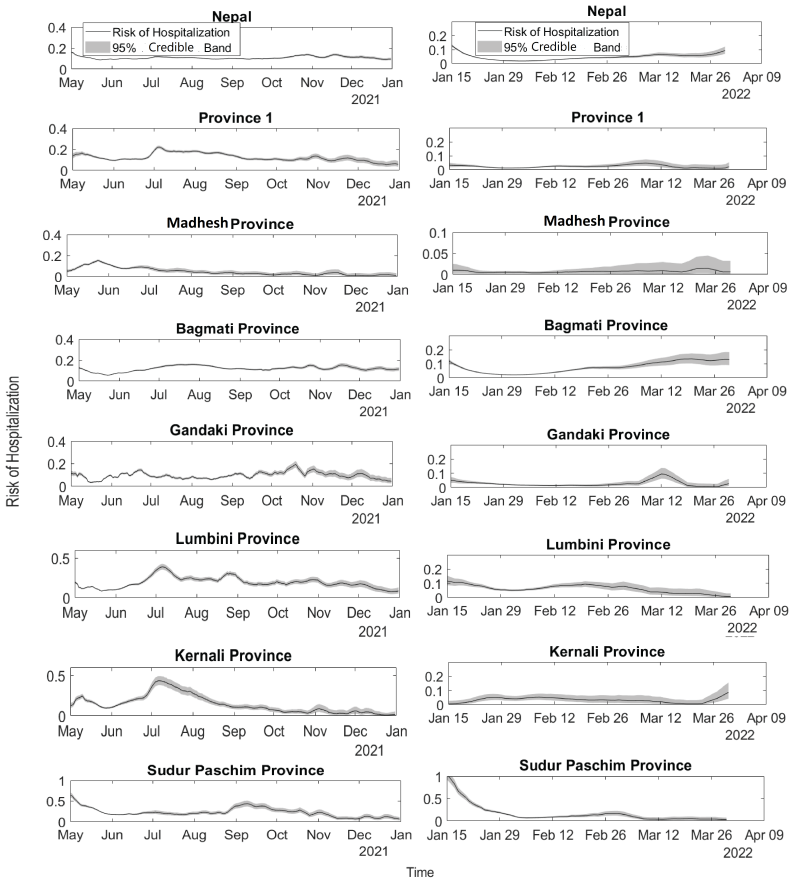

Figure 25: Risk of hospitalization during Delta and Omicron wave in Nepal and its provinces. The left column is the risk of hospitalization during the Delta wave, and the right column is the risk of hospitalization during the Omicron wave. The scaling on the y-axis differs depending on the province and the wave.

In Nepal, the risk of hospitalization of the Delta variant remains at 10% on average (min 7%, max 20%) and Province 1 shows a risk of hospitalization of 11% (min 6%, max 22%). Madhesh province had the lowest risk of hospitalization at 6% (min 5%, max 14%). Although many actual hospitalization cases are in the Bagmati province, the risk of hospitalization is 11% (min 10%, max 15%), similar to other regions. Besides the Madhesh province, Gandaki province also has a lower risk of hospitalization of 9.5% (min 5%, max 18%). The risk of hospitalization in both Lumbini and Karnali provinces is high [Lumbini: 19% (min 7%, max 38%); Karnali: 14% (min 3%, max 42%)]. In Sudur Paschim, the risk of hospitalization was initially high (68%) but later on around 21% (min 6%, max 43%). The initial higher risk of hospitalization in Sudur Paschim could be due to the high volume of returnees migrant workers from India.

The Omicron surge had substantially lower hospitalization rates than the Delta surge. The results in Fig. 25 (right column) show that the risk of hospitalization was 2.5% during the peak time of the Omicron wave in Nepal. At the end of March 2022, the hospitalization rate was again raised in Nepal as well as in Bagmati province. Sudur Paschim province had an extremely high risk of hospitalization during the mid of January, which could be due to the inclusion of the institutional isolation of returnee migrant workers in the data. Our estimates show that compared to the Delta wave (Fig. 25, left column), the hospitalization risk in Nepal and its provinces is significantly lower during the Omicron wave (Fig. 25, right column), falling to even less than 1% in some provinces (Nepal: 1.8%, 95% CrI [1.7%, 1.9%], Province 1: 1.2%, 95% CrI [1%, 1.5%], Madhesh: 0.38%, 95% CrI [0.17%, 0.7%], Bagmati: 2%, 95% CrI [1.9%, 2.1%], Gandaki: 1.3%, 95% CrI [0.97%, 1.75%], Lumbini: 1.3%, 95% CrI [0.29% 4.29%], Karnali: 0.6%, 95% CrI [0.022%, 3.18%], Sudur Paschim: 2.9%, 95% CrI [0.92%, 7.15%]). At the end of March 2022, the risk of hospitalization increased in Nepal and Bagmati province.

5.3.4 Impact of Non Pharmaceutical Interventions (NPIs) on Reducing the Risk of COVID-19 Infection

NPIs are known to play an important role in the mitigation of COVID-19. In general, restricting of mobility through NPIs, such as lockdown, reduces the contact rate, thereby reducing the risk of infection. Here, we used our model to quantify the impact of NPIs implemented by the Government of Nepal on reducing the risk of COVID-19. In Fig 26, we present the maximum risk of infection during the Delta wave with different control levels. In Bagmati province (the province with the highest risk), the maximum risk would have increased by 216.32% if the lockdown was not implemented during the Delta surge. Similarly, Madhesh province (a province with the lowest risk) would have increased by 216.61% if the lockdown was not implemented.

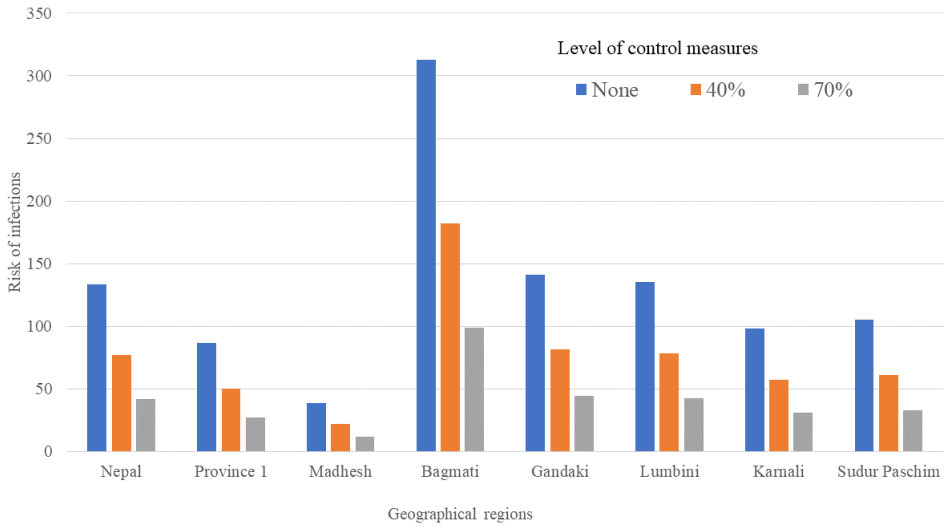

Figure 26: The maximum risk of infection under different control levels during the Delta wave in Nepal and its provinces.

The results in Fig. 27 show the trend of risk of infection during the Delta wave under different control levels. Our model estimates that if the lockdown had not been implemented during the Delta surge in Nepal, there would have been three times more new infections (Fig. 27). We also observed a similar impact trend of control strategies during the Omicron wave as in the Delta wave. For example, the risk of infection is reduced by about two-thirds due to the reduction of contact rate by 70% (Nepal: 30.42, 95% CrI [17.61, 46.43] to 9.6, 95% CrI [1.60, 17.61], Province 1: 16.30, 95% CrI [9.87, 24.03] to 5.15, 95% CrI [1.71, 9.44] per hundred thousand).

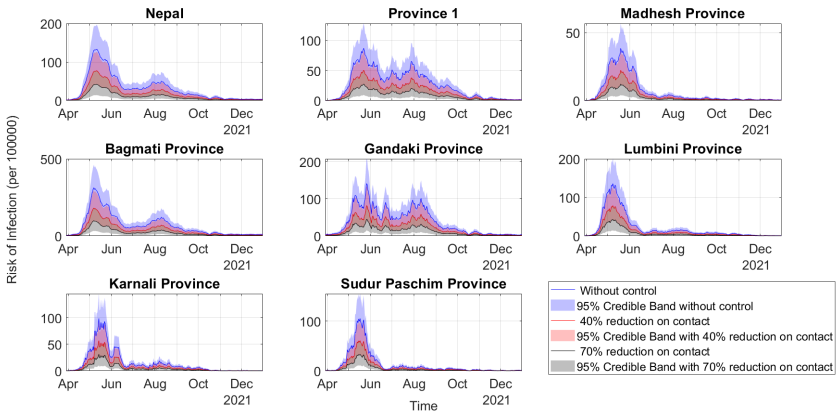

Figure 27: Effect of control measures on a reduction of risk of infection during the Delta wave.

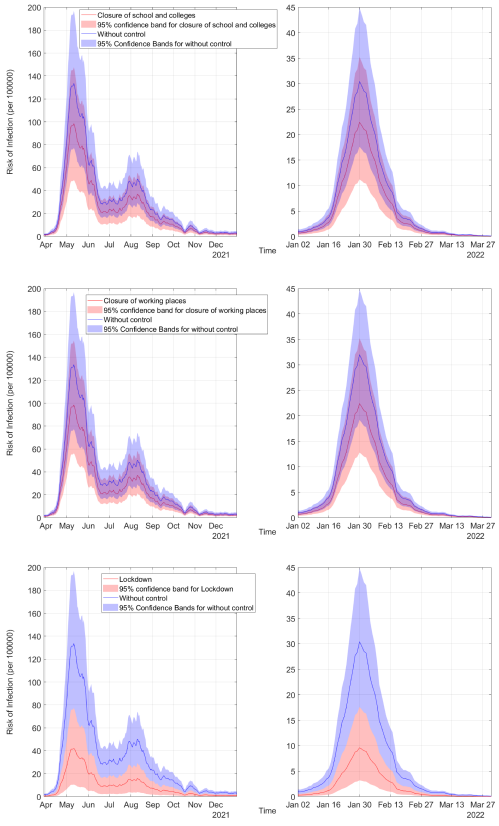

Figure 28: Effect of closures of school colleges, working places, and lockdown on reducing the risk of infection during the Delta and Omicron waves. The left column is for the Delta Wave, and the right column is for the Omicron Wave. The first row represents the impacts of the closure of schools and colleges, the second row represents the effects of closing working places, and the third row represents the effects of lockdown.

We also estimated the risk of infection under the closure of school/colleges and working places only during the Delta and Omicron waves (Fig. 28). We observed that closing schools and colleges (i.e., restriction of mobility of school/college age groups) and workplaces (i.e., restriction of mobility of the adult groups of age 25-59) can reduce the risk of infection by 26.30% while a complete lockdown reduces the risk of infections by 68.42% (during the Delta, none: 133.54, 95% CrI [77.33, 196.74], school/college closed: 98.42, 95% CrI [49.22 147.59], working place closed: 98.42, 95% CrI [56.25, 154.61], lockdown: 42.17, 95% CrI [14.06, 77.33]; during the Omicron wave, none: 30.42, 95% CrI [17.61, 46.43], schools/colleges closed: 22.41, 95% CrI [11.21, 33.62], working places closed: 22.42, 95% CrI [12.81, 36.82], lockdown: 8.00, 95% CrI [1.60, 17.61] per hundred thousand).

5.4 Discussion

The timely assessment of the epidemic trend and its potential burden is essential to minimize the epidemic disaster and manage the healthcare facilities. In order to allocate resources and design health policies during the early stages of a pandemic, it is necessary to estimate the risk of infection and risk of hospitalization. Generally, the risk of hospitalization remains the same throughout the transmission period for the same kind of strain. However, the pattern of hospitalization may vary depending on the geographic region, cultural background, level of education, way of life, access to medical services, and population group among which the disease is circulating [13, 87]. Even when more infections result in more patients being admitted to hospitals, the risk of hospitalization may not be constant over time.

The effective reproduction number is widely used to track the transmission rate during epidemics. However, due to variations in the size of the susceptible population, the number of actively infected individuals, and the population's pattern of contact, two regions with the same effective reproduction number may have different levels of vulnerability (risk) throughout the pandemic. To track the trend of an epidemic more precisely by including the most vital factors of disease transmission, we developed data-driven mathematical models which provide a timely estimation of the risk of infection and the risk of hospitalization during a pandemic. Our mathematical model of risk of infection considers the susceptible population, active infectious population, and contact pattern of the people in addition to the effective reproduction number. Similarly, our hospitalization risk model uniquely utilizes active hospitalized cases to

describe the temporal pattern of hospitalization trends. We implemented our models to the unique data sets of new COVID-19 cases and hospitalized cases in Nepal and its provinces. Furthermore, our models also allow us to determine how the implemented control strategies could effectively control disease.

The seven provinces of Nepal have a range of population contact patterns due to their diverse geographic locations, distinctive lifestyles, cultural traditions, economic conditions, and level of urbanization [134]. The recorded COVID-19 cases also varied throughout provinces [122]. Despite huge discrepancies among provinces, the reproduction numbers of COVID-19 of the Delta and Omicron waves across Nepal and its provinces are not considerably different (Fig. 23), indicating that reproduction numbers alone may not fully capture the disease trend. A noticeable difference in reproduction number between the Delta and Omicron surges regarding the non-pharmaceutical interventions is that the total lockdown needed to be implemented during the Delta wave, while for the Omicron variant, partial closure of schools and colleges helped fall the reproduction number below the threshold value one. In some provinces (Madhesh, Lumbini, Karnali, and Sudur Paschim), we noticed a wider range of credible intervals for the estimated Rt at the end of March 2022. This increased variability may be due to the fact that there were fewer reported new cases, with more fluctuations.

The risk of infection varies widely among provinces in both the Delta and Omicron waves despite the similar reproduction number. The ability of our model to capture the discrepancies among the provinces highlights the risk of infection as a critical indicator of the disease trend. Our results show a similar risk of infection in Nepal and in Bagmati province during the Delta and Omicron surges. However, in the case of other provinces, the risk of infection is less during the Omicron surge than during the Delta surge. Less risk of the Omicron is in contrast to what has been observed in other regions of the world, where the Omicron wave had a higher risk of infection than the Delta wave [58, 86, 108, **?**]. Note that 36% of Nepalese people were fully vaccinated, and 49% were vaccinated with at least one dose by 4 January 2022 [150]. Because of the low severity of the Omicron variant [31, 185], and the high coverage of vaccines, there were presumably fewer reported cases during the Omicron surge, which could be attributed to the low risk of infection as estimated by our model. During the Delta wave, infection risk rapidly increased and declined slowly. In contrast, during the Omicron wave, it rose and fell quickly, which may be due to the burnout of the susceptible population during previous waves or vaccinations, resulting in a faster

climb and decline of cases compared to the Delta wave.

A substantial strength of our models also lies in their ability to describe the discrepancies among provinces in the pattern of the risk of hospitalization. We observed these discrepancies throughout Nepal and its provinces (for example, 6% in Madhesh province and 21% in Sudur Paschim) during the Delta surge (Fig. 25). The disparities in the risk of hospitalization reflect the unequal distribution of healthcare facilities and the different living standards of the people in different provinces [39, 154]. For example, Madhesh province shares the border with Province 1, which has relatively better and larger hospitals. Therefore, many people from Madhesh province go to the hospitals of Province 1, causing a higher hospitalization rate in Province 1 than in Madhesh province. Bagmati province contains Kathmandu, the capital city, and other major cities such as Lalitpur, Bhaktapur, Bharatpur, Hetauda, and Dhulikhel, comprising the major hospitals of Nepal. Among the reported hospitalized cases $\sim 48\%$, were in this province [122], which may have included the hospitalization of people from other provinces as well.

Despite the fewer number of new cases and hospitalized cases, the rate of hospitalization in Karnali and Sudur Paschim was estimated to be high. Madhesh province, on the other hand, has a low risk of hospitalization and low reported new cases. Our model estimates a four times higher risk of hospitalization during the Delta surge than the Omicron surge in Nepal and most provinces (Fig. 25), consistent with the higher hospitalization during the Delta surge found in other studies [30, 41, 185]. The unusual risk of hospitalization seen in the Sudur Paschim is likely due to the data set. For example, on 1st January 2022, there were four new cases while seven persons were in hospital. From 1st to 12th January 2022, only 330 new cases were reported, but 395 active hospitalized cases were reported on 12th January, indicating more than 100% risk of hospitalization, as revealed in the model prediction. The higher active hospitalized cases of Sudur Paschim, compared to the new cases, could be due to the inclusion of the institutional isolation of returnee migrant workers in the data of active hospitalized cases.

We also used our model to evaluate the effectiveness of control strategies in suppressing infection rates. For the purpose of demonstration, we assumed different levels of control interventions (0%, 40%, and 70% reduction in contact rates) and estimated the corresponding risk of infection during the Delta surge (Fig. 26 & Fig. 27). Our results indicate that the risk of infection of COVID-19 would have been three times more if there were no lockdown (i.e., a lack of 70% reduction in contact) during the

Delta surge. We also found that school/college closures have a greater impact on the reduction of risk of infection (Fig. 28), supporting the Nepal government's strategy of closing schools and colleges first during the peak of the Omicron surge [92]. Our model supports that the effectiveness of the control strategy is linearly translated to the risk of infection (Fig. 26). Other studies [65, 96, 97, 174] have also reported that travel restrictions and non-pharmaceutical interventions have major impacts on the control of COVID-19 surges.

We acknowledge several limitations of our study. Although the population has a varied mixture pattern, we consider a homogeneous mixture in our model for estimating the risk of hospitalization so that every infected person has an equal probability of hospitalization. There are some uncertainties in the data used to compute the risk of infection and hospitalization. Underestimation and temporal inaccuracy (time lag between the time of infection/hospitalization and observation (record)) of the data also are two major factors that reduce the quality of the data we used. The better quality of data enhances the accuracy of the results of this study. Our model also does not consider the temporal variation in under-reporting, which might otherwise be interpreted as a variation in the risk of infection. Reported COVID-19 cases include only those individuals who were tested and confirmed to be positive.

Several studies [3, 4, 142, 156] have found asymptomatic or undiagnosed COVID-19-infected individuals who can significantly spread the virus. The detection of COVID-19 cases in Nepal is low [3], implying that the actual risk of infection might be quantitatively different from our estimations. A Hidden Markov Model (HMM) could be an extension of our model to account for the imperfect observation process of undiagnosed cases. Hospital admission is nonspecific because it does not necessarily specify the reason and might cover a wide range of severity. Individuals infected with SARS-COV-2 may be hospitalized, but not necessarily as a result of COVID-19. A study [48] estimated that 17 billion (UI 10–24) individuals, or 22% (UI 15–28) of the world's population, have at least one underlying condition that increases their chance of developing severe COVID-19 if they become infected (range from 5% of those younger than 20 years to $> 66\%$ of those who are 70 years or older). Also, a study [22] shows that among the COVID-19 patients hospitalized in Sukraraj Tropical and Infectious Disease Hospital of Nepal from January 2020 to January 2021, 64% had two or more comorbidities. Identifying an accurate number of hospitalized cases due to COVID-19 is necessary to accurately estimate the risk of hospitalization. Due to the unavailability of data regarding the number of new cases caused by the Delta and Omicron

variants in mixed disease dynamics, we did not consider the mixed diseases model.

In summary, we developed data-driven mathematical models to estimate the risk of infection and the risk of hospitalization during the pandemic. As demonstrated by the applications of these models to a unique data set of Nepal and its provinces, the risk of infection and hospitalization can capture critical features of epidemic trends. Our model can also be used in other places and for outbreaks of other infectious diseases. Real-time quantification of the risk of infection and hospitalization is essential to develop ideal policy guidelines and appropriate control strategies for bringing society out of the devastating pandemic.

CHAPTER 6

SUMMARY AND CONCLUSION

The main objectives of this work are to construct the comprehensive mathematical models for the analysis of COVID-19 transmission dynamics, explore spatial variations in COVID-19 transmission dynamics, particularly within the context of Nepal, and evaluate potential control measures. Additionally, the study aims to validate the developed mathematical models using multiple data sets, enabling the estimation of critical parameters along withe diseases thresholds; basic reproduction number (R_0) and the time-varying effective reproduction number (R_t) to enhance our understanding of the disease's spread and inform effective public health interventions. This work also aims to contribute novel tools, techniques and insights that advance our comprehension of COVID-19 risk and hospitalization. We summarized the overall work, conclusions, and some research plans for future directions.

6.1 Summary

In Chapter 2, the study provides the foundation by providing essential background information on epidemiology and mathematical modeling, introducing key theoretical analysis techniques utilized throughout the dissertation. Chapter 3 focuses on the development of a deterministic mathematical model that incorporates both imported and locally generated COVID-19 cases in Nepal, considering various control policies. This chapter also estimates crucial parameters, such as the basic and effective reproductive numbers, using case data from different phases of the epidemic, evaluating control strategies and predicting long-term dynamics. Chapter 4 extends the research by employing data-driven modeling to examine COVID-19 transmission patterns in high-risk and low-risk regions during the Delta surge, with a special focus on areas near the Nepal-India border and densely populated cities. Model validation, parameter es-

timation, and simulations are conducted using real-time data. Finally, in Chapter 5, novel techniques and insights that advance our comprehension of COVID-19 risk and hospitalization are proposed. These techniques are used to predict infection and hospitalization risks in real time, applying them to Nepal's COVID-19 data to estimate and assess the impact of the Delta and Omicron waves, as well as intervention strategies, on provincial communities and healthcare systems. In our study, we use MATLAB (The MathWorks, Inc.), R program for the numerical simulations.

6.2 Conclusion

Our work discussed in chapters 3 and 4 focuses on developing realistic epidemic mathematical models aimed at enhancing our understanding and predictive capabilities regarding the dynamics of infectious diseases, particularly COVID-19. Our approach diverges from simplification, as we prioritize the nuanced interplay of influential factors within real-world scenarios. Acknowledging the multifaceted nature of infectious disease transmission, including variables such as demographic characteristics, human behavior, non-pharmaceutical and pharmaceutical interventions, and healthcare infrastructure, our models incorporate these complexities. Consequently, our efforts result in representations of disease dynamics that faithfully mirror the intricacies of actual epidemiological situations. This, in turn, enhances the accuracy and utility of our work for informing public health strategies. An essential aspect of our work is also a parameter estimation, a critical process for optimizing our mathematical models. To achieve this, we employ statistical tools and techniques, including the nonlinear least squares method and Bayesian Inference. These methodologies enable us to precisely determine the most appropriate values for model parameters by fitting them with multiple datasets. This comprehensive approach refines our models while simultaneously providing a robust assessment of parameter uncertainty. The use of diverse datasets serves a dual purpose: it validates the reliability of our models and ensures their applicability across a wide range of epidemiological scenarios. This enhances the versatility and practicality of our findings, making them valuable for a broader range of applications in epidemiology and public health.

Our work described in Chapter 5 has an innovative advancement to precisely predict the dynamics of diseases along with the classical concept of the reproduction number. This extension provides a comprehensive understanding of disease dynamics by estimating the risks of infection and hospitalization. By doing so, we enable a

thorough assessment of the potential implications of disease spread within specific populations. These advancements furnish public health decision-makers with precise tools to adapt interventions, accounting not only for disease transmission dynamics but also for the potential strain on healthcare systems. In essence, our work significantly contributes to advancing epidemiological modeling, with practical applications that enhance public health protection.

6.3 Suggestions for Future Directions

We suggest the following areas for further study of the dynamic of the epidemic to be carried out for further study that may be appropriate to public health interventions:

- In modeling the first wave of COVID-19, we assumed a homogeneous mixing of the population, whereas for the Delta wave, our model incorporates two classes of susceptibilities. The susceptibility of the population network evolves over time upon contact with infectious agents. Therefore, employing mathematical modeling with multiple susceptibilities in dynamic networks enhances precision in capturing the dynamics of the disease.
- Within the mathematical framework for estimating risk, we used the average contact rate among the susceptible population. Varied contact rates within diverse susceptible populations contribute to refining the accuracy of the outcomes. To accommodate more impactful factors and their corresponding datasets, robust computational tools and techniques are required. The integration of machine learning and Artificial Intelligence (AI) into epidemiological models allows for leveraging extensive and dynamic datasets for real-time analysis and decision-making. This integration enhances the flexibility of models to adapt to changing scenarios, fostering a proactive approach in preparing for and responding to epidemics.

REFERENCES

[1] Nurul Absar, Nazim Uddin, Mayeen Uddin Khandaker, and Habib Ullah, *The efficacy of deep learning based LSTM model in forecasting the outbreak of contagious diseases*, Infectious Disease Modelling **7** (2022), no. 1, 170–183.

[2] Laith J Abu-Raddad, Hiam Chemaitelly, and Adeel A Butt, *Effectiveness of the BNT162b2 COVID-19 vaccine against the B. 1.1. 7 and B. 1.351 variants*, New England Journal of Medicine **385** (2021), no. 2, 187–189.

[3] Khagendra Adhikari, Ramesh Gautam, Anjana Pokharel, Meghnath Dhimal, Kedar Nath Uprety, and Naveen K Vaidya, *Insight into delta variant dominated second wave of COVID-19 in Nepal*, Epidemics (2022), 100642.

[4] Khagendra Adhikari, Ramesh Gautam, Anjana Pokharel, Kedar Nath Uprety, and Naveen K Vaidya, *Transmission dynamics of covid-19 in nepal: Mathematical model uncovering effective controls*, Journal of theoretical biology **521** (2021), 110680.

[5] Hafiz Farooq Ahmad, Huda Khaloofi, Zahra Azhar, Abdulelah Algosaibi, and Jamil Hussain, *An improved COVID-19 forecasting by infectious disease modelling using machine learning*, Applied Sciences **11** (2021), no. 23, 11426.

[6] Md Manjurul Ahsan, Shahana Akter Luna, and Zahed Siddique, *Machine-learning-based disease diagnosis: A comprehensive review*, Healthcare, vol. 10, MDPI, 2022, p. 541.

[7] ALJAZEERA, *Nepal starts 15-day covid lockdown as infections spike*, 2021.

[8] Philip W Anderson, *More is different: Broken symmetry and the nature of the hierarchical structure of science.*, Science **177** (1972), no. 4047, 393–396.

[9] Sina F Ardabili, Amir Mosavi, Pedram Ghamisi, Filip Ferdinand, Annamaria R Varkonyi-Koczy, Uwe Reuter, Timon Rabczuk, and Peter M Atkinson, *COVID-19 outbreak prediction with machine learning*, Algorithms **13** (2020), no. 10, 249.

[10] R Armitage and LB Nellums, *COVID-19 and the gypsy, roma and traveller population*, Public Health **185** (2020), 48.

[11] Shahir Asfahan, Maya Gopalakrishnan, Naveen Dutt, Ram Niwas, Gopal Chawla, Mehul Agarwal, and Mahendera Kumar Garg, *Using a simple open-source automated machine learning algorithm to forecast COVID-19 spread: A modelling study*, Advances in Respiratory Medicine **88** (2020), no. 5, 400–405.

[12] Maksat Ashyraliyev, Yves Fomekong-Nanfack, Jaap A Kaandorp, and Joke G Blom, *Systems biology: parameter estimation for biochemical models*, The FEBS journal **276** (2009), no. 4, 886–902.

[13] Prashant Athavale, Vijay Kumar, Jeremy Clark, Sumona Mondal, and Shantanu Sur, *Differential impact of COVID-19 risk factors on ethnicities in the united states*, Frontiers in public health (2021), 1954.

[14] Andrew Atkinson, Benjamin Ellenberger, Vanja Piezzi, Tanja Kaspar, Luisa Salazar-Vizcaya, Olga Endrich, Alexander B Leichtle, and Jonas Marschall, *Extending outbreak investigation with machine learning and graph theory: Benefits of new tools with application to a nosocomial outbreak of a multidrug-resistant organism*, Infection Control & Hospital Epidemiology **44** (2023), no. 2, 246–252.

[15] ———, *Extending outbreak investigation with machine learning and graph theory: Benefits of new tools with application to a nosocomial outbreak of a multidrug-resistant organism*, Infection Control & Hospital Epidemiology **44** (2023), no. 2, 246–252.

[16] Andrew S Azman and Francisco J Luquero, *From China: hope and lessons for COVID-19 control*, The Lancet Infectious Diseases **20** (2020), no. 7, 756–757.

[17] Jantien A Backer, Don Klinkenberg, and Jacco Wallinga, *Incubation period of 2019 novel coronavirus (2019-nCoV) infections among travellers from wuhan, China, 20–28 january 2020*, Eurosurveillance **25** (2020), no. 5, 2000062.

[18] Peter Bager, Jan Wohlfahrt, Jannik Fonager, Morten Rasmussen, Mads Albertsen, Thomas Yssing Michaelsen, Camilla Holten Møller, Steen Ethelberg, Rebecca Legarth, Mia Sarah Fischer Button, et al., *Risk of hospitalisation associated with infection with sars-cov-2 lineage b. 1.1. 7 in denmark: an observational cohort study*, The Lancet Infectious Diseases **21** (2021), no. 11, 1507–1517.

[19] Travis P Baggett, Harrison Keyes, Nora Sporn, and Jessie M Gaeta, *Prevalence of sars-cov-2 infection in residents of a large homeless shelter in boston*, Jama **323** (2020), no. 21, 2191–2192.

[20] Harvey Thomas Banks, Shuhua Hu, and W Clayton Thompson, *Modeling and inverse problems in the presence of uncertainty*, CRC Press, 2014.

[21] Anup Bastola, Ranjit Sah, Alfonso J Rodriguez-Morales, Bibek Kumar Lal, Runa Jha, Hemant Chanda Ojha, Bikesh Shrestha, Daniel KW Chu, Leo LM Poon, Anthony Costello, et al., *The first 2019 novel coronavirus case in Nepal*, The Lancet Infectious Diseases **20** (2020), no. 3, 279–280.

[22] Anup Bastola, Sanjay Shrestha, Richa Nepal, Kijan Maharjan, Bikesh Shrestha, Bimal Sharma Chalise, Pratistha Thapa, Pujan Balla, Alisha Sapkota, and Priyanka Shah, *Clinical mortality review of COVID-19 patients at Sukraraj Tropical and Infectious Disease Hospital, Nepal; a retrospective study*, Tropical Medicine and Infectious Disease **6** (2021), no. 3.

[23] Weissenbach Ben, *COVID-19 spirals out of control in Nepal: 'Every emergency room is full now'*, NATIONAL GEOGRAPHIC (2021).

[24] Daniel Bernoulli, *Essai d'une nouvelle analyse de la mortalité cause par la petite vérole et des avantages de l'inoculation pour la prévenir. histoire de l'académie royale des sciences avec les mémoires de mathématique et de physique tirés des registres de cette académie. paris 1766 (année 1760)*, History of Actuarial Science **8** (1766), 1766.

[25] ———, *Essai d'une nouvelle analyse de la mortalite causee par la petite verole*, Mem. Math. Phys. Acad. Roy. Sci., Paris **14** (2004), no. 5, 275–288.

[26] Jaime Berumen, Max Schmulson, Jesús Alegre-Díaz, Guadalupe Guerrero, Jorge Larriva-Sahd, Gustavo Olaiz, Rosa María Wong-Chew, Carlos Cantú-Brito, Ana Ochoa-Guzmán, Adrián Garcilazo-Ávila, Carlos González-Carballo, and Erwin Chiquete, *Risk of infection and hospitalization by COVID-19 in Mexico: a case-control study*, medRxiv (2020).

[27] R Bhandari and H Ellis-Peterson, *A hopeless situation': oxygen shortage fuels nepal's covid crisis*, The Guardian **10** (2021).

[28] Rajneesh Bhandari and Hannah Ellis Hannah Peterse, *A hopeless situation': oxygen shortage fuels Nepal's Covid crisis*, The Guardian (2021).

[29] Shital Bhandary, *Effectiveness of lockdown as COVID-19 intervention: official and computed cases in nepal*, Journal of Patan Academy of Health Sciences **7** (2020), no. 1, 37–41.

[30] Rajiv Bhatia and Jeffrey Klausner, *Estimating individual risks of COVID-19 associated hospitalization and death using publicly available data*, PLOS One **15** (2020), no. 12, e0243026.

[31] ———, *Estimating individual risks of COVID-19-associated hospitalization and death using publicly available data*, PLoS One **15** (2020), no. 12, e0243026.

[32] Gauri Bhuju, Ganga Ram Phaijoo, Dil Bahadur Gurung, et al., *Modeling transmission dynamics of COVID-19 in nepal*, Journal of Applied Mathematics and Physics **8** (2020), no. 10, 2167.

[33] Matthew Biggerstaff, Fredrick Scott Dahlgren, Julia Fitzner, Dylan George, Aspen Hammond, Ian Hall, David Haw, Natsuko Imai, Michael A Johansson, Sarah Kramer, et al., *Coordinating the real-time use of global influenza activity data for better public health planning*, Influenza and Other Respiratory Viruses **14** (2020), no. 2, 105–110.

[34] Alexandre Bolze, Elizabeth T Cirulli, Shishi Luo, Simon White, Dana Wyman, Andrew Dei Rossi, Tyler Cassens, Sharoni Jacobs, Jason Nguyen, JM Ramirez III, et al., *Rapid displacement of sars-cov-2 variant b. 1.1. 7 by b. 1.617. 2 and p. 1 in the united states*, MedRxiv (2021).

[35] Fred Brauer, *Mathematical epidemiology: Past, present, and future*, Infectious Disease Modelling **2** (2017), no. 2, 113–127.

[36] Ellen Brooks-Pollock, Leon Danon, Thibaut Jombart, and Lorenzo Pellis, *Modelling that shaped the early COVID-19 pandemic response in the UK*, 2021, p. 20210001.

[37] Ewen Callaway et al., *Delta coronavirus variant: scientists brace for impact*, Nature **595** (2021), no. 7865, 17–18.

[38] Finlay Campbell, Brett Archer, Henry Laurenson-Schafer, Yuka Jinnai, Franck Konings, Neale Batra, Boris Pavlin, Katelijn Vandemaele, Maria D Van Kerkhove, Thibaut Jombart, et al., *Increased transmissibility and global spread of sars-cov-2 variants of concern as at june 2021*, Eurosurveillance **26** (2021), no. 24, 2100509.

[39] Wen-Rui Cao, Prabin Shakya, Biraj Karmacharya, Dong Roman Xu, Yuan-Tao Hao, and Ying-Si Lai, *Equity of geographical access to public health facilities in nepal*, BMJ Global Health **6** (2021), no. 10, e006786.

[40] Central Bureau of Statistics (CBS), *Preliminary results of NationalPopulation Census,2078*, CBS, 2022.

[41] Centre for Disease Control and Prevention (CDC), *Rates of laboratory-confirmed COVID-19 hospitalizations by vaccination status*, September 2022, pp. 1–3.

[42] Robert Challen, Ellen Brooks-Pollock, Krasimira Tsaneva-Atanasova, and Leon Danon, *Meta-analysis of the SARS-CoV-2 serial interval and the impact of parameter uncertainty on the COVID-19 reproduction number*, MedRxiv (2020).

[43] Arnab Chanda, *COVID-19 in india: transmission dynamics, epidemiological characteristics, testing, recovery and effect of weather*, Epidemiology & Infection **148** (2020), e182.

[44] Nar Bahadur Chanda, Khagendra Adhikari, Ramesh Gautam, Anjana Pokharel, and Kedar Nath Uprety, *Estimating the effects of nonpharmaceutical interventions of covid-19 in sudurpaschim province, nepal*, Journal of Institute of Science and Technology **28** (2023), no. 1, 31–43.

[45] Hao-Yuan Cheng, Shu-Wan Jian, Ding-Ping Liu, Ta-Chou Ng, Wan-Ting Huang, Hsien-Ho Lin, et al., *Contact tracing assessment of COVID-19 transmission dynamics in Taiwan and risk at different exposure periods before and after symptom onset*, JAMA internal medicine **180** (2020), no. 9, 1156–1163.

[46] Jun Yong Choi, *COVID-19 in south korea*, Postgraduate medical journal **96** (2020), no. 1137, 399–402.

[47] I-Chun Chou and Eberhard O Voit, *Recent developments in parameter estimation and structure identification of biochemical and genomic systems*, Mathematical biosciences **219** (2009), no. 2, 57–83.

[48] Andrew Clark, Mark Jit, Charlotte Warren-Gash, Bruce Guthrie, Harry HX Wang, Stewart W Mercer, Colin Sanderson, Martin McKee, Christopher Troeger, Kanyin L Ong, et al., *Global, regional, and national estimates of the population at increased risk of severe COVID-19 due to underlying health conditions in 2020: a modelling study*, The Lancet Global Health **8** (2020), no. 8, e1003–e1017.

[49] Anne Cori, Neil M Ferguson, Christophe Fraser, and Simon Cauchemez, *A new framework and software to estimate time-varying reproduction numbers during epidemics*, American journal of epidemiology **178** (2013), no. 9, 1505–1512.

[50] Samuel Cusimano and Beckett Sterner, *Integrative pluralism for biological function*, Biology & Philosophy **34** (2019), 1–21.

[51] Sushma Dahal, Ruiyan Luo, Raj Kumar Subedi, Meghnath Dhimal, and Gerardo Chowell, *Transmission dynamics and short-term forecasts of covid-19: Nepal 2020/2021*, Epidemiologia **2** (2021), no. 4, 639–659.

[52] Ciara E Dangerfield, I David Abrahams, Chris Budd, Matt Butchers, Michael E Cates, Alan R Champneys, Christine SM Currie, Jessica Enright, Julia R Gog, Alain Goriely, et al., *Getting the most out of maths: How to coordinate mathematical modelling research to support a pandemic, lessons learnt from three initiatives that were part of the COVID-19 response in the UK*, Journal of Theoretical Biology **557** (2023), 111332.

[53] Department of Health and Social Care, *SPI-M modelling summary for pandemic influenza, Edition. Nov*, GOV. UK, 2018.

[54] Samath Dharmaratne, Supun Sudaraka, Ishanya Abeyagunawardena, Kasun Manchanayake, Mahen Kothalawala, and Wasantha Gunathunga, *Estimation of the basic reproduction number (R_0) for the novel coronavirus disease in Sri Lanka*, Virology Journal **17** (2020), no. 1, 1–7.

[55] Odo Diekmann, Johan Andre Peter Heesterbeek, and Johan AJ Metz, *On the definition and the computation of the basic reproduction ratio R0 in models for infectious diseases in heterogeneous populations*, Journal of mathematical biology **28** (1990), 365–382.

[56] Zoltan Domotor, *Philosophy of science, mathematical models in*, Mathematics of Complexity and Dynamical Systems, 2009.

[57] Vajeera Dorabawila, Dina Hoefer, Ursula E. Bauer, Mary T. Bassett, Emily Lutterloh, and Eli S. Rosenberg, *Risk of Infection and Hospitalization Among Vaccinated and Unvaccinated Children and Adolescents in New York After the Emergence of the Omicron Variant*, JAMA (2022).

[58] Zhanwei Du, Huaping Hong, Shuqi Wang, Lijia Ma, Caifen Liu, Yuan Bai, Dillon C Adam, Linwei Tian, Lin Wang, Eric HY Lau, et al., *Reproduction*

number of the Omicron variant triples that of the Delta variant, Viruses **14** (2022), no. 4, 821.

[59] EDCD, *COVID-19 Statistics: Nepal*, 2020a.

[60] _____, *Detailed epidemiological update COVID-19 – national and provinces*, 2020b.

[61] _____, *Epidemiological update on covid 19. epidemiology and diseases control division. nepal, (17 july 2020)*, 2020c.

[62] England, Public Heath, *Sars-cov-2 variants of concern and variants under investigation in england*, Technical briefing **23** (2021).

[63] PD En'Ko, *On the course of epidemics of some infectious diseases*, International journal of epidemiology **18** (1989), no. 4, 749–755.

[64] The New Indian Express, *Coronavirus infection in Nepal enters community transmission phase*, 2020.

[65] Neil M Ferguson, Daniel Laydon, Gemma Nedjati-Gilani, Natsuko Imai, Kylie Ainslie, Marc Baguelin, Sangeeta Bhatia, Adhiratha Boonyasiri, Zulma Cucunubá, Gina Cuomo-Dannenburg, et al., *Impact of non-pharmaceutical interventions (NPIs) to reduce COVID-19 mortality and healthcare demand*, Imperial College COVID-19 Response Team **20** (2020), no. 10.25561, 77482.

[66] Luca Ferretti, Chris Wymant, Michelle Kendall, Lele Zhao, Anel Nurtay, Lucie Abeler-Dörner, Michael Parker, David Bonsall, and Christophe Fraser, *Quantifying SARS-CoV-2 transmission suggests epidemic control with digital contact tracing*, science **368** (2020), no. 6491, eabb6936.

[67] Ivo M Foppa, *A historical introduction to mathematical modeling of infectious diseases: Seminal papers in epidemiology*, Academic Press, 2016.

[68] Tjede Funk, Anastasia Pharris, Gianfranco Spiteri, Nick Bundle, Angeliki Melidou, Michael Carr, Gabriel Gonzalez, Alejandro Garcia-Leon, Fiona Crispie, Lois O'Connor, et al., *Characteristics of sars-cov-2 variants of concern b. 1.1. 7, b. 1.351 or p. 1: data from seven eu/eea countries, weeks 38/2020 to 10/2021*, Eurosurveillance **26** (2021), no. 16, 2100348.

[69] Ryan B Ghannam and Stephen M Techtmann, *Machine learning applications in microbial ecology, human microbiome studies, and environmental monitoring*, Computational and Structural Biotechnology Journal **19** (2021), 1092–1107.

[70] Frank R Giordano, William P Fox, and Steven B Horton, *A first course in mathematical modeling*, Cengage Learning, 2013.

[71] GISAID, *Tracking of hcov19 variant.*, 2022.

[72] Taewan Goo, Catherine Apio, Gyujin Heo, Doeun Lee, Jong Hyeok Lee, Jisun Lim, Kyulhee Han, and Taesung Park, *Forecasting of the COVID-19 pandemic situation of korea*, Genomics & Informatics **19** (2021), no. 1.

[73] Gov. Nep, *Nepal labour migration report,2020*, Government of Nepal, Ministry of Labour, Employment and Social Security (2020).

[74] Nivedita Gupta, Harmanmeet Kaur, Pragya Yadav, Labanya Mukhopadhyay, Rima R Sahay, Abhinendra Kumar, Dimpal A Nyayanit, Anita M Shete, Savita Patil, Triparna Dutta Majumdar, et al., *Clinical characterization and genomic analysis of covid-19 breakthrough infections during second wave in different states of india (preprint)*, (2021).

[75] Linnéa Gyllingberg, Abeba Birhane, and David JT Sumpter, *The lost art of mathematical modelling*, Mathematical Biosciences (2023), 109033.

[76] Sara Hafeez, Misbahud Din, Fatima Zia, Muhammad Ali, and Zabta Khan Shinwari, *Emerging concerns regarding covid-19; second wave and new variant*, Journal of Medical Virology **93** (2021), no. 7, 4108.

[77] William Heaton Hamer, *The milroy lectures on epidemic diseases in england: The evidence of variability and of persistency of type; delivered before the royal college of physicians of london, march 1st, 6th, and 8th, 1906*, Bedford Press, 1906.

[78] Joel Hellewell, Sam Abbott, Amy Gimma, Nikos I Bosse, Christopher I Jarvis, Timothy W Russell, James D Munday, Adam J Kucharski, W John Edmunds, Fiona Sun, et al., *Feasibility of controlling COVID-19 outbreaks by isolation of cases and contacts*, The Lancet Global Health **8** (2020), no. 4, e488–e496.

[79] M Pear Hossain, Alvin Junus, Xiaolin Zhu, Pengfei Jia, Tzai-Hung Wen, Dirk Pfeiffer, and Hsiang-Yu Yuan, *The effects of border control and quarantine measures on the spread of COVID-19*, Epidemics **32** (2020), 100397.

[80] Tom Britton (auth.) Håkan Andersson, *Stochastic epidemic models and their statistical analysis*, 1 ed., Lecture Notes in Statistics 151, Springer-Verlag New York, 2000.

[81] IHME, *Tracking of hcov19 variant.*, 2021.

[82] VP Il'In, *Mathematical modeling and the philosophy of science*, Herald of the Russian Academy of Sciences **88** (2018), 81–88.

[83] IOM, *Migration in Nepal -a country profile 2019*, 2019.

[84] Salsabil Islam, Towhidul Islam, and Md Rabiul Islam, *New coronavirus variants are creating more challenges to global healthcare system: a brief report on the current knowledge*, Clinical pathology **15** (2022), 2632010X221075584.

[85] Kimihito Ito, Chayada Piantham, and Hiroshi Nishiura, *Predicted dominance of variant delta of SARS-CoV-2 before tokyo olympic games, japan, july 2021*, Eurosurveillance **26** (2021), no. 27, 2100570.

[86] ———, *Relative instantaneous reproduction number of Omicron SARS-CoV-2 variant with respect to the delta variant in Denmark*, Journal of Medical Virology **94** (2022), no. 5, 2265–2268.

[87] Sarah L Jackson, Sahar Derakhshan, Leah Blackwood, Logan Lee, Qian Huang, Margot Habets, and Susan L Cutter, *Spatial disparities of COVID-19 cases and fatalities in united states counties*, International Journal of Environmental Research and Public Health **18** (2021), no. 16, 8259.

[88] Waasila Jassat, Caroline Mudara, Lovelyn Ozougwu, Stefano Tempia, Lucille Blumberg, Mary-Ann Davies, Yogan Pillay, Terence Carter, Ramphelane Morewane, Milani Wolmarans, et al., *Difference in mortality among individuals admitted to hospital with covid-19 during the first and second waves in south africa: a cohort study*, The Lancet Global Health **9** (2021), no. 9, e1216–e1225.

[89] Niall PAS Johnson and Juergen Mueller, *Updating the accounts: global mortality of the 1918-1920" spanish" influenza pandemic*, Bulletin of the History of Medicine (2002), 105–115.

[90] D Joubert, JD Stigter, and J Molenaar, *Determining minimal output sets that ensure structural identifiability*, PLoS One **13** (2018), no. 11, e0207334.

[91] Hemanth Kumar Kandikattu, Chandra Sekhar Yadavalli, Sathisha Upparahalli Venkateshaiah, and Anil Mishra, *Vaccine efficacy in mutant sars-cov-2 variants*, International journal of cell biology and physiology **4** (2021), no. 1-2, 1.

[92] KATHMANDU POST, *Schools across Nepal shut until january 29 amid virus threat*, 2022.

[93] William O Kermack and Anderson G McKendrick, *Contributions to the mathematical theory of epidemics–I. 1927.*, Bulletin of mathematical biology **53** (1991), no. 1-2, 33–55.

[94] William Ogilvy Kermack and Anderson G McKendrick, *A contribution to the mathematical theory of epidemics*, Proceedings of the royal society of london. Series A, Containing papers of a mathematical and physical character **115** (1927), no. 772, 700–721.

[95] WO Kermack and AG McKendrick, *Contributions to the mathematical theory of epidemics—iii. further studies of the problem of endemicity*, Bulletin of mathematical biology **53** (1991), no. 1-2, 89–118.

[96] Adhikari Khagendra, Gautam Ramesh, Anjana Pokharel, Kedar Nath Uprety, and Naveen K. Vaidya, *Transmission dynamics of COVID-19 in Nepal: Mathematical model uncovering effective controls*, Journal of Theoretical Biology **521** (2021), no. 110680.

[97] Moritz UG Kraemer, Chia-Hung Yang, Bernardo Gutierrez, Chieh-Hsi Wu, Brennan Klein, David M Pigott, Open COVID-19 Data Working Group†, Louis Du Plessis, Nuno R Faria, Ruoran Li, et al., *The effect of human mobility and control measures on the COVID-19 epidemic in China*, Science **368** (2020), no. 6490, 493–497.

[98] Anthony YC Kuk and Stefan Ma, *The estimation of SARS incubation distribution from serial interval data using a convolution likelihood*, Statistics in Medicine **24** (2005), no. 16, 2525–2537.

[99] Laxman Singh Kunwar, *Emigration of Nepalese people and its impact*, Economic Journal of Development Issues (2015), 77–82.

[100] Stephen A Lauer, Kyra H Grantz, Qifang Bi, Forrest K Jones, Qulu Zheng, Hannah R Meredith, Andrew S Azman, Nicholas G Reich, and Justin Lessler,

The incubation period of coronavirus disease 2019 (COVID-19) from publicly reported confirmed cases: estimation and application, Annals of internal medicine **172** (2020), no. 9, 577–582.

[101] Chris L . Lehnig, Eyal Oren, and Naveen K. Vaidya, *Effectiveness of alternative semester break schedules on reducing COVID-19 incidence on college campuses*, Scientific Reports **12** (2021), no. 2116.

[102] Baisheng Li, Aiping Deng, Kuibiao Li, Yao Hu, Zhencui Li, Yaling Shi, Qianling Xiong, Zhe Liu, Qianfang Guo, Lirong Zou, et al., *Viral infection and transmission in a large, well-traced outbreak caused by the sars-cov-2 delta variant*, Nature communications **13** (2022), no. 1, 460.

[103] Qun Li, Xuhua Guan, Peng Wu, Xiaoye Wang, Lei Zhou, Yeqing Tong, Ruiqi Ren, Kathy SM Leung, Eric HY Lau, Jessica Y Wong, et al., *Early transmission dynamics in Wuhan, China, of novel coronavirus–infected pneumonia*, New England journal of medicine **382** (2020), no. 13, 1199–1207.

[104] Sunghoon Lim, Conrad S Tucker, and Soundar Kumara, *An unsupervised machine learning model for discovering latent infectious diseases using social media data*, Journal of biomedical informatics **66** (2017), 82–94.

[105] Natalie M Linton, Tetsuro Kobayashi, Yichi Yang, Katsuma Hayashi, Andrei R Akhmetzhanov, Sung-mok Jung, Baoyin Yuan, Ryo Kinoshita, and Hiroshi Nishiura, *Incubation period and other epidemiological characteristics of 2019 novel coronavirus infections with right truncation: a statistical analysis of publicly available case data*, Journal of clinical medicine **9** (2020), no. 2, 538.

[106] Sunil Pokharel Dipti Lata Lisa White, Nicholas Letchford and Rashid Zaman, *Modelling of COVID-19 strategies in Nepal*, 2020.

[107] Yang Liu, Julian W Tang, and Tommy TY Lam, *Transmission dynamics of the COVID-19 epidemic in england*, International Journal of Infectious Diseases **104** (2021), 132–138.

[108] Ying Liu and Joacim Rocklöv, *The effective reproductive number of the Omicron variant of SARS-CoV-2 is several times relative to Delta*, Journal of Travel Medicine **29** (2022), no. 3, taac037.

[109] Jamie Lopez Bernal, Nick Andrews, Charlotte Gower, Eileen Gallagher, Ruth Simmons, Simon Thelwall, Julia Stowe, Elise Tessier, Natalie Groves, Gavin

Dabrera, et al., *Effectiveness of covid-19 vaccines against the b. 1.617. 2 (delta) variant*, New England Journal of Medicine **385** (2021), no. 7, 585–594.

[110] George Macdonald, *The epidemiology and control of malaria.*, The Epidemiology and Control of Malaria. (1957).

[111] Manzoor Ahmad Malik, *Fragility and challenges of health systems in pandemic: early lessons from india's second wave of coronavirus disease 2019 (covid-19)*, Global Health Journal (2022).

[112] Maia Martcheva, *An introduction to mathematical epidemiology*, vol. 61, Springer, 2015.

[113] Michael T Meehan, Diana P Rojas, Adeshina I Adekunle, Oyelola A Adegboye, Jamie M Caldwell, Evelyn Turek, Bridget M Williams, Ben J Marais, James M Trauer, and Emma S McBryde, *Modelling insights into the COVID-19 pandemic*, Paediatric Respiratory Reviews **35** (2020), 64–69.

[114] Hongyu Miao, Xiaohua Xia, Alan S Perelson, and Hulin Wu, *On identifiability of nonlinear ODE models and applications in viral dynamics*, SIAM review **53** (2011), no. 1, 3–39.

[115] Sandra D Mitchell, *Biological complexity and integrative pluralism*, Cambridge University Press, 2003.

[116] Kenji Mizumoto and Gerardo Chowell, *Estimating risk for death from coronavirus disease, china, january–february 2020*, Emerging Infectious Diseases **26** (2020), no. 6, 1251.

[117] AG M'kendrick, *Applications of mathematics to medical problems*, Proceedings of the Edinburgh Mathematical Society **44** (1925), 98–130.

[118] MoHP, *Covid19-dashboard*, 2021.

[119] MoHP, GoN, *Health sector emergency response plan: Covid-19 pandemic (pp. 1–29)*, Government of Nepal, Ministry of Health and Population. Kathmandu, Nepal.

[120] ———, *COVID-19 Nepal*, 2020.

[121] ———, *Nepal national sero-prevalence survey for covid-19 october 2020.*, Government of Nepal, Ministry of Health and Population. Kathmandu, Nepal, 2020.

[122] MoHP, Nepal, *Nepal — Recent Updates*, Covid dash board (2022).

[123] Joël Mossong, Niel Hens, Mark Jit, Philippe Beutels, Kari Auranen, Rafael Mikolajczyk, Marco Massari, Stefania Salmaso, Gianpaolo Scalia Tomba, Jacco Wallinga, et al., *Social contacts and mixing patterns relevant to the spread of infectious diseases*, PLoS medicine **5** (2008), no. 3, e74.

[124] Khondoker Nazmoon Nabi, *Forecasting COVID-19 pandemic: A data-driven analysis*, Chaos, Solitons & Fractals **139** (2020), 110046.

[125] S Nebehay and E Farge, *Who classifies india variant as being of global concern*, 2021.

[126] Surendra Raj Nepal, *An analysis of COVID-19 cases in nepal: A modeling approach*, Journal of Institute of Science and Technology **25** (2020), no. 2, 80–92.

[127] Hiroshi Nishiura, Natalie M Linton, and Andrei R Akhmetzhanov, *Serial interval of novel coronavirus (COVID-19) infections*, International journal of infectious diseases **93** (2020), 284–286.

[128] Onlinekhabr, *Poor contract tracing in Kathmandu- two per infectious. onlinekhabr*, 2020.

[129] Christina Pagel and Christian A Yates, *Role of mathematical modelling in future pandemic response policy*, bmj **378** (2022).

[130] Shanthi Palaniappan, Ragavi V, and Beaulah David, *Prediction of epidemic disease dynamics on the infection risk using machine learning algorithms*, SN computer science **3** (2022), no. 1, 47.

[131] Basu Dev Pandey, Mya Myat Ngwe Tun, Kishor Pandey, Shyam Prakash Dumre, Khin Mya Nwe, Yogendra Shah, Richard Culleton, Yuki Takamatsu, Anthony Costello, and Kouichi Morita, *How an outbreak of covid-19 circulated widely in nepal: a chronological analysis of the national response to an unprecedented pandemic*, Life **12** (2022), no. 7, 1087.

[132] Kiran Raj Pandey, Anup Subedee, Bishesh Khanal, and Bhagawan Koirala, *Covid-19 control strategies and intervention effects in resource limited settings: A modeling study*, Plos one **16** (2021), no. 6, e0252570.

[133] Buddhi Pantha, Subas Acharya, Hem Raj Joshi, and Naveen K Vaidya, *Inter-provincial disparity of covid-19 transmission and control in nepal*, Scientific Reports **11** (2021), no. 1, 13363.

[134] Buddhi Pantha, Subas Acharya, Hem Raj Joshi, and Naveen K. Vaidya, *Inter-provincial disparity of COVID-19 transmission and control in Nepal*, Scitific Reports **11** (2021), no. 13363.

[135] Buddhi Pantha, Sunil Giri, Hem Raj Joshi, and Naveen K Vaidya, *Modeling transmission dynamics of rabies in nepal*, Infectious Disease Modelling **6** (2021), 284–301.

[136] Anjana Pokharel, Khagendra Adhikari, Ramesh Gautam, Kedar Nath Uprety, and Naveen K Vaidya, *Modeling transmission dynamics of measles in nepal and its control with monitored vaccination program*, Mathematical Biosciences and Engineering **19** (2022), no. 8.

[137] Arjun Poudel, *Highly contagious double mutant indian variant responsible for current surge of covid-19 cases*, 2021.

[138] Arjun Poudel, *Nepal reports new Omicron case*, THE KATHMANDU POST (2021).

[139] ———, *Omicron responsible for 88 percent of new COVID-19 infections in Nepal*, THE KATHMANDU POST (2022).

[140] Sangam Prasain, *Nepal's lockdown 2.0, new covid curbs on travel*, 2021.

[141] Kiesha Prem, Alex R Cook, and Mark Jit, *Projecting social contact matrices in 152 countries using contact surveys and demographic data*, PLOS Computational Biology **13** (2017), no. 9, e1005697.

[142] Giulia Pullano, Laura Di Domenico, Chiara E Sabbatini, Eugenio Valdano, Clément Turbelin, Marion Debin, Caroline Guerrisi, Charly Kengne-Kuetche, Cécile Souty, Thomas Hanslik, et al., *Underdetection of cases of COVID-19 in France threatens epidemic control*, Nature **590** (2021), no. 7844, 134–139.

[143] Sher Bahadur Pun, Shrawan Mandal, Lilanath Bhandari, Santoshananda Jha, Sagar Rajbhandari, Abdhesh Kumar Mishra, Bimal Sharma Chalise, and Rajesh Shah, *Understanding COVID-19 in Nepal*, (2020).

[144] Manesha Putra, Malavika Kesavan, Kerri Brackney, David N Hackney, and Kimberlyn M Roosa, *Forecasting the impact of coronavirus disease during delivery hospitalization: an aid for resource utilization*, American Journal of Obstetrics & Gynecology MFM **2** (2020), no. 3, 100127.

[145] Munsur Rahman, Kidist Bekele-Maxwell, LeAnna L Cates, HT Banks, and Naveen K Vaidya, *Modeling zika virus transmission dynamics: parameter estimates, disease characteristics, and prevention*, Scientific reports **9** (2019), no. 1, 10575.

[146] Balram Rai, Anandi Shukla, and Laxmi Kant Dwivedi, *Estimates of serial interval for COVID-19: A systematic review and meta-analysis*, Clinical Epidemiology and Global Health **9** (2021), 157–161.

[147] Bhatia Rajiv and Klausner Jeffrey, *Estimating individual risk of COVID-19 associated hospitalization and death using publicly available data*, Plos One **15** (2020).

[148] Nicolas Rashevsky, *Outline of a unified approach to physics, biology and sociology*, The bulletin of mathematical biophysics **31** (1969), 159–198.

[149] Ruy Freitas Reis, Bárbara de Melo Quintela, Joventino de Oliveira Campos, Johnny Moreira Gomes, Bernardo Martins Rocha, Marcelo Lobosco, and Rodrigo Weber Dos Santos, *Characterization of the covid-19 pandemic and the impact of uncertainties, mitigation strategies, and underreporting of cases in south korea, italy, and brazil*, Chaos, Solitons & Fractals **136** (2020), 109888.

[150] Hannah Ritchie, Edouard Mathieu, Lucas Rodés-Guirao, Cameron Appel, Charlie Giattino, Esteban Ortiz-Ospina, Joe Hasell, Bobbie Macdonald, Diana Beltekian, and Max Roser, *Coronavirus pandemic (COVID-19)*, Our World in Data (2020).

[151] Ronald Ross, *The prevention of malaria*, John Murray, 1911.

[152] ———, *An application of the theory of probabilities to the study of a priori pathometry.—part I*, Proceedings of the Royal Society of London. Series A, Containing Papers of a Mathematical and Physical Character **92** (1916), no. 638, 204–230.

[153] Satyaki Roy, Preetom Biswas, and Preetam Ghosh, *Spatiotemporal tracing of pandemic spread from infection data*, Scientific reports **11** (2021), no. 1, 17689.

[154] Eiko Saito, Stuart Gilmour, Daisuke Yoneoka, Ghan Shyam Gautam, Md Mizanur Rahman, Pradeep Krishna Shrestha, and Kenji Shibuya, *Inequality and inequity in healthcare utilization in urban nepal: a cross-sectional observational study*, Health Policy and Planning **31** (2016), no. 7, 817–824.

[155] Sho Saito, Yusuke Asai, Nobuaki Matsunaga, Kayoko Hayakawa, Mari Terada, Hiroshi Ohtsu, Shinya Tsuzuki, and Norio Ohmagari, *First and second covid-19 waves in japan: a comparison of disease severity and characteristics*, Journal of Infection **82** (2021), no. 4, 84–123.

[156] ———, *First and second COVID-19 waves in Japan: A comparison of disease severity and characteristics*, Journal of Infection **82** (2021), no. 4, 84–123.

[157] Omar Enzo Santangelo, Vito Gentile, Stefano Pizzo, Domiziana Giordano, and Fabrizio Cedrone, *Machine learning and prediction of infectious diseases: a systematic review*, Machine Learning and Knowledge Extraction **5** (2023), no. 1, 175–198.

[158] Subramanian Shankar, Sourya Sourabh Mohakuda, Ankit Kumar, PS Nazneen, Arun Kumar Yadav, Kaushik Chatterjee, and Kaustuv Chatterjee, *Systematic review of predictive mathematical models of covid-19 epidemic*, Medical journal armed forces India **77** (2021), S385–S392.

[159] B Shayak, Mohit Sharma, Richard H Rand, Awadhesh Kumar Singh, and Anoop Misra, *Transmission dynamics of COVID-19 and impact on public health policy*, MedRxiv (2020), 2020–03.

[160] Aziz Sheikh, Jim McMenamin, Bob Taylor, and Chris Robertson, *Sars-cov-2 delta voc in scotland: demographics, risk of hospital admission, and vaccine effectiveness*, The Lancet **397** (2021), no. 10293, 2461–2462.

[161] Subina Shrestha, *Hundreds of Nepalese stuck at india border amid COVID-19 lockdown*, Aljazeera [Internet] (2020).

[162] Paul E Smaldino, *Models are stupid, and we need more of them*, Computational social psychology (2017), 311–331.

[163] Herbert E Soper, *The interpretation of periodicity in disease prevalence*, Journal of the Royal Statistical Society **92** (1929), no. 1, 34–73.

[164] Gui-Quan Sun, Shi-Fu Wang, Ming-Tao Li, Li Li, Juan Zhang, Wei Zhang, Zhen Jin, and Guo-Lin Feng, *Transmission dynamics of COVID-19 in Wuhan, China: effects of lockdown and medical resources*, Nonlinear Dynamics **101** (2020), 1981–1993.

[165] Hideyuki Suzuki and Kazuyuki Aihara, *Universality in mathematical modeling: A comment on "surprising dynamics from a simple model"*, Mathematics Magazine **81** (2008), no. 4, 291–294.

[166] Khouloud Talmoudi, Mouna Safer, Hejer Letaief, Aicha Hchaichi, Chahida Harizi, Sonia Dhaouadi, Sondes Derouiche, Ilhem Bouaziz, Donia Gharbi, Nourhene Najar, et al., *Estimating transmission dynamics and serial interval of the first wave of COVID-19 infections under different control measures: a statistical analysis in Tunisia from February 29 to May 5, 2020*, BMC infectious Diseases **20** (2020), no. 1, 1–8.

[167] Biao Tang, Nicola Luigi Bragazzi, Qian Li, Sanyi Tang, Yanni Xiao, and Jianhong Wu, *An updated estimation of the risk of transmission of the novel coronavirus (2019-nCov)*, Infectious Disease Modelling **5** (2020), 248–255.

[168] The Himalayan Times , *Covid cases going up as restrictions eased in jhapa.*

[169] THE KATHMANDU POST, *No evidence of covid community transmission yet but infection cases could rise, who nepal representative says*, 2020a.

[170] ———, *With hundreds of thousands of migrants predicted to return home, nepal needs to brace for a crisis*, 2020b.

[171] THE RISING NEPAL, *63 people sent to Kharipati quarantine*, 2020.

[172] RN Thompson, JE Stockwin, Rolina D van Gaalen, JA Polonsky, ZN Kamvar, PA Demarsh, Elisabeth Dahlqwist, Siyang Li, Eve Miguel, Thibaut Jombart, et al., *Improved inference of time-varying reproduction numbers during infectious disease outbreaks*, Epidemics **29** (2019), 100356.

[173] Robin N Thompson, Jake E Stockwin, Rolina D van Gaalen, Jonny A Polonsky, Zhian N Kamvar, P Alex Demarsh, Elisabeth Dahlqwist, Siyang Li, Eve Miguel, Thibaut Jombart, et al., *Improved inference of time-varying reproduction numbers during infectious disease outbreaks*, Epidemics **29** (2019), 100356.

[174] Huaiyu Tian, Yonghong Liu, Yidan Li, Chieh-Hsi Wu, Bin Chen, Moritz UG Kraemer, Bingying Li, Jun Cai, Bo Xu, Qiqi Yang, et al., *An investigation of transmission control measures during the first 50 days of the COVID-19 epidemic in China*, Science **368** (2020), no. 6491, 638–642.

[175] Time, *World Health Organization declares COVID-19 a 'pandemic' here's what that means*, 2020.

[176] Maurizio Trevisan, Linh Cu Le, and Anh Vu Le, *The COVID-19 pandemic: a view from Vietnam*, American Journal of Public Health **110** (2020), no. 8, 1152–1153.

[177] Ashleigh R Tuite, David N Fisman, and Amy L Greer, *Mathematical modelling of covid-19 transmission and mitigation strategies in the population of ontario, canada*, Cmaj **192** (2020), no. 19, E497–E505.

[178] Katherine A Twohig, Tommy Nyberg, Asad Zaidi, Simon Thelwall, Mary A Sinnathamby, Shirin Aliabadi, Shaun R Seaman, Ross J Harris, Russell Hope, Jamie Lopez-Bernal, et al., *Hospital admission and emergency care attendance risk for SARS-CoV-2 delta (B. 1.617. 2) compared with alpha (B. 1.1. 7) variants of concern: a cohort study*, The Lancet Infectious Diseases **22** (2022), no. 1, 35–42.

[179] P. van den Driessche and James Watmough, *Reproduction numbers and subthreshold endemic equilibria for compartmental models of disease transmission*, Mathematical Biosciences **180** (2002), no. 1, 29–48.

[180] Pauline Van den Driessche and James Watmough, *Reproduction numbers and sub-threshold endemic equilibria for compartmental models of disease transmission*, Mathematical biosciences **180** (2002), no. 1-2, 29–48.

[181] J Leo van Hemmen, *Biology and mathematics: A fruitful merger of two cultures*, Biological cybernetics **97** (2007), no. 1, 1–3.

[182] Maria D Van Kerkhove and Neil M Ferguson, *Epidemic and intervention modelling: a scientific rationale for policy decisions? lessons from the 2009 influenza pandemic*, Bulletin of the World Health Organization **90** (2012), no. 4, 306–310.

[183] Robert Verity, Lucy C Okell, Ilaria Dorigatti, Peter Winskill, Charles Whittaker, Natsuko Imai, Gina Cuomo-Dannenburg, Hayley Thompson, Patrick GT

Walker, Han Fu, et al., *Estimates of the severity of coronavirus disease 2019: a model-based analysis*, The Lancet infectious diseases **20** (2020), no. 6, 669–677.

[184] Jacco Wallinga and Peter Teunis, *Different epidemic curves for severe acute respiratory syndrome reveal similar impacts of control measures*, American Journal of Epidemiology **160** (2004), no. 6, 509–516.

[185] Hui Wan, Jing-An Cui, and Guo-Jing Yang, *Risk estimation and prediction of the transmission of coronavirus disease-2019 (COVID-19) in the mainland of china excluding hubei province*, Infectious Diseases of Poverty **9** (2020), no. 1, 1–9.

[186] Liping Wang, Jing Wang, Hongyong Zhao, Yangyang Shi, Kai Wang, Peng Wu, and Lei Shi, *Modelling and assessing the effects of medical resources on transmission of novel coronavirus (COVID-19) in Wuhan, China*, Math. Biosci. Eng **17** (2020), no. 4, 2936–2949.

[187] B Weissenbach, *Covid-19 spirals out of control in nepal:"every emergency room is full now."*, Natl Geogr Mag (2021).

[188] BEN WEISSENBACH, *Covid-19 spirals out of control in nepal: 'every emergency room is full now'*, 2021.

[189] WHO, *Coronavirus disease 2019 (COVID-19) situation report. 2 april, 2020. world health organization (who).*, 2020a.

[190] _____, *COVID-19 strategy update. World Health Organization (WHO)*, 2020b.

[191] _____, *Situation update report 19 (26 August, 2020), coronavirus disease 2019 (covid-19), who country office for nepal*, 2020d.

[192] _____, *Situation update report 22 (16 september, 2020), coronavirus disease 2019 (covid-19), who country office for nepal*, 2020e.

[193] _____, *Situation update report 23 (23 september, 2020), coronavirus disease 2019 (covid-19), who country office for nepal*, 2020f.

[194] _____, *Situation update report 18 (19 Aug 2020), coronavirus diseases 2019 nepal, who country office for nepal*, 2020g.

[195] _____, *Criteria for releasing covid-19 patients from isolation*, 2021.

[196] ———, *Critical preparedness, readiness and response actions for COVID-19*, 2021.

[197] ———, *Weekly epidemiological update on covid-19 - 29 june 2021*, 2021b.

[198] Eugene P Wigner, *The unreasonable effectiveness of mathematics in the natural sciences*, Philosophical Reflections and Syntheses, Springer, 1995, pp. 534–549.

[199] Rasmus Grønfeldt Winther, *Mathematical modeling in biology: philosophy and pragmatics*, Frontiers in Plant Science **3** (2012), 102.

[200] World Health Organization, *Ethics and governance of artificial intelligence for health: WHO guidance*, (2021).

[201] Worldometer, *Coronavirus cases*, Worldometer (2022).

[202] ———, *CORONAVIRUS PANDEMIC*, 2023.

[203] Yong Xiang, Ruoyu Zhang, QIU Jinghong, and Hon-Cheong So, *Association of COVID-19 with risks of hospitalization and mortality from other disorders post-infection: A study of the UK Biobank*, medRxiv (2022).

[204] Yanni Xiao, Biao Tang, Jianhong Wu, Robert A Cheke, and Sanyi Tang, *Linking key intervention timing to rapid decline of the COVID-19 effective reproductive number to quantify lessons from mainland China*, International Journal of Infectious Diseases **97** (2020), 296–298.

[205] Hsiang-Yu Yuan, Axiu Mao, Guiyuan Han, Hsiangkuo Yuan, and Dirk Pfeiffer, *Effectiveness of quarantine measure on transmission dynamics of COVID-19 in Hong Kong*, medRxiv (2020), 2020–04.

[206] Juanjuan Zhang, Maria Litvinova, Wei Wang, Yan Wang, Xiaowei Deng, Xinghui Chen, Mei Li, Wen Zheng, Lan Yi, Xinhua Chen, et al., *Evolving epidemiology and transmission dynamics of coronavirus disease 2019 outside Hubei province, China: a descriptive and modelling study*, The Lancet Infectious Diseases **20** (2020), no. 7, 793–802.

[207] NS Zhong, BJ Zheng, YM Li, LLM Poon, ZH Xie, KH Chan, PH Li, SY Tan, Q Chang, JP Xie, et al., *Epidemiology and cause of severe acute respiratory syndrome (sars) in guangdong, people's republic of china, in february, 2003*, The Lancet **362** (2003), no. 9393, 1353–1358.

[208] N Zhu, D Zhang, W Wang, X Li, B Yang, J Song, X Zhao, B Huang, W Shi, R Lu, et al., *China novel coronavirus investigating and research team. china novel coronavirus investigating and research team. a novel coronavirus from patients with pneumonia in china, 2019*, N Engl J Med **382** (2020), no. 8, 727–733.

Appendix

Publications

1. **Adhikari, K.** Gautam, R. Pokharel, A., Uprety KN., Vaidya, NK., Data-Driven Models for the Risk of Infection and Hospitalization during a Pandemic: Case Study on COVID-19 in Nepal. *Journal of Theoretical Biology.*

2. **Adhikari, K.** Gautam, R. Pokharel, A., Uprety KN. Vaidya, NK. Transmission dynamics of COVID-19 in Nepal: Mathematical model uncovering effective controls, Journal of Theoretical Biology, Volume 521, 2021, 110680, ISSN 0022-5193,
https://doi.org/10.1016/j.jtbi.2021.110680.

3. **Adhikari, K.** Gautam, R. Pokharel, A., Uprety KN., Dhimal M.N, Vaidya, NK., Insight into delta variant dominated second wave of COVID-19 in Nepal, Epidemics (2022) 100642.

4. **Adhikari K,** Dhan Bahadur Shrestha DB, Gautam R, Pokharel A. Transmission Dynamics of COVID-19 in Nepal. Humanities and Social Sciences Journal, Volume 13, Number 1, 2021, pp.155–169.

5. Pokharel A, **Adhikari K,** Gautam R, Uprety KN, Vaidya NK, Campus A, Campus RR. Modeling transmission dynamics of measles in Nepal and its control with monitored vaccination program. Math Biosci Eng. 2022 Jan 1;19(8):8554-79.

6. Gautam, R., Pokharel, A., **Adhikari, K.,** Uprety, K.N. and Vaidya, N.K., 2022. Modeling malaria transmission in Nepal: impact of imported cases through cross-border mobility. Journal of Biological Dynamics, 16(1), pp.528-564.

7. Chanda NB, **Adhikari K,** Gautam R, Pokharel A, Uprety KN, Estimating effects of nonpharmaceutical interventions of COVID-19 in Sudurpaschim province, Nepal. *Journal of Institute of Science and Technology*, Vol. 28 No. 1 (2023), DOI: https://doi.org/10.3126/jist.v28i1.49044.

Conferences/Workshops/Seminars

1. **Instructor:** CIMPA Summer School in Data Visualization, Modeling, and Mathematical Tools, Kathmandu, Nepal, May 15-24, 2023.

   Presentation: Mathematical Models of COVID-19 in Nepal. Third International Conference on Applications of Mathematics to Nonlinear Sciences (AMNS-2023). May 25, 2023, Pokhara, Nepal.

2. **Presentation:** Data-Driven Models for the Risk of Infection and Hospitalization during a Pandemic: Case Study on COVID-19 in Nepal. National Conference on Mathematics & Its Applications (NCMA-2022) (11-13 June, 2022, Ilam).

4. **Presentation:** Transmission dynamics of COVID-19 in Nepal: Mathematical Models for Effective Control. (30 September, 2022, IIT, Indore), (Through CIMPA research help project)).

5. **Presentation:** Potential of Research Collaborations. An Auto-ethnography. Recovery and Resilience in an Uncertain World. Nepali Academics in America (15- 16, April, 2022.) (The 2022 NACA Conference).

6. **Instructor:** Data Visualization in Epidemic models. Infectious diseases workshop on "Mathematical Modeling for Epidemic Control and prevention" (21-24, June 2022). Nepal health research council.

7. **Presentation:** CIMPA Summer Research School in Mathematical Epidemiology (09/05/2022 to 20/05/2022). Dhaka University, Bangladesh.

8. Participation in the 13th Conference on Dynamical Systems Applied to Biology and Natural Sciences (DSABNS 2022) Mathematical and Theoretical Biology Group (MTB), Feb. 8- 11, 2022.

9. **Presentation:** Transmission Dynamics of COVID-19 in Nepal, in the 3rd International Conference on Frontiers of Science and Technology-2021 (ICFST-2021) India, August 13-14, 2021.

10. **Presentation:** Transmission Dynamics of COVID-19in Nepal: Assessment of Effective Controls. ICCA NEPAL 2021, organized by Nepal Mathematical Society:

11. **Poster presentation:** Transmission Dynamics of COVID-19 in Nepal: Assessment of Effective Controls in the 3rd Annual Meeting of the SIAM Texas-Louisiana Section, October 16 - 18, 2020.

Scholarly Awards/honors

- **PhD Research Fellowship:** GRAID (Graduate Research Assistantships in Developing Countries) Program, International Mathematical Union (IMU). Fellowship period: 06/01/2021 – 05/31/2025.
- **PhD Research Fellowship:** Nepal Academy of Science and Technology (NAST) PhD Research Grant Fellowship period: 2020-2023.
- **NMS-Fellowship-2020:** Nepal Mathematical Society.
- **Awarded paper:** Gautam, R., Pokharel, A., **Adhikari, K.**, Uprety, K. N., & Vaidya, N. K. (2022). Modeling malaria transmission in Nepal: impact of imported cases through cross-border mobility. Journal of Biological Dynamics, 16(1), 528-564. (Awarded as the best international paper of the year 2022-2023). Prof. Dr. Shankar Raj Pant Research Award-2021
- **Awarded paper: Adhikari, K.**, Gautam, R., Pokharel, A., Uprety, K. N., & Vaidya, N. K. (2021). Transmission dynamics of COVID-19 in Nepal: Mathematical model uncovering effective controls. Journal of theoretical biology, 521, 110680. (Awarded as the best international paper of the year 2021).
- CIMPA Research Visit Travel Support 9/15/2022-10/15/2022 for IIT, Indore, India

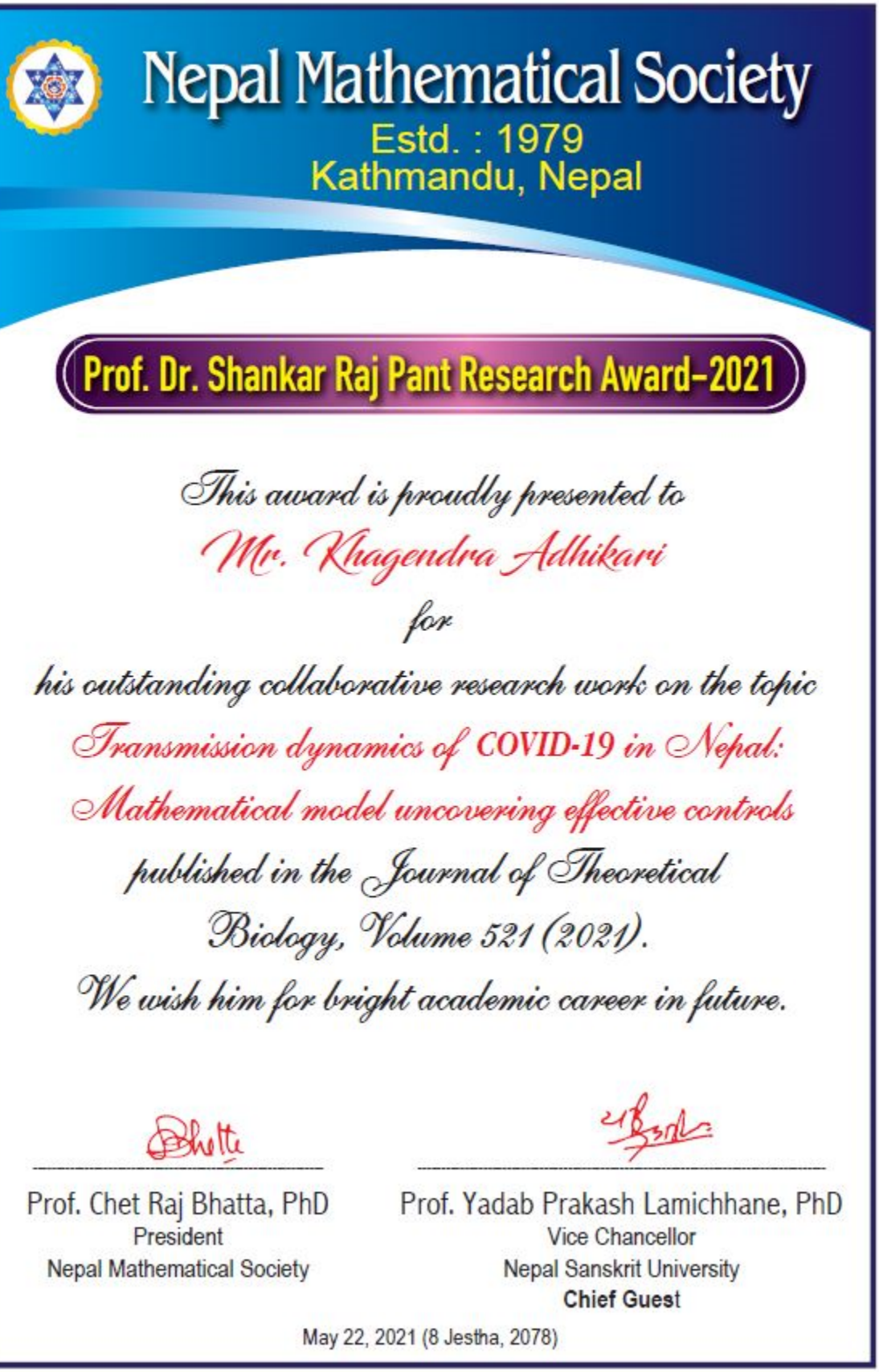

Nepal Mathematical Society

Estd. : 1979
Kathmandu, Nepal

Prof. Dr. Shankar Raj Pant Research Award-2021

This award is proudly presented to

Mr. Khagendra Adhikari

for

his outstanding collaborative research work on the topic

Transmission dynamics of COVID-19 in Nepal: Mathematical model uncovering effective controls

published in the Journal of Theoretical Biology, Volume 521 (2021).

We wish him for bright academic career in future.

Prof. Chet Raj Bhatta, PhD
President
Nepal Mathematical Society

Prof. Yadab Prakash Lamichhane, PhD
Vice Chancellor
Nepal Sanskrit University
Chief Guest

May 22, 2021 (8 Jestha, 2078)

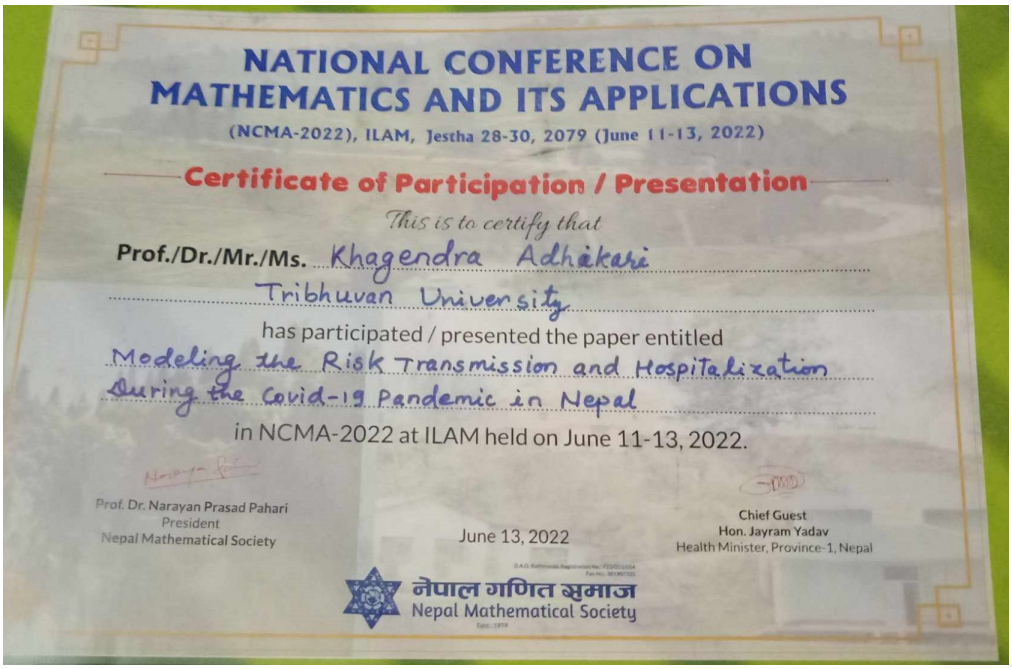

NATIONAL CONFERENCE ON
MATHEMATICS AND ITS APPLICATIONS

(NCMA-2022), ILAM, Jestha 28-30, 2079 (June 11-13, 2022)

Certificate of Participation / Presentation

This is to certify that

Prof./Dr./Mr./Ms. Khagendra Adhikari

Tribhuvan University

has participated / presented the paper entitled

Modeling the Risk Transmission and Hospitalization During the Covid-19 Pandemic in Nepal

in NCMA-2022 at ILAM held on June 11-13, 2022.

Prof. Dr. Narayan Prasad Pahari
President
Nepal Mathematical Society

June 13, 2022

Chief Guest
Hon. Jayram Yadav
Health Minister, Province-1, Nepal

नेपाल गणित समाज
Nepal Mathematical Society

CENTRAL DEPARTMENT OF MATHEMATICS

Tribhuvan University, Kathmandu, Nepal

CIMPA Summer School in Data Visualization, Modeling, and Mathematical Tools

Kathmandu, Nepal | May 15-24, 2023

CERTIFICATE OF APPRECIATION

This token of appreciation is presented to

Mr. Khagendra Adhikari

for his invaluable contribution to the Summer School as an instructor.

CIMPA

Dr. Shree Ram Khadka
Local Coordinator of the CIMPA School
Central Department of Mathematics
Tribhuvan University, Kathmandu, Nepal

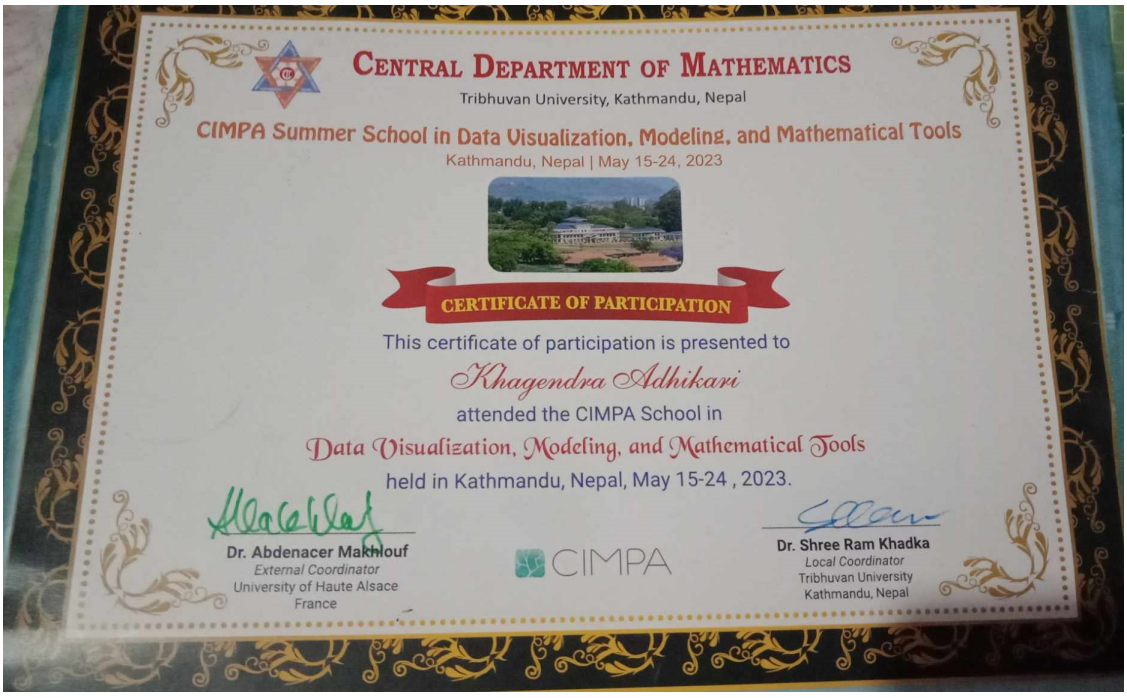

CENTRAL DEPARTMENT OF MATHEMATICS

Tribhuvan University, Kathmandu, Nepal

CIMPA Summer School in Data Visualization, Modeling, and Mathematical Tools

Kathmandu, Nepal | May 15-24, 2023

CERTIFICATE OF PARTICIPATION

This certificate of participation is presented to

Khagendra Adhikari

attended the CIMPA School in

Data Visualization, Modeling, and Mathematical Tools

held in Kathmandu, Nepal, May 15-24 , 2023.

Dr. Abdenacer Makhlouf
External Coordinator
University of Haute Alsace
France

CIMPA

Dr. Shree Ram Khadka
Local Coordinator
Tribhuvan University
Kathmandu, Nepal

CIMPA SUMMER RESEARCH SCHOOL

on

MATHEMATICAL EPIDEMIOLOGY/BIOLOGY

May 09-20, 2022

Certificate of Participation

This certificate is proudly presented to

Adhikari Khagendra

from the **Central Department of Mathematics, Tribhuvan University** for participating CIMPA (International Center for Pure & Applied Mathematics) Research School on Mathematical Epidemiology during May 09-20, 2022 at the Department of Mathematics, University of Dhaka, Bangladesh.

(Jorge Mozo Fernández)
External Coordinator
CIMPA Research School 2022

(Chandra Nath Podder)
Local Coordinator
CIMPA Research School 2022

Journal of Theoretical Biology 521 (2021) 110680

Contents lists available at ScienceDirect

Journal of Theoretical Biology

journal homepage: www.elsevier.com/locate/yjtbi

Transmission dynamics of COVID-19 in Nepal: Mathematical model uncovering effective controls

Khagendra Adhikari [a], Ramesh Gautam [b], Anjana Pokharel [c], Kedar Nath Uprety [d], Naveen K. Vaidya [e,f,g,*]

[a] Amrit Campus, Tribhuvan University, Kathmandu, Nepal
[b] Ratna Rajya Laxmi Campus, Tribhuvan University, Kathmandu, Nepal
[c] Padma Kanya Multiple Campus, Tribhuvan University, Kathmandu, Nepal
[d] Central Department of Mathematics, Tribhuvan University, Kathmandu, Nepal
[e] Department of Mathematics and Statistics, San Diego State University, San Diego, CA, USA
[f] Computational Science Research Center, San Diego State University, San Diego, CA, USA
[g] Viral Information Institute, San Diego State University, San Diego, CA, USA

ARTICLE INFO

Article history:
Received 26 November 2020
Revised 9 March 2021
Accepted 11 March 2021
Available online 24 March 2021

2010 MSC:
92B05

Keywords:
Biphasic epidemic
COVID-19
Mathematical model
Nepal
Open border

ABSTRACT

While most of the countries around the globe are combating the pandemic of COVID-19, the level of its impact is quite variable among different countries. In particular, the data from Nepal, a developing country having an open border provision with highly COVID-19 affected country India, has shown a biphasic pattern of epidemic, a controlled phase (until July 21, 2020) followed by an outgrown phase (after July 21, 2020). To uncover the effective strategies implemented during the controlled phase, we develop a mathematical model that is able to describe the data from both phases of COVID-19 dynamics in Nepal. Using our best parameter estimates with 95% confidence interval, we found that during the controlled phase most of the recorded cases were imported from outside the country with a small number generated from the local transmission, consistent with the data. Our model predicts that these successful strategies were able to maintain the reproduction number at around 0.21 during the controlled phase, preventing 442,640 cases of COVID-19 and saving more than 1,200 lives in Nepal. However, during the outgrown phase, when the strategies such as border screening and quarantine, lockdown, and detection and isolation, were altered, the reproduction number raised to 1.8, resulting in exponentially growing cases of COVID-19. We further used our model to predict the long-term dynamics of COVID-19 in Nepal and found that without any interventions the current trend may result in about 18.76 million cases (10.70 million detected and 8.06 million undetected) and 89 thousand deaths in Nepal by the end of 2021. Finally, using our predictive model, we evaluated the effects of various control strategies on the long-term outcome of this epidemics and identified ideal strategies to curb the epidemic in Nepal.

1. Introduction

Since the first reported case in China in December 2019 as a case of pneumonia of unknown cause, the novel corona virus disease (COVID-19) has spread rapidly all over the world, and on March 11, 2020, the World Health Organization (WHO) declared COVID-19 a pandemic (Time, 2020). As of September 16, 2020, more than 29 million cases of COVID-19 and more than 900 thousand deaths due to the disease have been reported worldwide (WHO, 2020c). In its global devastating effects on all aspects of human lives, the impact of the epidemic quite varies from country to country, thus the study focused on a specific country can provide better understanding of the disease and its control strategies.

In Nepal, the first case of COVID-19 was confirmed on January 23, 2020, which was also the first COVID-19 case in South Asia (GoN, 2020). After this first case found to be an infected Nepali student who had recently returned from Wuhan, China (Wiki, 2020), no additional case was reported until March 23, 2020. On March 24, 2020, the Government of Nepal implemented a country-wide lockdown including business closures and restrictions on movement within the country and access to flights in and out of the country (UN, 2020). In addition, the Government of Nepal aggressively initiated a border screen policy to quarantine people

* Corresponding author at: Department of Mathematics and Statistics, San Diego State University, San Diego, CA, USA.
E-mail address: nvaidya@sdsu.edu (N.K. Vaidya).

https://doi.org/10.1016/j.jtbi.2021.110680
0022-5193/

traveling to Nepal from abroad, to test them, and to isolate them if the test is positive. Because of such timely and aggressively implemented control strategies, the number of COVID-19 cases in Nepal remained relatively low (only 4% of the total cases from local transmission) until mid of July, 2020 (EDCD, 2020c), when these policies ended. Since these policies were lifted, the new cases began to grow dramatically, and as of September 16, 2020 the total of 58,327 cases (mostly from local transmission) have been reported (EDCD, 2020a). We define the epidemic phase from March 22 to July 21 as *the controlled phase*, during which the daily recorded cases remained significantly low, and the epidemic phase from July 22 to September 16 (end of the study) as *the outgrown phase*, during which the daily recorded COVID-19 cases exponentially increased. A detailed study of the biphasic epidemic trend of COVID-19 appeared in Nepal provides us with an opportunity to identify and evaluate effects of control strategies in the context of countries like Nepal, which is uniquely characterized by an open border provision with India, one of the highest COVID-19 affected countries.

Mathematical modeling using nonlinear systems has been an important tool for describing the dynamics of infectious diseases and evaluating the control strategies to curb epidemics (He et al., 2020; Hiroshi et al., 2020; Keeling and Rohani, 2008; Martcheva, 2015; Okuonghae and Omame, 2020; Vaidya and Lindi, 2015; Yang et al., 2020; Zhang et al., 2012; Rahman et al., 2019; Van den Driessche and Watmough, 2020). Deterministic mathematical models, including the SEIR (Susceptible-Exposed-Infected-Recovered) model, have been widely used in quantitative studies of COVID-19 pandemics. While some models were used to estimate the parameters, such as incubation period and infectious period (Backer et al., 2020; Linton et al., 2020; Liu et al., 2020b; Wan et al., 2020), others examined the effectiveness of control strategies, such as lockdown, detection and isolation, border screening, and medical resources (Hellewell et al., 2020; Shayak et al., 2020; Sun et al., 2020; Xiao et al., 2020; Chanda, 2020; Cheng et al., 2020; Faal et al., 2020; Ferretti and Chris, 2020; Wang et al., 2020). The quarantine for the traveler and suspected cases were also studied as the effective control measures for mitigating COVID-19 (Armitage and Nellums, 2020; Hossain et al., 2020; Liu et al., 2020a; Yuan et al., 2020). Regarding COVID-19 in Nepal, previous studies (Bhandary, 2020; Bhuju et al., 2020; Pun et al., 2020; White et al., 2020) have provided some insights into doubling time of new infections, early transmission trend, and the timing of the daily incidence burden in Nepal. However, none of the previous models have considered the entry of cases through the Nepal-India open border and border-related control strategies, which can be important factors because the travel history of recorded infectious people shows that more than 80% infectious cases came from abroad, especially from India, during the early period of epidemics (EDCD, 2020b; Rijal, 2020). Also, despite the Nepal government's effort of applying strategies, such as border screening, quarantine and isolation, poor handling policy at the border does exist, allowing many infected individuals to enter the community without quarantine (Shrestha, 2020).

In this study, we develop a deterministic mathematical model, which incorporates the imported as well as locally generated cases along with various policies implemented for the control of COVID-19 in Nepal. Using case data from both the controlled and outgrown phases of epidemics in Nepal, we estimated key parameters as well as the basic and effective reproductive numbers. Using our model, we evaluated the control strategies implemented in Nepal. Furthermore, we applied our model to predict the long-term dynamics of COVID-19 in Nepal, and provided the simulations to demonstrate how these control strategies can curb the epidemics in Nepal.

2. Method

2.1. Data source

The data used in this study was obtained from the Ministry of Health and Population, Epidemiology and disease control division (EDCD) of Nepal (EDCD, 2020a). Since March 22, 2020 is the last day of any single COVID-19 case in the country, we considered the data of COVID-19 from March 22. The government of Nepal started the countrywide lockdown and border screening from March 24 to July 21. Since the country returned into an almost no-policy state after the long route buses and national flights were fully opened on September 17, 2020 (WHO, 2020e), we considered the data until September 16, 2020. The data including quarantine, new cases, cumulative cases, and RT-PCR tests, were used in our model fitting and simulation. We note that during the initial phase of epidemic, most of the PCR tests performed were for the quarantined people and only a few for the community and front line workers (armed forces, hospital workers, civil workers, etc.). Therefore, we considered 80% of the PCR-tests performed were for the people who were quarantined.

2.2. Modeling basic transmission dynamics

We consider the transmission dynamics model based on the SEIR framework. We divide the whole population into five distinct compartments: S (susceptible), E (exposed), I_R (recorded infectious), I_N (non-recorded infectious), and R (recovered). In our model, susceptible individuals contract the virus when they come in contact with the non-recorded infectious individuals at the rate β. These exposed individuals become infectious at per capita rate δ with the proportion θ being recorded and $1-\theta$ remaining non-recorded. Individuals from both I_R and I_N classes get recovered with the rate η or die with the rate k. μ and Λ represent the per capita rate of natural mortality and the natural recruitment rate into the susceptible class. We represent the entry of individuals from abroad, mainly across the Nepal-India border, by the time-dependent rate $\lambda(t)$, among which the proportion ρ are infected and the remaining $(1-\rho)$ are susceptible.

2.3. Modeling control strategies implemented in Nepal

The main control strategies implemented by the government of Nepal are: (i) Border screening and quarantine, (ii) Lockdown, and (iii) Detection and isolation.

Border screening and quarantine. To model the border screening and quarantine strategy, we introduce a quarantined class, Q, to which $\phi\lambda(t)$ of individuals from abroad enter, where ϕ represents the rate of border screening. For these quarantined individuals PCR test is performed with rate τ and the tested individuals with positive result enter into the I_R class and are isolated. As the expected rate of positive test in people entering into the country is ρ, we assume that ρ represents the portion of the tested population getting positive result, while the remaining $(1-\rho)$ portion of the tested population show negative result and enter the susceptible class, S. Due to the limitation of PCR test, there were cases of individuals, including some without onset of the symptoms, being released from the quarantine center without performing PCR test. We assume that individuals leave the quarantined class without PCR test at the rate of γ. Among them, the portion ρ enters non-recorded infectious class and the remaining $(1-\rho)$ enters the susceptible class.

Lockdown. Lockdown strategy reduces the contact among individuals, and we assume the reduction of contact by ξ resulting in the transmission rate $\beta \to (1-\xi)\beta$. Since the strategy was altered

in two different phases, the controlled and the outgrown, we consider two different reduction rates of contact as follows.

$$\xi(t) = \begin{cases} \xi_c, & t \leqslant t_c, \\ \xi_o, & t > t_c, \end{cases}$$

where t_c represents the time when the epidemic phase changes corresponding to alteration of policies (July 21, 2020). As a result, the net infection rate becomes $\beta_c = (1-\xi_c)\beta$ and $\beta_o = (1-\xi_o)\beta$ before and after $t = t_c$, respectively.

Detection and isolation. As mentioned above, recorded infected individuals, I_R, in our model are isolated. Therefore, the detection and isolation strategy can be incorporated into our model by altering the rate θ. We introduce a parameter ψ to represent the effect of the detection so that the rate of individuals in exposed class, who are detected and recorded, changes as $\theta \to \psi\theta$. Since the strategy of testing for individuals in the general community was altered after the lockdown was lifted, we take two different detection rates for the controlled and outgrown phases as follows.

$$\psi(t) = \begin{cases} \psi_c, & t \leqslant t_c, \\ \psi_o, & t > t_c. \end{cases}$$

As a result, the net detection and isolation rate becomes $\theta_c = \psi_c\theta$ and $\theta_o = \psi_o\theta$ before and after $t = t_c$, respectively.

Combining all the control strategies implemented in Nepal into the basic transmission dynamics model, we obtain the model as shown in Fig. 1. The model is described by the following system of ordinary differential equations.

$$\frac{dQ}{dt} = \lambda(t)\phi - \tau Q - \mu Q - \gamma Q, \tag{1}$$

$$\frac{dS}{dt} = \Lambda + \lambda(t)(1-\phi)(1-\rho) + \tau(1-\rho)Q + \gamma(1-\rho)Q - \frac{\beta(t)SI_N}{N} - \mu S, \tag{2}$$

$$\frac{dE}{dt} = \frac{\beta(t)SI_N}{N} - (\delta+\mu)E, \tag{3}$$

$$\frac{dI_R}{dt} = \delta\theta(t)E + \rho\tau Q - (\eta+\mu+k)I_R, \tag{4}$$

$$\frac{dI_N}{dt} = \lambda(t)\rho(1-\phi) + \gamma\rho Q + \delta(1-\theta(t))E - (\eta+\mu+k)I_N, \tag{5}$$

$$\frac{dR}{dt} = \eta I_N + \eta I_R - \mu R. \tag{6}$$

Here, the total population is given by $N = Q + S + E + I_R + I_N + R$.

2.4. Estimation of population size and model parameters

Even though the first case of COVID-19 in Nepal was confirmed on January 23, 2020, no additional cases were reported until March 23, 2020. Therefore, we consider March 22, 2020 as the initial time $t = 0$ for our dynamical system model. The total population of Nepal in the census year 2011 was 26,494,504, which was projected to reach 29,704,501 by the end of 2019 (CBS, 2011). There are about 3 to 4 million Nepalese working in India (Kunwar, 2015; TKP, 2020b) and about 1.5 million Nepalese working in the Gulf countries and Malaysia (MoL, 2020; IOM, 2019), making approximately the total of 5 million Nepalese as seasonal migrants. Therefore, deducting 5 million people as migrants from the total population of 29,704,501, we get $N(0) = 25{,}000{,}000$. Also, 63 people came from abroad were sent to Kharipati quarantine (a quarantine centre) on March 21 (TRN, 2020). Therefore, we take $Q(0) = 63$. The first case identified on January 23, 2020 had been recovered (GoN, 2020) by the beginning of our dynamics, and hence we take $R(0) = 1$. Since the initial time of our dynamic model is the beginning of the epidemic, we assume $E(0) = 1$, $I_R(0) = 0$, and $I_N(0) = 1$.

Since the infected individuals remain in the exposed class for about 5.2 days until they become infectious (Stephen et al., 2020; Backer et al., 2020; WHO, 2020a), we take $\delta = 1/5.2 = 0.1923$ per day. Also, the infectious individuals get recovered in about 17 days (Time, 2020), implying the average recovery rate $\eta = 1/17 = 0.0588$ per day. We estimate the rate of death due to COVID-19 using the data taken from the official website of the Nepal government (GoN, 2020). Specifically, we take the average death rate from March 22 to September 16, 2020, and obtain the death rate $k = 0.000281$ per day. We take μ and Λ in such a way that the natural birth rate and death rate remain equal for the period of this pandemic. In addition, we use the quarantine and PCR data along with the model to estimate parameters τ and γ, which are related to people leaving quarantine center. We estimate the remaining parameters $\phi, \beta_c, \beta_o, \theta_c, \theta_o$ and ρ by using the least square fitting of the model to the daily recorded new case data.

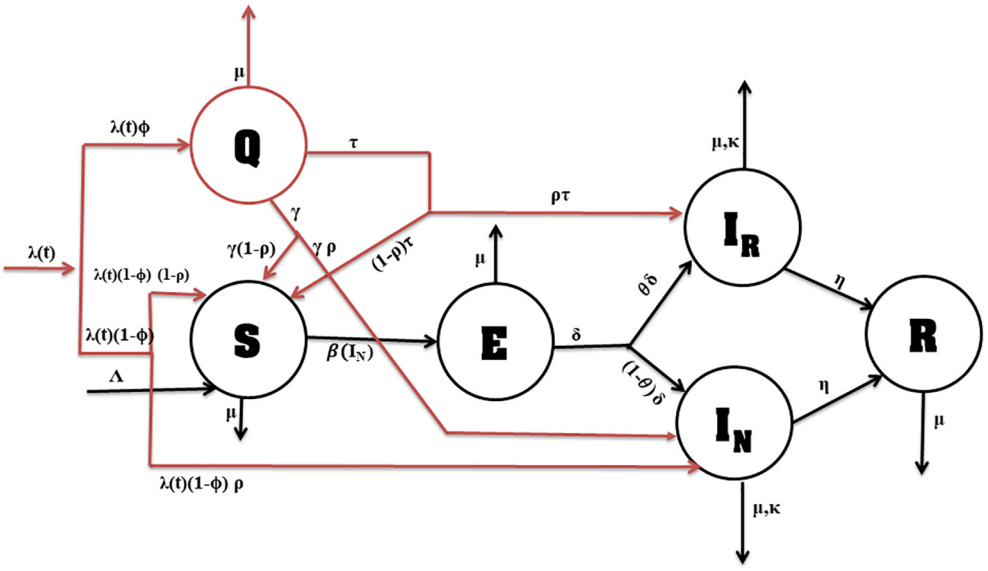

Fig. 1. *Schematic diagram of the model.* The arrow along with parameters shows the rate of flow from one compartment to another. The basic transmission dynamics of COVID-19 is shown in black color while the implemented control policies are indicated by red color.

2.5. Data fitting

We implemented the previous method (Rahman et al., 2019) to perform the data fitting and to identify a reasonable confidence interval of the estimated parameters. In brief, the method involves thorough process of consecutive reduction of number of parameters until the reasonable confidence intervals are identified. The process allowed us to identify the parameters $\phi, \beta_c, \beta_o, \theta_c, \theta_o$, and ρ that can be reasonably estimated from the available data. Further reduction of the number of parameters from the current six parameters provided a poor fit (F-test, p-value < 0.05).

For the model fitting the data available is the daily new cases of recorded infectious people. Using our model, the recorded new infections generated at time $t, L(t)$, can be computed using the following equation:

$$L(t) = \tau\rho Q(t) + \delta\theta E(t) \tag{7}$$

We solve the system of differential equations numerically using a fourth order Runge–Kutta method. We use the solutions to obtain the best-fit parameters via a nonlinear least squares regression method that minimizes the following sum of the squared residuals:

$$J(\phi, \beta_c, \beta_o, \theta_c, \theta_o, \rho) = \sum_{i=1}^{n} \left[L(t_i) - \bar{L}(t_i)\right]^2, \tag{8}$$

where $\phi, \beta_c, \beta_o, \theta_c, \theta_o$, and ρ are parameters to be estimated, and $L(t_k)$ and $\bar{L}(t_k)$ are the new cases of recorded infectious people predicted by the model and those given in the available data, respectively. Here, n represents the total number of data points used for the model fitting. To obtain the confidence limits for the estimated parameters, we compute the standard errors from the sensitivity matrix (S) by using the complex-step derivative techniques described previously (Banks et al., 2014; Banks and Joyner, 2018; Rahman et al., 2019).

Furthermore, we use the sensitivity-based method (Miao et al., 2011) to analyze the identifiability of these parameters. In particular, we found the matrix $S^T S$ to be of the full rank (rank = 6), which confirms the identifiability of the estimated parameters (Miao et al., 2011). In our study, all computations were carried out in MATLAB 2020a (The MathWorks, Inc.) using its various routines, including "ode45" (ODE solver) and "fmincon" (minimizer).

3. Results

3.1. Estimation of border screen

Given the open border of Nepal with India, one of the most COVID-19 infected countries, and related border screen and quarantine policies implemented by the Nepal government, the rate of border screening and quarantine is important for accurate evaluation of the policy. However, the official data of this information is not available. We use our model to estimate the rate of border screen and quarantine, $\phi\lambda(t)$, from the data of the active quarantine population, $\bar{Q}(t_i)$, and the number of PCR-tests performed, $PCR(t_i)$.

Using the fact that the natural death is negligible during the short period of epidemic (i.e., $\mu \approx 0$), we apply the model Eq. (1) at the data collected time t_i to obtain the following approximation:

$$\begin{aligned}\phi\lambda(t_i) &\approx \left.\frac{dQ}{dt}\right|_{t=t_i} + \tau Q(t_i) + \gamma Q(t_i)\\ &\approx \bar{Q}(t_i) - \bar{Q}(t_{i-1}) + \tau\bar{Q}(t_i) + \gamma\bar{Q}(t_i),\end{aligned}$$

where $t_i - t_{i-1} = 1$ day, as the data was recorded every day. In this expression, $\tau\bar{Q}(t_i)$ is given by $PCR(t_i)$, and $\gamma\bar{Q}(t_i)$ represents those leaving quarantine center without PCR test ($no\_PCR(t_i)$), implying

$$\phi\lambda(t_i) \approx \bar{Q}(t_i) - \bar{Q}(t_{i-1}) + PCR(t_i) + no\_PCR(t_i).$$

Since $\phi\lambda(t_i) \geqslant 0$, we obtain the minimum estimate of $no\_PCR(t_i)$ as

$$no\_PCR(t_i) \approx \begin{cases} \bar{Q}(t_i) - \bar{Q}(t_{i-1}) + PCR(t_i), & \text{if} \quad PCR(t_i) > \bar{Q}(t_{i-1}) - \bar{Q}(t_i), \\ 0, \quad \text{otherwise.} \end{cases}$$

Using data of active quarantine, $\bar{Q}(t_i)$, PCR tests, $PCR(t_i)$, and the estimated population leaving quarantine center without PCR, $no\_PCR(t_i)$, we then estimated the daily number of people border screened and entered into the quarantine, $\phi\lambda(t_i)$, until July 21, 2020 (the controlled phase). Our estimates show that the rate of border screen and quarantine was relatively low (less than 2 thousand per day) until the mid of May, 2020, and then the rate increased rapidly reaching a peak of about 16 thousand per day around mid-June. After the peak, the rate began to fall and reached a low level by the end of the first phase of epidemic (Fig. 2). Data shows that, after July 21 (the outgrown phase), the active quarantined population continues to decrease indicating less impact of these individuals on the epidemic during the outgrown phase. Therefore, for simplicity, we assume that $\phi\lambda(t_i)$ decreases linearly after July 21 (Fig. 2).

Furthermore, we use our model to estimate the per capita rate of individuals leaving quarantine center with (τ) and without (γ) PCR test. We can approximate these rates as follows:

$$\tau \approx \frac{1}{n}\sum_{i=1}^{n} PCR(t_i) \quad \text{and} \quad \gamma \approx \frac{1}{n}\sum_{i=1}^{n} no\_PCR(t_i).$$

Our calculation shows that the individuals leave the quarantine center at the rate $\tau = 0.06$ per day with PCR test and at the rate $\gamma = 0.00975$ per day without PCR test.

3.2. Epidemic pattern and model validation

We fitted our model to daily recorded new cases data of Nepal from both the controlled (March 22 to July 21) and the outgrown (July 21 to Sept 16) phases, and estimated six parameters $\phi, \beta_c, \beta_o, \theta_c, \theta_o$, and ρ. The values of the best estimates, along with their 95% confidence intervals, are provided in Table 1. As shown in Fig. 3a the model has an excellent agreement with the data of recorded new cases from both phases of the epidemic. In addition, we used our model to estimate the cumulative cases of COVID-19 during the entire period of study and compared our estimates with the data (Fig. 3b). Our model is capable of accurately predicting the

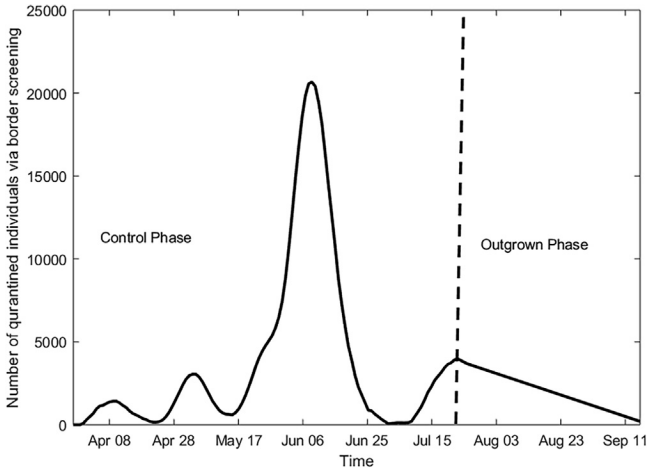

Fig. 2. *Estimation of border screen and quarantine.* Estimated number of daily quarantined individuals using the border screening and quarantine policy.

Table 1
Values of estimated and fixed parameters.

Parameters	Value	95% CI	Reference
β_c	0.052	[0.0085 0.0955]	Data fitting
β_o	0.248	[0.20 0.29]	Data fitting
θ_c	0.75	[0.64 0.85]	Data fitting
θ_o	0.57	[0.49 0.65]	Data fitting
ϕ	0.75	[0.64 0.85]	Data fitting
ρ	0.052	[0.04 0.063]	Data fitting
k	0.000281	Fixed	Calculated
γ	0.00975	Fixed	Calculated
τ	0.06	Fixed	Calculated
η	0.0588	Fixed	(Li et al., 2020)
δ	0.1923	Fixed	Stephen et al. (2020), Backer et al. (2020), WHO, (2020a)

cumulative cases of COVID-19 in Nepal for both epidemic phases, thereby validating our modeling approach.

In consistence with the data, the epidemic trend of the COVID-19 in Nepal predicted by our model shows that the recorded COVID-19 cases increased slowly until the mid of May, attained the peak of the controlled phase during the mid-June, and then decreased until the end of the first phase (the controlled phase), when the policies were altered. After the controlled phase, the cases again started to rise with a higher rate until the end of the study, giving the outgrown phase following the controlled phase. It's worth noting that the first peak observed during the controlled phase is around the same time when the maximum number of returned migrants were border-screened and quarantined (Fig. 2).

3.3. Importation vs local transmission of COVID-19 cases in Nepal

For countries like Nepal that shares open-border with another country (India) having one of the highest levels of COVID-19 cases, it is critical to identify the impact of importation through the border and the local transmission on the disease spread. We used our model to estimate the imported cases and the cases from local transmission, both recorded and non-recorded (Fig. 4). Our estimation shows that during the controlled phase of the epidemic, most of the COVID-19 cases in Nepal were imported, indicating the local transmission was well controlled. During this phase, the imported

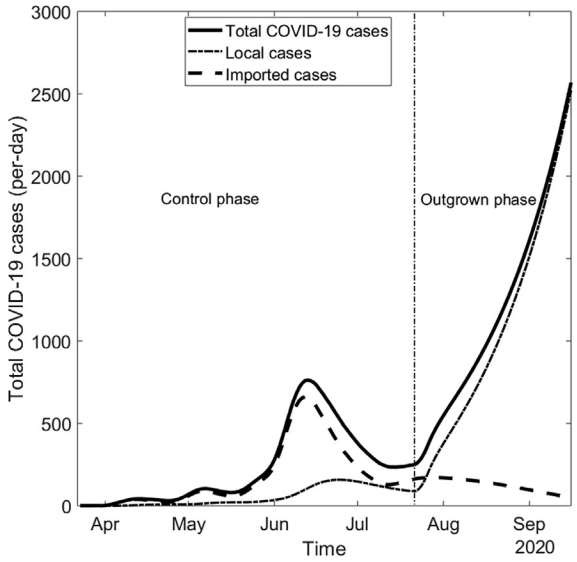

Fig. 4. *Contribution of Importation vs local transmission in COVID-19 cases.* Model estimation of the daily number of COVID-19 cases (solid line) along with the contributions from the importation through border (dashed line) and local transmission (dot-dashed line).

cases gradually increased while the local transmission remained significantly lower than the imported cases. The imported cases reached the maximum number (about 460) around July 01, consistent with the highest border screen (Fig. 2), and then gradually decreased for the entire period of our study.

While the local transmission was quite controlled during the controlled phase (only 6,577 cases), during the outgrown phase the local cases dramatically increased outcompeting the imported cases at the end of July. The outgrown phase (July 22-September 16, 2020) resulted in 67,073 total cases (recorded and non-recorded), out of which 60,123 ($\approx 90\%$) are from local transmission, by the end of our study (September 16, 2020). Note that the timing of the dominance of the local transmission over importation is consistent with the alteration of policies by the government of Nepal, especially the lifting of the lockdown.

3.4. Effectiveness of control strategies

From the epidemic trend it can be clearly seen that the major policies implemented by the government of Nepal, namely border

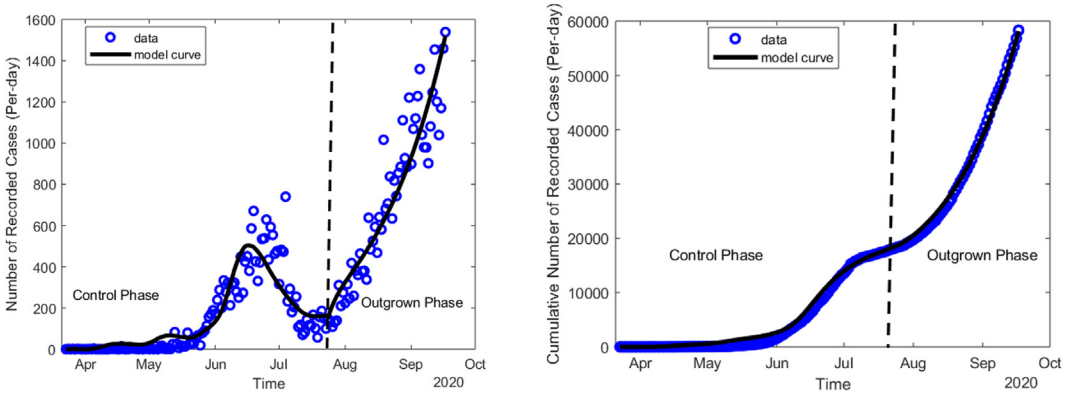

Fig. 3. *Data fitting and model validation.* (a) Recorded daily new cases of COVID-19 data (circle) along with the best fit of the model prediction (line). (b) Cumulative cases over entire study period estimated using the model (line) along with the data (circle).

screening and quarantine, lockdown, and detection and isolation, were significantly effective because the disease spread was well-controlled while the policies were in place and became out of control once the policies were lifted. We can use our model parameters ϕ, ξ, and ψ to quantify the effectiveness of these policies, border screen and quarantine, lockdown, and detection and isolation, respectively, on controlling COVID-19 epidemic in Nepal during the controlled phase. Our model shows that the epidemic dynamics would have been quite worse (19,090 new cases per day during the peak) if these policies were not implemented (Fig. 5a). Through these policies, 442,640 cases were prevented and 1,216 lives were saved during the period of controlled phase (real scenario from the official data: 17,994 cumulative cases and 40 deaths).

We also estimated the effectiveness of each of the policies individually (Fig. 5b). Removing each policy (border screen and quarantine, lockdown, and detection and isolation) at a time, our model predicts the peak infectious case of 1339, 4199, 884, respectively. As per our model estimation, in the absence of border screen and quarantine, lockdown, and detection and isolation, one at a time, the total cumulative cases would have reached 42050, 162400, 38920, respectively, taking the Nepalese lives of 162, 497, 138, respectively. Among these three policies lockdown was found to be the most significant, followed by the border screening and quarantine, and then by the detection and isolation. These results show that the detection and isolation does not seem to have significant impact on the reduction of infections and deaths on the early phase, compared to other two strategies, presumably because of the less local transmission due to the strict lockdown. However, the detection and isolation may have important role and significant impact during the outgrown phase when the local transmission becomes the leading cause of infection.

3.5. Long-term prediction and potential control in Nepal

In this section, we present our model prediction of epidemic outcome, especially the new cases, cumulative cases, and the total deaths, in Nepal by the end of the year 2021. If the current trend continues without any interventions, our model predicts that the peak value of daily new cases will reach 144,600 (82,420 recorded and 62,180 non-recorded) on March 4, 2021 (Fig. 6a). With this epidemic trend, Nepal will suffer from the cumulative cases of 18.76 million (10.70 million recorded and 8.06 million non-recorded) and the total COVID-19-related deaths of 87 thousand by the end of 2021 (Fig. 6b).

At the current situation of the limited pharmaceutical prevention, applying public health measures, including the ones the government of Nepal implemented during the controlled phase, are the most promising control mearues (MoHP, 2020; WHO, 2020b). We now assess the impact of these control measures on curbing COVID-19 epidemics from September 2020 to December 2021. Since the current trend (the outgrown phase) shows that the imported COVID-19 cases are not important compared to the local transmission, we particularly focus on two control strategies, the lockdown and the detection and isolation. Note that the current value of infection rates is $\beta = \beta_o$ and the detection rate is $\theta = \theta_o$ (Table 1). In our model, the level of lockdown and detection and isolation can be incorporated using the parameters ξ and ψ, respectively.

Our model predicts that both the lockdown (reduction on β) and the detection and isolation (increment in θ) are significantly impactful on curbing COVID-19 epidemic burden in Nepal (Fig. 7). For example, 50% reduction of contact through lockdown (i.e., $\xi = 0.5$) can reduce the cumulative number from the base-case of 18.7 million to 426 thousand and the total deaths from 87 thousand to 20 thousand. Similarly, 1.4 times increment in the detection and isolation rate (i.e., $\psi = 1.4$) can bring the cumulative cases down to 494 thousand and the total death down to 13 thousand.

3.6. Reproduction number

The basic reproduction number, R_0, is an average number of secondary infections generated by a single infectious individual in a completely susceptible population. For infectious diseases, it is an important threshold, which helps determine whether outbreak occurs ($R_0 > 1$) or is avoided ($R_0 < 1$) (Martcheva, 2015). We used the Next Generation Matrix method (Diekmann et al., 1990; Van den Driessche and Watmough, 2020) to derive the expression of R_0 for our model (see Appendix) and obtained

$$R_0 = \frac{\beta_c \delta (1-\theta_c) S^*}{(\delta+\mu)(\eta+k+\mu)(Q^*+S^*)},$$

where

$$S^* = \frac{\Lambda}{\mu} + \frac{\lambda(0)(\tau+\gamma+\mu(1-\phi))}{\mu(\tau+\gamma+\mu)} \quad \text{and} \quad Q^* = \frac{\lambda(0)\phi}{\tau+\gamma+\mu}.$$

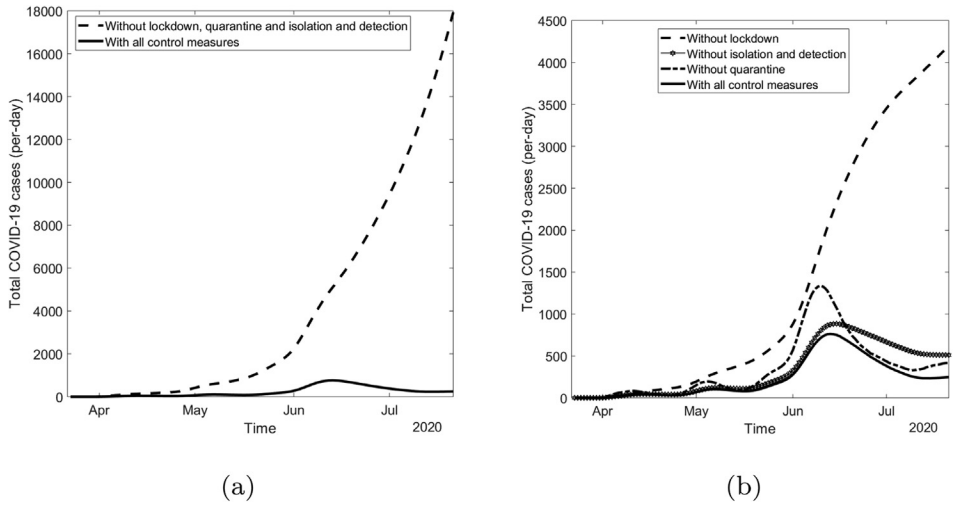

Fig. 5. *Effect of control strategies.* Daily new covid-19 cases (a) with (solid line) and without (dashed line) all control strategies in combination, and (b) with (solid line) and without one policy at a time, border screening and quarantine (dot-dashed line), lockdown (dashed line) and detection and isolation (star-line).

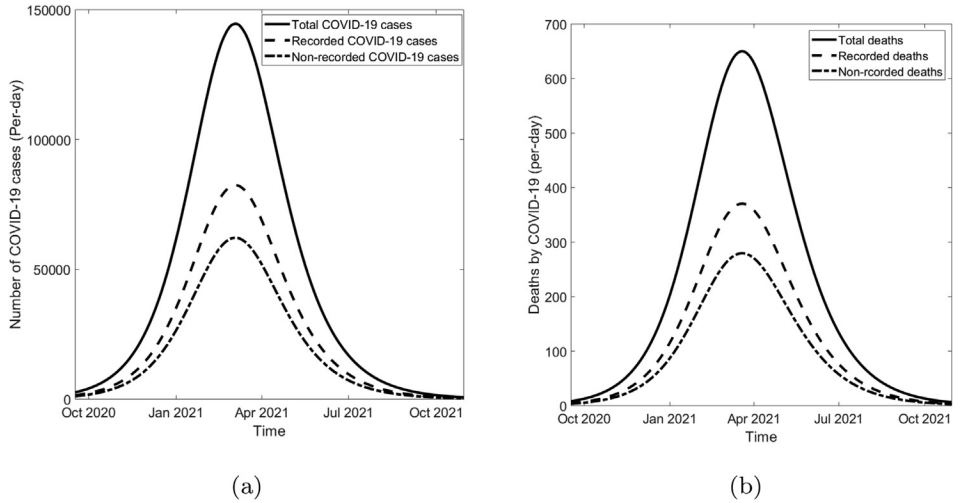

Fig. 6. *Long-term dynamics of COVID-19 in Nepal.* Long-term dynamics of (a) daily new cases and (b) daily deaths due to COVID-19, predicted by our model. Here, the current (Oct 2020) peak of the new cases and daily deaths are 1,127 and 4, respectively..

As expected, we are able to theoretically establish R_0 as the outbreak threshold for our model, as stated in the following theorem:

Theorem 1. *Disease free equilibrium point of the system of Eqs. (1)–(6) is asymptotically stable if $R_0 < 1$ and unstable if $R_0 > 1$.*

The proof of the theorem is given in Appendix. Using the estimated parameters, we found the value of $R_0 = 0.21$ for Nepal. $R_0 < 1$ implies that the outbreak was avoided at the time the locally infected case was introduced in March 2020. The successful control is consistent with the fact that the local transmission during early epidemic period was negligible with the majority of infections coming from abroad. Furthermore, we found that if the government of Nepal had not timely implemented policies (i.e., if we replace β_c by β_o and θ_c by θ_o), the basic reproduction number would have been $R_0 = 1.8$. Using our model, we also performed analysis to identify the level of lockdown (ξ) and the level of detection and isolation (ψ) required to assure the value of R_0 less than unity so that the epidemic is avoided. The resulting combinations of these two policies, which can avoid the epidemic, are shown in Fig. 8a. For example, a policy with combination of 22% reduction in contact due to lockdown ($\xi = 0.22$) and 1.2 times increase in detection and isolation ($\psi = 1.2$) can make R_0 less than unity, thereby avoiding epidemic to occur.

While the basic reproduction number provides the important information about the beginning of the epidemic, the average number of the secondary infections varies over time, mainly due to alteration of implementation of policies over the epidemic period. To describe the time varying average number of secondary cases more accurately, we considered the effective reproduction number, R_t. The value of R_t allows us to track whether the epidemic at time t is in increasing ($R_t > 1$) or decreasing ($R_t < 1$) trend. For our model, the effective reproduction number is given by

$$R_t = \frac{\beta(t)\delta(1-\theta(t))S(t)}{(\delta+\mu)(\eta+k+\mu)N(t)}.$$

Using the estimated parameters, we observed that the value of effective reproduction number $R(t)$ remains about 0.21 until July 21 (Fig. 8b), indicating that the local transmission is under control during the controlled phase. However, around July-21 (the date of end of policies), the effective reproduction number rapidly

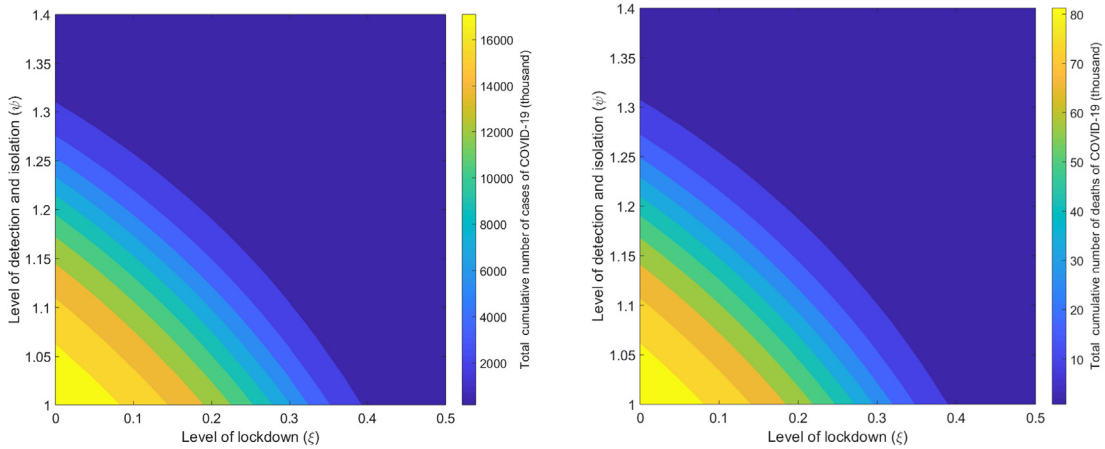

Fig. 7. *Long-term impact of control policies.* Model prediction of (a) the cumulated cases and (b) the cumulative deaths due to COVID-19 by December 2021, under the different levels of lockdown and detection and isolation.

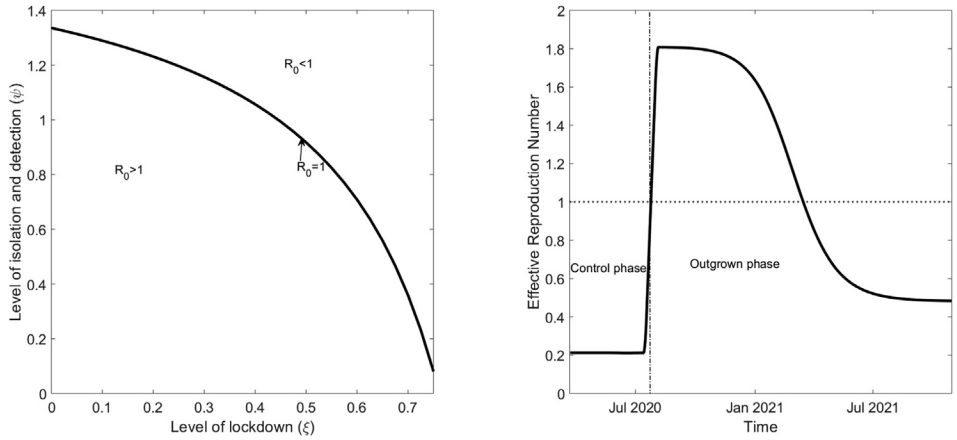

Fig. 8. *Reproduction numbers.* (a) Parameter space showing the level of lockdown (ξ) and the level of detection and isolation (ψ) that make R_0 less than or greater than 1. (b) Effective reproduction number of COVID-19 ($R_t = 1$) in Nepal until December 2021.

increased and reached 1.80 indicating the rapid local transmission during the outgrown phase. The long-term prediction of our model shows that the value of R_t remains greater than unity until March 2021 (increasing trend). After March 2021, the epidemic will observe the decreasing trend (i.e, $R_t < 1$).

4. Discussion

In this study, we focused on modeling COVID-19 epidemic in Nepal, which shares an open border with India, one of the most affected countries in the world. Since a large number of Nepalese, especially male labor migrants, work in India, the mobility across the Nepal-India open border has directly affected COVID-19 cases in Nepal, causing considerable number of imported cases through the migrant workers coming from India (EDCD, 2020c). Despite a large number of inflow of COVID-19 cases from India, the timely implementation of the Nepal Government's policies, namely (i) border screen and quarantine, (ii) lockdown, and (iii) detection and isolation, was successful in controlling the epidemic for about four months until these policies were lifted on July 21, 2020. After the policies were lifted, the cases surged uncontrollably, resulting in a biphasic trend of COVID-19 in Nepal, the controlled phase (until July 21, 2020) and the outgrown phase (after July 21, 2020). In order to evaluate these successful control policies, here we took advantage of modeling and data of unique epidemic in Nepal with biphasic trend resulting from the combination of case-inflow through the Nepal-India border and control policy implementation. Our novel model, which is capable of excellently describing the COVID-19 data from Nepal, has provided number of important insights into transmission dynamics and related effective control policies.

Using our model and the available data from the ministry of health and population, we estimated the key parameters related to COVID-19 transmission and control in Nepal. Based on our model, we identified quite distinct transmission rate (β) and distinct rate of detection and isolation (θ) between two phases of epidemics, showing that the policies implemented were indeed significantly effective. The timely implementation of policies was able to maintain the low level of effective reproduction number (≈ 0.21) while the polices were in place, and upon lifting the policies the effective reproduction number rapidly rose to 1.80. As per our model evaluation, with these policies the government of Nepal was able to prevent more than 444 thousand cases and save more than 1,200 lives. Among these three policies, "lockdown" was found to be the most effective, followed by "border screen and quarantine" and then by "detection and isolation".

Consistent with the data based on the travel history of recorded infectious people (more than 80% came from aboard, especially from India) (EDCD, 2020b; Rijal, 2020), our result also shows that about 70% of COVID-19 cases in Nepal were imported during the controlled phase. Despite inflow of significant number of COVID-19 cases from India, the local transmission remains well controlled during the controlled phase of epidemic, implying that the "border screening and quarantine" policy in combination with other policies implemented by the government of Nepal was key to avoid a potential early surge of cases from local transmission. Our model predicts a high rate of local transmission, consistent with the data, during the outgrown phase (i.e., after the policies were lifted on July 21, 2020). As a result, the contribution of the local transmission to epidemics became significantly high outcompeting the importation after July 21, 2020. We note that along the line of our results, various reports and updates on the situation of Nepal (Pun et al., 2020; NIE, 2020; EDCD, 2020b; TKP, 2020a; WHO, 2020d; WHO, 2020e; WHO, 2020g) also claim that there were small number of local transmissions before July 21, 2020 and the mass community transmission has become noticeable only after lifting the policies on July 21, 2020.

Based on the current epidemic trend identified by our model, we predict that without any interventions about 18 million Nepalese ($\sim 70\%$ of the total population) will be infected with COVID-19 by the end of 2021. The model predicts that the current increasing trend of daily new cases will continue to increase reaching the peak level of about 144 thousand new cases per day on March 04, 2021. However, we also acknowledge that there is a possibility for the peak time to occur earlier, as projected by some studies (White et al., 2020), if the government reduces the testing of asymptomatic cases (i.e., reduces the detection and isolation in our model) as mentioned in (OLK, 2020). Because Nepal is in the high risk zone of COVID-19 due to its poor health system and porous borders with India, potential epidemic outcomes predicted by our model strongly recommend the urgent implementation of control strategies.

Since the pharmaceutical control of COVID-19 is not widely available, most of the countries have been implementing the non-pharmaceutical approaches, including the ones implemented by the government of Nepal, for mitigating COVID-19 transmissions. As identified by our model in the context of Nepal, many

countries, such as China, Taiwan, and South Korea, which have been successful to control the epidemics, also applied the strict lockdown, meticulous testing and tracking, and massive isolation of people, precise and widespread contact tracing and testing (Azman and Luquero, 2020; Choi, 2020; Trevisan et al., 2020; Cheng et al., 2020) as effective means of epidemic control. Therefore, we also evaluated the local transmission related control strategies "Lockdown" and "Detection and isolation" in the context of Nepal, and identified the level of these policies required for successful mitigation of potential COVID-19 surge in Nepal. For example, our result shows that the lockdown level that can reduce the contact rate by 50% will decrease the peak of new cases of COVID-19 below 2,600, significantly less than the predicted base-case of 144 thousand. In this level of lockdown, the cumulative cases will also reduce from 18 million to less than 200 thousand. Similarly, the total COVID-19 cases can be reduced to 494 thousand if the detection and isolation policy is increased by 1.4 times the base case. Importantly, our model has identified that for a significantly large level of the detection and isolation (for example, greater than 1.6 time the base case), the disease spread can be avoided without needing a high level of lockdown.

We acknowledge several limitations of our study. We used the limited data sets available publicly from the ministry of health and population of Nepal. Because of poor policy at the border, the data related to border screen need to be carefully considered. The detailed data with accurate border screening and quarantine will improve the predictions of our model. While the testing program for border screened population was better documented, the testing for local community is less understood, which may have slightly impacted on our estimates of detection and isolation rate. However, we conducted sensitivity of this parameter over the wider range. We have ignored the spatial heterogeneity on the dynamics and policy implementation, especially among seven provinces of Nepal. Not all provinces equally share border with India and also cases distribution is not uniform. For example, Gandaki province has sporadic transmission (WHO, 2020f) while other six provinces (Province 1, Province 2, Bagmati, Lumbini, Karnali and Sudurpaschim) show clusters of cases. Therefore, future studies on province-wise analysis of COVID-19 transmission along with inter-province mobility will help for better implementation of effective control strategies.

In summary, we developed a novel mathematical model to uncover effective control strategies that were implemented in unique biphasic epidemic trend in Nepal, under the influence of human mobility across the open-border with India, one of the most COVID-19 affected countries in the world. Quantification of these successful control strategies through distinct two phases of epidemic in Nepal (the controlled phase and the outgrown phase) has provided us with opportunity to evaluate the impact of these strategies to curb potential surge in Nepal. Our results may provide important policy guidance for devising the appropriate control strategies for bringing Nepal out from the devastating pandemic.

CRediT authorship contribution statement

Khagendra Adhikari: Formal analysis, Investigation, Methodology, Writing - original draft. **Ramesh Gautam:** Formal analysis, Investigation, Methodology, Writing - original draft. **Anjana Pokharel:** Formal analysis, Investigation, Methodology, Writing - original draft. **Kedar Nath Uprety:** Formal analysis, Supervision, Writing – review and editing. **Naveen K. Vaidya:** Conceptualization, Formal analysis, Supervision, Writing - review & editing.

Declaration of Competing Interest

The authors declare that they have no known competing financial interests or personal relationships that could have appeared to influence the work reported in this paper.

Acknowledgments

KA acknowledges Nepal Academy of Science and Technology (NAST) for Ph.D. Fellowship. AP acknowledges the financial support from International Mathematical Union (IMU) through the Graduate Research Assistantships in Developing Countries (GRAID) award 2020. KA, RG and AP acknowledge the Nepal Mathematical Society (NMS) for the NMS Ph.D. Fellowship Award 2020. The work of NKV was supported by NSF grants DMS-1951793, DMS-1616299, DMS-1836647, and DEB-2030479 from National Science Foundation of USA and the UGP award from San Diego State University.

Appendix A

A.1. Derivation of basic reproduction number, R_0, using the next generation matrix

We first obtain the disease free equilibrium, $\mathscr{E}^*$, of the model system. Using the pre-pandemic condition $\lambda = \lambda(0)$ and the disease-free conditions $E = 0$, $I_R = 0$, $I_N = 0$, we obtain $\rho = 0$. Then the model system provides the following disease free equilibrium:

$$\mathscr{E}^* = (S^*, Q^*, 0, 0, 0, 0),$$

where

$$S^* = \frac{\Lambda}{\mu} + \frac{\lambda(0)(\tau+\gamma+\mu(1-\phi))}{\mu(\tau+\gamma+\mu)} \quad \text{and} \quad Q^* = \frac{\lambda(0)\phi}{\tau+\gamma+\mu}.$$

According to the next generation matrix method, we divide the compartments used in the model into two groups: infected $\vec{x} = (x_i, i = 1,2,3) = (E, I_R, I_N)$ and non-infected group $\vec{y} = (y_j, j = 1,2,3) = (S, Q, R)$. Then the model system can be written as:

$$x_i' = f_i(\vec{x}, \vec{y}) \quad \text{and} \quad y_j' = g_j(\vec{x}, \vec{y}) \quad \text{for} \quad i,j = 1,2,3.$$

We now write the right hand side of the system of infected compartments as $f_i(\vec{x}, \vec{y}) = F_i(\vec{x}, \vec{y}) - V_i(\vec{x}, \vec{y})$, where $F_i(\vec{x}, \vec{y})$ contains the terms representing the new infections in compartment i and $V_i(\vec{x}, \vec{y})$ contains the terms containing the difference between the transfer of individuals out of and into the compartment i:

$$\begin{pmatrix} F_1 \\ F_2 \\ F_3 \end{pmatrix} = \begin{pmatrix} \frac{\beta(t)SI_N}{S+Q+E+R+I_N+I_R} \\ 0 \\ 0 \end{pmatrix},$$

$$\begin{pmatrix} V_1 \\ V_2 \\ V_3 \end{pmatrix} = \begin{pmatrix} (\delta+\mu)E \\ (\eta+k+\mu)I_R - \delta\theta(t)E \\ (\eta+k+\mu)I_N - \delta(1-\theta(t))E \end{pmatrix}.$$

We now take the values $\beta(t) = \beta_c$ and $\theta(t) = \theta_c$ corresponding to the beginning of the epidemic, and construct the following two matrices using $F = \left(\frac{\partial F_i}{\partial x_j}\right)\Big|_{\mathscr{E}^*}$ and $V = \left(\frac{\partial V_i}{\partial x_j}\right)\Big|_{\mathscr{E}^*}$.

$$F = \begin{pmatrix} 0 & 0 & \frac{\beta_c S^*}{Q^*+S^*} \\ 0 & 0 & 0 \\ 0 & 0 & 0 \end{pmatrix}, \quad V = \begin{pmatrix} \delta+\mu & 0 & 0 \\ -\delta\theta_c & \eta+k+\mu & 0 \\ -\delta(1-\theta_c) & 0 & \eta+k+\mu \end{pmatrix}.$$

These matrices allow use to compute the second generation matrix as follows:

$$FV^{-1} = \begin{pmatrix} \frac{\beta_c\delta(1-\theta_c)S^*}{(\delta+k+\mu)(\eta+k+\mu)(Q^*+S^*)} & 0 & \frac{\beta_c S^*}{(\eta+k+\mu)(Q^*+S^*)} \\ 0 & 0 & 0 \\ 0 & 0 & 0 \end{pmatrix},$$

whose eigenvalues are 0, 0, and $\frac{\beta_c\delta(1-\theta_c)S^*}{(\delta+\mu)(\eta+k+\mu)(Q^*+S^*)}$. Then the basic reproduction number is given by the dominant eigenvalue. Therefore,

$$R_0 = \frac{\beta_c\delta(1-\theta_c)S^*}{(\delta+\mu)(\eta+k+\mu)(Q^*+S^*)}.$$

A.2. Proof of Theorem 1

Jacobian of the system of Eqs. (2)–(6) evaluated at the disease free equilibrium, $\mathscr{E}^*$, is

$$\begin{pmatrix} -\mu & \gamma(1-\rho_1)+(1-\rho)\tau & 0 & 0 & -\frac{\beta_c S^*}{Q^*+S^*} & 0 \\ 0 & -(\tau+\gamma+\mu) & 0 & 0 & 0 & 0 \\ 0 & 0 & -(\delta+\mu) & 0 & \frac{\beta_c S^*}{Q^*+S^*} & 0 \\ 0 & \rho\tau & \delta\theta_c & -(\eta+k+\mu) & 0 & 0 \\ 0 & \gamma\rho_1 & \delta(1-\theta_c) & 0 & -(\eta+k+\mu) & 0 \\ 0 & 0 & 0 & \eta & \eta & -\mu \end{pmatrix}.$$

The eigenvalues of this Jacobian are given by

$$\lambda_1 = -\mu, \lambda_2 = -\mu, \lambda_3 = -(\eta+k+\mu), \lambda_4 = -(\gamma+\tau+\mu),$$

$$\lambda_5 = \frac{-(\delta+\eta+2\mu+k) - \sqrt{(\delta+\eta+2\mu+k)^2 - 4(\delta+\mu)(\eta+\mu+k)(1-R_0)}}{2},$$

and

$$\lambda_6 = \frac{-(\delta+\eta+2\mu+k) + \sqrt{(\delta+\eta+2\mu+k)^2 - 4(\delta+\mu)(\eta+\mu+k)(1-R_0)}}{2}.$$

We can clearly observe that all the eigenvalues are negative if $R_0 < 1$. Therefore, the disease free equilibrium, $\mathscr{E}^*$, is asymptotically stable if $R_0 < 1$ and unstable if $R_0 > 1$.

References

Armitage, R., Nellums, L.B., 2020. COVID-19 and the Gypsy, Roma and Traveller population. Public Health 185, 48. https://doi.org/10.1016/j.puhe.2020.06.003.

Azman, A.S., Luquero, F.J., 2020. From China: hope and lessons for COVID-19 control. Lancet Infect Dis 20 (7), 756–757. https://doi.org/10.1016/S1473-3099(20)30264-4.

Backer, J.A., Klinkenberg, D., Wallinga, J., 2020. Incubation period of 2019 novel coronavirus (2019-nCoV) infections among travellers from Wuhan, China, 20-28 January 2020. Euro Surveill 25(5). https://doi.org/10.2807/1560-7917.ES.2020.25.5.2000062.

Banks, H.T., Joyner, M.L., 2018. Information content in data sets: A review of methods for interrogation and model comparison. Journal of Inverse and Ill-Posed Problems 26. https://doi.org/10.1515/jiip-2017-0096.

Banks, H.T., Hu, S., Tompson, W.C., 2014. Modeling and Inverse Problems in the Presence of Uncertainty. CRC Press, Boca Raton London.

Bhandary, S., 2020. Effectiveness of lockdown as COVID-19 intervention: official and computed cases in Nepal. Journal of Patan Academy of Health Sciences 7 (1), 37–41. https://doi.org/10.3126/jpahs.v7i1.28861.

Bhuju, G., Phaijoo, G., Gurung, D., 2020. Modeling transmission dynamics of COVID-19 in Nepal. Journal of Applied Mathematics and Physics 8 (10), 2167–2173. https://doi.org/10.4236/jamp.2020.810162.

CBS, 2011. National Population and Housing Census 2011 (Population Projection 2011-2031), Central Bureau of Statistics, Nepal, Volume 08, NPHC 2011. URL: https://cbs.gov.np/wp-content/upLoads/2018/12/PopulationProjection2011-2031.pdf (Accessed: 2020-09-10).

Chanda, A., 2020. COVID-19 in India: transmission dynamics, epidemiological characteristics, testing, recovery and effect of weather. Epidemiology and Infection 148, e182, 1–10. https://doi.org/10.1017/S09.

Cheng, H.Y., Jian, S.W., Liu, D.P., Ng, T.C., Huang, W.T., Lin, H.H., et al., 2020. Contact tracing assessment of COVID-19 transmission dynamics in Taiwan and risk at different exposure periods before and after symptom onset. JAMA Intern Med 180 (9), 1156–1163. https://doi.org/10.1001/jamainternmed.

Choi, J.Y., 2020. Covid-19 in South Korea. Postgrad. Med. J. 96, 399–402. https://doi.org/10.1136/postgradmedj-2020-137738.

Diekmann, O., Heesterbeek, J.A.P., Metz, J.A.J., 1990. On the definition and the computation of the basic reproduction ratio R_0 in models for infectious diseases in heterogeneous populations. J. Math. Biol. 28 (4), 365–382. https://doi.org/10.1007/BF00178324 hdl:1874/8051. PMID 2117040. S2CID 22275430.

EDCD, 2020a. COVID-19 Statistics: Nepal. Epidemiology and Disease Control Division. URL: https://portal.edcd.gov.np/covid19/. Accessed: 2020-09-17.

EDCD, 2020b. Detail epidemiological update COVID-19-National and Provinces, 11 August 2020. Epidemiology and diseases control Division, Nepal. URL: http://edcd.gov.np/news/download/epidemiological-update-on-covid-19-11-aug-2020. Accessed: 2020-09-26.

EDCD, 2020c. Epidemiological Update on COVID 19. Epidemiology and diseases control Division. Nepal, (17 July 2020). URL: http://edcd.gov.np/news/download/epidemiological-update-on-covid-19-17-july-2020. Accessed:2020-09-27.

Faal, N., Ivn, A., Delfim, F.M.T., Juan, J.N., 2020. Mathematical modeling of COVID-19 transmission dynamics with a case study of Wuhan. Chaos Solitons Fract 135, 109846. https://doi.org/10.1016/j.chaos.2020.109846.

Ferretti, L., Chris, W., 2020. Quantifying SARS-CoV-2 transmission suggests epidemic control with digital contact tracing. Science 368 (6491), eabb6936. https://doi.org/10.1126/science.abb6936.

GoN, 2020. COVID-19 Nepal. Government of Nepal, URL: https://covidnepal.org. Accessed: 2020-09-18.

He, S., Peng, Y., Sun, K., 2020. SEIR modeling of the COVID-19 and its dynamics. Nonlinear Dyn 101, 1667–1680. https://doi.org/10.1007/s11071-020-05743-y.

Hellewell, J., Abbott, S., Gimma, A., Bosse, N.K., Jarvis, C.I., Russell, T.W., et al., 2020. Feasibility of controlling COVID-19 outbreaks by isolation of cases and contacts. Lancet Glob Health 8 (4), e488–e496. https://doi.org/10.1016/S2214-109X(20)30074-7.

Hiroshi, N., Natalie, M.L., Andrei, R.A., 2020. Serial interval of novel corona virus (COVID-19) infections.International. J. Infect. Dis. 93, 284–286. https://doi.org/10.1016/j.chaos.2020.109846.

Hossain, M.P., Junus, A., Zhu, X., Jia, P., Pfeiffer, D., Yuan, H.Y., 2020. The effects of border control and quarantine measures on the spread of COVID-19. Epidemics 32,100397. https://doi.org/10.1016/j.epidem.2020.100397.

IOM, 2019. Migration in Nepal -A COUNTRY PROFILE 2019. Kathmandu, Nepal. International Organization for Migration. URL: https://publications.iom.int/system/files/pdf/mp_nepal_2019.pdf.

Keeling, M.J., Rohani, P., 2008. Modeling Infectious Diseases in Humans and Animals. Princeton University Press. https://doi.org/10.2307/j.ctvcm4gk0. 41 William Street Princeton, NJ 08540-5237 USA. http://www.jstor.org/stable/j.ctvcm4gk0.

Kunwar, S.K., 2015. Emigration of Nepalese People and Its Impact. Econ. J. Develop. Issue 19 (20), 77–82.

Li, Q., Guan, X., Wu, P., Wang, X., Zhou, L., Tong, Y., et al., 2020. Early transmission dynamics in Wuhan, China, of novel coronavirus–infected pneumonia.. N Engl J Med 382 (13), 1199–1207. https://doi.org/10.1056/NEJMoa2001316.

Linton, N.M., Kobayashi, T., Yang, Y., Hayashi, K., Akhmetzhanov, A.R., Jung, S.M., Yuan, B., Kinoshita, R., Nishiura, H., 2020. Incubation period and other epidemiological characteristics of 2019 novel coronavirus infections with right truncation: a statistical analysis of publicly available case data. J. Clin. Med. 9, 538. https://doi.org/10.3390/jcm9020538.

Liu, Y., Tang, J.W., Lam, T.Y., 2020a. Transmission Dynamics of the COVID-19 Epidemics in England. Cold Spring Harbor Laboratory Press. https://doi.org/10.1101/2020.06.30.20143743.

Liu, Z., Magal, P., Seydi, O., Webb, G.A, 2020. COVID-19 epidemic model with latency period. Infect. Dis. Model. 5, 323–337. https://doi.org/10.1016/j.idm.2020.03.003.

Martcheva, M., 2015. An Introduction to Mathematical Epidemiology, ISSN 2196-9949. In: Texts in Applied Mathematics. Springer, ISBN 978-1-4899-7612-3.

MoHP, 2020. Critical preparedness, readiness and response actions for COVID-19, 2020. Ministry of Health and Population, Government of Nepal. URL: https://www.who.int/publications/i/item/critical-preparedness-readiness-and-response-actions-for-covid-19. Accessed: 2020-09-18.

MoL, 2020. Nepal Labour Migration Report,2020. Government of Nepal, Ministry of Labour, Employment and Social Security. URL: https://moless.gov.np/wp-content/uploads/2020/03/Migration-Report-2020-English.pdf. Accessed: 2020-09-17.

Miao, H., Xia, X., Perelson, A.S., Wu, H., 2011. On identifiability of nonlinear ODE models and applications in viral dynamics. SIAM Rev. 53 (1), 3–39. https://doi.org/10.1137/090757009.

NIE, 2020. Coronavirus infection in Nepal enters community transmission phase. The New Indian Express. URL: https://www.newindianexpress.com/world/2020/sep/02/coronavirus-infection-in-nepal-enters-community-transmission-phase-2191464.html. Accessed: 2020-09-26.

Okuonghae, D., Omame, A., 2020. Analysis of a mathematical model for COVID-19 population dynamics in Lagos, Nigeria. Chaos Solitons Fract. 139,. https://doi.org/10.1016/j.chaos.2020.110032 110032.

OLK, 2020. Poor contract tracing in Kathmandu- Two per infectious. Onlinekhabr. URL: https://www.onlinekhabar.com/2020/09/894783. Accessed: 2020-09-27.

Pun, S.B., Mandal, S., Bhandari, L., Jha, S., Rajbhandari, S., Mishra, A.K., Chalise, B.S., Shah, R., 2020. Understanding COVID-19 in Nepal. J. Nepal Health Res. Counc. 18 (1), 126–127.

Rahman, M., Bekele-Maxwell, K., Cates, L.L., Banks, H.T., Vaidya, N.K., 2019. Modeling Zika virus transmission dynamics: parameter estimates, disease characteristics, and prevention. Sci. Rep. 9 (1), 10575. doi:10.1038/s41598-019-46218-4.

Rijal, A., 2020. 99% COVID-19 cases in Nepal asymptomatic, 97% Imported. The Rising Nepal. URL: https://risingnepaldaily.com/main-news/99-covid-19-cases-in-nepal-asymptomatic-97-imported. Accessed: 2020-09-27.

Shayak, B., Sharma, M.M., Rand, R.H., Singh, A.K., Misra, A., 2020. Transmission dynamics of COVID-19 and impact on public health policy. medRxiv. https://doi.org/10.1101/2020.03.29.20047035.

Shrestha, S., 2020. Hundreds of Nepalese stuck at India border amid COVID-19 lockdown. ALJAZERA. URL: https://www.aljazeera.com/news/2020/04/01/hundreds-of-nepalese-stuck-at-india-border-amid-covid-19-lockdown/. Accessed: 2020-06-26.

Stephen, A.L., Kyra, H.G., Qifang, B.I., Forrest, K.J., Qulu, Z., Hannah, R.M., Andrew, S. A., Nicholas, G.R., Justin, L., 2020. The Incubation Period of Coronavirus Disease 2019 (COVID-19) from publicly reported confirmed cases: estimation and application. Ann. Intern. Med. 172, 577–582. https://doi.org/10.7326/M20-0504.

Sun, G.Q., Wang, S.F., Li, M.T., Li, L., Zhang, J., Zhang, W., Jin, Z., Feng, G.L., 2020. Transmission dynamics of COVID-19 in Wuhan, China: effects of lockdown and medical resources. Nonlinear Dynamics Jun 24, 1–13. https://doi.org/10.1007/s11071-020-05770-9.

Time, 2020. World Health Organization Declares COVID-19 a 'Pandemic' Here's What That Means. URL: https://time.com/5791661/who-coronavirus-pandemic-declaration/. Accessed:2020-08-04.

TKP, 2020. No evidence of Covid community transmission yet but infection cases could rise, WHO Nepal representative says.THE KATHMANDU POST. 10 June, 2020. URL: https://tkpo.st/2YkDnKV. Accessed:2020: 09-26.

TKP, 2020. With hundreds of thousands of migrants predicted to return home, Nepal needs to brace for a crisis. THE KATHMANDU POST (22 April, 2020). URL: https://tkpo.st/2xNRgYL. Accessed: 2020-08-02.

Trevisan, M., Le, L.C., Le, A.V., 2020. The COVID-19 pandemic: a view from Vietnam. Am. J. Public Health 110, 1152–1153. https://doi.org/10.2105/AJPH.2020.305751.

TRN, 2020. Sixty three People Sent To Kharipati Quarantine. The Rising Nepal. URL: https://risingnepaldaily.com/mustread/63-people-sent-to-kharipati-quarantine. Accessed: 2020-05-10.

UN, 2020. COVID-19 Nepal: Preparedness and Response Plan (NPRP) April-2020. UNITED NATIONS, Nepal. URL: https://www.who.int/docs/default-source/nepal-documents/novel-coronavirus/covid-19-nepal-preparedness-and-response-plan-(nprp)-draft-april-9.pdf?sfvrsn=808a970a_2.

Vaidya, N.K., Lindi, M.W., 2015. Avian influenza dynamics under periodic environmental conditions. SIAM J. Appl. Math. 75 (2), 443–467. https://doi.org/10.1137/140966642.

Van den Driessche, P., Watmough, J., 2020. Reproduction numbers and sub-threshold endemic equilibria for compartmental models of disease transmission. Mathematical Biosciences 180, 29–48. https://doi.org/10.1016/S0025-5564(02)00108-6. PMID 12387915.

Wan, H., Cui, J., Yang, G., 2020. Risk estimation and prediction of the transmission of coronavirus disease-2019 (COVID-19) in the mainland of China excluding Hubei province. Infect. .Dis Poverty 9 (116). https://doi.org/10.1186/s40249-020-00683-6.

Wang, L., Wang, J., Zhao, H., Shi, Y., Wang, P., Wu, Shi, L.. 2020. Modeling and assessing the effects of medical resources on transmission of novel corona virus (covid19) in Wuhan, China. Math. Biosci. Eng. 17 (4), 2936–2949. https://doi.org/10.3934/mbe.2020173.

White, L., Letchford, N., Pokharel, S., Lata, D., Zaman, R. 2020. Modelling of COVID-19 Strategies in Nepal Final Report, Oxford Policy Management Limited Registered in England. URL: https://reliefweb.int/sites/reliefweb.int/files/resources/Nepal_COVID-19_modelling_-_final_published.pdf. Accessed: 2020-08-17.

WHO, 2020a. Coronavirus disease 2019 (COVID-19) Situation Report. 2 April, 2020. World Health Organization (WHO). URL: https://www.who.int/docs/default-source/coronaviruse/situation-reports/20200402-sitrep-73-Covid-19.pdf/. Accessed: 2020-06-04.

WHO, 2020b. COVID-19 Strategy Update. World Health Organization (WHO). URL: https://www.who.int/docs/default-source/coronaviruse/covid-strategy-update-14april2020.pdf?sfvrsn=29da3ba0_12. Accessed: 2020-08-12.

WHO, 2020c. WHO Coronavirus Disease (COVID-19) Dashboard URL: https://covid19.who.int/. Accessed: 2020-09-21.

WHO, 2020d. Situation Update Report 19 (26 August, 2020), Coronavirus disease 2019 (COVID-19), WHO Country Office for Nepal. URL: https://www.who.int/docs/default-source/nepal-documents/novel-coronavirus/who-nepal-sitrep/19-who-nepal-sitrep-covid-19.pdf?sfvrsn=c9fe7309_2. Accessed: 2020-09-26.

WHO, 2020e. Situation Update Report 22 (16 September, 2020), Coronavirus disease 2019 (COVID-19), WHO Country Office for Nepal. URL: https://www.who.int/docs/default-source/nepal-documents/novel-coronavirus/who-nepal-sitrep/22-who-nepal-sitrep-covid-19.pdf?sfvrsn=df7c946a_2. Accessed: 2020-09-26.

WHO, 2020f. Situation Update Report 23 (23 September, 2020), Coronavirus disease 2019 (COVID-19), WHO Country Office for Nepal. URL: https://www.who.int/docs/default-source/nepal-documents/novel-coronavirus/who-nepal-sitrep/23-who-nepal-sitrep-covid-19.pdf?sfvrsn=1c07f023_2. Accessed: 2020-09-25.

WHO, 2020g. Situation Update Report 18 (19 Aug 2020), Coronavirus Diseases 2019 Nepal, WHO Country Office for Nepal. URL: https://www.who.int/docs/default-source/nepal-documents/novel-coronavirus/who-nepal-sitrep/18-who-nepal-sitrep-covid-19-23082020.pdf?sfvrsn=6fb20500_2. Accessed: 2020-09-16.

Wiki, 2020. COVID-19 pandemic in Nepal. URL:https://en.wikipedia.org/wiki/COVID-19_pandemic_in_Nepal. Accessed: 2020-09-26.

Xiao, Y., Tang, B., Wu, J., Cheke, R.A., Tang, S., 2020. Linking key intervention timings to rapid decline of the COVID-19 effective reproductive number to quantify lessons from mainland China. Int. J. Infect. Dis. 97, 296–298. https://doi.org/10.1016/j.ijid.2020.06.030.

Yang, Z., Zeng, Z., Wang, K., Wong, S.S., Liang, W., Zanin, M., et al., 2020. Modified SEIR and AI prediction of the epidemics trend of COVID-19 in China under public health interventions. J. Thorac. Dis. 12, 165–174. https://doi.org/10.21037/jtd.2020.02.64.

Yuan, H.Y., Mao, A., Han, G., Yuan, H., Pfeiffer, D., 2020. Effectiveness of quarantine measure on transmission dynamics of COVID-19 in Hong Kong. medRxiv 2020.04.09.20059006; doi: https://doi.org/10.1101/2020.04.09.20059006.

Zhang, H., Small, M., Fu, X., Sun, G., Wang, B., 2012. Modeling the influence of information on the coevolution of contact networks and the dynamics of infectious diseases. Physica D: Nonlinear Phenom. 241 (18), 1512–1517. https://doi.org/10.1016/j.physd.2012.05.011.

Epidemics 41 (2022) 100642

Contents lists available at ScienceDirect

Epidemics

journal homepage: www.elsevier.com/locate/epidemics

Insight into Delta variant dominated second wave of COVID-19 in Nepal

Khagendra Adhikari [a], Ramesh Gautam [b], Anjana Pokharel [c], Meghnath Dhimal [d,e], Kedar Nath Uprety [f], Naveen K. Vaidya [g,h,i,*]

[a] Amrit Campus, Tribhuvan University, Kathmandu, Nepal
[b] Ratna Rajya Laxmi Campus, Tribhuvan University, Kathmandu, Nepal
[c] Padma Kanya Multiple Campus, Tribhuvan University, Kathmandu, Nepal
[d] Nepal Health Research Council, Kathmandu, Nepal
[e] Global Institute for Interdisciplinary Studies, Lalitpur, Nepal
[f] Central Department of Mathematics, Tribhuvan University, Kathmandu, Nepal
[g] Department of Mathematics and Statistics, San Diego State University, San Diego, CA, USA
[h] Computational Science Research Center, San Diego State University, San Diego, CA, USA
[i] Viral Information Institute, San Diego State University, San Diego, CA, USA

ARTICLE INFO

Keywords:
Delta variant
COVID-19
Nepal
Hospitalization
Vaccination

ABSTRACT

Objective: To study the spreading nature of Delta variant (B.1.617.2) dominated COVID-19 in Nepal to help the policymakers assess and manage health care facilities and vaccination programs.

Methods: Deterministic mathematical models in the form of systems of ordinary differential equations were developed to describe the COVID-19 transmission in the high- and the low-risk regions of Nepal. The models were validated using the multiple data sets containing daily new cases in the whole country, the high-risk region, the low-risk region, and cases needing medical care, ICU, and ventilator.

Results: We found the reproduction number of $R_t = 4.2$ at the beginning of the second wave, larger than the first wave (~1.8 estimated previously), indicating that the transmissibility of Delta variant is higher than the wild-type circulated during the first wave. Model predicts that ~5% of the COVID-19 cases were reported in Nepal, estimating the seroprevalence of ~63.9% as of July 2021, consistent with the survey conducted by the Government of Nepal. The seroprevalence was expected to reach 94.46% by April 2022, among which ~46% would have both infection and vaccination. The expected cases from September 2021 to April 2022 is 111,300, among which 11,890 people might need medical care, 3590 need ICU, and 953 need ventilators. The COVID-19 cases and medical care needs could be significantly reduced with proper implementation of vaccination and social distancing.

Conclusions: The data-driven mathematical models are useful to assess control programs in resource-limited countries. The appropriate combination of vaccination and social distancing are necessary to keep the pandemic under-control and manage the medical care facilities in Nepal.

1. Introduction

The COVID-19 pandemic caused by the novel coronavirus (SARS-CoV-2) continues with multiple waves worldwide. The pandemic has already generated more than 587 million cases and 6.43 million deaths worldwide as of August 6, 2022 (Worldometer, 2022). Among the several waves of COVID-19 caused by the different variants of the virus, the Delta variant (B.1.617.2) was the dominating strain during the second wave (June 2021 to December 2021 (GISAID, 2022)) until it was suppressed by new Omicron variant. The World Health Organization (WHO) classified the Delta variant as a global concern on May 10, 2021, when it had already spread to more than 30 countries (Nebehay and Farge, 2021). Notably, the Delta variant circulating during the second wave was more infectious (Bolze et al., 2021b; Callaway, 2021; Campbell and Archer, 2021; Jassat et al., 2021; WHO, 2021b) than the wild type, and caused the highest number of cases and deaths compared to other waves in Nepal (MoHP, 2021).

The crisis of Delta variant COVID-19 surge was catastrophic in Nepal, significantly ruining the fragile health care system after the second week of March 2021 (Weissenbach, 2021). With the country's population of

* Correspondence to: Department of Mathematics and Statistics, San Diego State University, 5500 Campanile Drive, San Diego, CA 92182 USA.
E-mail address: nvaidya@sdsu.edu (N.K. Vaidya).

https://doi.org/10.1016/j.epidem.2022.100642
Received 10 December 2021; Received in revised form 6 September 2022; Accepted 5 October 2022
Available online 6 October 2022

only 30 million, infections during the second wave soared to over 9000 new cases per day recorded in the first week of May 2020 (MoHP, 2021; Poudel, 2021). As of September 1, 2021, the total COVID-19 related death in Nepal is 10,770, among which more than 7770 were during the second wave (MoHP, 2021). In May 2021, the whole-genome sequencing tests of 35 swab samples confirmed 34 of them as Delta variants (97%) (Poudel, 2021). Note that Alpha variant (B1.1.7) and K417N (AY.1.), a sub-lineage of B.1.617.2, have also been identified in Nepal (MoHP, 2020b).

In response to the second wave of COVID-19, the Government of Nepal implemented the lockdown on April 29, 2021, beginning from Kathmandu, the capital city, and later extending to all parts of the country (ALJAZEERA, 2021). Despite the lockdown for about four months and implemented vaccination, the transmission of the disease was still significantly high (2052 new cases and 20 deaths on September 1, 2021 (MoHP, 2021)). The potential devastation of this pandemic is highly unpredictable, primarily due to significant asymptomatic and undiagnosed cases (Baggett et al., 2020; Li et al., 2020; MoHP, 2020a; Reis et al., 2020). Moreover, the transmission dynamics of the second wave of COVID-19 was quite different from the first wave because of the availability of COVID-19 vaccination, improved treatment strategies, and a higher infectivity of the Delta variant (Hafeez et al., 2021; Ito et al., 2021). During the second wave, a higher reproduction number has been reported (EPH, 2021; WHO, 2021b), and also infected individuals experienced more severe infection resulting in a higher rate of hospitalization (Bager et al., 2021; Funk et al., 2021; Gupta et al., 2021; Sheikh et al., 2021). Different vaccines are found to have varying effects in the community across different regions of the world depending on the variants (Abu-Raddad et al., 2021; Bernal et al., 2021). Therefore, it is critical to gain insight into the unique transmission pattern and potential burden of COVID-19 in Nepal to design policies for the proper management of health care facilities and vaccination.

In this study, we implemented a data-driven modeling approach to study the COVID-19 transmission dynamics focused on two separate regions (high-risk and low-risk). Considering two different regions is essential in the context of Nepal because of the Nepal-India open border and largely populated cities in some regions, making them higher than others. Especially all the districts of the Terai region connected to India and populated cities such as Kathmandu, Surkhet, Pokhara, Lalitpur, Bhaktapur, and Chitwan are taken as a high-risk region. We validated our model by fitting it to the multiple real-time data sets containing new recorded cases from the high- and low-risk regions as well as the hospitalized, Intensive Care Unit (ICU), and Ventilator cases, and estimating key parameters of the model in a realistic range. We estimated the effective reproduction number and predicted the hospital beds, ICU, and Ventilators that would be needed in Nepal until April 2022. Moreover, we extended our model to explore how various vaccination programs would reduce the epidemic burden in Nepal.

2. Methods

2.1. Data

The data used in this study is obtained from the Ministry of Health and Population, Government of Nepal (MoHP, 2021). We used the data from 14 March to 15 September 2021 to fit the model. The six different data sets, the daily new cases of the whole country, the high-risk and low-risk regions, and number of patients in medical care, ICU, and ventilators were used in our model fitting and simulation.

2.2. Transmission dynamics model

In our transmission dynamics model based on the SEIR framework, we incorporated the medical care, ICU, and Ventilator compartments for both high- and low-risk regions to study the second wave of COVID-19 in Nepal. Schematic diagram and short description of the model are provided in Fig. 1, and the detailed description along with model equations is provided in the GitHub public repository (Adhikari, 2021).

2.3. Parameter estimation and model fitting to data

Since the new cases began to increase from March 14, 2021, we took March 14, 2021, as the initial time ($t = 0$) to initiate the second wave. The total population of Nepal in the census year 2011 was 26,494,504, and it is projected to be 29,996,478 at the end of 2020 (CBS, 2011). About 3.5 million Nepalese live in India as migrant workers (Kuwar, 2015; Prasain, 2021), so we did not include this population in our study. Using 14.4% [95% CI: 11.8–17.0] seroprevalence found in the October 2020 (MoHP, 2020a), our previous model (Adhikari et al., 2021) allowed us to estimate the seroprevalence on March 14, 2021, to be 24%. We deducted both seroprevalence and migrant population from the total population and took the initial susceptible population of 19.29 million for this study. Out of these susceptible populations, high and low-risk regions constitute 65% and 35%, respectively (CBS, 2011). The baseline values of all state variables are provided in the GitHub public repository (Adhikari, 2021).

The lockdown in Kathmandu valley was started on March 29, 2021, and gradually extended to almost all parts of the country (ALJAZEERA, 2021). To model this scenario, we defined the transmission rate $\beta_2(t)$ and $\beta_3(t)$ as follows:

$$\beta_2(t) = \begin{cases} \beta_H, & if \quad t \le 47, \\ \beta_H \quad ((1-c_b)exp(-r_H(t-47)) + c_b), & if \quad t > 47, \end{cases}$$

$$\beta_3(t) = \begin{cases} \beta_L, & if \quad t \le 47, \\ \beta_L \quad ((1-c_b)exp(-r_L(t-47)) + c_b), & if \quad t > 47, \end{cases}$$

where β_H and β_L represent the transmission rates before lockdown on the high-risk region and the low-risk region, respectively. Following the lockdown (at day 47), the transmission rates of high-risk and low-risk regions decay at the rates r_H and r_L, respectively. We further estimate the different values of r_H and r_L for different time periods according to the different levels of lockdown. We took c_b= 0.3 assuming up to 70% reduction on contacts during the prolonged lockdown period (Coburn et al., 2009). Note that the transmission of diseases by the recorded infectious remains the same regardless of the lockdown situation.

Since the inter-region mobility is quite different during the lockdown period from the pre-lockdown period, we considered two different mobility rates, $\gamma(t) = \gamma_1$, and γ_2, for the period of pre-lockdown and lockdown, respectively. The remaining parameters were estimated from data fitting by using the least square method. The details of data fitting are explained in the GitHub public repository (Adhikari, 2021).

2.4. Calculation of the reproduction number

The reproduction number (R_t) is an average number of secondary infections generated by a single infectious individual (You et al., 2020), which captures the increasing ($R_t > 1$) and decreasing (R_t<1) trend of the infection. We calculated the reproduction number by using our dynamical system model and also using the Maximum Likelihood Method (MLM) from the daily reported incidence using the EpiStem package of R-program (Thompson et al., 2019) (see the GitHub public repository (Adhikari, 2021) for the reproduction number formulation).

2.5. Modeling vaccination program

We assumed the vaccination for individuals in all compartments, except the recorded infectious, medical care, ICU, and ventilator compartments, because the individuals were not vaccinated while they are infected or in medical care. To incorporate the vaccination program into the model, we further divide each vaccination-eligible compartment

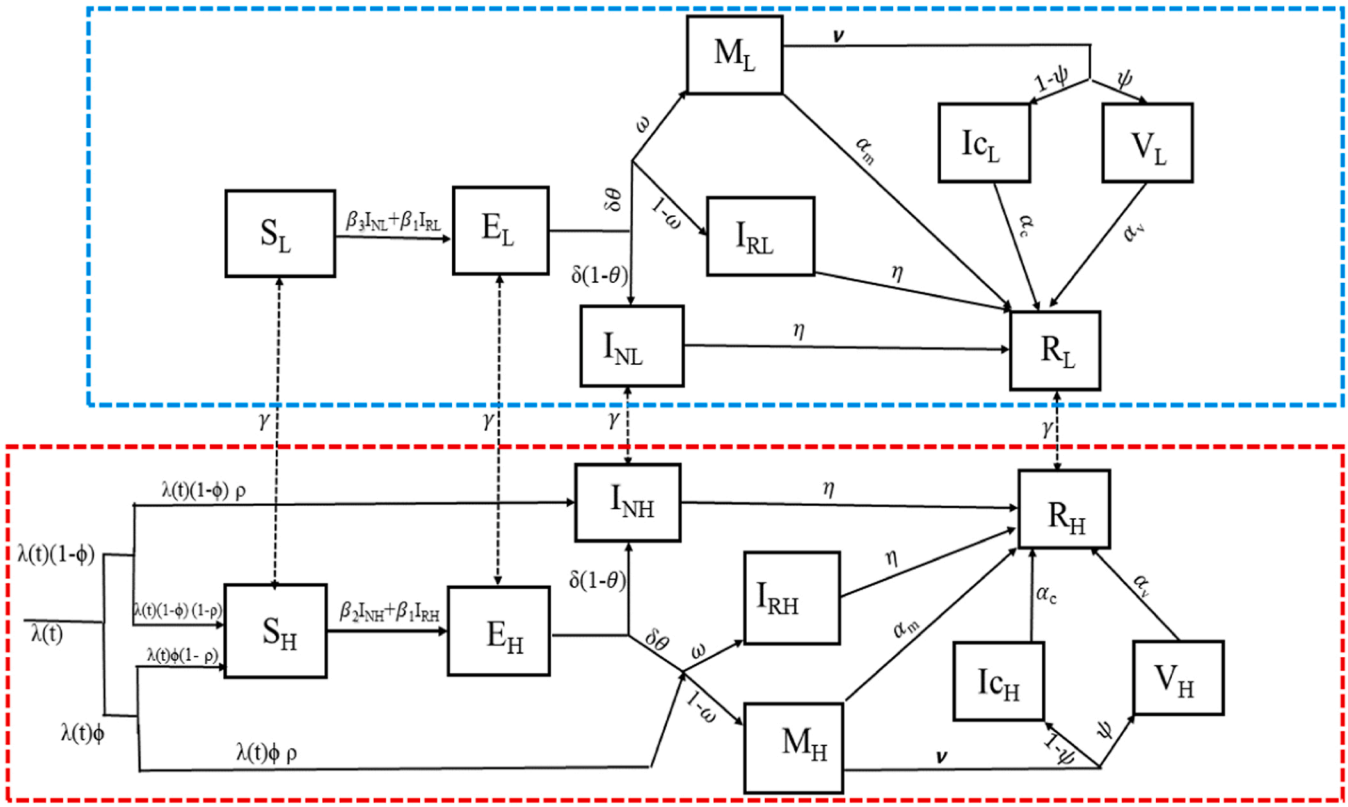

Fig. 1. Compartmental diagram of the Model. The red box denotes the high-risk region and blue the low-risk region. Here we divided the population into sixteen distinct compartments: S_H, S_L (susceptible), E_H, E_L (exposed), I_{RH}, I_{RL} (recorded infectious), I_{NH}, I_{NL}, (non-recorded infectious), M_H, M_L (Medical care), I_{CH}, I_{CL} (ICU), V_H, V_L (Ventilator) and R_H, R_L (recovered), where the suffixes H and L are used to indicate the high- and low-risk regions, respectively. $\wedge_H$ and $\wedge_L$ represent the recruitment rates due to birth and $\lambda(t)$ is the rate of entry of the immigrants from abroad to the high-risk region. Among the immigrants, a portion ϕ is tested by the antigen, and the rest $(1-\phi)$ entered the community without the antigen test. The ρ portion of immigrants with a positive test enter I_{RH} class and the remaining with a negative test enters S_H class. The immigrants without antigen test are entered to S_H and I_{NH} with the same portion $1-\rho$ and ρ, respectively. There is no recruitment from immigration in the low-risk region as it does not have a border with India. γ is the mobility rate between two regions. The transmission rate from the recorded infectious classes are β_1 for both regions, and that from non-recorded infectious classes in high- and low-risk regions are β_2 and β_3, respectively. The incubation period is represented by $\frac{1}{\delta}$. θ is the rate of being recorded, among which a portion ω enter M_H and M_L, and a portion $(1-\omega)$ enter I_{RH}, and I_{RL}, respectively. From M_H and M_L classes, the severe patients enter high medical care at the rate υ among them (1-ψ) portion enter I_{CH}, I_{CL}, and ψ portion enter V_H, and V_L at the rate ν. The recovery rate of I_{RH}, I_{NH}, I_{RL}, and I_{NL} classes is η and that of (M_H, M_L), (I_{CH}, I_{CL}), and (V_H, V_L) are α_m, α_c, and α_v, respectively. The natural death rate of all the classes is μ and the disease-induced death rate for recorded and non-recorded infectious individuals are k and k', respectively, and that of individuals in medical care, ICU, and ventilator are k_1, k_2 and k_3, respectively. A detailed description of the model and system of differential equations are provided in the GitHub public repository (Adhikari, 2021).

into vaccinated and unvaccinated sub-compartments and transfer individuals from unvaccinated to vaccinated compartment upon receiving vaccinations. We assumed that the vaccinated individuals are less susceptible to infection, less vulnerable for medical care, and immune during the study period. The extended model diagram with the vaccination program is presented in the GitHub public repository (Adhikari, 2021).

3. Results

3.1. Pattern of the second wave of COVID-19 in Nepal and model validation

We used the extended model to fit the data and future predictions. The model was fitted to the multiple data sets consisting altogether 1116 data points simultaneously (186 data points of each of the daily recorded new cases in the whole country, the high-risk region, and the low-risk region, and cases in medical care, ICU, and ventilator) (Fig. 2). The large number of 6 different kinds of data points allowed us to estimate the unique parameters. In the beginning, the vaccination level in Nepal was negligible, but from middle of July 2021, the vaccination rate was significantly increased. So, we also incorporated the realistic vaccination program in our basic model fitting. The model is in excellent agreement with each data set, asserting the validation of our model.

The second wave increased rapidly until the 1st week of May 2021, hitting the highest new cases of 9070 on May 6, 2021. The implementation of lockdown reduces the new cases in both the high- and low-risk regions, but the effect observed in the low-risk region was one month delayed compared to the high-risk region. After the relaxation in lockdown in some places of the high- and low-risk regions, the COVID-19 cases resurged from mid-July of 2021, forcing these places to impose the second lockdown (For example, Jhapa district imposed the second lockdown from the last week of July 2021 and then relaxed from the second week of August 2021 (The Himalayan, 2021)). As revealed in Fig. 2, during the first peak of the second wave, the hospital beds, ICUs, and ventilators needed were below the capacity allocated by the government. The estimated parameters are given in Table 1.

3.2. Forecasting of the second wave of COVID-19 in Nepal

The long-term prediction of the disease dynamics using the dynamical system model is widely accepted. There are many mathematical models (Chowdhury et al., 2020; Goscé et al., 2020; Hachtel et al., 2022; Putra et al., 2020; Shankar et al., 2021; Tuite et al., 2020), which have

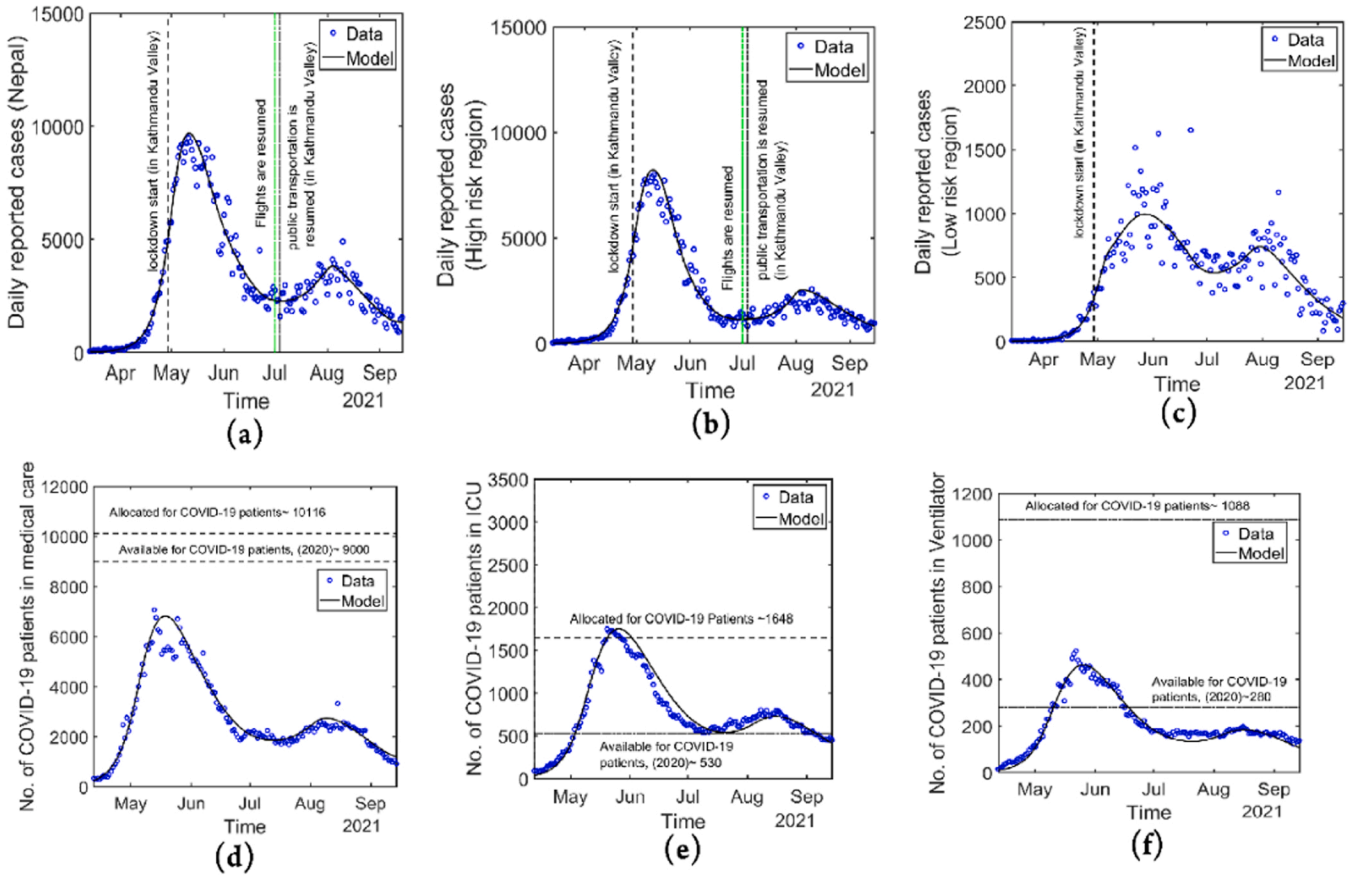

Fig. 2. Model Fitting to Multiple Data Sets. Daily reported cases of the whole country Nepal (a), the high-risk region (b), and the low-risk region (c), and cases in medical care (d), ICU (e), and ventilator (f). Solid lines represent the model prediction, and the circles represent the data. We take different decay rates r_H and r_L of transmission to address the different level of lockdown in different parts as follows: $r_{\mathrm{H}} = 0$ ($0 \leq t$ 47, Pre lockdown time), 0.082 ($47 \leq t$ 95, Lockdown to all regions), −0.05 ($95 \leq t$ 193 186, Partial relockdown in some parts), and $r_L = 0$ ($0 \leq t < 47$, Pre lockdown time), 0.033 ($47 \leq t < 105$, Lockdown starts and extend to other parts), −0.038 ($105 \leq t < 135$, Relaxation of lockdown), 0.038 ($135 \leq t < 185$ Partial relockdown in some places).

been used to predict the long-term behavior of pandemic in different places of the world. Here, we used our extended model to predict the long-term trend of the epidemic from 16 September 2021 to the end of April 2022 with the scenario of gradual relaxation of lockdown to reach the pre-lockdown phase. We would like to mention our long-term prediction includes short-term predictions as in some previous studies (Dahal et al., 2021; IHME, 2021). We also used our model to evaluate the various vaccination programs that the Nepal Government could implement. The trend of the epidemic with the level of vaccination implemented by the government (Fig. 3) shows a steady decrease to an almost extinct level with no cases of hospitalization at the end of April 2022. However, we note that our prediction was for the scenario in which no novel strain of SARS-CoV-2 would dominate the transmission. As per model estimations, 111,300 new cases would be reported, with 11,890 people needing medical care, 3590 needing ICU, and 950 needing ventilators, from September 16, 2021, to April 30, 2022.

3.3. Estimation of reproduction number in Nepal

We first estimated the reproduction number (R_t) from the data using the Maximum Likelihood Method (MLM). As mentioned earlier, the April 14 was the starting date of the second wave of COVID-19 in Nepal. Taking the 7 day-window for the calculation of R_t (see method section), we estimated the reproduction number from 21 April 2021–15 September 2021 (the last data considered). We observed that before the lockdown, R_t reached up to 2 in both the high- and low-risk regions as well as in the whole country (around the 3rd week of April), indicating that the significant community transmission of the disease had already occurred before the lockdown.

While R_t estimated from the data provides valuable information regarding the disease trend, it lacks the asymptomatic cases, which may be the dominating spreader of the disease. To overcome this limitation, we also estimated the time-dependent reproduction number (R_t) by using our model. As expected, the model predicted a higher value of the reproduction number of 4.2 due to the asymptomatic cases. R_t decreases rapidly after the implementation of the lockdown (Fig. 4). Around the 1st week of June, it fell below 1 and again raised following the partial relaxation of lockdown. This trend of R_t well-describes the trends of new cases in both high-and low-risk regions.

Under the complete national-level lockdown, it took one month longer in the low-risk region to bring R_t below 1 compared to the high-risk region. Our model also allowed us to predict a long-term R_t up until 30 April 2022. According to our model prediction, R_t remained less than the threshold value 1, indicating the decreasing trends of new cases in both regions (Fig. 4) throughout the pandemic until April 2022.

3.4. Estimates of seroprevalence

The antibody of COVID-19 forms in the body due to the viral infection and/or vaccination. Estimating the seroprevalence is practically essential for COVID-19, mainly because of a large portion of unreported infected individuals. We assumed that recovered and/or vaccinated people remain immune during the simulation period. We estimated 63.9% seroprevalence (Fig. 5) as of the end of July. We also used our model to predict the expected seroprevalence during the pandemic until April 2022 (Fig. 5). As predicted by our model, the seroprevalence

Table 1
Parameters of the model.

Symbol	Description	Value	References
β_1	transmission rate of recorded infectious people of high and low risk region	0.005	Data fitting
β_H	transmission rate of non-recorded infectious people of high region	0.525	Data fitting
β_L	transmission rate of non-recorded infectious people of low-risk region	0.235	Data fitting
θ	detection rate	0.05	Data fitting
ϕ	border screening rate	0.1	Data fitting
ρ	positivity rate of migrant workers at border	0.1	(MoHP, 2021)
k	disease induced death rate of reported non- hospitalized infected	0.0002	Data fitting
k'	disease induced death rate of non-reported non-hospitalized infected	0.00002	Data fitting
k_1, k_2, k_3	disease induced death rate in medical care, ICU, and ventilator	0.001,0.041,0.071	Data fitting
γ_1, γ_2	mobility rate between high and low risk regions before and after lockdown	0.015, 0.0001	Data fitting
ω	proportion of infected who need medical care	0.1125	Data fitting
τ	rate of admission on ICU from medical care	0.1	Data fitting
ν	rate of admission on high medical care (ventilator and ICU)	0.05	Data fitting
Ψ	proportion of infected who need ventilator	0.21	Data fitting
$\alpha_m, \alpha_c, \alpha_v$	recovery rate from medical care, ICU, and ventilator	0.092,0.1,0.0625	Data fitting
η	recovery rate of infectious without medical care	0.0588	(WHO, 2021a)
δ	incubation period	0.1923	(Linton et al., 2020)

reached ~89% in December 2021 and ~95% in April 2022.

Moreover, our model allows us to identify whether the seroprevalence achieved is due to vaccination, actual infection, or both. Among the ~89% seroprevalence achieved by December 31, 2021, ~7% are from vaccination, ~52% are from infection, and ~30% are from both vaccination and infection. Similarly, ~7%, ~42%, and ~46% are expected contributions from vaccination, infection, and both, respectively, towards the total seroprevalence of ~95% by April 30, 2022.

3.5. Role of vaccination in the mitigation of COVID-19 in Nepal

Here, we considered different vaccination scenarios under the complete relaxation of non-pharmaceutical interventions and used the model to predict the outcome of the pandemic under these vaccination programs. Based on the literature, we modeled the effectiveness of vaccination using a 50% reduction in infection and a 90% reduction in hospitalization for vaccinated people. While we used this level of effectiveness for demonstration purposes, the simulations with other values produce a similar qualitative behavior with a slight quantitative difference.

The Government of Nepal had set the target to vaccinate 71.6% of the people from the eligible age groups (MoHP, 2021). Therefore, we focus on vaccination programs targeting 71.6% of the eligible population by a specific timeframe. The vaccination rate (ζ), in our model with the target to cover 71.6% eligible population by vaccination timeframe, T, can be calculated using $\zeta = \frac{-\ln(1-\frac{71.6}{100})}{T}$ (Pantha et al., 2021a). For varying vaccination timeframes from October 31, 2021, to April 30, 2022, and the varying level of lockdown from 0% to 80%, we simulated our model to predict maximum daily cases, the total cases, the total deaths, the total medical cares, the total ICUs, and the total ventilators, during the pandemic until April 2022 (Fig. 6).

With the level of vaccination implemented and complete relaxation of the lockdown, the peak value of new cases is 2232 per day. However, the peak could be reduced to ~ 1726, 1966, 2070 and 2134 per day, respectively, when the vaccination timeframe is set to the end of October 2021, December 2021, February 2022, and April 2022. Our model simulations show that the total number of cases by the end of April 2022 could be reduced from 154,000 to 62,000, 94,000, 119,000, and 132,000 by setting the vaccination timeframe at the end of October 2021, December 2021, February 2022, and April 2022, respectively. With these vaccination programs, i.e., the time frame of the end of October 2021, December 2021, February 2022, and April 2022, the number of recorded deaths could be reduced from 1509 to 686, 1017, 1196, and 1316, respectively. Similarly, these vaccination timeframes could reduce the total medical patients from 16,610 to 5885, 9965, 12,150, and 14,080, respectively. In this case, the total ICU patients could be reduced from 4941 to 1964, 3147, 3790, and 4220, respectively, and ventilator patients could be reduced from 1305 to 522, 836, 1007, and 1122, respectively (Fig. 6).

4. Discussion

The timely characterization of the COVID-19 wave is essential for policy intervention to overcome the devastating impacts of the pandemic. Here, we developed a data-driven mathematical model to describe Nepal's unique delta variant-dominated second wave of COVID-19. Using multiple data sets simultaneously and considering two distinct high- and low-risk regions are unique features with more practical applications in our model. Our results provide a great insight into some relevant scenarios of COVID-19 in Nepal and predict the impact of potential vaccination programs on mitigating the burden of the pandemic, helping policymakers design proper health care facilities and vaccination strategies.

We identified the distinct pattern of the Delta wave in high- and low-risk regions regarding its magnitude and time period. As expected, most of the cases (>80%) were recorded in high-risk region and it peaked about one month earlier than low-risk region. Such spatial disparity on the pandemic trend was also found in the previous study (Pantha et al., 2021b), which performed the province-wise analysis of the first wave of COVID-19 in Nepal. The increasing trend of the epidemics remained for the period of April-May 2021 in high-risk region and for the period of May-June 2021 in low-risk region.

The delta variant was the dominant variant during the second wave of COVID-19 in Nepal. As per our model estimates, the reproduction number of $R_t = 4.2$ at the beginning of the Delta variant dominated second wave is higher than the first wave (~1.8) (Adhikari et al., 2021), indicating a significantly higher virus transmission during the second wave than the first wave. The maximum likelihood method gives a relatively low effective reproduction number (~2) at the peak time of epidemic that is similar to the other study (Dahal et al., 2021). The higher transmissibility of the Delta variant observed in our study is supported by the previous studies in different parts of the world (Campbell and Archer, 2021; Funk et al., 2021; Saito et al., 2021; Bolze et al., 2022; Li et al., 2021) and higher reproduction numbers in many other reports and studies (Campbell and Archer, 2021; Ito et al., 2021; WHO, 2021b). While the national implementation of lockdown caused the reproduction number to decrease to below the threshold value 1, the effect seen in the low-risk region was about a month delayed compared to the high-risk region. Such inter-regional disparity highlights that regional level policy, and thus regional level modeling, is needed for more effective control of the local-level outbreak. The inter-region discrepancy overserved in our estimated R_t is consistent with the inter-provincial disparity identified in Pantha et al. (Pantha et al.,

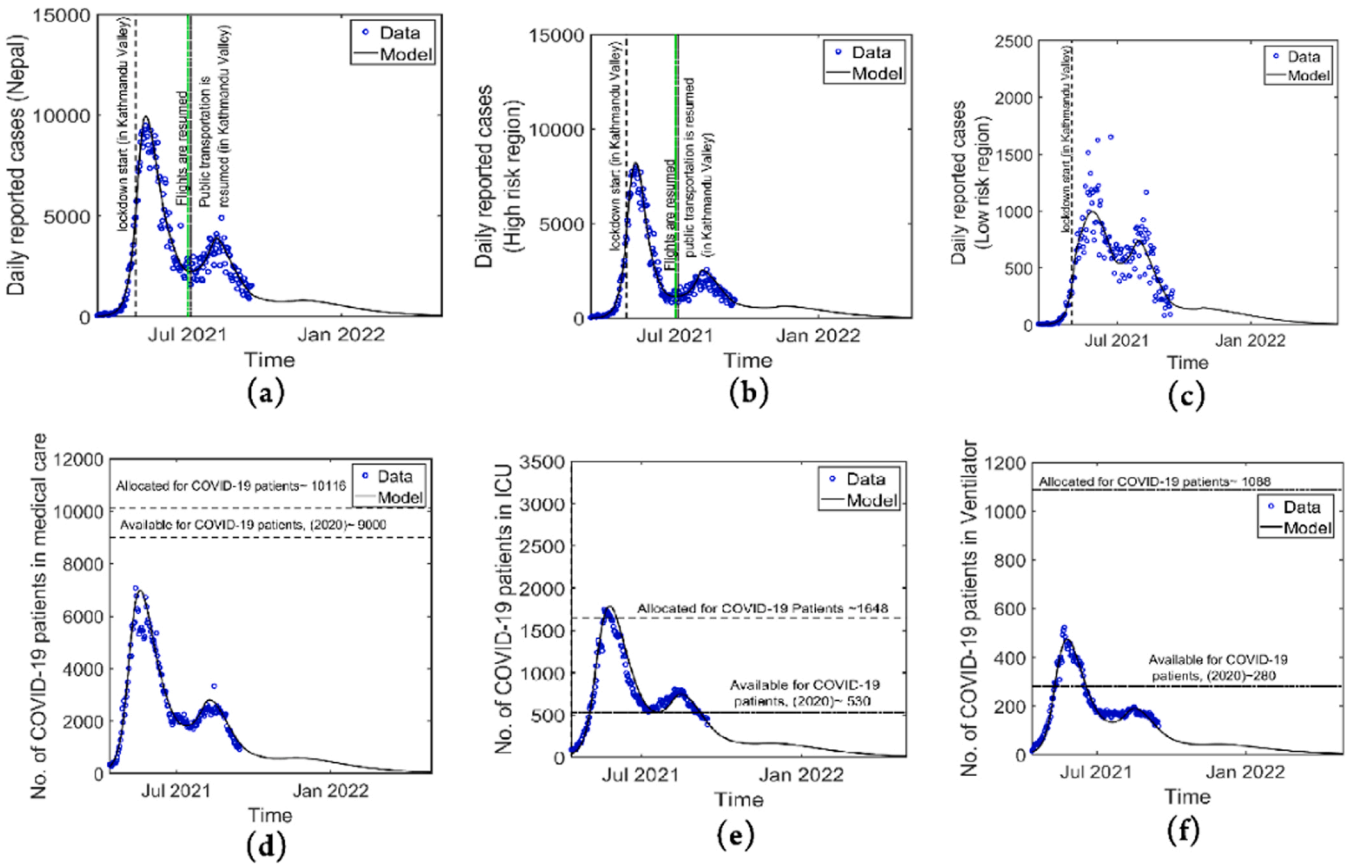

Fig. 3. Long term Prediction of the Model. Prediction of daily reported cases of the whole country Nepal (a), the high-risk region (b), and the low-risk region (c), and cases in medical care (d), ICU (e), and ventilator (f), predicted by the model until April 30, 2022.

2021b) during the first wave of COVID-19 in Nepal.

The potential transmission from the undiagnosed cases is one of the most contributing factors to the uncertainty of the COVID-19 pandemic, causing extreme difficulty for its control. Estimating this critical transmission rate from undiagnosed cases requires a large-scale seroprevalence survey, which is often limited by resources in developing countries like Nepal. We implemented our data-driven dynamical system-based model to estimate this transmission rate. We found a significantly high transmission rate from undiagnosed cases (~95%), consistent with the seroprevalence survey of the Government of Nepal (MoHP). Our model predicts ~63% seroprevalence in Nepal at the end of July 2021, consistent with the result (~68.6%) from the Nepal Government's survey (MoHP). With the level of vaccination implemented, the model predicts that ~95% of people were immune to the circulating strains of COVID-19 by the end of April 2022. Among these immune people, about 46% had experienced both vaccination and actual infection.

For developing countries like Nepal, timely assessment of expected burden is critical to avoid an overwhelming situation in hospitals and medical facilities. Our simulation results identified the duration of hospitalization of the COVID-19 patients in Nepal (7 days in normal medical care, 7.2 days in ICU, and 7.5 days in ventilators) shorter than that noted in other studies (Ben, 2021; Li et al., 2020; Twohig et al., 2022; Gupta et al., 2021). As in many other studies (Saito et al., 2021; Twohig et al., 2022; Verity et al., 2020; Jassat et al., 2021), Nepal faced a significant increase in the hospitalization burden due to the delta-variant compared to the wild-type. Based on our model analysis, we found the hospitalization of ~11.25% of recorded cases in Nepal, similar to the rates identified in other countries (~9.2%–25%) (Bager et al., 2021; Gupta et al., 2021). Among the hospitalized patients, ~35% of them needed extensive medical care, such as ICU and ventilator. According to the report on May 2020 (MoHP, 2020b), Nepal had 26,930 hospital beds, 1595 ICU beds, and 840 ventilators, including the government and private sectors. The Government of Nepal planned to allocate one-third of these facilities for COVID-19 patients. Later, the Government of Nepal extended its capacity to 10,116 hospital beds, 1648 ICUs, and 1088 ventilators for COVID-19 patients (MoHP, 2021). Interestingly, these data show that the predicted total hospitalization burden remains below the total capacity of Nepal even though the country is expected to have limited medical resources and prevention programs. However, we note that during the peak time (last of May 2021), many national and international media (Ben, 2021; Bhandari and Hannah Peterse, 2021; Prasain, 2021; ReliefWeb, 2021) covered the news about a shortage of hospital beds, ICU, ventilators, and oxygen cylinders. This discrepancy may be attributed to mismanagement of the hospital infrastructure and/or underreporting of patients. We also note that the low hospital rate may partially be attributable to the hospitalization of only complicated cases or scarcity of the hospital beds at the time of peak (Ben, 2021; Prasain, 2021; ReliefWeb, 2021).

The significant impact of the vaccination, including against the new variants, has been reported (Abu-Raddad et al., 2021; Bernal et al., 2021). Both vaccination programs and the relaxation of lockdown were ongoing in Nepal after the September 2021. We implemented our model to predict the potential epidemic trends and medical care needed (hospital bed, ICU, ventilator) for various coverage rates of vaccination programs and levels of lockdown during the pandemic until April 2022 (Fig. 6). Our model predictions of 111,300 cases, 11,890 hospitalizations, 3590 ICUs, and 950 ventilators by the end of April 2022 is also compatible with the prediction of IHME model (IHME, 2021). The results on vaccination and lockdown provide information on suitable strategies for Nepal to manage medical care and the pandemic burden.

We acknowledge some limitations of our study. Daily new cases may be affected by the number of tests and the positivity rate, which were not

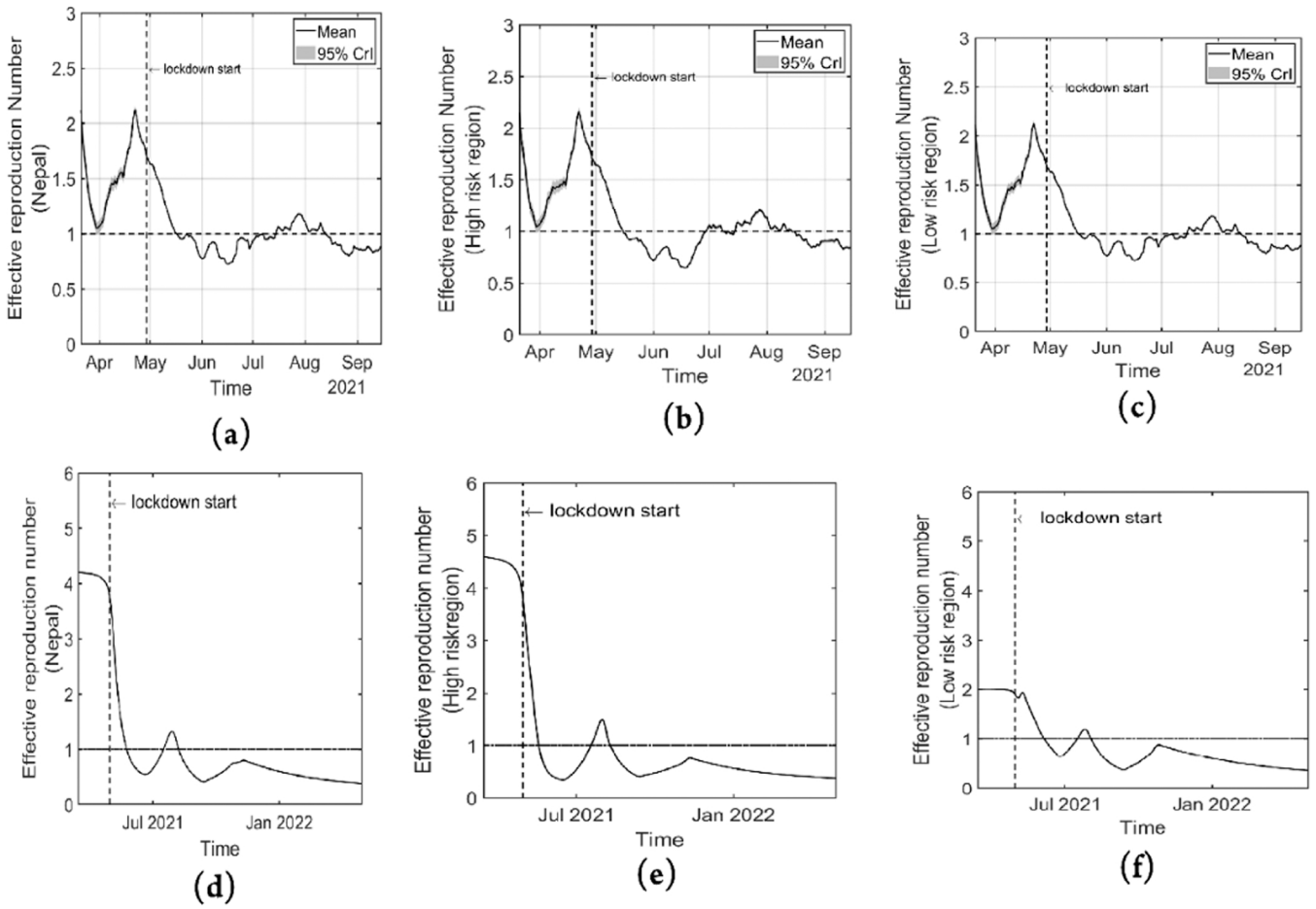

Fig. 4. Reproduction number. Time-dependent reproduction number of COVID-19 estimated from the recorded data for the whole country Nepal (a), the high-risk region (b), and the low-risk region (c). Time-dependent reproduction number of COVID-19 estimated from the model for the whole country Nepal (d), the high-risk region (e), and the low-risk region (f). Note that the higher reproduction number estimated from the model is presumably due to the unreported cases. The horizontal lines indicate the threshold value, $R_t = 1$, above (below) which shows an increasing (decreasing) trend of the disease spread. The model allowed us to predict R_t for the longer time up until April 2022.

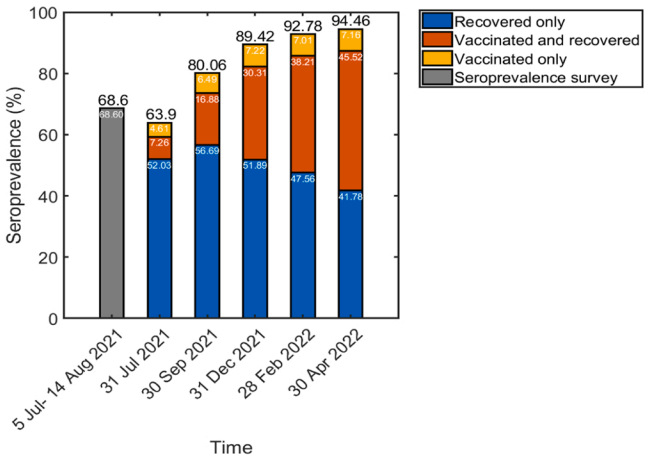

Fig. 5. Estimation of seroprevalence. The predicted seroprevalence achieved due to actual infection only, vaccination only, and both. The first bar represents the survey data by the Government of Nepal.

considered into our model. The inherent complexities of an unfolding epidemic, human behavior, implementation timing, and governmental policy change may have some impact on our predictions. We ignored the spatial heterogeneity in the dynamics within each region, the high- and low-risk regions. Furthermore, the inhomogeneity of the age structures of the study population was ignored. These questions can be addressed by heterogeneous and/or age-structured models, but more granular data is required. We considered high- and low-risk districts based on interconnections with India, a highly affected country by Delta variant, population density, and mobility pattern. The lack of data and information might have caused some uncertainty in categorizing districts into high- or low-risk regions. For example, our model classified the Makawanpur district, which is connected to high-risk districts (Chitwan, Lalitpur, and three Tarai districts), as low-risk due to its low density, low mobility pattern (a hilly district), and low infected cases. Moreover, because of the lockdown implemented during the second wave, there was less mobility across the districts, making Makawanpur a low-risk district despite its high-risk neighboring districts. Our long-term predictions were under the assumption that a novel strain would not appear for the study period. Therefore, the results need to be interpreted when the viral evolution and emergence of more severe strains are absent.

In summary, our data-driven model reveals some essential and insightful facts regarding the Delta-dominated second wave of COVID-19 in Nepal. In-depth exploration of the potential discrepancy between the actual epidemic burden and the recorded data suggests the policymakers revisit the gaps between the plan and practice of management of the pandemic. Estimated seroprevalence, new COVID-19 cases, and the hospitalization burdens under vaccination can provide helpful information for designing plans to control the pandemic in Nepal.

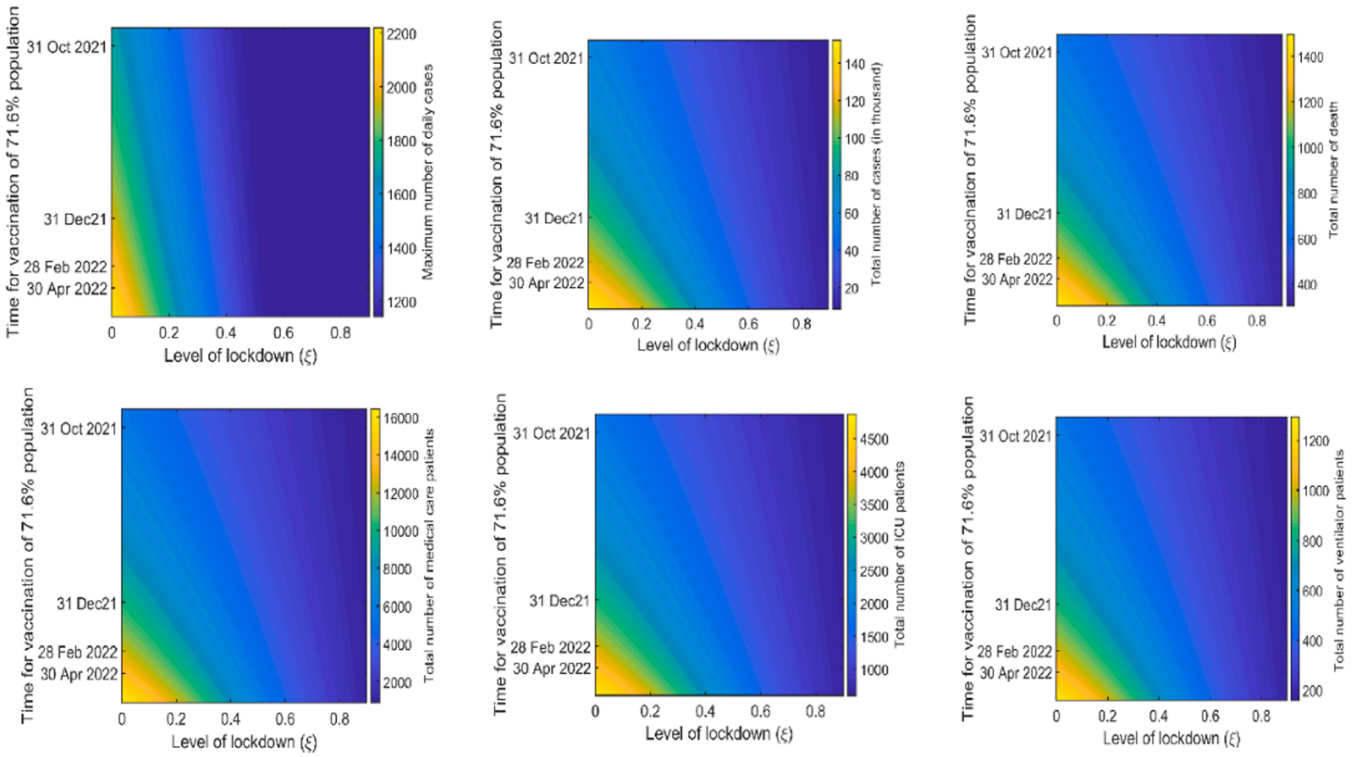

Fig. 6. Assessment of vaccination and lockdown program combined. The predicted peak value of the daily cases (a), total cases (b), total death (c), medical care cases (d), ICU cases (e), and ventilator cases (f) during the period from September 01, 2021, to April 30, 2022, for varying vaccination target timeframe and lockdown level.

CRediT authorship contribution statement

Khagendra Adhikari: Formal analysis, Investigation, Methodology, Writing – original draft. **Ramesh Gautam**: Formal analysis, Investigation, Methodology, Writing – original draft. **Anjana Pokharel**: Formal analysis, Investigation, Methodology, Writing – original draft. **Meghnath Dhimal**: Formal analysis, Writing – review & editing. **Kedar Nath Uprety**: Formal analysis, Supervision, Writing – review & editing. **Naveen K. Vaidya**: Conceptualization, Formal analysis, Supervision, Writing – review & editing.

Declaration of Competing Interest

The authors declare that they have no known competing financial interests or personal relationships that could have appeared to influence the work reported in this paper.

Acknowledgments

This research is supported by the GRAID (Graduate Research Assistantships in Developing Countries) awards from the International Mathematical Union (IMU). KA acknowledges the Nepal Academy of Science and Technology (NAST) for Ph.D. Fellowship. RG acknowledges the University Grants Commission (UGC) Nepal for Ph.D. Fellowship 2021. The work of NKV was supported by NSF grants DMS-1951793 and DEB-2030479 from the National Science Foundation of USA and UGP award from San Diego State University.

References

Abu-Raddad, L.J., Chemaitelly, H., Butt, A.A., 2021. Effectiveness of the BNT162b2 Covid-19 vaccine against the B. 1.1. 7 and B. 1.351 variants. N. Engl. J. Med. 385, 187–189. https://doi.org/10.1056/NEJMc2104974.

Adhikari, K., 2021. Supplementary Materials. https://github.com/Khagendra38/Supplimentary_material_COVID-19_Nepal_Nepal/blob/main/supplimentary_material_COVID-19_Nepal.pdf.

Adhikari, K., Gautam, R., Pokharel, A., Uprety, K.N., Vaidya, N.K., 2021. Transmission dynamics of COVID-19 in Nepal: mathematical model uncovering effective controls, 110680-110680 J. Theor. Biol. 521. https://doi.org/10.1016/j.jtbi.2021.110680.

ALJAZEERA, 2021. Nepal starts 15-day COVID lockdown as infections spike. ALJAZERA News. https://www.aljazeera.com/news/2021/4/29/nepal-starts-15-day-covid-lockdown-as-infections-spike. (Accessed 21 May 2021).

Bager, P., Wohlfahrt, J., Fonager, J., Rasmussen, M., Albertsen, M., Michaelsen, T.Y., Møller, C.H., Ethelberg, S., Legarth, R., Button, M.S.F., Gubbels, S., Voldstedlund, M., Mølbak, K., Skov, R.L., Fomsgaard, A., Krause, T.G., 2021. Risk of hospitalisation associated with infection with SARS-CoV-2 lineage B.1.1.7 in Denmark: an observational cohort study. Lancet Infect. Dis. 0, 1–11. https://doi.org/10.1016/S1473-3099(21)00290-5.

Baggett, T.P., Keyes, H., Sporn, N., 2020. Prevalence of SARS-CoV-2 infection in residents of a large homeless shelter in Boston. JAMA 323, 2191–2192. https://doi.org/10.1001/jama.2020.6887.

Bernal, J.L., Andrews, N., Gower, C., Gallagher, E., Simmons, R., Thelwall, S., Stowe, J., Tessier, E., Groves, N., Dabrera, G., et al., 2021. Effectiveness of Covid-19 vaccines against the B. 1.617. 2 (Delta) variant. N. Engl. J. Med. 2021; 385:585-594.

Ben, W., 2021. COVID-19 spirals out of control in Nepal: 'Every emergency room is full now. NATIONAL GEOGRAPHIC News. https://www.nationalgeographic.com/culture/article/a-pandemic-surge-threatens-livelihoods-in-nepal#:~:text=Shrestha%2C%20AP%20Images-,COVID%2D19%20spirals%20out%20of%20control%20in%20Nepal%3A%20'Every,one%20of%20India's%20neighboring%20nations.&text=India's%20crisis%20shows%20how%20oxygen,medicine%20not%20everyone%20can%20access.

Bhandari, R., Hannah Peterse, H.E., 2021. A hopeless situation': oxygen shortage fuels Nepal's Covid crisis. Theguardian. https://www.theguardian.com/world/2021/may/10/hopeless-situation-oxygen-shortage-fuels-nepal-covid-crisis. (Accessed 2 September 2021).

Bolze, A., Cirulli, E.T., Luo, S., White, S., Wyman, D., Dei Rossi, A., Cassens, T., Jacobs, S., Nguyen, J., Ramirez, J.M., Sandoval, E., Wang, X., Wong, D., Becker, D., Laurent, M., Lu, J.T., Isaksson, M., Washington, N.L., Lee, W., 2022. Rapid displacement of SARS-CoV-2 variant B.1.1.7 by B.1.617.2 and P.1 in the United States Cell Report Medicine. Cell Report Medicine 3 (3), 1–10. https://doi.org/10.1016/j.xcrm.2022.100564.

Callaway, E., 2021. Delta coronavirus variant: scientists brace for impact. Nature NEWS. https://www.nature.com/articles/d41586-021-01696-3. (Accessed 2 September 2021).

Campbell, F., Archer, B., 2021. Increased transmissibility and global spread of SARS-CoV-2 variants of concern as at June 2021. Eur. Surveill. 26, 2100509. https://doi.org/10.2807/1560-7917.ES.2021.26.24.2100509.

CBS, 2011. Population monograph of Nepal (Volume I). Central Bureau of Statistics (Nepal), Kathmandu, Nepal.
Chowdhury, R., Heng, K., Shawon, M.S.R., Goh, G., Okonofua, D., Ochoa-Rosales, C., Gonzalez-Jaramillo, V., Bhuiya, A., Reidpath, D., Prathapan, S.J.E. j o e, 2020. Dynamic interventions to control COVID-19 pandemic: a multivariate prediction modelling study comparing 16 worldwide countries. Eur. J. Epidemiol. 35, 389–399. https://doi.org/10.1007/s10654-020-00649-w.
Coburn, B.J., Wagner, B.G., Blower, S., 2009. Modeling influenza epidemics and pandemics: insights into the future of swine flu (H1N1). BMC Med. 7, 1–8. https://doi.org/10.1186/1741-7015-7-30.
Dahal, S., Luo, R., Subedi, R.K., Dhimal, M., Chowell, G., 2021. Transmission dynamics and short-term forecasts of COVID-19: Nepal 2020/2021. Epidemiologia 2, 639–659. https://doi.org/10.3390/epidemiologia2040043.
Funk, T., Pharris, A., Spiteri, G., Bundle, N., Melidou, A., Carr, M., Gonzalez, G., Garcia-Leon, A., Crispie, F., O'Connor, L., Murphy, N., Mossong, J., Vergison, A., Wienecke-Baldacchino, A.K., Abdelrahman, T., Riccardo, F., Stefanelli, P., Di Martino, A., Bella, A., Lo Presti, A., Casaca, P., Moreno, J., Borges, V., Isidro, J., Ferreira, R., Gomes, J.P., Dotsenko, L., Suija, H., Epstein, J., Sadikova, O., Sepp, H., Ikonen, N., Savolainen-Kopra, C., Blomqvist, S., Möttönen, T., Helve, O., Gomes-Dias, J., Adlhoch, C., 2021. Characteristics of SARS-CoV-2 variants of concern B.1.1.7, B.1.351 or P.1: data from seven EU/EEA countries, weeks 38/2020 to 10/2021. Eur. Surveill. 26, 2100348. https://doi.org/10.2807/1560-7917.ES.2021.26.16.2100348.
2021 WHO. 2021, Weekly epidemiological update on COVID-19-1 June 2021. https://www.who.int/publications/m/item/weekly-epidemiological-update-on-covid-19—1-june-2021. (Accessed 1 July 2021).
EPH., 2021. SARS-CoV-2 variants of concern and variants under investigation in England. technical briefing 20, pp. september 2. England Public Health. https://assets.publishing.service.gov.uk/government/uploads/system/uploads/attachment_data/file/1009243/Technical_Briefing_20.pdf.
GISAID, 2022. Tracking of hCov19 variant. https://gisaid.org/hcov19-variants/. (Accessed 22 March 2022).
Goscé, L., Phillips, A., Spinola, P., Gupta, R.K., Abubakar, Ibrahim, 2020. Modelling SARS-COV2 spread in London: approaches to lift the lockdown. J. Infect. 81, 260–265. https://doi.org/10.1016/j.jinf.2020.05.037.
Gupta, N., Kaur, H., Yadav, P., Mukhopadhyay, L., Sahay, R.R., Kumar, A., Nyayanit, D. A., Shete, A.M., Patil, S., Majumdar, T., Rana, S., Gupta, S., Narayan, J., Vijay, N., Barde, P., Natrajan, G., Kumari, B.A., Kumari, M.P., Biswas, D., Iravane, J., Raut, S., Dutta, S., Devi, S., Barua, P., Gupta, P., Borkakoty, B., Kalita, D., Dhingra, K., Fomda, B., Joshi, Y., Goyal, K., John, R., Ashok, Dhodapkar, R., Pandit, P., Devi, S., Dudhmal, M., Kinariwala, D., Khandelwal, N., Tiwari, Y.K., Khatri, P.K., Gupta, A., Khatri, H., Malhotra, B., Nagasundaram, M., Dar, L., Sheikh, N., Aggarwal, N., Abraham, P., 2021. Clinical characterization and Genomic analysis of COVID-19 breakthrough infections during second wave in different states of India. Viruses. 2021 Sep; 13(9): 1782. doi: 10.3390/v13091782.
Hachtel, G.D., Stack, J.D., Hachtel, J.A., 2022. Forecasting and modeling of the COVID-19 pandemic in the USA with a timed intervention model. Sci. Rep. 12, 1–14. https://doi.org/10.1038/s41598-022-07487-8.
Hafeez, S., Din, M., Zia, F., Ali, M., Shinwari, Z.K., 2021. Emerging concerns regarding COVID-19; second wave and new variant. J. Med. Virol. 93, 4108–4110. https://doi.org/10.1002/jmv.26979.
IHME, 2021. COVID-19 Projections. https://covid19.healthdata.org/nepal?view=cumulative-deaths&tab=trend.(Accessed 2 Auguest 2022).
Ito, K., Piantham, C., Nishiura, H., 2021. Predicted domination of variant Delta of SARS-CoV-2 before Tokyo Olympic games, Japan. Euro Surveill 2021;26(27) doi:10.2807/1560-7917.ES.2021.26.27.2100570.
Jassat, W., Mudara, C., Ozougwu, L., Tempia, S., Blumberg, L., Davies, M.-A., Pillay, Y., Carter, T., Morewane, R., Wolmarans, M., von Gottberg, A., Bhiman, J.N., Walaza, S., Group, D.A.T.C.O.V.A., Cohen, C., 2021. Difference in mortality among individuals admitted to hospital with COVID-19 during the first and second waves in South Africa: a cohort study. The Lancet Global Health, 9 (9), e1216 - e1225. doi:10.1016/S2214-109X(21)00289-8.
Kuwar, L.S., 2015. Emigration of Nepalese people and its impact. Econ. J. Dev. (Issue 19), 77–82.
Li, B., Deng, A., Li, K., Hu, Y., Li, Z., Xiong, Q., Liu, Z., Guo, Q., Zou, L., Zhang, H., Zhang, M., Ouyang, F., Su, J., Su, W., Xu, J., Lin, H., Sun, J., Peng, J., Jiang, H., Zhou, P., Hu, T., Luo, M., Zhang, Y., Zheng, H., Xiao, J., Liu, T., Che, R., Zeng, H., Zheng, Z., Huang, Y., Yu, J., Yi, L., Wu, J., Chen, J., Zhong, H., Deng, X., Kang, M., Pybus, O.G., Hall, M., Lythgoe, K.A., Li, Y., Yuan, J., He, J., Lu, J., 2021. Viral infection and transmission in a large, well-traced outbreak caused by the SARS-CoV-2 Delta variant. *Nat Commun* **13**, 460 (2022). doi: 10.1038/s41467-022-28089-y.
Li, Q., Guan, X., Wu, P., Wang, X., Zhou, L., Tong, Y., Ren, R., Leung, K.S.M., Lau, E.H.Y., Wong, J.Y., Xing, X., Xiang, N., Wu, Y., Li, C., Chen, Q., Li, D., Liu, T., Zhao, J., Liu, M., Tu, W., Chen, C., Jin, L., Yang, R., Wang, Q., Zhou, S., Wang, R., Liu, H., Luo, Y., Liu, Y., Shao, G., Li, H., Tao, Z., Yang, Y., Deng, Z., Liu, B., Ma, Z., Zhang, Y., Shi, G., Lam, T.T.Y., Wu, J.T., Gao, G.F., Cowling, B.J., Yang, B., Leung, G.M., Feng, Z., 2020. Early transmission dynamics in Wuhan, China, of novel coronavirus–infected pneumonia. N. Engl. J. Med. 382, 1199–1207. https://doi.org/10.1056/NEJMoa2001316.
Linton, N.M., Kobayashi, T., Yang, Y., Hayashi, K., Akhmetzhanov, A.R., Jung, S. M, Yuan, B., Kinoshita, R., Nishiura, H., 2020. Incubation period and other epidemiological characteristics of 2019 novel coronavirus infections with right truncation: a statistical analysis of publicly available case data. J. Clin. Med. 9, 538. https://doi.org/10.3390/jcm9020538.
MoHP, 2020a. Nepal National Sero-Prevalence Survey for COVID-19 October 2020. Government of Nepal, Ministry of Health and Population. Kathmandu, Nepal.
MoHP, 2020b. Health Sector Emergency Response Plan, COVID-19 pandemic. Health Sector Emergency Response Plan, COVID-19 pandemic. Kathmandu, Nepal.
Nebehay, S., Farge, E., 2021. WHO classifies India variant as being of global concern. REUTERS. https://www.reuters.com/business/healthcare-pharmaceuticals/who-designates-india-variant-being-global-concern-2021-05-10/. (Accessed 10 July 2021).
Pantha, B., Giri, S., Joshi, H.R., Vaidya, N.K., 2021a. Modeling transmission dynamics of rabies in Nepal. Infect. Dis. Model 6, 284–301. https://doi.org/10.1016/j.idm.2020.12.009.
MoHP, 2021. COVID19-Dashboard. https://covid19.mohp.gov.np/.
Pantha, B., Acharya, S., Joshi, H.R., Vaidya, N.K., 2021b. Inter-provincial disparity of COVID-19 transmission and control in Nepal. Sci. Rep. 11, 1–16.
Poudel, A., 2021. Highly contagious double mutant Indian variant responsible for current surge of Covid-19 cases. KATHMANDU POST. https://kathmandupost.com/health/2021/05/18/highly-contagious-double-mutant-indian-variant-responsible-for-current-surge-of-covid-19-cases. (Accessed 20 June 2021).
Prasain, S., 2021. Nepal's lockdown 2.0, new Covid curbs on travel. https://kathmandupost.com/money/2021/04/28/explained-nepal-s-lockdown-2-0-new-covid-curbs-on-travel. (Accessed 1 september 2021).
Putra, M., Kesavan, M., Brackney, K., Hackney, D.N., Roosa, K.M., 2020. Forecasting the impact of coronavirus disease during delivery hospitalization: an aid for resource utilization. Am. J. Obstetrics Gynecol. MFM 2, 100127.
Reis, R.F., de Melo Quintela, B., de Oliveira Campos, J., Gomes, J.M., Rocha, B.M., Lobosco, M., dos Santos, R.W., 2020. Characterization of the COVID-19 pandemic and the impact of uncertainties, mitigation strategies, and underreporting of cases in South Korea, Italy, and Brazil. Chaos Solitons Fractals 136, 109888.
ReliefWeb, 2021. Second wave of Covid-19 causes alarm - Nepal. https://reliefweb.int/report/nepal/second-wave-covid-19-causes-alarm?gclid=Cj0KCQjw5oiMBhDtARIsAJi0qk1Tlz_52IRdDhPJHhTqHNPwjA8w3uj9x6fXUMlUzyFBCOEy6EpDWx4aAkIvEALw_wcB. (Accessed 2 september 2021).
Saito, S., Asai, Y., Matsunaga, N., Hayakawa, K., Terada, M., Ohtsu, H., Tsuzuki, S., Ohmagari, N., 2021. First and second COVID-19 waves in Japan: a comparison of disease severity and characteristics. J. Infect. 82, 84–123. https://doi.org/10.1016/j.jinf.2020.10.033.
Shankar, S., Mohakuda, S.S., Kumar, A., Nazneen, P., Yadav, A.K., Chatterjee, K., Chatterjee, K.J.M. j a f I., 2021. Systematic review of predictive mathematical models of COVID-19 epidemic. Med. J. Armed Forces India 77, S385–S392.
Sheikh, A., McMenamin, J., Taylor, B., Robertson, C., 2021. SARS-CoV-2 Delta VOC in Scotland: demographics, risk of hospital admission, and vaccine effectiveness. Lancet 397 (10293). https://doi.org/10.1016/S0140-6736(21)01358-1.
The Himalayan, 2021. COVID cases going up as restrictions eased in Jhapa. The Himalayan Times. https://thehimalayantimes.com/nepal/covid-cases-going-up-as-restrictions-eased-in-jhapa. (Accessed 10 september 2021).
Thompson, R.N., Stockwin, J.E., van Gaalen, R.D., Polonsky, J.A., Kamvar, Z.N., Demarsh, P.A., Dahlqwist, E., Li, S., Miguel, E., Jombart, T., Lessler, J., Cauchemez, S., Cori, A., 2019. Improved inference of time-varying reproduction numbers during infectious disease outbreaks. Epidemics 29, 100356.
Tuite, A.R., Fisman, D.N., Greer, A.L., 2020. Mathematical modelling of COVID-19 transmission and mitigation strategies in the population of Ontario, Canada. Cmaj 192, E497–E505. https://doi.org/10.1503/cmaj.200476.
Twohig, K.A., Nyberg, T., Zaidi, A., Thelwall, S., Sinnathamby, M.A., Aliabadi, S., Seaman, S.R., Harris, R.J., Hope, R., Lopez-Bernal, J., et al., 2022. Hospital admission and emergency care attendance risk for SARS-CoV-2 delta (B. 1.617. 2) compared with alpha (B. 1.1. 7) variants of concern: a cohort study. Lancet Infect. Dis. 22 (1), 35–42.
Verity, R., Okell, L.C., Dorigatti, I., Winskill, P., Whittaker, C., Imai, N., Cuomo-Dannenburg, G., Thompson, H., Walker, P.G.T., Fu, H., Dighe, A., Griffin, J.T., Baguelin, M., Bhatia, S., Boonyasiri, A., Cori, A., Cucunubá, Z., FitzJohn, R., Gaythorpe, K., Green, W., Hamlet, A., Hinsley, W., Laydon, D., Nedjati-Gilani, G., Riley, S., van Elsland, S., Volz, E., Wang, H., Wang, Y., Xi, X., Donnelly, C.A., Ghani, A.C., Ferguson, N.M., 2020. Estimates of the severity of coronavirus disease 2019: a model-based analysis. Lancet Infect. Dis. 20, 669–677. https://doi.org/10.1016/S1473-3099(20)30243-7.
Weissenbach, B., 2021. NATIONAL GEOGRAPHIC. https://www.nationalgeographic.com/culture/article/a-pandemic-surge-threatens-livelihoods-in-nepal. (Accessed 10 September 2021).
WHO, 2021a. Criteria for releasing COVID-19 patients from isolation, vol. 2021.
WHO, 2021b. Weekly epidemiological update on COVID-19 - 29 June 2021, vol. 2021.
Worldometer, 2022. COVID-19 CORONAVIRUS PANDEMIC. https://www.worldometers.info/coronavirus/.
You, C., Deng, Y., Hu, W., Sun, J., Lin, Q., Zhou, F., Pang, C.H., Zhang, Y., Chen, Z., Zhou, X.-H., 2020. Estimation of the time-varying reproduction number of COVID-19 outbreak in China. Int. J. Hyg. Environ. Health 228, 113555.

Supplementary Materials

Insight into Delta Variant Dominated Second Wave of COVID-19 in Nepal

Khagendra Adhikari[a], Ramesh Gautam[b], Anjana Pokharel[c], Meghnath Dhimal[d,1], Kedar Nath Uprety[f], Naveen K. Vaidya[g,h,i,*]

[a] *Amrit Campus, Tribhuvan University, Kathmandu, Nepal*
[b] *Ratna Rajya Laxmi Campus, Tribhuvan University, Kathmandu, Nepal*
[c] *Padma Kanya Multiple Campus, Tribhuvan University, Kathmandu, Nepal*
[d] *Nepal Health Research Council, Kathmandu, Nepal*
[e] *Global Institute for Interdisciplinary Studies, Lalitpur, Nepal*
[f] *Central Department of Mathematics, Tribhuvan University, Kathmandu, Nepal*
[g] *Department of Mathematics and Statistics, San Diego State University, San Diego, CA, USA*
[h] *Computational Science Research Center, San Diego State University, San Diego, CA, USA*
[i] *Viral Information Institute, San Diego State University, San Diego, CA, USA*

---

1. Transmission dynamics model

To develop a transmission dynamics model based on the $SEIR$ framework, the total population is divided into high- and low-risk regions. The high-risk region consists of 22 districts, which have an open border with India and/or have highly populous cities, such as Kathmandu, Kaski, Chitawan, and Surkhet. The remaining districts belong to the low-risk region. The map of Nepal showing the high and low risk region is shown in the figure 1.

*Corresponding author
Email address: nvaidya@sdsu.edu (Naveen K. Vaidya)

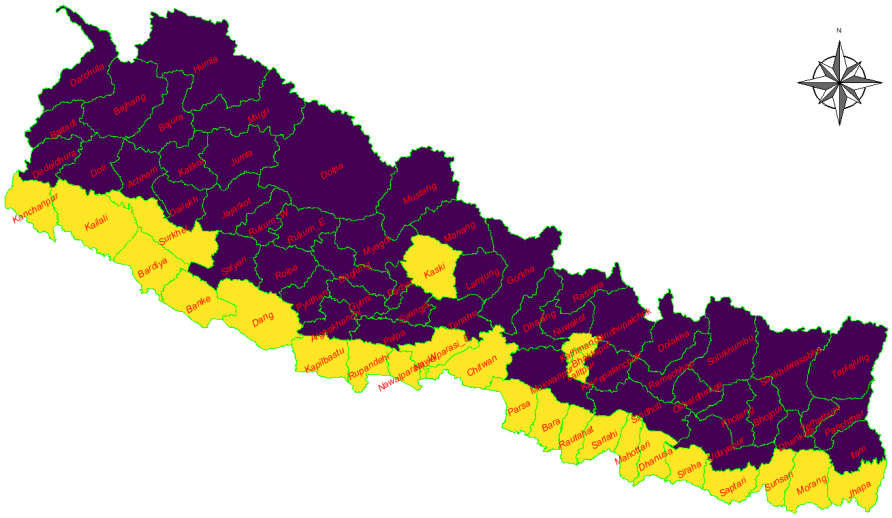

Figure 1: **A map of Nepal**. To create the map, the data (shapefile format) was obtained from the official webpage (`http://dos.gov.np`) of the government of Nepal (Accessed on April 23, 2021). The map was then created using cartography package in R 4.3.1. The yellow region constitute the districts of high risk region and that of deep blue is low risk region.

The population of each region is divided into sixteen distinct compartments: S_H, S_L (susceptible), E_H, E_L (exposed), I_{RH}, I_{RL} (recorded infectious), I_{RH}, I_{NL} (non-recorded infectious), M_H, M_L (Medical care), I_{cH}, I_{cL} (ICU), V_H, V_L (Ventilator) and R_H, R_L (recovered), where the suffixes H and L are used to indicate the high- and low-risk regions, respectively. Λ_H and Λ_L represent the birth rate in the high and the low-risk regions, respectively.

The immigrants from abroad enter only the high-risk region at the rate of $\lambda(t)$. Among the immigrants $\lambda(t)$, a portion ϕ is tested by the antigen, and the rest $(1-\phi)$ entered to the community without the antigen test. The portion ρ of the immigrants with a positive test result entered the recorded infected class (I_{RH}) of the high-risk region and the remaining immigrants (negative test result) entered the susceptible class. The immigrants without antigen test entered to the susceptible and non-recorded infectious (I_{NH}) with the same portion as that of tested immigrants. Since the low-risk region does not have a border

with India, there is no recruitment from immigration in low-risk regions.

$\gamma(t)$ represents the mobility rate between two regions with corresponding classes (susceptible, exposed, non-recorded infectious, and recovered). The transmission rate from recorded infected individuals of both regions, non-recorded infectious individuals in the high-risk region, and non-recorded infectious individuals in low-risk region are denoted by β_1, $\beta_2(t)$, and $\beta_3(t)$, respectively. The exposed individuals become infectious at the rate of δ, among which a portion θ are recorded and the remaining $(1-\theta)$ remain non-recorded in both regions.

Among the recorded infectious, a portion ω of infected entered the medical care class, and the remaining $(1-\omega)$ enter the class without medical care in both regions. From the medical care class, the severe patients enter an extreme medical care class at the rate ν, among whom a portion ψ require the ventilators and the remaining $(1-\psi)$ portion are admitted to ICU. The rate of recovery from the recorded class without medical care and non-recorded infectious class is denoted by η and those from medical care, ICU, and ventilator are denoted by $\alpha_m,\ \alpha_c,$ and α_v, respectively. The natural death rate is denoted by μ and the disease-induced death rate for recorded and non-recorded infectious are k and k', respectively. The disease-induced death rate for medical, ICU, and ventilator are $k_1,\ k_2$, and k_3, respectively. The schematic diagram of the model is shown in Figure 2.

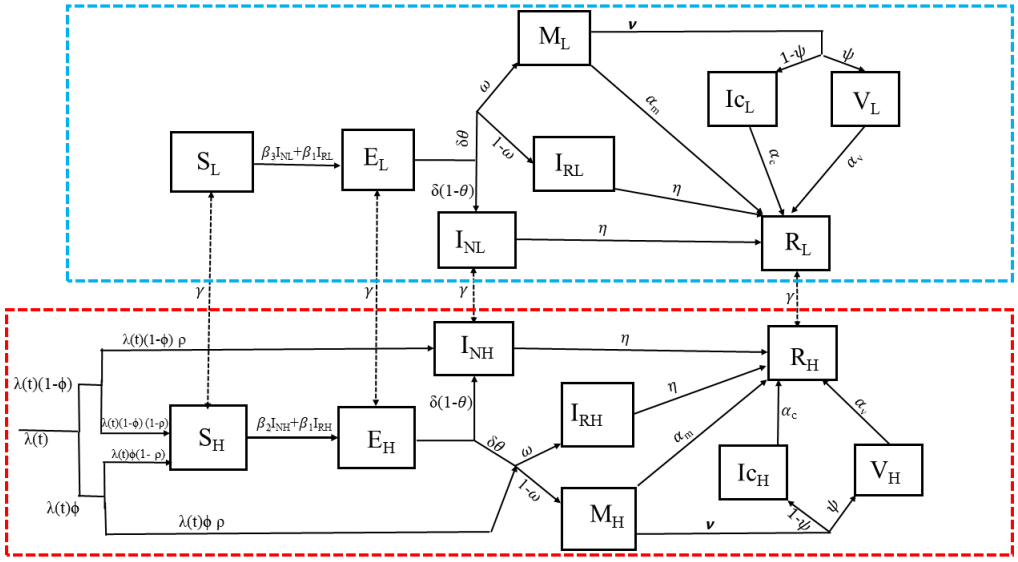

Figure 2: **The compartmental diagram of the model**. The compartments within the red box and the blue box belong to the high- and the low-risk regions, respectively. The arrow represents the transfer from one compartment to another. For clarity, the natural and disease-induced death rates are not shown in the diagram.

The dynamical system consisting of ODEs of the model is as follows:

$$\frac{dS_H}{dt} = \Lambda_H + \gamma S_L - \frac{(\beta_2 I_{\mathrm{NH}} + \beta_1 I_{\mathrm{RH}})\, S_H}{N_H} - (\gamma+\mu)S_H + \lambda(1-\rho)(1-\phi) + \lambda(1-\rho)\phi \tag{1}$$

$$\frac{dS_L}{dt} = \Lambda_L + \gamma S_H - \frac{(\beta_3 I_{NL} + \beta_1 I_{\mathrm{RL}})\, S_L}{N_L} - (\gamma+\mu)S_L \tag{2}$$

$$\frac{dE_H}{dt} = \frac{(\beta_2 I_{\mathrm{NH}} + \beta_1 I_{\mathrm{RH}})\, S_H}{N_H} + \gamma E_L - (\gamma+\delta+\mu)E_H \tag{3}$$

$$\frac{dE_L}{dt} = \frac{(\beta_3 I_{NL} + \beta_1 I_{RL})\, S_L}{N_L} + \gamma E_H - (\gamma+\delta+\mu)E_L \tag{4}$$

$$\frac{dI_{NH}}{dt} = \delta(1-\theta)E_H + \gamma I_{NL} - (\eta+k'+\mu)I_{NH} + \lambda\rho(1-\phi) - \gamma I_{NH} \tag{5}$$

$$\frac{dI_{NL}}{dt} = \delta(1-\theta)E_L + \gamma I_{NH} - (\eta+k'+\mu)I_{NL} - \gamma I_{NL} \tag{6}$$

$$\frac{dI_{RH}}{dt} = \delta\theta(1-\omega)E_H + \lambda\rho\phi(1-\omega) - (\eta+k+\mu)I_{\mathrm{RH}} \tag{7}$$

$$\frac{dI_{RL}}{dt} = \delta\theta(1-\omega)E_L - (\eta+k+\mu)I_{RL} \tag{8}$$

$$\frac{dM_H}{dt} = \delta\theta E_H\omega + \lambda\rho\omega\phi - (k_1+\mu+\alpha_m+\nu)\, M_H \tag{9}$$

$$\frac{dM_L}{dt} = \delta\theta\omega E_L - (\alpha_m+k_1+\mu+\nu)\, M_L \tag{10}$$

$$\frac{dI_{cH}}{dt} = \nu(1-\psi)M_H - (\alpha_c+k_2+\mu)\, I_{cH} \tag{11}$$

$$\frac{dI_{cL}}{dt} = \nu(1-\psi)M_L - (\alpha_c+k_2+\mu)\, I_{cL} \tag{12}$$

$$\frac{dV_H}{dt} = \nu\psi M_H - (\alpha_c+k_3+\mu)\, V_H \tag{13}$$

$$\frac{dV_L}{dt} = \nu\psi M_L - (\alpha_c+k_3+\mu)\, V_L \tag{14}$$

$$\frac{dR_H}{dt} = \alpha_c I_{cH} + \alpha_m M_H + \eta(I_{RH}+I_{NH}) + \alpha_v V_H + \gamma R_L - (\mu+\gamma)R_H \tag{15}$$

$$\frac{dR_L}{dt} = \alpha_c I_{cL} + \gamma R_H + \alpha_m M_L + \eta(I_{NL}+I_{RL}) + \alpha_v V_L - (\gamma+\mu)R_L. \tag{16}$$

Here, $N_H = S_H + E_H + I_{RH} + I_{NH} + M_H + I_{cH} + V_H + R_H$ and $N_L = S_L + E_L + I_{RL} + I_{NL} + M_L + I_{cL} + V_L + R_L$.

2. Modeling vaccination program

We extended our model to incorporate the vaccination program by further dividing each compartment into vaccinated and non-vaccinated compartments

except the recorded infectious compartments and medical compartments. For our study period, we assumed that there is no loss of immunity of vaccinated and recovered people. In the vaccinated compartments, there is a reduced infection rates and a reduced rates of hospitalization and medical care. The schematic compartmental diagram of the model with vaccination program is shown in Figure 3.

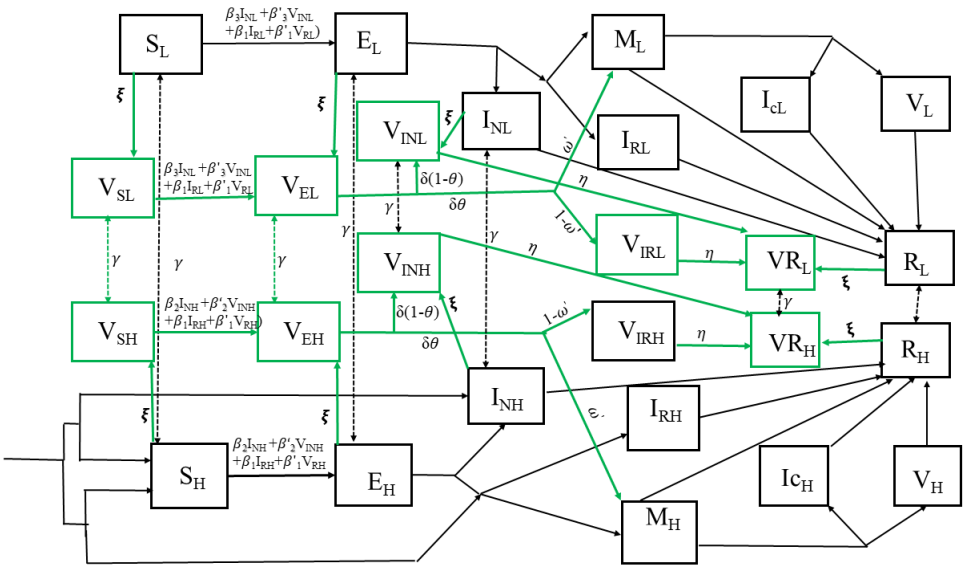

Figure 3: **The compartmental diagram of the model with vaccination**. The green boxes represent the vaccinated compartments. All other rates of transfer between compartments are the same as in Figure 2 except transmission rates and hospitalization rates ($\beta_i', i = 1, 2, 3$, and ω').

3. Computation of reproduction number

3.1. Next generation method

3.1.1. Reproduction number of the whole country

First we calculate the diseases free equilibrium point. At the disease free equilibrium point the portion of positive antigen test is zero, i.e $\rho = 0$, and we use the pre-pandamic condition $\lambda = \lambda(0)$ and $E_H = E_L = I_{RH} = I_{RL} = I_{NH} =$

$I_{NL} = M_H = M_L = I_{cH} = I_{cL} = V_H = V_L = 0$. We get the following disease free equilibrium point: $E^* = (S_H^*, S_L^*, 0, 0, 0, 0, 0, 0, 0, 0, 0, 0, 0, 0, 0, 0)$, where

$$S_H^* = \frac{\lambda(0)(\gamma+\mu) + (\gamma+\mu)\Lambda_H + \gamma\Lambda_L}{\mu(2\gamma+\mu)},\ S_L^* = \frac{\gamma\lambda(0) + \gamma\Lambda_H + (\gamma+\mu)\Lambda_L}{\mu(2\gamma+\mu)}.$$

We now divide the compartments into two groups: infected $\vec{x} = (x_i, i = 1, 2, ..., 12) = (E_H, E_L,$
$I_{RH}, I_{RL}, I_{NH}, I_{NL}, M_H, M_L, I_{cH}, I_{cL}, V_H, V_L)$ and non-infected $\vec{y} = (y_j, j = 1, 2, 3, 4) = (S_H, S_L, R_H, R_L)$. Then the system (1-16) can be written as:

$$x_i' = f_i(\vec{x}, \vec{y}) \text{ and } y_j' = g_j(\vec{x}, \vec{y}) \text{ for } i = 1, 2, ..., 12, j = 1, 2, 3, 4.$$

The right hand side of the system of infected compartments can be written as: $f_i(\vec{x}, \vec{y}) = F_i(\vec{x}, \vec{y}) - V_i(\vec{x}, \vec{y})$, where $F_i(\vec{x}, \vec{y})$ contains the terms representing the new infections in compartment i and $V_i(\vec{x}, \vec{y})$ contains the terms containing the difference between the transfer of individuals out of and into the compartment i. Then we construct the following two matrices using $F = \left(\frac{\partial F_i}{\partial x_i}\right)$ and $V = \left(\frac{\partial V_i}{\partial x_i}\right)$ at the diseases free equilibrium (DFE) point as follows:

$$F = \begin{pmatrix} A_{6\times6} & 0_{6\times6} \\ 0_{6\times6} & 0_{6\times6} \end{pmatrix},\ V = \begin{pmatrix} B_{8\times6} & 0_{6\times6} \\ 0_{4\times6} & C_{6\times6} \end{pmatrix},$$

where

$$A = \begin{pmatrix} 0 & 0 & \frac{\beta_1 S_H^*}{N_L^*} & 0 & \frac{\beta_H S_H^*}{N_H^*} & 0 \\ 0 & 0 & 0 & \frac{\beta_1 S_L^*}{N_L} & 0 & \frac{\beta_L S_L^*}{N_L^*} \\ 0 & 0 & 0 & 0 & 0 & 0 \\ 0 & 0 & 0 & 0 & 0 & 0 \\ 0 & 0 & 0 & 0 & 0 & 0 \\ 0 & 0 & 0 & 0 & 0 & 0 \end{pmatrix},$$

$$B = \begin{pmatrix} \gamma+\delta+\mu & -\gamma & 0 & 0 & 0 & 0 \\ -\gamma & \gamma+\delta+\mu & 0 & 0 & 0 & 0 \\ -\delta\theta(1-\omega) & 0 & k+\eta+\mu & 0 & 0 & 0 \\ 0 & -\delta\theta(1-\omega) & 0 & k+\eta+\mu & 0 & 0 \\ -\delta(1-\theta) & 0 & 0 & 0 & \gamma+\eta+\mu+k' & -\gamma \\ 0 & -\delta(1-\theta) & 0 & 0 & -\gamma & \gamma+\eta+\mu+k' \\ -\delta\theta\omega & 0 & 0 & 0 & 0 & 0 \\ 0 & -\delta\theta\omega & 0 & 0 & 0 & 0 \end{pmatrix},$$

and

$$C = \begin{pmatrix} p & 0 & 0 & 0 & 0 & 0 \\ 0 & p & 0 & 0 & 0 & 0 \\ -\nu(1-\psi) & 0 & q & 0 & 0 & 0 \\ 0 & -\nu(1-\psi) & 0 & q & 0 & 0 \\ -\nu\psi & 0 & 0 & 0 & r & 0 \\ 0 & -\nu\psi & 0 & 0 & 0 & r \end{pmatrix}.$$

Here $p = k_1 + \mu + \alpha_m$, $\quad q = \alpha_c + k_2 + \mu$, and $r = k_3 + \mu + \alpha_v$.

The largest eigenvalue of the matrix FV^{-1} gives the basic reproduction number as follows:

$$R_0 = \frac{1}{2}\left(D + \sqrt{D^2 - 4E}\right), \tag{17}$$

where

$$D = \frac{\beta_1 T_1 S_H^* N_L^* + \beta_1 T_1 S_L^* N_H^* + \beta_2 T_3 S_H^* N_L^* + \beta_3 T_3 S_L^* N_H^*}{N_H^* N_L^*},$$

$$E = \frac{S_H^* S_L^* \left(\beta_1^2 T_1^2 - \beta_1^2 T_2^2 + (\beta_2+\beta_3)\,\beta_1 T_1 T_3 - (\beta_2+\beta_3)\,\beta_1 T_2 T_4 + \beta_2\beta_3\left(T_3^2 - T_4^2\right)\right)}{N_H^* N_L^*},$$

$$T_1 = \frac{\delta\theta(1-\omega)(\gamma+\delta+\mu)}{(\delta+\mu)(2\gamma+\delta+\mu)(\eta+k+\mu)}, \qquad T_2 = \frac{\gamma\delta\theta(1-\omega)}{(\delta+\mu)(2\gamma+\delta+\mu)(\eta+k+\mu)},$$

$$T_3 = \frac{\gamma\delta(1-\theta)\,(2\gamma+\delta+\eta+k'+2\mu)}{(\delta+\mu)N_L(2\gamma+\delta+\mu)\,(\eta+k'+\mu)\,(2\gamma+\eta+k'+\mu)},$$

and $\quad T_4 = \dfrac{\delta(1-\theta)\left(\delta\eta+\delta\mu+\eta\mu+\gamma\,(2\gamma+\delta+\eta+k'+2\mu)+\delta k'+\mu k'+\mu^2\right)}{(\delta+\mu)(2\gamma+\delta+\mu)\,(\eta+k'+\mu)\,(2\gamma+\eta+k'+\mu)}.$

At the Diseases Free Eqilibrium (DFE) point, $S_H^* = N_H^*$, and $S_L^* = N_L^*$, then the basic reproduction number is obtained as:

$$R_0 = \frac{1}{2}\left(2\beta_1 T_1 + \beta_2 T_3 + \beta_3 T_3 + \sqrt{4\beta_2\beta_3 T_4^2 + 4\beta_1\beta_3 T_2 T_4 + 4\beta_1^2 T_2^2 + (\beta_2 - \beta_3)^2 T_3^2 + 4\beta_1\beta_2 T_2 T_3}\right). \tag{18}$$

The corresponding effective reproduction number is obtained by making the respective state variables of 17 as function of t.

3.1.2. Reproduction number of the high-risk region

Similar to the section 3.1.1, we construct the following two matrices for high risk region at DFE point as follows:

$$F_H = \begin{pmatrix} 0 & \frac{\beta_1 S_H^*}{N_H^*} & \frac{\beta_2 S_H^*}{N_H^*} & 0 & 0 & 0 \\ 0 & 0 & 0 & 0 & 0 & 0 \\ 0 & 0 & 0 & 0 & 0 & 0 \\ 0 & 0 & 0 & 0 & 0 & 0 \\ 0 & 0 & 0 & 0 & 0 & 0 \\ 0 & 0 & 0 & 0 & 0 & 0 \end{pmatrix}$$

$$V_H = \begin{pmatrix} \gamma+\delta+\mu & 0 & 0 & 0 & 0 & 0 \\ -\delta\theta(1-\omega) & k+\eta+\mu & 0 & 0 & 0 & 0 \\ -\delta(1-\theta) & 0 & k'+\gamma+\eta+\mu & 0 & 0 & 0 \\ -\delta\theta\omega & 0 & 0 & \mu+\nu+k_1+\alpha_m & 0 & 0 \\ 0 & 0 & 0 & -\nu(1-\psi) & \mu+k_2+\alpha_c & 0 \\ 0 & 0 & 0 & -\nu\psi & 0 & \mu+k_3+\alpha_v \end{pmatrix}.$$

The dominated Eigenvalue of $F_H V_H^{-1}$ gives the basic reproduction number of the high-risk region as follows.

$$R_{H0} = \frac{S_H^*\delta\left(\beta_2(1-\theta)(\eta+k+\mu) + \theta\beta_1(1-\omega)(\gamma+\eta+k'+\mu)\right)}{N_H^*(\gamma+\delta+\mu)(\eta+k+\mu)(\gamma+\eta+k'+\mu)}. \tag{19}$$

. Using $N_H^* = S_H^*$ for DFE point, we obtain

$$R_{H0} = \frac{\delta\left(\beta_2(1-\theta)(\eta+k+\mu) + \theta\beta_1(1-\omega)(\gamma+\eta+k'+\mu)\right)}{(\gamma+\delta+\mu)(\eta+k+\mu)(\gamma+\eta+k'+\mu)}. \tag{20}$$

The corresponding effective reproduction number is obtained by making the respective state variables of 19 as function of t.

3.1.3. Reproduction number of the low-risk region

Similar to the section 3.1.1, we construct the following two matrices for low risk region at DFE point as follows:

$$F_L = \begin{pmatrix} 0 & \frac{\beta_1 S_L^*}{N_L^*} & \frac{\beta_3 S_L^*}{N_L^*} & 0 & 0 & 0 \\ 0 & 0 & 0 & 0 & 0 & 0 \\ 0 & 0 & 0 & 0 & 0 & 0 \\ 0 & 0 & 0 & 0 & 0 & 0 \\ 0 & 0 & 0 & 0 & 0 & 0 \\ 0 & 0 & 0 & 0 & 0 & 0 \end{pmatrix}$$

and

$$V_L = \begin{pmatrix} \gamma+\delta+\mu & 0 & 0 & 0 & 0 & 0 \\ -\delta\theta(1-\omega) & k+\eta+\mu & 0 & 0 & 0 & 0 \\ -\delta(1-\theta) & 0 & k'+\gamma+\eta+\mu & 0 & 0 & 0 \\ -\delta\theta\omega & 0 & 0 & \mu+\nu+k_1+\alpha_m & 0 & 0 \\ 0 & 0 & 0 & -\nu(1-\psi) & \mu+k_2+\alpha_c & 0 \\ 0 & 0 & 0 & -\nu\psi & 0 & \mu+k_3+\alpha_v \end{pmatrix}.$$

The dominated eigenvalue of $F_H V_H^{-1}$ gives the basic reproduction number as follows.

$$R_{L0} = \frac{S_L^* \delta \left(\beta_1 \theta(1-\omega)(\gamma+\eta+k'+\mu) + \beta_3(1-\theta)(\eta+k+\mu)\right)}{N_L^*(\gamma+\delta+\mu)(\eta+k+\mu)(\gamma+\eta+k'+\mu)}. \tag{21}$$

Using $N_L^* = S_L^*$ for DFE point, we obtain

$$R_{L0} = \frac{\delta \left(\beta_1 \theta(1-\omega)(\gamma+\eta+k'+\mu) + \beta_3(1-\theta)(\eta+k+\mu)\right)}{(\gamma+\delta+\mu)(\eta+k+\mu)(\gamma+\eta+k'+\mu)}. \tag{22}$$

The corresponding effective reproduction number is obtained by making the respective state variables of 22 as function of t.

3.1.4. Maximum likelihood method on data

There are number of methods to estimate the basic reproduction number from the disease incidence data. Among them, the method proposed by White and Pagano [5, 6] known as the maximum likelihood method (MLM), is widely used in many studies.

We also calculate the effective Reproduction number (R_t) from the daily incidence data as a marker for the decrease or surge in infections from the real-time data. Time-varying R_t can be calculated using the time series of the infections and generation time distribution [3]. We use the approach developed by Thompson et al [2] for the estimation of effective reproduction numbers using the EpiEstem package of the R program. We take the mean serial interval as 4.7 days days, with an SD of 2.9 days days based on the previous study [4].

3.2. Parameter estimation and model fitting to data

3.2.1. Data fitting

The model is fitted to the multiple data sets, containing the daily new cases of the whole country, the high-risk and low-risk regions, and patients in medical care, ICU, and ventilators. From our model, the recorded new infections in Nepal, the high-risk region, and the low-risk region, the number of patients in medical care, ICU and ventilator at time t can be computed using the following respective equations:

$$L_r(t) = \delta\theta E_H + \lambda(t)\phi\rho + \delta\theta E_L, \tag{23}$$

$$L_{rh}(t) = \delta\theta E_H + \lambda(t)\phi\rho, \tag{24}$$

$$L_{rl}(t) = \delta\theta E_L, \tag{25}$$

$$L_m(t) = \delta\omega\theta(E_H+E_L)+\lambda(t)\phi\rho\omega-\alpha_m(M_H+M_L)-k_1(M_H+M_L)-\nu(M_H+M_L), \tag{26}$$

$$L_c(t) = \nu(1-\psi)(M_H+M_L) - (k_2+\alpha_c)(M_H+M_L), \tag{27}$$

$$L_v(t) = \nu\psi(M_H+M_L) - (k_3+\alpha_v)(V_H+V_L). \tag{28}$$

We solve the system of differential equations numerically using a fourth-order Runge-Kutta method. We use the solutions to obtain the best-fit parameters via a nonlinear least-squares regression method that minimizes the following sum of the squared residuals:

$$J = \sum_{i=1}^{n} \big[\big(L_r(t_i) - \bar{L_r}(t_i)\big)^2 + \big(L_{rh}(t_i) - \bar{L_{rh}}(t_i)\big)^2 + \big(L_{rl}(t_i) - \bar{L_{rl}}(t_i)\big)^2 + \big(L_m(t_i) - \bar{L_m}(t_i)\big)^2 + \big(L_c(t_i) - \bar{L_c}(t_i)\big)^2 + \big(L_v(t_i) - \bar{L_v}(t_i)\big)^2 \big].$$

Here, $\beta_1, \beta_H, \beta_L, \theta, r_H, r_L, \gamma_1, \gamma_2, \omega, \nu, \psi, \alpha_m, \alpha_c, \alpha_v, \nu, k, k', k_1, k_2$, and k_3 are parameters to be estimated. $L_r(t_k), L_{rh}(t_i), L_{rl}(t_i), L_m(t_i), L_c(t_i), L_v(t_i)$ are model values and $\bar{L_r}(t_i), \bar{L_{rh}}(t_i), \bar{L_{rl}}(t_i), \bar{L_m}(t_i), \bar{L_c}(t_i), \bar{L_v}(t_i)$ are those given in the available data of the respective classes. n represents the total number of data points used for the model fitting.

In our study, all computations were carried out in MATLAB 2020a (The MathWorks, Inc.).

3.2.2. Initial values of the state variables

Description	State variables	Base Value	Reference
Susceptible population in high risk region	$S_H(0)$	12,818,000	Calculated
Susceptible population in low risk region	$S_L(0)$	6,479,000	Calculated
Exposed population in high risk region	$E_H(0)$	100	Assumed
Exposed population in low risk region	$E_L(0)$	80	Assumed
Recorded infectious population in high risk region	$I_{RH}(0)$	200	Assumed
Recorded infectious population in low risk region	$I_{RL}(0)$	100	Assumed
Non-Recorded infectious population in high risk region	$I_{NH}(0)$	1000	Assumed
Non-Recorded infectious population in low risk region	$I_{NL}(0)$	800	Assumed
Patients in medical care in high risk region	$M_H(0)$	0	Assumed
Patients in medical care in low risk region	$M_L(0)$	0	Assumed
Patients in medical care in high risk region	$I_{cH}(0)$	0	Assumed
Patients in medical care in low risk region	$M_{cL}(0)$	0	Assumed
Patients in medical care in high risk region	$V_H(0)$	0	Assumed
Patients in medical care in low risk region	$V_L(0)$	0	Assumed
Recovered population in high risk region	$R_H(0)$	460,8000	Calculated
Recovered population in low risk region	$R_L(0)$	256,8000	Calculated

References

[1] Adhikari K, Gautam R, Pokharel A, Uprety KN, Vaidya NK. Transmission dynamics of COVID-19 in Nepal: Mathematical model uncovering effective controls. Journal of Theoretical Biology. 2021;521:110680.

[2] Thompson RN, Stockwin JE, van Gaalen RD, Polonsky JA, Kamvar ZN, Demarsh PA, et al. Improved inference of time-varying reproduction numbers during infectious disease outbreaks. Epidemics. 2019;29:100356.

[3] Cori, A, Ferguson, NM, Fraser C, Cauchemez, S. A new framework and

software to estimate time-varying reproduction numbers during epidemics. American Journal of Epidemiology. 2013;178:1505-1512.

[4] Nishiura H, Linton NM, Akhmetzhanov AR. Serial interval of novel coronavirus (COVID-19) infections. International journal of infectious diseases. 2020;93: 284–286.

[5] You C, Deng Y, Hu W, Sun J, Lin Q, et al. Estimation of the time-varying reproduction number of COVID-19 outbreak in China. International Journal of Hygiene and Environmental Health.2020;228.

[6] Forsberg WL, Pagano M. A likelihood-based method for real-time estimation of the serial interval and reproductive number of an epidemic. 2008;27:2999-3016.

Journal of Theoretical Biology 574 (2023) 111622

Contents lists available at ScienceDirect

Journal of Theoretical Biology

journal homepage: www.elsevier.com/locate/yjtbi

Data-driven models for the risk of infection and hospitalization during a pandemic: Case study on COVID-19 in Nepal

Khagendra Adhikari [a], Ramesh Gautam [b], Anjana Pokharel [c], Kedar Nath Uprety [d], Naveen K. Vaidya [e,f,g,*]

[a] Amrit Campus, Tribhuvan University, Kathmandu, Nepal
[b] Ratna Rajya Laxmi Campus, Tribhuvan University, Kathmandu, Nepal
[c] Padma Kanya Multiple Campus, Tribhuvan University, Kathmandu, Nepal
[d] Central Department of Mathematics, Tribhuvan University, Kathmandu, Nepal
[e] Department of Mathematics and Statistics, San Diego State University, San Diego, CA, USA
[f] Computational Science Research Center, San Diego State University, San Diego, CA, USA
[g] Viral Information Institute, San Diego State University, San Diego, CA, USA

ABSTRACT

The newly emerging pandemic disease often poses unexpected troubles and hazards to the global health system, particularly in low and middle-income countries like Nepal. In this study, we developed mathematical models to estimate the risk of infection and the risk of hospitalization during a pandemic which are critical for allocating resources and planning health policies. We used our models in Nepal's unique data set to explore national and provincial-level risks of infection and risk of hospitalization during the Delta and Omicron surges. Furthermore, we used our model to identify the effectiveness of non-pharmaceutical interventions (NPIs) to mitigate COVID-19 in various groups of people in Nepal. Our analysis shows no significant difference in reproduction numbers in provinces between the Delta and Omicron surge periods, but noticeable inter-provincial disparities in the risk of infection (for example, during Delta (Omicron) surges, the risk of infection of Bagmati province is: ~ 98.94 (89.62); Madhesh province: ~ 12.16 (5.1); Karnali province ~31.16 (3) per hundred thousands). Our estimates show a significantly low level of hospitalization risk during the Omicron surge compared to the Delta surge (hospitalization risk is: ~ 10% in Delta and ~ 2.5% in Omicron). We also found significant inter-provincial disparities in the hospitalization rate (for example, ~ 6% in Madhesh province and ~ 21% in Sudur Paschim) during the Delta surge. Moreover, our results show that closing only schools, colleges, and workplaces reduces the risk of infection by one-third, while a complete lockdown reduces the infections by two-thirds. Our study provides a framework for the computation of the risk of infection and the risk of hospitalization and offers helpful information for controlling the pandemic.

1. Introduction

The COVID-19 pandemic has expanded globally in multiple waves, resulting in considerable clinical expenses due to the emergence of new Corona Virus strains. Despite the global control efforts and the development of vaccines, the disease has triggered a catastrophic impact with more than 692.58 million cases and more than 6.90 million deaths as of 3 August 2023 (Worldometer, 2023). Notably, during the pandemic, a lack of knowledge about the risk of circulating new strains, which may be more contagious and capable of evading the immune response of previously infected or vaccinated individuals, may lead to unusually high cases (Islam et al., 2022). Due to the uncertainty and variability in disease severity across different strains, there are often insufficient resources and preparedness, resulting in overwhelmed hospitalizations and shortages of medical staff, equipment, and beds. Consequently, individuals may postpone seeking medical attention and neglect preventive measures, which can ultimately increase the risk of death, as witnessed in Nepal and India during the Delta variant outbreak (Adhikari et al., 2022; Malik, 2022). The uncertainty on the risk of infection and hospitalization may have a greater impact, especially on developing countries like Nepal, because of the resource limitations. Thus, estimating the real-time risk of infection and hospitalization is crucial for assessing disease transmission and managing medical resources to minimize the burden of pandemics.

Nepal, one of the least developed countries in the world, has been severely impacted by the COVID-19 pandemic (Adhikari et al., 2022; Ben, 2021; Bhandari and Hannah Peterse, 2021). Specifically, the second and third waves with the respective Delta and Omicron variants swept across the country from the beginning of April 2021, resulting in one million cases and 12,019 deaths (MoHP, 2022) until 1 December 2022. During the peak of the second wave of COVID-19 (end of May 2021), Nepal experienced a terrifying shortage of hospital beds, ICU beds, ventilators, and oxygen cylinders, which resulted in a loss of potentially preventable lives (Ben, 2021; Bhandari and Hannah Peterse,

* Corresponding author at: .
E-mail address: nvaidya@sdsu.edu (N.K. Vaidya).

https://doi.org/10.1016/j.jtbi.2023.111622
Received 24 January 2023; Received in revised form 11 August 2023; Accepted 12 September 2023
Available online 19 September 2023

2021). The first case of Omicron in Nepal was detected on 6 December 2021 (Poudel, 2021). On 23 January 2022, the Omicron variant constituted 88% of the new cases (Poudel, 2022) and then quickly swept across the country but with significantly less severe cases than the Delta wave (Worldometer, 2023; MoHP, 2022).

The seven provinces of Nepal have various contact patterns of population because of the diverse geographical areas, distinct lifestyles, cultural practices, economic circumstances, and levels of urbanization in these areas (Pantha et al., 2021), which also pose challenges in testing and reporting COVID-19 cases. As a result, each of Nepal's seven provinces had specific vulnerabilities during Delta and Omicron surges. These distinctive features highlight the importance of context-specific distinct Nepalese data set with a multi-phasic trend of disease dynamics to perform an in-depth analysis of the risk of infection and hospitalization in the context of the geographic and demographic heterogeneity among the provinces of Nepal.

The effective reproduction number is widely used to assess the speed of an epidemic; if it is greater than one, the disease is rising (van den Driessche and Watmough, 2002). However, due to the differences in the size of the susceptible population, the number of infected individuals, and the population's contact pattern, two localities with the same effective reproduction number may be vulnerable in different magnitudes (different magnitudes of incidence) during the pandemic. In such situations, estimating the risk of infection and hospitalization is essential, which can better describe epidemic status and healthcare capabilities. Limited clinical case studies (Dorabawila et al., 2022; Berumen et al., 2020; Lehnig et al., 2021; Tang et al., 2020; Rajiv and Jeffrey, 2020; Xiang et al., 2022) and a handful of mathematical models (Bhatia and Klausner, 2020; Wan et al., 2020; Mizumoto and Chowell, 2020; Meehan et al., 2020) estimate the risk of infection and hospitalization. However, none of these studies have combined mathematical models with real-time incidence data, active hospitalization, and population contact patterns, constituting the essential factors associated with disease transmission and controls. Such data-driven mathematical models can accurately estimate and quantify the real-time risk of infection and hospitalization during the pandemic (Adhikari et al., 2022; Pantha et al., 2021; Nabi, 2020).

In this study, we developed data-driven models to estimate the real-time risk of infection and hospitalization. Then we implemented our models on the data of COVID-19 in Nepal to estimate the province-wise time-dependent reproduction numbers, the risk of disease, and the risk of hospitalization. Using our models, we compared the Delta and Omicron waves and their impacts on the province-level community and healthcare systems. Furthermore, we used our model to evaluate the effects of intervention policies on the risk of infections.

2. Methods

2.1. Data

The countrywide and province-wise data were obtained from various available sources, including the official websites of the Ministry of Health and Population Nepal (MoHP, 2022) and the Central Bureau of Statistics (Central Bureau of Statistics (CBS), 2022). We considered the data containing the daily new COVID-19 cases and the active hospitalization cases in seven provinces of Nepal from 1 April 2021 to 31 March 2022, covering both Delta and Omicron waves. Based on the information about the circulating viral strains, we assumed that the Delta surge occurred between 1 April and 30 December 2021 and that the Omicron surge occurred from 1 January to 31 March 2022.

The contact rate, which depends upon the mobility of the population, plays a vital role in disease transmission. Since the population is a heterogeneous mixture of different age groups with different mobility and contact patterns, we utilized a previous study's age-specific contact rates for Nepal (Prem et al., 2017). Here, a contact is defined as either skin-to-skin contact, such as a kiss or handshake (a physical contact), or a two-way conversation with three or more words in the physical presence of another person but no skin-to-skin contact (a nonphysical contact) (Prem et al., 2017). Based on the previous studies (Prem et al., 2017; Mossong et al., 2008), we estimated an average of 19.31 contacts per person daily. The contact matrix, including population mixing patterns and distribution of contacts by age groups, is presented in Fig. 1. We calculated the group-wise contact rate using the weighted arithmetic mean of contact rates of different age groups. Details of the study design and data collection procedure of contact rate are provided in the previous study (Prem et al., 2017).

Table 1
Total population of Nepal and its provinces. The third column contains the populations used in our study.

Regions	Total population	Population for the study (0.9255 × Total population)
Nepal	29,136,808	26,966,116
Province 1	4,972,021	4,601,605
Madhesh province	6,126,288	5,669,880
Bagmati province	6,084,082	5,630,818
Gandaki province	2,479,745	2,295,004
Lumbini province	5,124,225	4,742,470
Karnali province	1,694,889	1,568,620
Sudur Paschim province	2,711,270	2,509,280

We took the total population of Nepal and its seven provinces from the recently published results of the population census of Nepal (2021) (Central Bureau of Statistics (CBS), 2022). Since about 7.45% of Nepalese are in foreign countries (Central Bureau of Statistics (CBS), 2022), we only took 92.55% of the total population for our study. The total population and population used in our study are given in Table 1. We assumed the infectious period of the Delta variant to be 10 days (Herrero, 2021) and that of the Omicron variant to be 7 days (Ontario Agency for Health Protection and Promotion (Public Health Ontario), 2021; Walensky, 2021).

2.2. Estimation of the effective reproduction number (R_t)

The effective reproduction number, R_t, is the real-time estimation of the reproduction number that represents the average number of secondary infections from an infected individual in his/her infectious period at time t (Thompson et al., 2019). Here, we used the Maximum Likelihood Method (MLM) described in the previous studies (Cori et al., 2013; Thompson et al., 2019) to estimate the effective reproduction number. We require two data sets to estimate R_t using MLM: the number of new cases (incidence of cases) over time and the generation time (time duration between the primary and secondary infection). The generation time is usually not observable but can be approximated with the serial interval (Kuk and Ma, 2005), which is defined as the time between the onset of symptoms of primary cases and that of secondary cases (Wallinga and Teunis, 2004). Many studies (Zhang et al., 2020; Talmoudi et al., 2020; Challen et al., 2020; Rai et al., 2021) have reported that the serial interval follows a Gamma distribution with certain means and standard deviations.

Assuming that the secondary cases at time t generated by the cases infected at time s ($s = 1, 2, \dots, t$) follow the Poisson distribution with mean $R_t\psi_t = R_t \sum_{s=1}^{t} I_{t-s} w_s$, where $\psi_t = \sum_{s=1}^{t} I_{t-s} w_s$ and w_s is a Gamma distribution of serial interval describing the infectiousness at time s after infection, the likelihood function of secondary cases is

$$L(R_t) = \frac{(R_t\psi_t)^{I_t}\, e^{-R_t\psi_t}}{I_t!}.$$

We assumed that the reproduction rate R_t remains constant over the small time period $[t-\tau,\ \ t]$ and is denoted as $R_{t,\tau}$. The likelihood of the secondary cases over the time period $[t-\tau,\ \ t]$ with given previous incidences $I_0, I_1, \dots, I_{t-\tau-1}$ is

$$L(R_{t,\tau}) = \prod_{s=t-\tau}^{t} \frac{(R_{s,\tau}\psi_{s,\tau})^{I_s}\, e^{-R_{s,\tau}\psi_{s,\tau}}}{I_s!}. \quad (1)$$

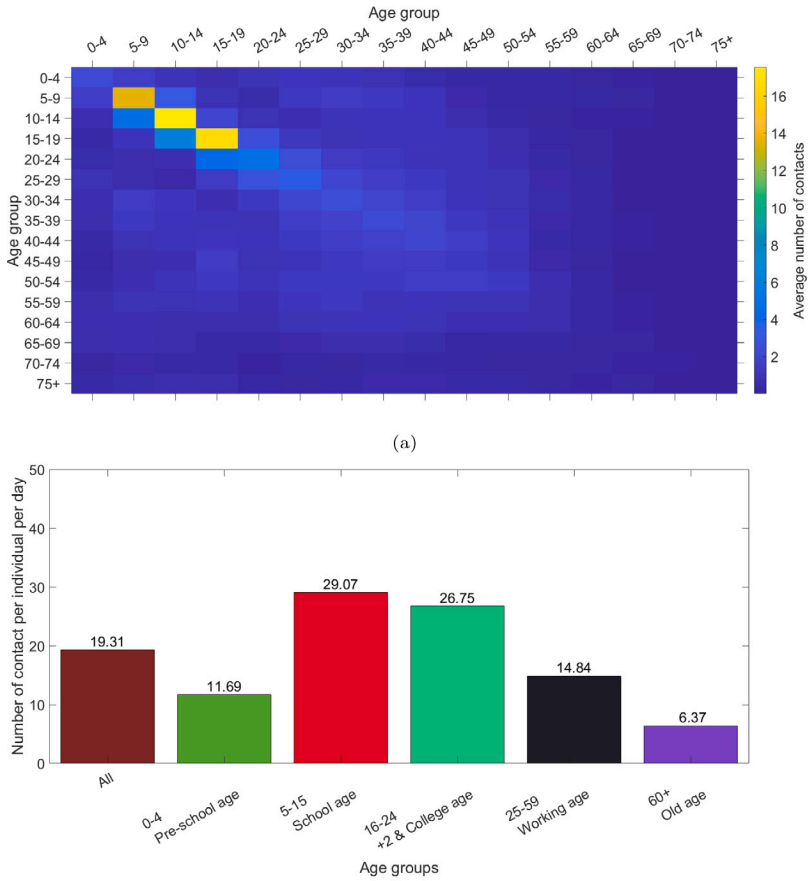

Fig. 1. (a) Age-specific contact matrix for Nepal (Prem et al., 2017). The two axes that start at the top left of the matrix represent the age groups that make up the population. (b) The average number of contacts per individual per day of different age groups in Nepal. The age groups are split into the following categories: preschool, school, 10+2 and college, working, and old age.

Using a Bayesian framework with a Gamma distributed prior with parameters (a, b), the posterior joint distribution of $R_{t,\tau}$ is given by a Gamma distribution with the parameters

$$\left(a + \sum_{s=t-\tau}^{t} I_s, \quad \frac{1}{\frac{1}{b} + \sum_{s=t-\tau}^{t} \psi_s} \right).$$

For our base-case computations, we used the serial interval with the Gamma distribution with a mean of 4.7 days and a standard deviation of 2.9 days for the Delta variant (Musa et al., 2020), and a mean of 3.5 days and standard deviation of 2.4 days for the Omicron variant (Backer et al., 2022). For the computation of reproduction numbers, we used the 'EpiEstim' package of R-software (R 4.2.1) (Cori et al., 2013; Thompson et al., 2019).

2.3. Estimation of risk of infection

We assumed that C_t represents the instantaneous contacts of an individual at time t and C is the average (expected) number of daily contacts. We assumed the contact (C_t) follows a Poisson distribution with mean C, i.e., $C_t \sim \text{Pois}(C)$. We further assumed that N is the total population, which we assumed to be constant during the short period of a single surge, and I_t and I_t^A are the number of new infections and active infections at time t, respectively. Taking ζ as the average infectious period (in days), $I_t^A = \sum_{s=t-\zeta}^{t} I_s$. Thus, the average contacts of an individual with the infectious people at time t is $C_t I_t^A / N$.

We now assume P_t to be the probability that a single contact with infectious people leads to successful infection and S_t to be the number of susceptible individuals at time t. Then the number of new infections at time t is $C_t \frac{I_t^A}{N} P_t S_t$. Also, since the effective reproduction number is R_t, the number of new infections generated by a single infectious individual at time t is R_t/ζ. On average, the total new cases generated by all infectious people I_t^A at time t is $R_t I_t^A/\zeta$. Thus we have

$$C_t \frac{I_t^A}{N} P_t S_t = R_t I_t^A / \zeta$$
$$\implies P_t = R_t N / (\zeta C_t S_t),$$

which gives the probability of infection at a single contact with an infectious person. Then, $(1 - P_t)$ represents the probability that a single contact with infectious people does not result in a successful infection. There are $C_t I_t^A / N$ contacts of an individual with infectious people at time t. Then, the probability that non of these contacts with infectious people results in a successful infection is $(1 - P_t)^{C_t I_t^A / N}$. Thus, the probability of infections (i.e., the risk of infection at time t) is

$$1 - (1 - P_t)^{C_t I_t^A / N}.$$

The computations of the risk of infection were carried out in MATLAB 2021a (The MathWorks, Inc.).

2.4. Estimation of risk of hospitalization

We considered time-to-hospitalization a random variable because it is randomly influenced by various factors, such as the severity of illness,

access to healthcare, demographic factors, the geographic variation that are subject to variation and uncertainty. These factors can differ both across individuals and geographic regions, resulting in heterogeneity in the distribution of time-to-hospitalization. We assume g_h to be the probability distribution of the time-to-hospitalization after becoming infected at time h and $\mathcal{H}_t$ to be the risk of hospitalization at time t of an infection. Therefore, the number of new hospitalized cases at time t is $\mathcal{H}_t \sum_{h=1}^{t} I_{t-h} g_h = \mathcal{H}_t \lambda_t$, where $\lambda_t = \sum_{h=1}^{t} I_{t-h} g_h$. Denoting ν as the average duration of the stay at the hospital, the number of active hospitalized cases at time t is

$$\sum_{j=t-\nu+1}^{t} \mathcal{H}_j \lambda_j.$$

We assumed that the active hospitalization cases follow the Poisson process. Then the likelihood of active hospitalized cases H_t with given hospitalization rate $\mathcal{H}_t$, incidences $I_0, I_1, I_2, \ldots, I_t$, and distribution g_h is:

$$P(H_t|I_0, I_1, I_2, \ldots, I_t, g_h, \mathcal{H}_t) = \frac{\left(\sum_{j=t-\nu+1}^{t} \mathcal{H}_j \lambda_j\right)^{H_t} e^{-\sum_{j=t-\nu+1}^{t} \mathcal{H}_j \lambda_j}}{H_t!}.$$

Using a Bayesian framework with a Gamma distributed prior with parameters (θ, ϕ) for $\mathcal{H}_t$, i.e., $\mathcal{H}_t \sim \text{Gamma}(\theta, \phi)$, the posterior joint distribution of $\mathcal{H}_t$ is

$$\begin{aligned} & P(\mathcal{H}_t|I_0, I_1, I_2, \ldots, I_t, H_t, g_h) \\ \propto\ & P(H_t|I_0, I_1, I_2, \ldots, I_t, g_h, \mathcal{H}_t)\ P(\mathcal{H}_t) \\ =\ & \frac{\left(\sum_{j=t-\nu+1}^{t} \mathcal{H}_j \lambda_j\right)^{H_t} e^{-\sum_{j=t-\nu+1}^{t} \mathcal{H}_j \lambda_j}}{H_t!} \cdot \frac{\mathcal{H}^{\theta-1} e^{-\frac{\mathcal{H}}{\phi}}}{\Gamma(\theta)\phi^{\theta}}. \end{aligned}$$

Since the stay in hospital is shorter than the surge period, we assumed that $\mathcal{H}_t$ is constant for the time period $t-\nu$ to t. Then we obtained

$$\begin{aligned} & P(\mathcal{H}_t|I_0, I_1, I_2, \ldots, I_{t-\nu}, H_t, g_h) \\ \propto\ & \frac{\mathcal{H}_t^{H_t} \left(\sum_{j=t-\nu+1}^{t} \lambda_j\right)^{H_t} e^{-\mathcal{H}_t \sum_{j=t-\nu+1}^{t} \lambda_j}}{H_t!} \frac{\mathcal{H}_t^{\theta-1} e^{-\frac{\mathcal{H}_t}{\phi}}}{\Gamma(\theta)\phi^{\theta}} \\ \propto\ & \left(\mathcal{H}_t^{H_t+\theta-1} e^{-\mathcal{H}_t\left(\sum_{j=t-\nu+1}^{t} \lambda_j + 1/\phi\right)}\right) \frac{\left(\sum_{j=t-\nu+1}^{t} \lambda_j\right)^{H_t}}{H_t!}. \end{aligned}$$

Note that we used the Gamma distributed prior conjugate to the Poisson likelihood. From the expression above, the posterior distribution of $\mathcal{H}_t$, given the new cases and active hospitalized cases, conditional on the post-infection hospitalization timing distribution g_h, is a Gamma distribution with parameters

$$\left(\theta + H_t,\ \frac{1}{\frac{1}{\phi} + \sum_{j=t-\nu+1}^{t} \lambda_j}\right).$$

We obtained a sample of a certain size (m) drawn from this posterior distribution of $\mathcal{H}_t$ given new cases and active hospitalized data from which the posterior mean and 95% Credible Interval (CrI) of $\mathcal{H}_t$ were computed. Since the exact time of infection is not observable and people only admit to the hospital if they feel some complications, the time between the infection and hospitalization cannot be precisely measured. For our simulation, we considered a gamma-distributed duration between infection and hospital admission, with a mean of 3 days and a standard deviation of 2 days.

The computations of the risk of hospitalization were carried out in MATLAB 2021a (The MathWorks, Inc.).

2.5. Impact of non-pharmaceutical interventions (NPIs)

To model different levels of control interventions, we applied corresponding percentage reductions in average contact rates, e.g., a 70% control intervention would result in a 70% reduction in contact rates. As the Nepal Government implemented a significant level of lockdown during the Delta wave, we considered the 70% control intervention as the base case. During the Omicron wave, only primary and secondary schools were closed for a short period (from 11 January to 29 January 2022) (Kathmandu Post, 2022), which we did not expect to have a significant impact, so we assumed a 0% control intervention for the Omicron wave.

In our modeling, the overall impact of NPIs was represented by the reduction of contact rate, which we considered to be 0%, 40%, and 70% for simulations with different levels of control interventions. For the impact of NPIs in age groups (schools, colleges, and working), we reduced the contact rate of the respective age group by 70% while keeping the contact rates of other groups unchanged and calculated the corresponding average contact rates. With these assumptions and based on the previous study (Prem et al., 2017), we estimated the contact rates of 13.79 for the closure of schools and colleges, 14.65 for the closure of working places, and 5.79 for the lockdown.

3. Results

3.1. Reproduction number

As meniontedearlier, the reproduction number indicates the trend of disease spread throughout the population (Dharmaratne et al., 2020). Specifically, if it is more than 1, the disease spread has an increasing trend, and if it is less than 1, the spread has a decreasing trend (van den Driessche and Watmough, 2002).

In Fig. 2 (left column), we present our estimates of the effective reproduction number in Nepal and its provinces from 21 April to 31 December 2021 (the Delta wave). The reproduction number was higher than the threshold value one at the beginning of April 2021. Except for Gandaki province, the reproduction number in Nepal and all of its provinces exceeded two and peaked in the middle of April 2021 (Nepal: 2.20, 95% CrI [2.166, 2.23], Province 1: 2.18, 95% CrI [2.04, 2.32], Madhesh: 2.61, 95% CrI [2.12, 3.14], Bagmati: 2.28, 95% CrI [2.23, 2.33], Gandaki: 1.84, 95% CrI [1.79, 1.89], Lumbini: 2.29, 95% CrI [2.28, 2.30], Karnali: 2.44, 95% CrI [1.68, 3.32], and Sudur Paschim: 2.63, 95% CrI [2.38, 2.89]). These early R_t values indicate that at the beginning of the Delta wave, the infections were rapidly spreading across the country in a short period of time. The reproduction rate in Nepal and its provinces began to fall below the threshold value one after the middle of May 2021 (Nepal: May 17; Province 1, Bagmati, and Gandaki: May 16; Madhesh: May 25; Lumbini: May 14; Karnali: May 24; Sudur Paschim: May 14 2021). Madhesh, Karnali, and Sudur Paschim provinces, where fewer cases were reported, showed greater fluctuations in the temporal pattern of the effective reproduction number.

The first incidence of Omicron in Nepal was detected on 6 December 2021 (Poudel, 2021). After the first week of January 2022, cases surged and spread rapidly. On January 23 2022, 80% of new cases were Omicron (Poudel, 2022). So, we estimate the effective reproduction number from 1 January to 31 April 2022 to characterize the period of the Omicron surge (Fig. 2, right column). The reproduction number in Nepal and all provinces were at the threshold level ($R_t = 1$) in December 2021 during the Delta wave (Fig. 2, left column). After that, it rose quickly, peaking around the middle of January (Nepal: 2.17,

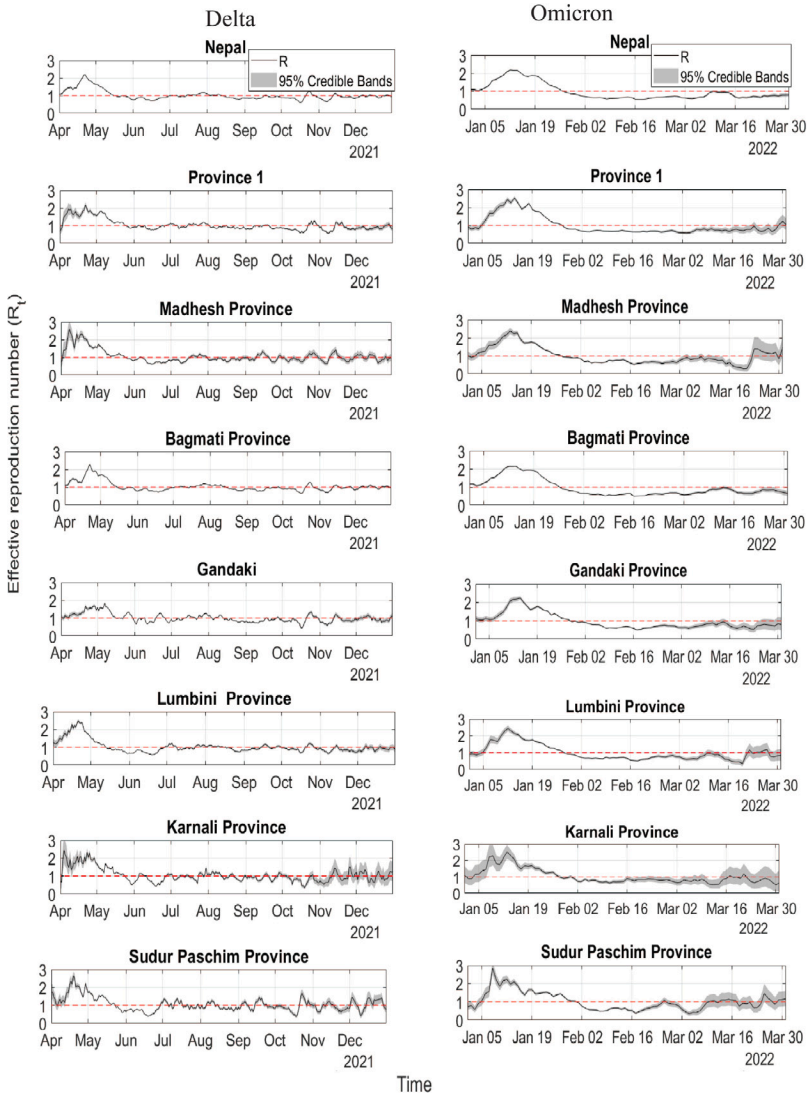

Fig. 2. The time-dependent effective reproduction number of COVID-19 in Nepal and its seven provinces during the Delta (Left column) and Omicron (Right column) waves. The gray-shaded region is the 95% credible interval for R_t. The horizontal red dashed line indicates the threshold value $R_t = 1$. The left column is the effective reproduction number during the Delta wave, and the right column is for the Omicron wave.

95% CrI [2.14, 2.21]; Province 1: 2.26, 95% CrI [2.15, 2.38]; Madhesh: 2.38, 95% CrI [2.21, 2.56]; Bagmati: 2.16, 95% CrI [2.13, 2.19]; Gandaki: 2.24, 95% CrI [2.130, 2.34]; Lumbini: 2.43, 95% CrI [2.27, 2.60]; Karnali: 2.52, 95% CrI [2.12, 2.96]; and Sudur Paschim: 2.85, 95% CrI [2.47, 3.25]), before rapidly dropping below the threshold value of one from the last week of January 2022 for the rest of the year. We observed that the reproduction number remained greater than one for about a month (1st to last week of January 2022) during the Omicron surge. In certain provinces (Madhesh, Lumbini, Karnali, and Sudur Paschim), we noticed a wider range of credible intervals for the estimated R_t at the end of April 2022. This increased variability may be due to the fact that there were fewer reported new cases, with more fluctuations. The results shown in Fig. 2 reveal that the reproduction numbers related to the Omicron and Delta variants are not considerably different even though quite different COVID-19 cases were reported in Nepal and all its provinces.

3.2. Risk of infection

The timely estimation of the risk of infection is essential to track the dynamics of the diseases and valuable to determine the need for amplification or the relaxation of public health control measures. We used our model to compare the risk of infection of COVID-19 during Delta and Omicron surges in Nepal and its provinces. The estimated maximum risk of infection of Delta surge in Nepal and its provinces is shown in Table 2. The temporal pattern of the risk of infection during the Delta and Omicron surges is shown in Fig. 3.

The risk of infection during the Delta wave increased sharply from mid-April 2021 and peaked in the second week of May 2021 in Nepal (Fig. 3, left column). The Bagmati province, which contains Nepal's most densely populated capital city, had the peak risk for infection two weeks sooner than the other provinces (first week of May 2021). Our estimates showed that Bagmati province was the highest risk zone (98.94, 95% CrI [32.99, 181.31] per hundred thousand), while Madhesh province remained the lowest risk zone (12.16, 95% CrI [4.05, 22.29] per hundred thousand) (Table 2). Interestingly, despite being the most densely populated province (600 people/km^2) (Central Bureau of Statistics (CBS), 2022) and having a larger R_t value, the Madhesh province had a lower risk of infection compared to other regions.

We also estimated the risk of COVID-19 infection during the Omicron wave (1 January to 31 March 2022). The temporal pattern of the risk of infection during the Omicron surge is shown in Fig. 3 (right column), and the estimated risk is shown in Table 2. Starting from a minimal risk at the beginning of January 2022, the risk of infection

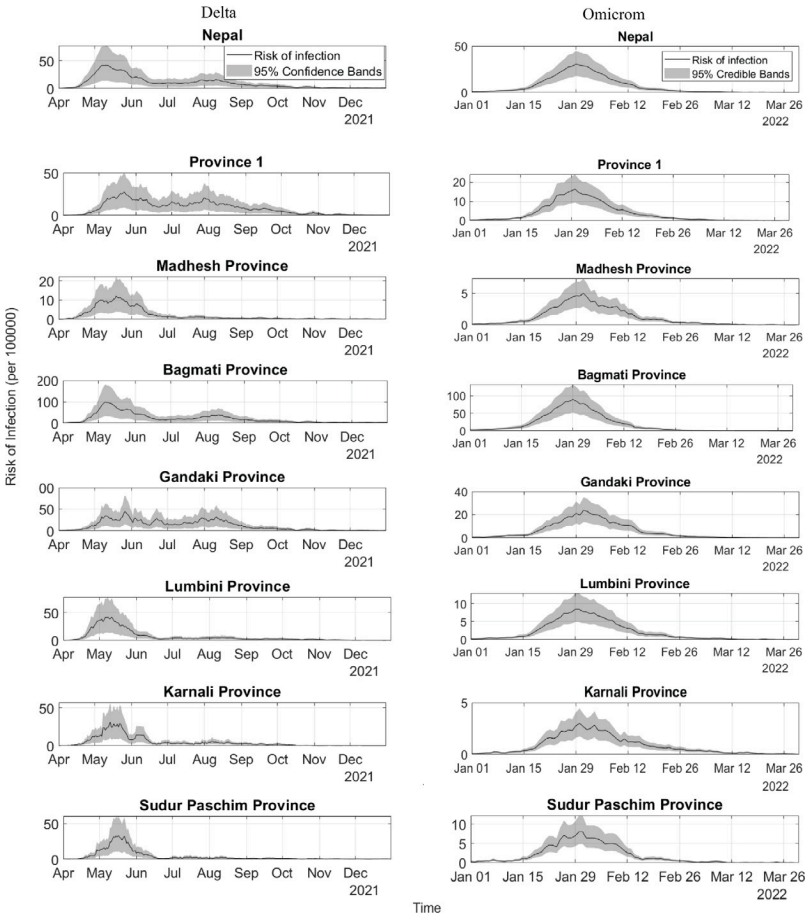

Fig. 3. Risk of infection (per thousand hundred) due to Delta and Omicron variants of Nepal and its seven provinces. The first column is the risk of infection during the Delta wave, and the second column is the risk of infection during the Omicron wave. The scaling on the *y*-axis differs depending on the province and wave.

Table 2
The maximum risk of infection and time of highest risk of COVID-19 during Delta and Omicron variant of Nepal and its seven provinces.

Risk of infection of Delta variant			
Regions	Risk of infection (per 100 000)	95% CrI	Time of highest risk
Nepal	42.19	[14.06, 77.33]	11 May, 2021
Province 1	27.49	[9.16, 50.40]	23 May, 2021
Madhesh	12.16	[4.05, 22.29]	19 May, 2021
Bagmati	98.94	[32.99, 181.31]	7 May, 2021
Gandaki	44.53	[14.84, 81.62]	26 May, 2021
Lumbini	42.89	[14.30, 78.63]	8 May, 2021
Karnali	31.16	[10.39, 57.13]	14 May, 2021
Sudur Paschim	33.26	[11.08, 60.97]	17 May, 2021
Risk of infection of Omicron variant			
Nepal	30.42	[17.61 46.43]	30 Jan, 2022
Province 1	16.30	[9.87, 24.03]	31 Jan, 2022
Madhesh	5.01	[2.63, 7.65]	1 Feb, 2022
Bagmati	89.62	[56.61, 132.05]	30 Jan, 2022
Gandaki	21.35	[13.48, 31.47]	1 Feb, 2022
Lumbini	8.46	[4.90, 12.47]	31 Jan, 2022
Karnali	3.00	[1.74, 4.43]	31 Jan, 2022
Sudur Paschim	8.03	[4.64, 11.83]	27 Jan, 2022

reached the highest level among provinces in a short period of time (3 weeks) around the fourth week of January 2022. During this time, we observed a considerable disparity in maximum risk of infection across Nepal and its provinces, ranging from 3.00, 95% CrI [1.74, 4.43] per hundred thousand in Karnali to 89.62, 95% CrI [56.61, 132.05] per hundred thousand in Bagmati. Furthermore, during the Delta surge, Madhesh province had a low (5.01, 95% CrI[2.63, 7.65] per hundred thousand) risk of infection at the peak time of the Omicron surge. The higher uncertainty, i.e., a larger width of credible intervals, for estimates may attribute to the fluctuation of the data set of new cases. The fluctuation of daily new cases may be due to the poor recording of daily testing and detected positive cases.

We found a considerable difference in the patterns of risk of infection between the two waves of COVID-19 in Nepal. The risk of infection during the Delta wave was abruptly increased, and with a complete lockdown, it took about one month to decline, but in the Omicron wave, it climbed and fell quickly without lockdown. Furthermore, during the Delta surge, the maximum risk of infection was slightly higher than the Omicron surge in Nepal (38.69%) and Bagmati province (10%) but significantly higher in Gandaki (108.57%), Lumbini (407%), Karnali (938.66%), and Sudur Paschim (314%) than that of the Omicron surge. The Bagmati province was the most vulnerable to both Delta and Omicron surges, while the rest of the provinces were more vulnerable to the Delta surge than the Omicron surge.

3.3. Risk of hospitalization

We calculated the risk of hospitalization using our model to the available data on active hospitalizations with COVID-19 in Nepal and its provinces. The results shown in Fig. 4 (left column) illustrate the risk that COVID-19 patients are admitted to hospitals in Nepal and its provinces during the Delta surge (1 May to 31 December 2021).

In Nepal, the risk of hospitalization of the Delta variant remains at 10% on average (min 7%, max 20%), and Province 1 shows a risk of hospitalization of 11% (min 6%, max 22%). Madhesh province had

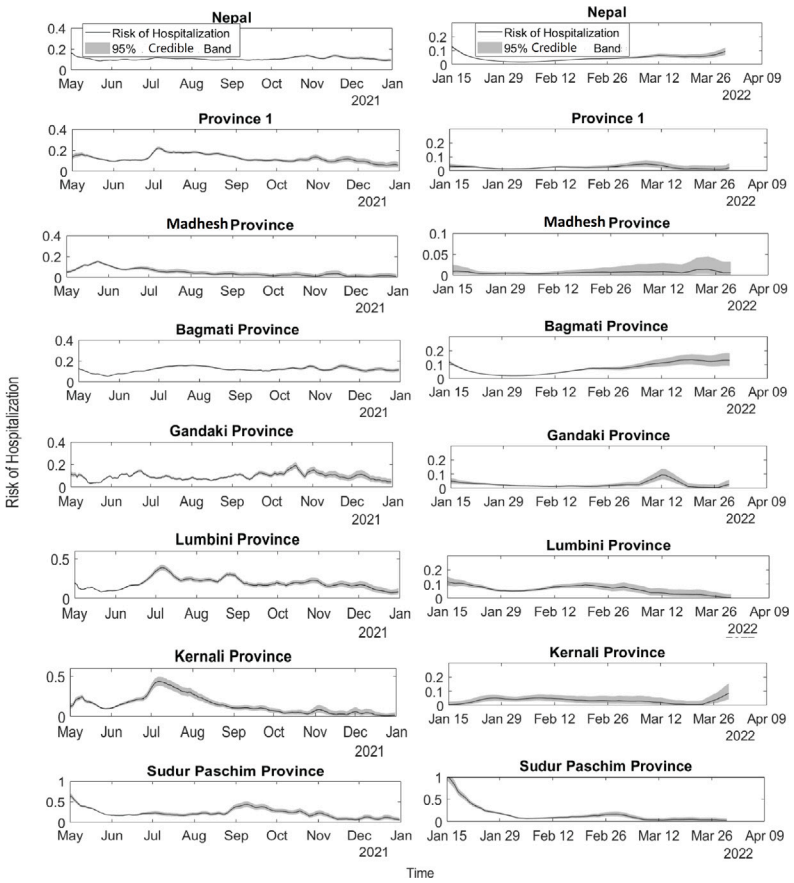

Fig. 4. Risk of hospitalization during Delta and Omicron wave in Nepal and its provinces. The left column is the risk of hospitalization during the Delta wave, and the right column is the risk of hospitalization during the Omicron wave. The scaling on the y-axis differs depending on the province and the wave.

the lowest risk of hospitalization at 6% (min 5%, max 14%). Although many actual hospitalization cases are in the Bagmati province, the risk of hospitalization is 11% (min 10%, max 15%), similar to other regions. Besides the Madhesh province, Gandaki province also has a lower risk of hospitalization of 9.5% (min 5%, max 18%). The risk of hospitalization in both Lumbini and Karnali provinces is high [Lumbini: 19% (min 7%, max 38%); Karnali: 14% (min 3%, max 42%)]. In Sudur Paschim, the risk of hospitalization was initially high (68%) but later on around 21% (min 6%, max 43%). The initial higher risk of hospitalization in Sudur Paschim could be due to the high volume of returnees migrant workers from India.

The Omicron surge had substantially lower hospitalization rates than the Delta surge. The results in Fig. 4 (right column) show that the risk of hospitalization was 2.5% during the peak time of the Omicron wave in Nepal. At the end of March 2022, the hospitalization rate was again raised in Nepal as well as in Bagmati province. Sudur Paschim province had an extremely high risk of hospitalization during the mid of January, which could be due to the inclusion of the institutional isolation of returnee migrant workers in the data. Our estimates show that compared to the Delta wave (Fig. 4, left column), the hospitalization risk in Nepal and its provinces is significantly lower during the Omicron wave (Fig. 4, right column), falling to even less than 1% in some provinces (Nepal: 1.8%, 95% CrI [1.7%, 1.9%], Province 1: 1.2%, 95% CrI [1%, 1.5%], Madhesh: 0.38%, 95% CrI [0.17%, 0.7%], Bagmati: 2%, 95% CrI [1.9%, 2.1%], Gandaki: 1.3%, 95% CrI [0.97%, 1.75%], Lumbini: 1.3%, 95% CrI [0.29% 4.29%], Karnali: 0.6%, 95% CrI [0.022%, 3.18%], Sudur Paschim: 2.9%, 95% CrI [0.92%, 7.15%]). At the end of March 2022, the risk of hospitalization increased in Nepal and Bagmati province.

3.4. Impact of Non Pharmaceutical Interventions (NPIs) on reducing the risk of COVID-19 infection

NPIs are known to play an important role in the mitigation of COVID-19. In general, restricting of mobility through NPIs, such as lockdown, reduces the contact rate, thereby reducing the risk of infection. Here, we used our model to quantify the impact of NPIs implemented by the Government of Nepal on reducing the risk of COVID-19. In Fig. 5, we present the maximum risk of infection during the Delta wave with different control levels. In Bagmati province (the province with the highest risk), the maximum risk would have increased by 216.32% if the lockdown was not implemented during the Delta surge. Similarly, Madhesh province (a province with the lowest risk) would have increased by 216.61% if the lockdown was not implemented.

The results in Fig. 6 show the trend of risk of infection during the Delta wave under different control levels. Our model estimates that if the lockdown had not been implemented during the Delta surge in Nepal, there would have been three times more new infections (Fig. 6). We also observed a similar impact of control strategies on the trend of risk of infection during the Omicron wave as in the Delta wave. For example, the risk of infection is reduced by about two-thirds due to the reduction of contact rate by 70% (Nepal: 30.42, 95% CrI [17.61, 46.43] to 9.6, 95% CrI [1.60, 17.61], Province 1: 16.30, 95% CrI [9.87, 24.03] to 5.15, 95% CrI [1.71, 9.44] per hundred thousand).

We also estimated the risk of infection under the closure of school/colleges and working places only during the Delta and Omicron waves (Fig. 7). We observed that closing schools and colleges (i.e., restriction of mobility of school/college age groups) and workplaces (i.e., restriction of mobility of the adult groups of age 25–59) can reduce the risk of infection by 26.30% while a complete lockdown reduces the

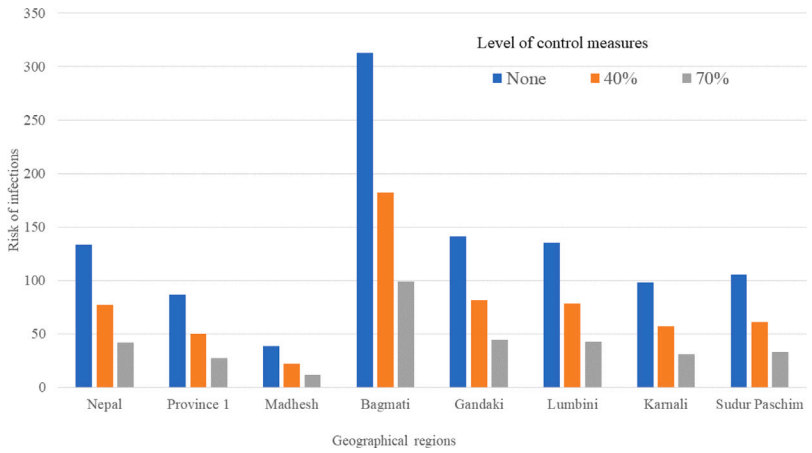

Fig. 5. The maximum risk of infection under different control levels during the Delta wave in Nepal and its provinces.

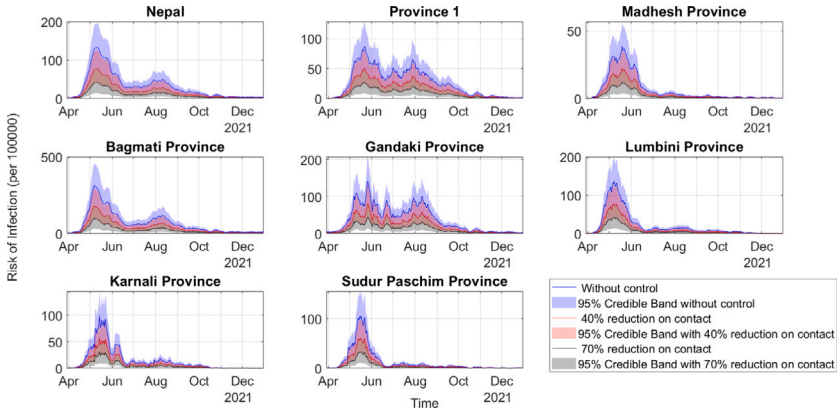

Fig. 6. Effect of control measures on a reduction of risk of infection during the Delta wave. Here, for a baseline computation, we took the average contact rate of 5.65 contacts per person per day during the Delta wave and assumed that lockdown reduces the contact rate by 70% (Coburn et al., 2009). To observe the impact of the lockdown, we used our model to estimate the risk of infection for 70% (5.79 contacts per person per day), 40% (11.58 contacts per person per day), and 0% (19.31 contacts per person per day) reduction of contact rate.

risk of infections by 68.42% (during the Delta, none: 133.54, 95% CrI [77.33, 196.74], school/college closed: 98.42, 95% CrI [49.22 147.59], working place closed: 98.42, 95% CrI [56.25, 154.61], lockdown: 42.17, 95% CrI [14.06, 77.33]; during the Omicron wave, none: 30.42, 95% CrI [17.61, 46.43], schools/colleges closed: 22.41, 95% CrI [11.21, 33.62], working places closed: 22.42, 95% CrI [12.81, 36.82], lockdown: 8.00, 95% CrI [1.60, 17.61] per hundred thousand).

4. Discussion

The timely assessment of the epidemic trend and its potential burden is essential to minimize the epidemic disaster and manage the healthcare facilities. In order to allocate resources and design health policies during the early stages of a pandemic, it is necessary to estimate the risk of infection and risk of hospitalization. Generally, the risk of hospitalization remains the same throughout the transmission period for the same kind of strain. However, the pattern of hospitalization may vary depending on the geographic region, cultural background, level of education, way of life, access to medical services, and population group among which the disease is circulating (Jackson et al., 2021; Athavale et al., 2021). Even when more infections result in more patients being admitted to hospitals, the risk of hospitalization may not be constant over time.

The effective reproduction number is widely used to track the transmission rate during epidemics. However, due to variations in the size of the susceptible population, the number of actively infected individuals, and the population's pattern of contact, two regions with the same effective reproduction number may have different levels of vulnerability (risk) throughout the pandemic. To track the trend of an epidemic more precisely by including the most vital factors of disease transmission, we developed data-driven mathematical models which provide a timely estimation of the risk of infection and the risk of hospitalization during a pandemic. Our mathematical model of risk of infection considers the susceptible population, active infectious population, and contact pattern of the people in addition to the effective reproduction number. Similarly, our hospitalization risk model uniquely utilizes active hospitalized cases to describe the temporal pattern of hospitalization trends. We implemented our models to the unique data sets of new COVID-19 cases and hospitalized cases in Nepal and its provinces. Furthermore, our models also allow us to determine how the implemented control strategies could effectively control the disease.

The seven provinces of Nepal have a range of population contact patterns due to their diverse geographic locations, distinctive lifestyles, cultural traditions, economic conditions, and level of urbanization (Pantha et al., 2021). The recorded COVID-19 cases also varied throughout provinces (MoHP, 2022). Despite huge discrepancies among provinces, the reproduction numbers of COVID-19 of the Delta and Omicron waves across Nepal and its provinces are not considerably

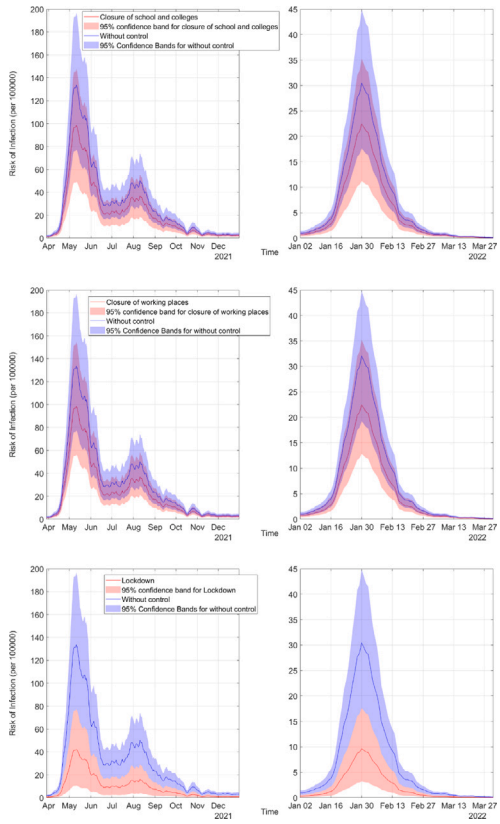

Fig. 7. Effect of closures of school colleges, working places, and lockdown on reducing the risk of infection during the Delta and Omicron waves. The left column is for the Delta wave, and the right column is for the Omicron wave. The first row represents the impacts of the closure of schools and colleges, the second row represents the effects of closing working places, and the third row represents the effects of lockdown.

different (Fig. 2), indicating that reproduction numbers alone may not fully capture the disease trend. A noticeable difference in reproduction number between the Delta and Omicron surges regarding the non-pharmaceutical interventions is that the total lockdown was needed to be implemented during the Delta wave, while during Omicron wave, partial closure of schools and colleges were enough for the reproduction number to fall below the threshold value one. In some provinces (Madhesh, Lumbini, Karnali, and Sudur Paschim), we noticed a wider range of credible intervals for the estimated R_t at the end of March 2022. This increased variability may be due to the fact that there were fewer reported new cases, with more fluctuations.

The risk of infection varies widely among provinces in both the Delta and Omicron waves despite the similar reproduction number. The ability of our model to capture the discrepancies among the provinces highlights the risk of infection as a critical indicator of the disease trend. Our results show a similar risk of infection in Nepal and in Bagmati province during the Delta and Omicron surges. However, in the case of other provinces, the risk of infection is less during the Omicron surge than during the Delta surge. Less risk of the Omicron is in contrast to what has been observed in other regions of the world, where the Omicron wave had a higher risk of infection than the Delta wave (Liu and Rocklöv, 2022; Du et al., 2022; Ito et al., 2022). Note that 36% of Nepalese people were fully vaccinated, and 49% were vaccinated with at least one dose by 4 January 2022 (Ritchie et al., 2020). Because of the low severity of the Omicron variant (Bhatia and Klausner, 2020; Wan et al., 2020), and the high coverage of vaccines, there were presumably fewer reported cases during the Omicron surge, which could be attributed to the low risk of infection as estimated by our model. During the Delta wave, infection risk rapidly increased and declined slowly. In contrast, during the Omicron wave, it rose and fell quickly, which may be due to the burnout of the susceptible population during previous waves or vaccinations, resulting in a faster climb and decline of cases compared to the Delta wave.

A substantial strength of our models also lies in their ability to describe the discrepancies among provinces in the pattern of the risk of hospitalization. We observed these discrepancies throughout Nepal and its provinces (for example, 6% in Madhesh province and 21% in Sudur Paschim) during the Delta surge (Fig. 4). The disparities in the risk of hospitalization reflect the unequal distribution of healthcare facilities and the different living standards of the people in different provinces (Cao et al., 2021; Saito et al., 2016). For example, Madhesh province shares the border with Province 1, which has relatively better and larger hospitals. Therefore, many people from Madhesh province go to the hospitals of Province 1, causing a higher hospitalization rate in Province 1 than in Madhesh province. Bagmati province contains Kathmandu, the capital city, and other major cities such as Lalitpur, Bhaktapur, Bharatpur, Hetauda, and Dhulikhel, comprising the major hospitals of Nepal. Among the reported hospitalized cases ~48%, were in this province (MoHP, 2022), which may have included the hospitalization of people from other provinces as well.

Despite the fewer number of new cases and hospitalized cases, the rate of hospitalization in Karnali and Sudur Paschim was estimated to be high. Madhesh province, on the other hand, has a low risk of hospitalization and low reported new cases. Our model estimates a four times higher risk of hospitalization during the Delta surge than the Omicron surge in Nepal and most provinces (Fig. 4), consistent with the higher hospitalization during the Delta surge found in other studies (Bhatia and Klausner, 2020; Wan et al., 2020; Centre for Disease Control and Prevention (CDC), 2022). The unusual risk of hospitalization seen in the Sudur Paschim is likely due to the data set. For example, on 1st January 2022, there were four new cases while seven persons were in hospital. From 1st to 12th January 2022, only 330 new cases were reported, but 395 active hospitalized cases were reported on 12th January, indicating more than 100% risk of hospitalization, as revealed in the model prediction. The higher active hospitalized cases of Sudur Paschim, compared to the new cases, could be due to the inclusion of the institutional isolation of returnee migrant workers in the data of active hospitalized cases.

We also used our model to evaluate the effectiveness of control strategies in suppressing infection rates. For the purpose of demonstration, we assumed different levels of control interventions (0%, 40%, and 70% reduction in contact rates) and estimated the corresponding risk of infection during the Delta surge (Figs. 5 & 6). Our results indicate that the risk of infection of COVID-19 would have been three times more if there were no lockdown (i.e., a lack of 70% reduction in contact) during the Delta surge. We also found that school/college closures have a greater impact on the reduction of risk of infection (Fig. 7), supporting the Nepal government's strategy of closing schools and colleges first during the peak of the Omicron surge (Kathmandu Post, 2022). Our model supports that the effectiveness of the control strategy is linearly translated to the risk of infection (Fig. 5). Other studies (Tian et al., 2020; Kraemer et al., 2020; Ferguson et al., 2020; Adhikari et al., 2021) have also reported that travel restrictions and non-pharmaceutical interventions have major impacts on the control of COVID-19 surges.

We acknowledge some limitations of our study. Although the population has a varied mixture pattern, we consider a homogeneous mixture in our model for estimating the risk of hospitalization so that every infected person has an equal probability of hospitalization. There are some uncertainties in the data used to compute the risk of infection and hospitalization. Underestimation and temporal inaccuracy (time lag between the time of infection/hospitalization and observation (record)) of the data also are two major factors that reduce the quality of the data we used. The better quality of data enhances the accuracy of the results of this study. Our model also does not consider the temporal

variation in under-reporting, which might otherwise be interpreted as a variation in the risk of infection. Reported COVID-19 cases include only those individuals who were tested and confirmed to be positive.

Several studies (Adhikari et al., 2021; Pullano et al., 2021; Adhikari et al., 2022; Saito et al., 2021) have found asymptomatic or undiagnosed COVID-19-infected individuals who can significantly spread the virus. The detection of COVID-19 cases in Nepal is low (Adhikari et al., 2022), implying that the actual risk of infection might be quantitatively different from our estimations. A Hidden Markov Model (HMM) could be an extension of our model to account for the imperfect observation process of undiagnosed cases. Hospital admission is nonspecific because it does not necessarily specify the reason and might cover a wide range of severity. Individuals infected with SARS-COV-2 may be hospitalized, but not necessarily as a result of COVID-19. A study (Clark et al., 2020) estimated that 17 billion (UI 10–24) individuals, or 22% (UI 15–28) of the world's population, have at least one underlying condition that increases their chance of developing severe COVID-19 if they become infected (range from 5% of those younger than 20 years to > 66% of those who are 70 years or older). Also, a study (Bastola et al., 2021) shows that among the COVID-19 patients hospitalized in Sukraraj Tropical and Infectious Disease Hospital of Nepal from January 2020 to January 2021, 64% had two or more comorbidities. Identifying an accurate number of hospitalized cases due to COVID-19 is necessary to accurately estimate the risk of hospitalization. Due to the unavailability of data regarding the number of new cases caused by the Delta and Omicron variants in mixed disease dynamics, we did not consider the mixed diseases model.

In summary, we developed data-driven mathematical models to estimate the risk of infection and the risk of hospitalization during the pandemic. As demonstrated by the applications of these models to a unique data set of Nepal and its provinces, the risk of infection and hospitalization can capture critical features of epidemic trends. Our model can also be used in other places and for outbreaks of other infectious diseases. Real-time quantification of the risk of infection and hospitalization is essential to develop ideal policy guidelines and appropriate control strategies for bringing society out of the devastating pandemic.

CRediT authorship contribution statement

Khagendra Adhikari: Formal analysis, Investigation, Methodology, Numerical simulation, Writing – original draft. **Ramesh Gautam:** Formal analysis, Review and editing. **Anjana Pokharel:** Formal analysis, Review and editing. **Kedar Nath Uprety:** Formal analysis, Supervision, Review and editing. **Naveen K. Vaidya:** Conceptualization, Formal analysis, Supervision, Review and editing.

Declaration of competing interest

None.

Data availability

The compiled data and codes that are analyzed will be available in the request of readers.

Acknowledgments

This research is supported by the GRAID (Graduate Research Assistantships in Developing Countries) awards from the International Mathematical Union (IMU), Germany. KA acknowledges the Nepal Academy of Science and Technology (NAST) for Ph.D. Fellowship. RG acknowledges the University Grants Commission (UGC) Nepal for Ph.D. Fellowship 2021. The work of NKV was supported by NSF, USA grants DMS-1951793 and DEB-2030479 from the National Science Foundation of USA and the UGP award from San Diego State University, USA.

References

Adhikari, K., Gautam, R., Pokharel, A., Dhimal, M., Uprety, K.N., Vaidya, N.K., 2022. Insight into delta variant dominated second wave of COVID-19 in Nepal. Epidemics 100642. http://dx.doi.org/10.1016/j.epidem.2022.100642.

Adhikari, K., Gautam, R., Pokharel, A., Uprety, K.N., Vaidya, N.K., 2021. Transmission dynamics of COVID-19 in Nepal: Mathematical model uncovering effective controls. J. Theoret. Biol. 521 (110680), http://dx.doi.org/10.1016/j.jtbi.2021.110680.

Athavale, P., Kumar, V., Clark, J., Mondal, S., Sur, S., 2021. Differential impact of COVID-19 risk factors on ethnicities in the United States. Front. Public Health 1954.

Backer, J.A., Eggink, D., Andeweg, S.P., Veldhuijzen, I.K., van Maarseveen, N., Vermaas, K., Vlaemynck, B., Schepers, R., van den Hof, S., Reusken, C.B., et al., 2022. Shorter serial intervals in SARS-CoV-2 cases with Omicron BA. 1 variant compared with delta variant, the netherlands, 13 to 26 december 2021. Eurosurveillance 27 (6), 2200042. http://dx.doi.org/10.2807/1560-7917.ES.2022.27.6.2200042.

Bastola, A., Shrestha, S., Nepal, R., Maharjan, K., Shrestha, B., Chalise, B.S., Thapa, P., Balla, P., Sapkota, A., Shah, P., 2021. Clinical mortality review of COVID-19 patients at sukraraj tropical and infectious disease hospital, nepal; a retrospective study. Trop. Med. Infect. Dis. 6 (3), http://dx.doi.org/10.3390/tropicalmed6030137.

Ben, W., 2021. COVID-19 spirals out of control in nepal: 'every emergency room is full now'. Natl. Geogr. URL https://www.nationalgeographic.com/culture/article/a-pandemic-surge-threatens-livelihoods-in-nepal.

Berumen, J., Schmulson, M., Alegre-Díaz, J., Guerrero, G., Larriva-Sahd, J., Olaiz, G., Wong-Chew, R.M., Cantú-Brito, C., Ochoa-Guzmán, A., Garcilazo-Ávila, A., González-Carballo, C., Chiquete, E., 2020. Risk of infection and hospitalization by COVID-19 in Mexico: a case-control study. http://dx.doi.org/10.1101/2020.05.24.20104414, medRxiv.

Bhandari, R., Hannah Peterse, H.E., 2021. A hopeless situation': oxygen shortage fuels nepal's covid crisis. Guardian URL https://www.theguardian.com/world/2021/may/10/hopeless-situation-oxygen-shortage-fuels-nepal-covid-crisis.

Bhatia, R., Klausner, J., 2020. Estimating individual risks of COVID-19 associated hospitalization and death using publicly available data. PLOS One 15 (12), e0243026.

Cao, W.-R., Shakya, P., Karmacharya, B., Xu, D.R., Hao, Y.-T., Lai, Y.-S., 2021. Equity of geographical access to public health facilities in nepal. BMJ Glob. Health 6 (10), e006786. http://dx.doi.org/10.1136/bmjgh-2021-006786.

Central Bureau of Statistics (CBS), 2022. Preliminary Results of NationalPopulation Census, 2078. CBS, URL https://censusnepal.cbs.gov.np/Home/Details?tpid=5&dcid=3479c092-7749-4ba6-9369-45486cd67f30&tfsid=17.

Centre for Disease Control and Prevention (CDC), 2022. Rates of laboratory-confirmed COVID-19 hospitalizations by vaccination status. pp. 1–3, URL https://covid.cdc.gov/covid-data-tracker/#covidnet-hospitalizations-vaccination.

Challen, R., Brooks-Pollock, E., Tsaneva-Atanasova, K., Danon, L., 2020. Meta-analysis of the SARS-CoV-2 serial interval and the impact of parameter uncertainty on the COVID-19 reproduction number. http://dx.doi.org/10.1101/2020.11.17.20231548, MedRxiv.

Clark, A., Jit, M., Warren-Gash, C., Guthrie, B., Wang, H.H., Mercer, S.W., Sanderson, C., McKee, M., Troeger, C., Ong, K.L., et al., 2020. Global, regional, and national estimates of the population at increased risk of severe COVID-19 due to underlying health conditions in 2020: a modelling study. Lancet Glob. Health 8 (8), e1003–e1017. http://dx.doi.org/10.1016/S2214-109X(20)30264-3.

Coburn, B.J., Wagner, B.G., Blower, S., 2009. Modeling influenza epidemics and pandemics: insights into the future of swine flu (H1N1). BMC Med. 7 (1), 1–8. http://dx.doi.org/10.1186/1741-7015-7-30.

Cori, A., Ferguson, N.M., Fraser, C., Cauchemez, S., 2013. A new framework and software to estimate time-varying reproduction numbers during epidemics. Am. J. Epidemiol. 178 (9), 1505–1512. http://dx.doi.org/10.1093/aje/kwt133.

Dharmaratne, S., Sudaraka, S., Abeyagunawardena, I., Manchanayake, K., Kothalawala, M., Gunathunga, W., 2020. Estimation of the basic reproduction number (R_0) for the novel coronavirus disease in Sri Lanka. Virol. J. 17 (1), 1–7. http://dx.doi.org/10.1186/s12985-020-01411-0.

Dorabawila, V., Hoefer, D., Bauer, U.E., Bassett, M.T., Lutterloh, E., Rosenberg, E.S., 2022. Risk of infection and hospitalization among vaccinated and unvaccinated children and adolescents in New York after the emergence of the Omicron variant. JAMA http://dx.doi.org/10.1001/jama.2022.7319.

Du, Z., Hong, H., Wang, S., Ma, L., Liu, C., Bai, Y., Adam, D.C., Tian, L., Wang, L., Lau, E.H., et al., 2022. Reproduction number of the Omicron variant triples that of the Delta variant. Viruses 14 (4), 821. http://dx.doi.org/10.3390/v14040821.

Ferguson, N.M., Laydon, D., Nedjati-Gilani, G., Imai, N., Ainslie, K., Baguelin, M., Bhatia, S., Boonyasiri, A., Cucunubá, Z., Cuomo-Dannenburg, G., et al., 2020. Impact of non-pharmaceutical interventions (NPIs) to reduce COVID-19 mortality and healthcare demand. Imp. Coll. COVID-19 Response Team 20 (10.25561), 77482. http://dx.doi.org/10.25561/77482.

Herrero, L., 2021. How contagious is delta? How long are you infectious? Is it more deadly? A quick guide to the latest science. Conversation TheConversation.http://theconversation.com/how-contagious-is-delta-how-long-are-you-infectious-is-it-more-deadly-a-quick-guide-to-the-latest-science-165538.

Islam, S., Islam, T., Islam, M.R., 2022. New coronavirus variants are creating more challenges to global healthcare system: a brief report on the current knowledge. Clin. Pathol. 15, 2632010X221075584.

Ito, K., Piantham, C., Nishiura, H., 2022. Relative instantaneous reproduction number of Omicron SARS-CoV-2 variant with respect to the delta variant in Denmark. J. Med. Virol. 94 (5), 2265–2268. http://dx.doi.org/10.1002/jmv.27560.

Jackson, S.L., Derakhshan, S., Blackwood, L., Lee, L., Huang, Q., Habets, M., Cutter, S.L., 2021. Spatial disparities of COVID-19 cases and fatalities in United States counties. Int. J. Environ. Res. Public Health 18 (16), 8259. http://dx.doi.org/10.3390/ijerph18168259.

Kathmandu Post, 2022. Schools across Nepal shut until january 29 amid virus threat. URL https://kathmandupost.com/national/2022/01/10/schools-across-nepal-shut-until-january-29-amid-virus-threat.

Kraemer, M.U., Yang, C.-H., Gutierrez, B., Wu, C.-H., Klein, B., Pigott, D.M., Open COVID-19 Data Working Group†, Du Plessis, L., Faria, N.R., Li, R., et al., 2020. The effect of human mobility and control measures on the COVID-19 epidemic in China. Science 368 (6490), 493–497. http://dx.doi.org/10.1126/science.abb42.

Kuk, A.Y., Ma, S., 2005. The estimation of SARS incubation distribution from serial interval data using a convolution likelihood. Stat. Med. 24 (16), 2525–2537. http://dx.doi.org/10.1002/sim.2123.

Lehnig, C.L., Oren, E., Vaidya, N.K., 2021. Effectiveness of alternative semester break schedules on reducing COVID-19 incidence on college campuses. Sci. Rep. 12 (2116), http://dx.doi.org/10.1038/s41598-022-06260-1.

Liu, Y., Rocklöv, J., 2022. The effective reproductive number of the Omicron variant of SARS-CoV-2 is several times relative to Delta. J. Travel Med. 29 (3), taac037. http://dx.doi.org/10.1093/jtm/taac037.

Malik, M.A., 2022. Fragility and challenges of health systems in pandemic: early lessons from India's second wave of coronavirus disease 2019 (COVID-19). Glob. Health J. http://dx.doi.org/10.1016/j.glohj.2022.01.006.

Meehan, M.T., Rojas, D.P., Adekunle, A.I., Adegboye, O.A., Caldwell, J.M., Turek, E., Williams, B.M., Marais, B.J., Trauer, J.M., McBryde, E.S., 2020. Modelling insights into the COVID-19 pandemic. Paediatr. Respir. Rev. 35, 64–69. http://dx.doi.org/10.1016/j.prrv.2020.06.014.

Mizumoto, K., Chowell, G., 2020. Estimating risk for death from coronavirus disease, China, january–february 2020. Emerg. Infect. Diseases 26 (6), 1251. http://dx.doi.org/10.3201/eid2606.200233.

MoHP, N., 2022. Nepal | recent updates. Covid Dash Board URL https://covid19.mohp.gov.np/.

Mossong, J., Hens, N., Jit, M., Beutels, P., Auranen, K., Mikolajczyk, R., Massari, M., Salmaso, S., Tomba, G.S., Wallinga, J., et al., 2008. Social contacts and mixing patterns relevant to the spread of infectious diseases. PLoS Med. 5 (3), e74. http://dx.doi.org/10.1371/journal.pmed.0050074.

Musa, S.S., Zhao, S., Wang, M.H., Habib, A.G., Mustapha, U.T., He, D., 2020. Estimation of exponential growth rate and basic reproduction number of the coronavirus disease 2019 (COVID-19) in Africa. Infect. Dis. Poverty 9 (1), 1–6. http://dx.doi.org/10.1186/s40249-020-00718-y.

Nabi, K.N., 2020. Forecasting COVID-19 pandemic: A data-driven analysis. Chaos Solitons Fractals 139, 110046.

Ontario Agency for Health Protection and Promotion (Public Health Ontario), 2021. COVID-19 omicron variant of concern and communicability-what we know so far. URL https://www.publichealthontario.ca/-/media/documents/ncov/covid-wwksf/2022/01/wwksf-omicron-communicability.pdf?sc_lang=en.

Pantha, B., Acharya, S., Joshi, H.R., Vaidya, N.K., 2021. Inter-provincial disparity of COVID-19 transmission and control in Nepal. Sci. Rep. 11 (13363), http://dx.doi.org/10.1038/s41598-021-92253-5.

Poudel, A., 2021. Nepal reports new Omicron case. Kathmandu Post URL https://kathmandupost.com/health/2021/12/22/nepal-reports-new-omicron-case-third-to-date.

Poudel, A., 2022. Omicron responsible for 88 percent of new COVID-19 infections in Nepal. Kathmandu Post URL https://kathmandupost.com/health/2022/01/23/omicron-responsible-for-88-percent-of-new-covid-19-infections-in-nepal.

Prem, K., Cook, A.R., Jit, M., 2017. Projecting social contact matrices in 152 countries using contact surveys and demographic data. PLoS Comput. Biol. 13 (9), e1005697. http://dx.doi.org/10.1371/journal.pcbi.1005697.

Pullano, G., Di Domenico, L., Sabbatini, C.E., Valdano, E., Turbelin, C., Debin, M., Guerrisi, C., Kengne-Kuetche, C., Souty, C., Hanslik, T., et al., 2021. Underdetection of cases of COVID-19 in France threatens epidemic control. Nature 590 (7844), 134–139. http://dx.doi.org/10.1038/s41586-020-03095-6.

Rai, B., Shukla, A., Dwivedi, L.K., 2021. Estimates of serial interval for COVID-19: A systematic review and meta-analysis. Clin. Epidemiol. Glob. Health 9, 157–161. http://dx.doi.org/10.1016/j.cegh.2020.08.007.

Rajiv, B., Jeffrey, K., 2020. Estimating individual risk of COVID-19 associated hospitalization and death using publicly available data. Plos One 15, http://dx.doi.org/10.1371/journal.pone.0243026.

Ritchie, H., Mathieu, E., Rodés-Guirao, L., Appel, C., Giattino, C., Ortiz-Ospina, E., Hasell, J., Macdonald, B., Beltekian, D., Roser, M., 2020. Coronavirus pandemic (COVID-19). Our World Data URL https://ourworldindata.org/coronavirus.

Saito, S., Asai, Y., Matsunaga, N., Hayakawa, K., Terada, M., Ohtsu, H., Tsuzuki, S., Ohmagari, N., 2021. First and second COVID-19 waves in Japan: A comparison of disease severity and characteristics. J. Infect. 82 (4), 84–123. http://dx.doi.org/10.1016/j.jinf.2020.10.033.

Saito, E., Gilmour, S., Yoneoka, D., Gautam, G.S., Rahman, M.M., Shrestha, P.K., Shibuya, K., 2016. Inequality and inequity in healthcare utilization in urban nepal: a cross-sectional observational study. Health Policy Plan. 31 (7), 817–824.

Talmoudi, K., Safer, M., Letaief, H., Hchaichi, A., Harizi, C., Dhaouadi, S., Derouiche, S., Bouaziz, I., Gharbi, D., Najar, N., et al., 2020. Estimating transmission dynamics and serial interval of the first wave of COVID-19 infections under different control measures: a statistical analysis in Tunisia from february 29 to may 5, 2020. BMC Infect. Dis. 20 (1), 1–8. http://dx.doi.org/10.1186/s12879-020-05577-4.

Tang, B., Bragazzi, N.L., Li, Q., Tang, S., Xiao, Y., Wu, J., 2020. An updated estimation of the risk of transmission of the novel coronavirus (2019-nCov). Infect. Dis. Model. 5, 248–255. http://dx.doi.org/10.1016/j.idm.2020.02.001.

Thompson, R., Stockwin, J., van Gaalen, R.D., Polonsky, J., Kamvar, Z., Demarsh, P., Dahlqwist, E., Li, S., Miguel, E., Jombart, T., et al., 2019. Improved inference of time-varying reproduction numbers during infectious disease outbreaks. Epidemics 29, 100356. http://dx.doi.org/10.1016/j.epidem.2019.100356.

Tian, H., Liu, Y., Li, Y., Wu, C.-H., Chen, B., Kraemer, M.U., Li, B., Cai, J., Xu, B., Yang, Q., et al., 2020. An investigation of transmission control measures during the first 50 days of the COVID-19 epidemic in China. Science 368 (6491), 638–642. http://dx.doi.org/10.1126/science.abb610.

van den Driessche, P., Watmough, J., 2002. Reproduction numbers and sub-threshold endemic equilibria for compartmental models of disease transmission. Math. Biosci. 180 (1), 29–48. http://dx.doi.org/10.1016/S0025-5564(02)00108-6.

Walensky, R.P., 2021. CDC updates and shortens recommended isolation and quarantine period for general population: media statement for immediate release: Monday, december 27, 2021. URL https://stacks.cdc.gov/view/cdc/112951.

Wallinga, J., Teunis, P., 2004. Different epidemic curves for severe acute respiratory syndrome reveal similar impacts of control measures. Am. J. Epidemiol. 160 (6), 509–516. http://dx.doi.org/10.1093/aje/kwh255.

Wan, H., Cui, J.-A., Yang, G.-J., 2020. Risk estimation and prediction of the transmission of coronavirus disease-2019 (COVID-19) in the mainland of China excluding Hubei province. Infect. Dis. Poverty 9 (1), 1–9.

Worldometer, 2023. Coronavirus cases. Worldometer URL https://www.worldometers.info/coronavirus/.

Xiang, Y., Zhang, R., Jinghong, Q., So, H.-C., 2022. Association of COVID-19 with risks of hospitalization and mortality from other disorders post-infection: A study of the UK Biobank. http://dx.doi.org/10.1101/2022.03.23.22272811, medRxiv.

Zhang, J., Litvinova, M., Wang, W., Wang, Y., Deng, X., Chen, X., Li, M., Zheng, W., Yi, L., Chen, X., et al., 2020. Evolving epidemiology and transmission dynamics of coronavirus disease 2019 outside Hubei province, China: a descriptive and modelling study. Lancet Infect. Dis. 20 (7), 793–802. http://dx.doi.org/10.1016/S1473-3099(20)30230-9.